VNIVERSITAT DE VALÈNCIA

New Physics adventures in the LHC age

Javier Fuentes Martín

IFIC, Universitat de València - CSIC

Tesis doctoral, Mayo 2017
Doctorado en Física

Directores de tesis:

Antonio Pich Zardoya, Jorge Portolés Ibáñez
y Pedro David Ruiz Femenía

Antonio Pich Zardoya, Catedrático del Departamento de Física Teórica de la Universitat de València,
Jorge Portolés Ibáñez, Científico Titular del Consejo Superior de Investigaciones Científicas (CSIC), y
Pedro David Ruiz Femenía, Profesor Visitante del Departamento de Física Teórica de la Universidad Autónoma de Madrid,

Certifican:

Que la presente memoria, "New Physics adventures in the LHC age", ha sido realizada bajo su dirección en el Instituto de Física Corpuscular, centro mixto de la Universidad de Valencia y del CSIC, por Javier Fuentes Martín y constituye su tesis para optar al grado de Doctor en Física.

Y para que así conste, en cumplimiento de la legislación vigente, presenta en el Departamento de Física Teórica de la Universidad de Valencia la referida Tesis Doctoral, y firman el presente certificado.

Valencia, a 15 de Mayo de 2017.

Antonio Pich Zardoya Jorge Portolés Ibáñez Pedro David Ruiz Femenía

Dedicada con cariño a mis padres
y a mi hermana Lauri

Contents

Glossary

$\overline{\text{MS}}$ Modified Minimal Subtraction. 93

2HDM Two-Higgs-Doublet Model. 18

3HFPQ Three-Higgs Flavored PQ. 221

A2HDM Aligned Two-Higgs-Doublet Model. 24

ADMX Axion Dark Matter experiment. 49

APV Atomic Parity Violation. 123

ATLAS A Toroidal LHC ApparatuS. 8

BFM Background Field Method. 58

BGL Branco–Grimus–Lavoura. 25

BSM Beyond the Standard Model. 238

CASPEr Cosmic Axion Spin Precession Experiment. 51

CAST CERN Axion Solar Telescope. 49

CERN European Organization for Nuclear Research, acronym derived from the French name: "Conseil Européen pour la Recherche Nucléaire". 8

CKM Cabbibo–Kobayashi–Maskawa. 9

CL Confidence Level. 123

CMS Compact Muon Solenoid. 8

CP Charge Conjugation Parity. 9

DFSZ Dine–Fischler–Srednicki–Zhitnitsky. 43

DM Dark Matter. 14

EDM Electric Dipole Moment. 51

EFT Effective Field Theory. 29

EOM Equations Of Motion. 59

EW Electroweak. 3

FCNC Flavor Changing Neutral Current. 10

GIM Glashow–Iliopoulos–Maiani. 237

HFAG Heavy Flavor Averaging Group. 163

HLM Henning–Lu–Murayama. 96

IAXO International Axion Observatory. 49

KSVZ Kim–Shifman–Vainshtein–Zakharov. 43

LAMPF Los Alamos Meson Physics Facility. 232

LEP Large Electron-Positron collider. 35

LFUV Lepton-Flavor Universality Violation. 72

LHC Large Hadron Collider. 8

LHCb Large Hadron Collider beauty experiment. 13

MFV Minimal Flavor Violation. 141

MSSM Minimal Supersymmetric Standard Model. 23

NFC Natural Flavor Conservation. 22

NP New Physics. 13

NTP Neutrino Trident Production. 123

NWA Narrow-Width Approximation. 124

PDG Particle Data Group. 159

PMNS Pontecorvo–Maki–Nakagawa–Sakata. 10

PQ Peccei-Quinn. 38

QCD Quantum chromodynamics. 35

RGE Renormalization Group Evolution. 24

SM Standard Model. 3

SMEFT Standard Model Effective Field Theory. 58

SSB Spontaneous Symmetry Breaking. 6

UV Ultraviolet. 22

vev vacuum expectation value. 6

VL Vector-Like. 148

WC Wilson Coefficient. 57

WD White Dwarf. 232

WET Weak Effective Theory. 58

Agradecimientos (*acknowledgments*)

> "But I don't want to go among mad people," Alice remarked. "Oh, you can't help that," said the Cat: "we're all mad here. I'm mad. You're mad." "How do you know I'm mad?" said Alice. "You must be," said the Cat, "or you wouldn't have come here."
>
> — *Lewis Carroll*, Alice in Wonderland

Al fin llega el esperado momento en que doy por concluida la tesis y empiezo a recordar a todos aquellos que me hacen rememorar mis años de doctorado con una sonrisa. Son muchas las personas a las que quiero agradecer profundamente por su ayuda, compañía, apoyo y por conseguir que no me volviera loco durante los momentos críticos o, al menos, por mantenerme dentro de los límites de cordura socialmente aceptables. Dada mi naturaleza despistada, estoy seguro de que dejaré a muchos sin agradecer. Les pido que no se enfaden y, a cambio, prometo compensar con birra.

Quiero comenzar agradeciendo por triplicado a mis directores: Jorge, Pedro y Toni, por todo lo que he aprendido con ellos durante mi doctorado y por el enorme apoyo que siempre me han dado. A los tres les quiero dar las gracias por sus correcciones y comentarios sobre esta tesis, los cuales, sin lugar a dudas, han contribuido a mejorarla considerablemente.

Mis interacciones con Toni han sido más escasas, pero no por ello menos gratificantes y fructíferas. Siempre me ha fascinado la claridad con la que ve y sabe transmitir la Física. Si algo lamento de mi años de doctorado es no haber interaccionado más con él. Quiero agradecerle su constante apoyo y sus consejos en los momentos de duda.

Muchas de las cosas que ahora sé se las debo a las largas discusiones en mail y en pizarra que tuve con Pedro. Más de una vez (y dos y tres...) sus preguntas me han hecho replantearme lo que creía que ya sabía y me han ayudado enormemente a ir un poco más allá y a abordar la Física de otra manera, razones por las que le estoy profundamente agradecido.

A Jorge le quiero dedicar una mención especial en estos agradecimientos. Cuando lo conocí durante mis años de carrera, supe inmediatamente que sería el mejor director de tesis... y desde luego no me equivoqué. Desde el primer momento, Jorge ha sido capaz de proponerme proyectos interesantes, estar ahí siempre que lo necesitaba y a su vez darme libertad para colaborar con otros investigadores. Jorge ha

estado siempre atento y disponible, ofreciéndome ayuda y consejo incluso para temas que iban más allá de su labor de director de tesis. Siempre recordaré los momentos de bloqueo en los que decidía acudir a su despacho y volvía con un conocimiento más profundo del tema en cuestión; así como también los momentos de relax en los que hablábamos de todo y nada, y de los que siempre acababa aprendiendo algo interesante. En fin, sólo quiero manifestar el inmenso agradecimiento que le tengo por todo y aprovechar para recordarle que no se librará fácilmente de mi.

También quiero dar las gracias a Alejandro por su ayuda y colaboraciones constantes desde mis primeros años en el doctorado. Con él he aprendido muchísima Física y seguramente aprenderé mucha más aún. *Of course, I also owe enormous gratitude to the rest of my collaborators: Hugo, Martin, Sofiane, Avelino, Javier, Andi, Admir and Gino, without whom this thesis would have been completely impossible. I had the luck to find in them not only great physicists but also very nice people, making my collaborations with them a fantastic experience.*

Gracias también a mis compañeros del IFIC con los que he tenido el placer de disfrutar tanto discutiendo de Física como a nivel personal. Quiero agradecer a todos los miembros del grupo de Física Nuclear, entre los que he estado de polizón todos estos años, por ser tan agradables conmigo e integrarme en su grupo. Por supuesto he de agradecer a mis súper compañeros de despacho, Pedro y Vinicius, que generaran el ambiente tan genial que tenemos en el despacho y por todas las cosas que hemos hecho juntos: los desayunos de marqués, los findes del equipo snowboard, las partidas de rol... También doy las gracias a mis next-to-leading compañeros de despacho: Edu, Rafa, Jorgivan y Astrid por contribuir a ese buen ambiente general. Agradezco especialmente a Miguel por darme un respiro con las clases durante los momentos más intensos de la tesis.

También tengo el placer de haber conocido grandes amigos, algunos de ellos en el IFIC, que de un modo u otro han contribuido a hacer mi estancia en Valencia fuera considerablemente mejor: Sebas, Javi, Pablo, Quim, Christoph y muchos más, gracias por todo. Por supuesto también agradezco haberme encontrado con Antonio, Laura y Pablo, los cuáles han sabido aguantar estoicamente mis discusiones durante las comidas (creo que en el fondo les gustaban, a veces...) y con los que he compartido merecidos momentos de relax, en especial esas partidas de escape, que tanto ayudaron a desconectar. Y cómo no también quiero agradecer a Clara, Julián y Quique por ser unas personas tan especiales. Estos años sin duda no habrían sido lo mismo sin Julián y nuestras movidas. Clara llegó en la recta final del doctorado pero entró pisando fuerte. Sin duda me lo he pasado genial con vosotros, ¡y espero seguir haciéndolo! *I would also like to thank my dear friend Marija for all the nice moments we spent together during the PhD and for her constant support during these years, even offering her home when I was homeless.* Por supuesto también doy las gracias a Jordi por obligarme a desconectar en los momentos de saturación hinchándome a vino y cerveza a la menor oportunidad posible. Y claro, también por las discusiones sobre Física, parecidas a una montaña rusa, que he tenido el placer de disfrutar con él. ¡Espero que todos me visitéis por Zurich!

I also had the occasion to meet great people during my research stays at Los Alamos and Zurich. I am grateful to Vincenzo and the rest of the members of the T-2 Theory Division of Los Alamos National Laboratory for hosting me during my

research stay, and specially to Saori and Felix, for making my stay there much more enjoyable. I also want to give my deepest thanks to Gino and all the people from the University of Zurich for making my stay there absolutely fantastic. I did not only find great coworkers in Zurich but also good friends. Thanks to Marzia, Dario, Danny, Sokratis, Admir, David, Andrea, and Carmelina for being so nice to me while I was there. I also had the luck to meet great people in Zurich outside academia, thanks Amogha, Tung, Evelyn, Tom, Pablo and many others for all the great moments. I will see you all soon!

I am really thankful to the evaluators of this thesis: José, Verónica, Arcadi, Gino, Avelino, Juanjo and Arantza for dedicating part of their time on preparing the reports, y especialmente a José y a Verónica por hacer el esfuerzo de venir a Valencia para formar parte del tribunal de tesis. Agradezco doblemente a Avelino por realizar una lectura de la tesis tan detallada y por sus comentarios y correcciones, siempre acertados, que la han hecho algo mejor.

También aprecio enormemente el apoyo económico que he recibido durante el doctorado por parte de la Universidad de Valencia bajo el programa "Atracciò de Talent" y desde el grupo para la participación en seminarios, conferencias y congresos.

Quiero terminar estas líneas dando las gracias a mi familia por su dedicación, apoyo y comprensión, especialmente durante los momentos más difíciles, sabiendo entender que no siempre podía estar disponible y apoyándome continuamente desde la distancia.

List of publications

This Ph.D. thesis is based on the following publications:

1. **Effective Aligned 2HDM with a DFSZ-like invisible axion**,
   Alejandro Celis, Javier Fuentes-Martín, Hugo Serôdio,
   Physics Letters B 737 (2014) 185–190, arXiv:1407.0971 [hep-ph]

2. **An invisible axion model with controlled FCNCs at tree level**,
   Alejandro Celis, Javier Fuentes-Martín, Hugo Serôdio,
   Physics Letters B 741 (2015) 117-123, arXiv:1410.6217 [hep-ph]

3. **A class of invisible axion models with FCNCs at tree level**,
   Alejandro Celis, Javier Fuentes-Martín, Hugo Serôdio,
   JHEP 1412 (2014) 167, arXiv:1410.6218 [hep-ph]

4. **Family non-universal Z' models with protected flavor-changing interactions**,
   Alejandro Celis, Javier Fuentes-Martín, Martin Jung, Hugo Serôdio,
   Physical Review D 92 (2015) 1, 015007, arXiv:1505.03079 [hep-ph]

5. **Non-abelian gauge extensions for B-decay anomalies**,
   Sofiane M. Boucenna, Alejandro Celis, Javier Fuentes-Martín, Avelino Vicente, Javier Virto,
   Physics Letters B 760 (2016) 214-219, arXiv:1604.03088 [hep-ph]

6. **Integrating out heavy particles with functional methods: a simplified framework**,
   Javier Fuentes-Martín, Jorge Portolés, Pedro Ruiz-Femenía,
   JHEP 1609 (2016) 156, arXiv:1607.02142 [hep-ph]

7. **Phenomenology of an $\mathbf{SU(2) \times SU(2) \times U(1)}$ model with lepton-flavor non-universality**,
   Sofiane M. Boucenna, Alejandro Celis, Javier Fuentes-Martín, Avelino Vicente, Javier Virto,
   JHEP 1612 (2016) 059, arXiv:1608.01349 [hep-ph]

8. **Lepton Flavor Non-Universality in B decays from Dynamical Yukawas**,
   Andreas Crivellin, Javier Fuentes-Martín, Admir Greljo, Gino Isidori,
   Physics Letters B 766 (2016) 77-85, arXiv:1611.02703 [hep-ph]

During my Ph.D. I have also co-authored the following publications that did not enter in the thesis:

1. **Instanton-mediated baryon number violation in non-universal gauge extended models**,
   Javier Fuentes-Martín, Jorge Portolés, Pedro Ruiz-Femenía,
   JHEP 1501 (2015) 134, arXiv:1411.2471 [hep-ph]

2. **DsixTools: The Standard Model Effective Field Theory Toolkit**,
   Alejandro Celis, Javier Fuentes-Martín, Avelino Vicente, Javier Virto,
   Eur.Phys.J. C77 (2017) no.6, 405, arXiv:1704.04504 [hep-ph]

and the preprint

1. **Gauge-invariant implications of the LHCb measurements on Lepton-Flavour Non-Universality**,
   Alejandro Celis, Javier Fuentes-Martín, Avelino Vicente, Javier Virto,
   arXiv:1704.05672 [hep-ph]

Finally, I have authored the following proceedings:

1. **Baryon and lepton number violating effective operators in a non-universal extension of the Standard Model**,
   Javier Fuentes-Martín,
   Proceedings of "XIth Quark Confinement and the Hadron Spectrum",
   Saint-Petersburg (Russia), September 8-12 (2014),
   AIP Conf.Proc. 1701 (2016) 070002

2. **A class of Z' models with non-universal couplings and protected flavor-changing interactions**,
   Javier Fuentes-Martín,
   Proceedings of the EPS-HEP 2015 conference,
   Vienna (Austria), July 22-29 (2015),
   PoS EPS-HEP2015 (2015) 577

Preface

"Begin at the beginning," the King said gravely,
"and go on till you come to the end: then stop."

— *Lewis Carroll*, Alice in Wonderland

Particle Physics is currently living an age of exploration that started with the observation at the LHC of the Higgs boson, providing the Standard Model of strong and electroweak interactions the final eluding piece that completes it. While this theory is extremely successful, it is commonly accepted that it is not the final one since it cannot answer all the theoretical questions and experimental observations. It is thus expected that New Physics that extends the Standard Model will appear soon, though this might well be only a hope. This thesis compiles some of the adventures in the Quest for New Physics. It is organized in three parts: Part I introduces the main subjects of the thesis and sets the notation and frameworks that are used later. This part contains topics that are of common knowledge in the literature and it is intended as a broad introduction. On the contrary, Part II is specifically devoted to compile the scientific research that was done during the Ph.D. and therefore it is more technical than the previous part. Part III contains a comprehensive summary of the thesis in Spanish.

Part I is organized as follows. In Chapter 1 we introduce the Standard Model, its main features, and several theoretical and experimental issues that this framework cannot explain. The rest of this part is dedicated to the analysis of various extensions of the Standard Model. In particular, in Chapter 2 we introduce the two-Higgs-doublet model, a minimal extension where an additional Higgs doublet is added to the scalar sector of the theory. In this chapter, special emphasis is placed in the two-Higgs-doublet model flavor problem and its solutions. Chapter 3 presents the Strong CP problem in some detail, together with a discussion on the Peccei–Quinn solution and its associated phenomenology. In Chapter 4 we introduce the concept of Effective Field Theories and show how to construct them from a given ultraviolet model using functional techniques. We also introduce examples of Effective Field Theories within the Standard Model framework that stand for a complementary approach in the search for New Physics. Finally, in Chapter 5 we present the recent experimental anomalies in B-physics data and discuss their main implications.

While Part I follows a more linear discussion, with each chapter based on the previous ones, Part II is structured in three, essentially unrelated, chapters. Chapter 6 extends to the one-loop order the functional methods for the construction of Effective Field Theories introduced in Chapter 4. In Chapter 7 we present three

models aimed to provide an explanation to the B-physics anomalies. These are based in various extensions of the Standard Model gauge sector, each predicting different characteristic experimental signatures. Chapter 8 introduces two invisible axion models that include additional features which are not present in the original implementations.

Part III contains a single chapter that summarizes in Spanish the major goals, procedures and results of the present thesis.

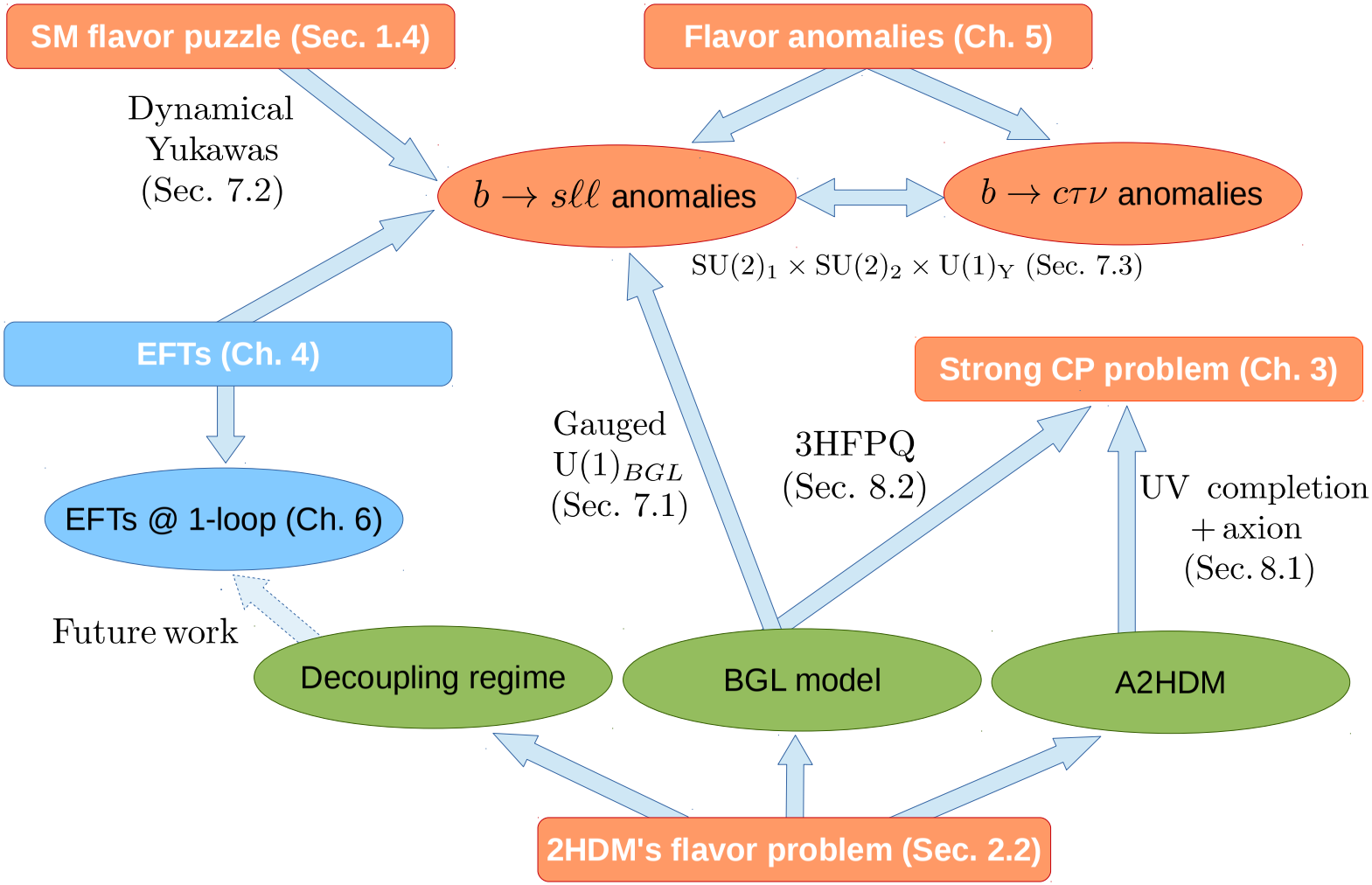

Thesis concept map

Part I

The Standard Model and some of its extensions

CHAPTER 1

A brief story of the Standard Model

> It sounds plausible enough tonight, but wait until tomorrow. Wait for the common sense of the morning.
>
> — *H.G. Wells*, The time machine

The SM [1–4] is the theory that compiles our current knowledge of the strong and EW interactions. In this theory the concept of symmetry plays a central role. Its fundamental degrees of freedom are fields that correspond to representations of the Lorentz symmetry, i.e. the spin-zero Higgs, spin-one-half quarks and leptons, and the spin-one gauge bosons; and the Lagrangian that characterizes the interactions among these fields is invariant under the local symmetry group $\mathrm{SU(3)_c} \times \mathrm{SU(2)_L} \times \mathrm{U(1)_Y}$. The use of these symmetry principles provides an elegant and simple framework that is able to describe with great accuracy most of the known experimental data in particle physics, making the SM one of the greatest successes of Modern Physics. In this chapter we will briefly present this theory and describe its main features (see Ref. [5] for a more detailed review on the SM). Also, at the end, we will present some open questions of this theory that serve as motivation for going beyond this framework, setting the ground for the next chapters.

1.1 The SM Lagrangian and its particle content

The SM is a quantum field theory based on the principles of locality, causality and renormalizability, invariant under the Lorentz symmetry and the $\mathcal{G}_{\mathrm{SM}} \equiv \mathrm{SU(3)_c} \times \mathrm{SU(2)_L} \times \mathrm{U(1)_Y}$ gauge group. In this framework, the interactions are mediated by bosons such as the Higgs or the gauge bosons. Contrary to the Higgs, the gauge fields are completely defined in terms of the gauge symmetry. We have eight massless gluons, G^{α}_{μ}, for the strong interactions, associated to the $\mathrm{SU(3)_c}$ gauge group; while the gauge bosons associated to the $\mathrm{SU(2)_L} \times \mathrm{U(1)_Y}$ symmetry are the massless photon, A_μ, that mediates the electromagnetic interactions, and three massive bosons, the $W^{\pm}_{\mu}$ and the Z_μ, mediators of the weak interactions. Since in the SM both the mediators of electromagnetism and those of the weak force are generated by the $\mathrm{SU(2)_L} \times \mathrm{U(1)_Y}$ gauge group, this symmetry is commonly denoted as the EW symmetry and these forces are said to be unified. The observed matter

Type	Particle	$SU(3)_c$	$SU(2)_L$	$U(1)_Y$
Quarks	q_L	**3**	**2**	1/6
	u_R	**3**	**2**	2/3
	d_R	**3**	**2**	−1/3
Leptons	ℓ_L	**1**	**2**	−1/2
	e_R	**1**	**1**	−1
Higgs	ϕ	**1**	**2**	1/2

Table 1.1: *The SM matter content (plus the Higgs) and their gauge quantum numbers.*

content, the fermions, are given in terms of fields of definite chirality

$$\begin{aligned} q_L &= \begin{pmatrix} u_L \\ d_L \end{pmatrix}, \qquad u_R\,, \qquad d_R\,, \\ \ell_L &= \begin{pmatrix} \nu_L \\ e_L \end{pmatrix}, \qquad e_R\,. \end{aligned} \tag{1.1}$$

The fermions appear in five different representations of the SM gauge group, these are shown in Table 1.1 together with the one of the Higgs. Quarks and leptons are found in three copies, which are commonly denoted as families or flavors. As we will see later, in the SM the different families have the same gauge interactions, situation that is called gauge *universality*, and only differ in their Yukawa couplings, see Section 1.1.3 for more details. The different flavors of quarks and leptons are denoted as

$$u \equiv \begin{pmatrix} u \\ c \\ t \end{pmatrix}, \qquad d \equiv \begin{pmatrix} d \\ b \\ s \end{pmatrix}, \qquad e \equiv \begin{pmatrix} e \\ \mu \\ \tau \end{pmatrix}, \qquad \nu \equiv \begin{pmatrix} \nu_e \\ \nu_\mu \\ \nu_\tau \end{pmatrix}. \tag{1.2}$$

The SM Lagrangian, that describes the interactions among all these particles, can be generically parameterized as

$$\mathcal{L}_{\rm SM} = \mathcal{L}_{g+f} + \mathcal{L}_H + \mathcal{L}_Y\,, \tag{1.3}$$

where $\mathcal{L}_{g+f}$ includes the SM gauge and fermion kinetic terms and interactions, $\mathcal{L}_H$ contains the Higgs kinetic term and potential, and $\mathcal{L}_Y$ describes the interactions between the Higgs and the fermions. We proceed to describe each of these terms in the following sections.

1.1.1 The fermion and gauge sectors

The free Lagrangian for the SM fermions ($\psi = q_L^0, \ell_L^0, u_R^0, d_R^0, e_R^0$)[1]

$$\mathcal{L}_f = \overline{\psi}\, i\partial\!\!\!/\, \psi\,, \tag{1.4}$$

[1]Here the 0 superscript in the fermion fields denotes that they are not in the mass-diagonal eigenbasis. This will be clear in Section 1.1.3 where we introduce the Yukawa interactions.

is invariant under the global $\mathrm{SU(3)_c} \times \mathrm{SU(2)_L} \times \mathrm{U(1)_Y}$, but not under local transformations of this symmetry. We can promote the symmetry of the Lagrangian to a local one by replacing the derivative in Eq. (1.4) by a covariant derivative. This covariant derivative is completely fixed by the symmetry transformation, and requires the introduction of a spin-one field for each of the generators of the group: the gauge fields G^α_μ ($\alpha = 1, \ldots, 8$), W^a_μ ($a = 1, 2, 3$) and B_μ,

$$D_\mu \psi \equiv \left(\partial_\mu - i g_c \, G^\alpha_\mu T^\alpha P_q - i g \, W^a_\mu T^a P_L - i g' B_\mu Y_\psi\right) \psi. \tag{1.5}$$

Here, $T^\alpha = \lambda^\alpha/2$ and $T^a = \tau^a/2$ are the $\mathrm{SU(3)_c}$ and $\mathrm{SU(2)_L}$ generators, with λ^α and τ^a the Gell-Mann and the Pauli matrices respectively. The chiral projectors are defined as $P_{L,R} = 1/2(1 \mp \gamma_5)$, and $P_q = P_u + P_d$ where P_f ($f = u, d, e$) projects the fermion multiplet ψ into the corresponding fermion. The values of the hypercharge, Y_ψ, are given in the fifth column of Table 1.1. The introduction of this new derivative generates an interaction among gauge fields and fermions whose strength is controlled by the gauge couplings: g_c, g and g'. As anticipated, since all the SM families have the same gauge symmetry transformations, the interactions among the SM fermions and gauge bosons are flavor universal. If one also includes a kinetic term for the gauge bosons, so they can propagate, we arrive at the following gauge-invariant Lagrangian

$$\mathcal{L}_{g+f} = -\frac{1}{4} G^\alpha_{\mu\nu} G^{\mu\nu\,\alpha} - \frac{1}{4} W^a_{\mu\nu} W^{\mu\nu\,a} - \frac{1}{4} B_{\mu\nu} B^{\mu\nu} + \overline{\psi}\, i \not{D}\, \psi + \mathcal{L}_{\mathrm{GF}} + \mathcal{L}_{\mathrm{ghost}}\,. \tag{1.6}$$

In this expression, the field-strength tensors are fixed by gauge invariance and read

$$\begin{aligned} G^\alpha_{\mu\nu} &= \partial_\mu G^\alpha_\nu - \partial_\nu G^\alpha_\mu + g f_{\alpha\beta\gamma} G^\beta_\mu G^\gamma_\nu, \\ W^a_{\mu\nu} &= \partial_\mu W^a_\nu - \partial_\nu W^a_\mu + g \epsilon_{abc} W^b_\mu W^c_\nu, \\ B_{\mu\nu} &= \partial_\mu B_\nu - \partial_\nu B_\mu. \end{aligned} \tag{1.7}$$

Due to the non-Abelian nature of the $\mathrm{SU(3)_c}$ and the $\mathrm{SU(2)_L}$ symmetries, the kinetic terms for the corresponding gauge fields also generate self interactions. These terms play a crucial role in the explanation of several key features of the strong interactions, such as confinement and asymptotic freedom [6–8]. Apart from the aforementioned terms, one should also include two additional pieces to the Lagrangian. Vector fields contain more degrees of freedom than the gauge fields. In order to get rid of the extra degrees of freedom without losing explicit Lorentz covariance, it is usual to include a gauge fixing term in the Lagrangian, $\mathcal{L}_{\mathrm{GF}}$. Moreover, one should also include the ghost Lagrangian, $\mathcal{L}_{\mathrm{ghost}}$, for consistency of the theory [9].

It can be shown that the Lagrangian constructed under the principles of gauge symmetry is renormalizable [10]. However, gauge invariance does not allow for a mass term for the gauge bosons and SM fermions, in contradiction with the experimental observations. The direct introduction of the mass terms would explicitly break the symmetry rendering the theory non-renormalizable. Therefore, we need a mechanism that is able to give masses to the gauge bosons and fermions while preserving the renormalizability of the theory. We introduce this mechanism in the next section.

1.1.2 The scalar sector

As already stated, the Lagrangian introduced in Eq. (1.6) is unable to account for the observed gauge boson masses. There is however an elegant solution to this problem that receives the name of Brout–Englert–Higgs mechanism [11, 12]. The idea consists in constructing a theory with a fully symmetric Lagrangian, but whose vacuum is not invariant under the symmetry. This can be achieved in a rather minimal way by introducing a complex scalar $\mathrm{SU}(2)_\mathrm{L}$ doublet, the Higgs doublet. The most general renormalizable Lagrangian for the Higgs doublet can be written as

$$\mathcal{L}_H = (D_\mu \phi)^\dagger D^\mu \phi - V(\phi)\,, \qquad V(\phi) = m_\phi^2 \left(\phi^\dagger \phi\right) + \frac{\lambda}{2}\left(\phi^\dagger \phi\right)^2\,, \tag{1.8}$$

where, as in the fermion sector, the covariant derivative has been introduced to render the Lagrangian locally invariant under $\mathcal{G}_\mathrm{SM}$ transformations and is defined as

$$D_\mu \phi \equiv \left(\partial_\mu - \frac{1}{2} i g \tau^a W_\mu^a - \frac{1}{2} i g' B_\mu\right)\phi\,. \tag{1.9}$$

The vacuum of the theory can be obtained by minimizing the scalar potential

$$\left.\frac{\partial V}{\partial \phi}\right|_{\phi=\langle\phi\rangle} = 0\,, \tag{1.10}$$

where the vacuum configuration of the Higgs doublet, $\langle\phi\rangle \equiv \langle 0|\,\phi\,|0\rangle$, can be generically parameterized in terms of its norm $|\langle\phi\rangle| \equiv v/\sqrt{2}$, with v denoting the Higgs vev. For $m_\phi^2 > 0$ the condition in Eq (1.10) gives just one extremum at $v = 0$. However, for $m_\phi^2 < 0$ the potential has two extrema

$$v = 0\,, \qquad v = \sqrt{\frac{-2m_\phi^2}{\lambda}}\,. \tag{1.11}$$

If one imposes the condition $\lambda > 0$, so that the potential is bounded from below, it is straightforward to see that those correspond, respectively, to a local maximum and a global minimum of the scalar potential, see Figure 1.1. As we can see from this figure, there is an infinite set of degenerate vacua in this case. However, choosing one of those vacua triggers a SSB of the SM gauge symmetry

$$\mathcal{G} \xrightarrow{\text{SSB}} \mathrm{SU}(3)_\mathrm{c} \times \mathrm{U}(1)_\mathrm{em}\,, \tag{1.12}$$

where we identified the unbroken U(1) with the symmetry associated to the electromagnetic force, $\mathrm{U}(1)_\mathrm{em}$, for phenomenological reasons. The Golstone theorem [13] states that the spontaneous breaking of a symmetry leads to the appearance of a set of massless bosons, one for each of the broken generators. These are the so-called Golstone bosons. Interestingly, when the broken symmetry is a gauge symmetry, the Golstone bosons get "eaten" by the gauge fields and become the longitudinal components of these fields, providing a mass for these gauge bosons. This can be easily seen if we parametrize the Higgs doublet in the following way

$$\phi = e^{i\frac{\varphi^a \tau^a}{2v}} \begin{pmatrix} 0 \\ \frac{1}{\sqrt{2}}(v+h) \end{pmatrix}\,, \tag{1.13}$$

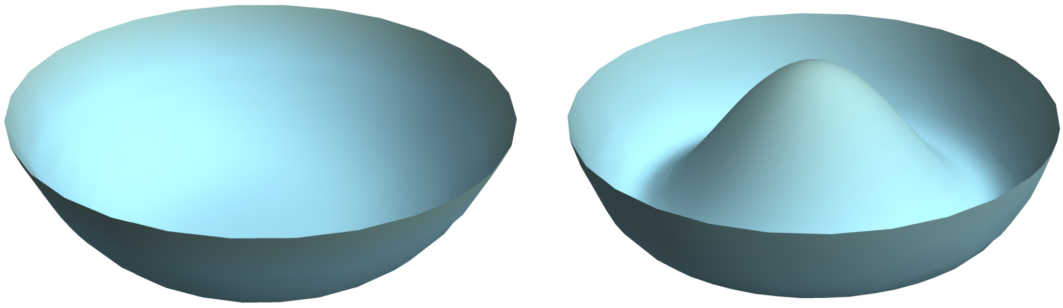

Figure 1.1: *Higgs potential for $m_\phi^2 > 0$ (left) and $m_\phi^2 < 0$ (right). In the second case, there are flat directions of degenerate vacua associated to the would-be Golstone bosons, φ_a; the Higgs, h, corresponds to an excitation in the radial direction.*

where the Golstone bosons, φ^a, related to excitations along the minima of the scalar potential are isolated in the exponential factor. The so-called Higgs boson, h, is on the other hand associated to the radial excitation of the Higgs doublet. We can use the local $\mathrm{SU(2)_L}$ gauge invariance to rotate away the Goldstones, which effectively consists in setting $\varphi^a = 0$ in Eq. (1.13). This rotation corresponds to the choice of a specific gauge that receives the name of *unitary gauge*. In this gauge, the kinetic term for the Higgs doublet can be rewritten as (here $\tan\theta_W = g'/g$)

$$(D_\mu\phi)^\dagger\, D^\mu\phi = \frac{1}{2}\partial_\mu h\,\partial^\mu h + (v+h)^2\left(\frac{g^2}{4}W_\mu^\dagger\, W^\mu + \frac{g^2}{8\cos^2\theta_W}Z_\mu\, Z^\mu\right), \qquad (1.14)$$

where one can see that the physical gauge bosons, defined as a linear combination of the ones introduced in Eq. (1.5), receive a mass proportional to the vev of the Higgs

$$M_W = \frac{1}{2}\,gv\,, \qquad M_Z = \frac{1}{2\cos\theta_W}\,gv\,, \qquad (1.15)$$

while the photon, given by a different combination of the EW gauge fields, remains massless. This is what one would expect from symmetry arguments given that the $\mathrm{U(1)_{em}}$ remains unbroken. The expression in Eq. (1.14) also has other important implications:

- We can see that the masses of the $W^\pm$ and the Z are not independent but instead they follow the tree-level relation

$$\rho \equiv \frac{M_W^2}{M_Z^2\cos^2\theta_W} = 1\,. \qquad (1.16)$$

  The value of the ρ parameter has been experimentally tested to a great accuracy and is found in good agreement with the SM prediction, which is slightly different from one due to radiative corrections.

- While the Goldstone bosons are "eaten" by the gauge fields in order to provide them a mass, the introduction of the Higgs doublet implies the appearance

of a new scalar, the Higgs boson. This elusive particle that was predicted in the 1960's was finally found at CERN by the ATLAS [14] and CMS [15] collaborations in 2012, providing a confirmation to the Brout–Englert–Higgs mechanism.

- The tree-level couplings of the Higgs boson to the $W^{\pm}$ and the Z are completely fixed and are proportional to the square of the gauge boson masses. This also implies that the Higgs has no tree-level coupling to photons, which is however generated at one loop. Current experimental measurements of these couplings at the LHC are compatible with the SM prediction [16].

Finally, by introducing the expression in Eq. (1.13) into the scalar potential in Eq. (1.8),

$$V(h) = \frac{1}{2} M_h^2 \, h^2 + \frac{M_h^2}{2v} \, h^3 + \frac{M_h^2}{8v^2} \, h^4 - \frac{M_h^2 v^2}{8} \,, \tag{1.17}$$

we see that the Higgs boson acquires a mass proportional to its vev: $M_h = \sqrt{\lambda}\, v$, as well as cubic and quartic self-interactions that are proportional to its mass. Given that the mass of the Higgs boson is a well-known parameter, $M_H = 125.09 \pm 0.21\,(\text{stat.}) \pm 0.11\,(\text{syst.})$ GeV [17], this implies that the Higgs self-couplings are completely fixed in the SM. Testing this key prediction of the SM is very challenging and there is currently no significant experimental bound on such couplings.

1.1.3 The Yukawa interactions

The gauge symmetry not only forbids a mass term for the gauge bosons but also for the SM fermions. This is a consequence of having fermions with different symmetry transformations for each chirality. However, the same mechanism used to give masses to the $W^{\pm}$ and Z gauge bosons can also be used to provide masses to the fermions. Since we introduced a Higgs doublet, we can now write the following gauge-invariant Yukawa Lagrangian

$$-\mathcal{L}_Y = \overline{\psi} \left(\widetilde{\phi}\, y_u \, P_u P_R + \phi \, y_d \, P_d P_R + \phi \, y_e \, P_e P_R \right) \psi + h.c. \,, \tag{1.18}$$

where the charge conjugated field $\widetilde{\phi} = i\tau^2 \phi^*$ is also a $\mathrm{SU(2)_L}$ doublet of opposite hypercharge, and the Yukawa couplings, $y_{u,d,e}$, are general 3×3 matrices in flavor space. After SSB, using the unitary gauge we can simply rewrite this Lagrangian into

$$-\mathcal{L}_Y = \left(1 + \frac{h}{v} \right) \left(\overline{u_L^0} \, M_u \, u_R^0 + \overline{d_L^0} \, M_d \, d_R^0 + \overline{e_L^0} \, M_e \, e_R^0 + h.c. \right) \,, \tag{1.19}$$

which contains the sought-after mass terms for the fermions. Here the mass matrices

$$M_u = \frac{v}{\sqrt{2}} \, y_u \,, \qquad M_d = \frac{v}{\sqrt{2}} \, y_d \,, \qquad M_e = \frac{v}{\sqrt{2}} \, y_e \,, \tag{1.20}$$

are not diagonal in general but they can be diagonalized by means of a bi-unitary transformation of the fermion fields

$$u^0_{L,R} = U_{uL,R}\, u_{L,R}\,, \quad d^0_{L,R} = U_{dL,R}\, d_{L,R}\,, \quad e^0_{L,R} = U_{eL,R}\, e_{L,R}\,, \tag{1.21}$$

chosen appropriately so that

$$\begin{aligned} U^\dagger_{uL} M_u U_{uR} &= D_u = \mathrm{diag}\,(m_u,\, m_c,\, m_t)\ , \\ U^\dagger_{dL} M_d U_{dR} &= D_d = \mathrm{diag}\,(m_d,\, m_s,\, m_b)\ , \\ U^\dagger_{eL} M_e U_{eR} &= D_e = \mathrm{diag}\,(m_e,\, m_\mu,\, m_\tau)\ , \end{aligned} \tag{1.22}$$

yielding the following form for the Yukawa Lagrangian in the fermion mass-diagonal eigenbasis

$$-\mathcal{L}_Y = \left(1 + \frac{h}{v}\right)\left(\overline{u_L}\, D_u\, u_R + \overline{d_L}\, D_d\, d_R + \overline{e_L}\, D_e\, e_R + h.c.\right)\ . \tag{1.23}$$

From this equation we see that the SM predicts that the Higgs boson couples flavor-diagonally to the physical fermions with a coupling proportional to their masses. This is another important prediction of the SM that can only be tested at the LHC for the heaviest fermions, with an accuracy of $\mathcal{O}(10\%)$. So far, all the experimental measurements are compatible with the SM expectations [16].

1.2 Flavor dynamics of the SM

The fact that we had to perform a rotation in flavor space to get the fermions in their mass-diagonal eigenbasis, has important implications in the SM phenomenology. The weak interactions of the $W^\pm$ with fermions, which are obtained from the covariant derivative defined in Eq. (1.5), are given by

$$\mathcal{L}_{\mathrm{CC}} = \frac{g}{\sqrt{2}}\left[W^\dagger_\mu \left(\overline{u^0_L}\gamma^\mu d^0_L + \overline{\nu^0_L}\gamma^\mu e^0_L\right) + h.c.\right]\ . \tag{1.24}$$

Therefore, when rotating to the fermion mass basis,

$$\mathcal{L}_{\mathrm{CC}} = \frac{g}{\sqrt{2}}\left[W^\dagger_\mu \left(\overline{u_L}\gamma^\mu\, V d_L + \overline{\nu_L}\gamma^\mu e_L\right) + h.c.\right]\ , \tag{1.25}$$

we find that the charged weak current is not diagonal because of the misalignment between the up- and down-quark rotations, which is parameterized in terms of the so-called CKM matrix, $V = U^\dagger_{uL} U_{dL}$,

$$V = \begin{pmatrix} V_{ud} & V_{us} & V_{ub} \\ V_{cd} & V_{cs} & V_{cb} \\ V_{td} & V_{ts} & V_{tb} \end{pmatrix}\ . \tag{1.26}$$

This unitary matrix, whose elements have to be determined experimentally, introduces a source of CP-violation. The measured values of the CKM matrix elements

	λ	A	$\overline{\rho}$	$\overline{\eta}$
CKMfitter	0.22506 ± 0.00050	0.811 ± 0.026	$0.124^{+0.019}_{-0.018}$	0.356 ± 0.011
UTfit	0.22496 ± 0.00048	0.823 ± 0.013	0.141 ± 0.019	0.349 ± 0.012

Table 1.2: *Fitted values of the Wolfenstein parameters from the global fits of the CKMfitter Group [19, 20] and the UTfit Collaboration [21, 22]. Here the barred parameters are defined in terms of the original ones as* $(\overline{\rho}, \overline{\eta}) = (1 - \lambda^2/2)\,(\rho, \eta)$.

have a very hierarchical structure. This is nicely illustrated in the Wolfenstein parametrization [18]

$$V = \begin{pmatrix} 1 - \frac{\lambda^2}{2} & \lambda & A\lambda^3\,(\rho - i\eta) \\ -\lambda & 1 - \frac{\lambda^2}{2} & A\lambda^2 \\ A\lambda^3\,(1 - \rho - i\eta) & -A\lambda^2 & 1 \end{pmatrix} + \mathcal{O}\left(\lambda^4\right) , \tag{1.27}$$

where the CKM is written as an expansion in the small parameter $\lambda \simeq 0.23$. The current experimental values of the Wolfenstein parameters from the global fits to flavor observables by the CKMfitter Group [19,20] and the UTfit Collaboration [21, 22] are given in Table 1.2. Flavor-changing transitions in the charged currents therefore appear suppressed by the off-diagonal elements of the CKM matrix, which is the only source of flavor violation in the SM.

It is important to stress that no flavor violations appear at tree-level in the neutral currents. Since these relate fermions of the same type, the transformations in Eq. (1.21) cancel due to unitarity. The SM therefore predicts no tree-level FCNC. Note however that these are generated in the SM at one-loop and are exactly related to the CKM matrix. Also notice that the unbroken $\mathrm{U}(1)_{\mathrm{em}}$ yields a further suppression of the photon-mediated FCNCs, which appear proportional to the fermion masses.

Finally note that in Eq. (1.25) there is no equivalent matrix for the lepton sector. This is a consequence of having assumed that neutrinos are massless, which allows us to perform a neutrino flavor redefinition to compensate the rotation in the charged lepton sector. However, if neutrino masses are included, this redefinition is no longer possible and an analogous unitary matrix appears in the lepton sector. This is the so-called PMNS matrix. As with the CKM matrix, the value of the PMNS matrix elements have to be determined experimentally. However contrary to the CKM, this matrix shows a rather anarchic structure, with most of its entries being of similar size.

1.3 Accidental symmetries of the SM

An interesting property of the SM is that it presents several accidental symmetries. These are symmetries that are not imposed in the construction of the theory but appear accidentally from the restrictions enforced by the gauge symmetry, the particle content, and the imposition of renormalizability; though nothing forbids

non-renormalizable symmetry-breaking terms. These symmetries are very interesting because they have important phenomenological implications, and because they might be hinting at hidden dynamics where they are not an accident but rather a fundamental symmetry of a larger theory. The SM Lagrangian has the following accidental global symmetries at the classical level

$$\mathrm{U}(1)_{\mathrm{B}} \times \mathrm{U}(1)_{e} \times \mathrm{U}(1)_{\mu} \times \mathrm{U}(1)_{\tau}\,, \tag{1.28}$$

corresponding to the total baryon number, B, and each of the lepton-family numbers, L_e, L_μ and L_τ, which contain the total lepton number, L, as a diagonal subgroup. The presence of these accidental symmetries forbids processes such as $\mu \to e\gamma$ and is the reason behind the stability of the proton. These symmetries are anomalous and get explicitly broken by non-perturbative quantum effects. Though this symmetry breaking effects are negligible at low temperatures, they may play an important role in the explanation of the matter-antimatter asymmetry (see discussion below), or when one aims for the construction of an extended gauge sector. Of the four Abelian symmetries only the subgroup corresponding to one of the combinations of lepton-family numbers $\mathrm{U}(1)_{\alpha-\beta}$ ($\alpha, \beta = e, \mu, \tau$, with $\alpha \neq \beta$) remains anomaly free in the SM [23–25]. Interestingly, if one includes three right-handed neutrinos, singlet under the SM gauge group, to account for neutrino masses, the global accidental anomaly-free symmetry of the theory is extended to [26]

$$\mathrm{U}(1)_{\mathrm{B-L}} \times \mathrm{U}(1)_{\mathrm{e}-\mu} \times \mathrm{U}(1)_{\mu-\tau}\,. \tag{1.29}$$

These accidental symmetries will get either partially or totally broken once we include the information from the neutrino sector. For instance, we know from the measured values of the PMNS matrix that the $\mathrm{U}(1)_{\mathrm{e}-\mu} \times \mathrm{U}(1)_{\mu-\tau}$ is broken. On the other hand, the $\mathrm{U}(1)_{\mathrm{B-L}}$ could be preserved if neutrinos have Dirac masses.

Apart from these symmetries of the SM Lagrangian, there are other interesting accidental symmetries that are not realized in the full Lagrangian but only in some parts of it. One of those symmetries is the *custodial symmetry*. The Higgs Lagrangian, $V(\phi)$, is invariant not only under the gauge $\mathrm{SU}(2)_{\mathrm{L}} \times \mathrm{U}(1)_{\mathrm{Y}}$ but also under a global $\mathrm{SO}(4) \equiv \mathrm{SU}(2)_{\mathrm{L}} \times \mathrm{SU}(2)_{\mathrm{R}}$ transformation. This can be easily seen by writing the Higgs doublet in terms of a four-dimensional vector of real scalar fields, $\vec{\phi} = (\phi_1, \phi_2, \phi_3, \phi_4)$, and noting that one has for the terms in the potential

$$\left(\phi^\dagger \phi\right) = \vec{\phi} \cdot \vec{\phi}\,, \tag{1.30}$$

which is invariant under four-dimensional rotations. After SSB, the symmetry $\mathrm{SU}(2)_{\mathrm{L}} \times \mathrm{SU}(2)_{\mathrm{R}}$ gets spontaneously broken down to the diagonal subgroup $\mathrm{SU}(2)_{\mathrm{V}}$. This symmetry is the reason for the tree-level relation among the gauge bosons masses given in Eq. (1.16). However, as anticipated, the custodial symmetry is not a true accidental symmetry of the full Lagrangian and gets explicitly broken by the gauging of the $\mathrm{U}(1)_{\mathrm{Y}}$ symmetry and the deviations from the relation $y_u = y_d$. As a result, one obtains small departures from $\rho = 1$ at higher orders in perturbation theory. Since these are small sources of symmetry breaking, the custodial symmetry remains as a good approximate symmetry and extensions of the SM that do not include this approximate symmetry typically receive very strong bounds from the experimental measurements of the ρ parameter.

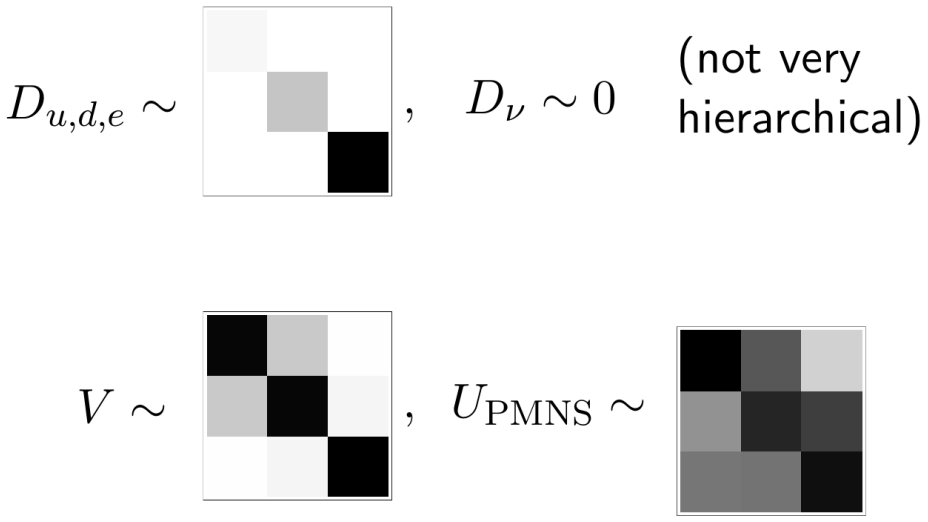

Figure 1.2: *Illustration of the observed patterns of SM fermion masses and mixings. Lighter color in the matrix elements indicates entries that are more suppressed as compared with the darker ones.*

Another important approximate symmetry of the SM is the *flavor symmetry*. In the absence of Yukawa couplings, the SM has a large accidental global symmetry [27–29]

$$\begin{aligned}\mathcal{G}_F \equiv\, & \mathrm{SU}(3)_q \times \mathrm{SU}(3)_d \times \mathrm{SU}(3)_u \times \mathrm{SU}(3)_\ell \times \mathrm{SU}(3)_e \\ & \times \mathrm{U}(1)_\mathrm{Y} \times \mathrm{U}(1)_\mathrm{B} \times \mathrm{U}(1)_e \times \mathrm{U}(1)_\mu \times \mathrm{U}(1)_\tau \times \mathrm{U}(1)_u \times \mathrm{U}(1)_d\,,\end{aligned} \tag{1.31}$$

The flavor symmetry may be of great importance in the understanding of the precise structure of the Yukawa couplings, which in the SM are just free parameters, and might provide some insight about a possible underlying flavor dynamics. This possibility has been analyzed in many works, see for instance the ones in Refs. [27–33].

1.4 What lies beyond the SM

The SM provides our best understanding of the physics at the high-energy scale and reproduces current data with an amazing agreement. However, there are several hints for an extended framework both from the theoretical and the experimental side. From the theory point of view, the SM present several unsatisfactory issues:

- **The strong CP problem:** As we will see in Chapter 3, the inclusion of non-perturbative effects in the gauge sector of the SM gives rise to the appearance of a new term in the Lagrangian that violates CP. However, there is no experimental evidence for such source of CP violation. Since the SM lacks a mechanism to forbid this term, one should introduce a large tunning of parameters to account for experimental observation.

- **The flavor puzzle:** There is no explanation in the SM why there are three families. Moreover, as can be seen in Figure 1.2, the SM fermion masses and mixings follow a rather particular structure, characterized by having very hierarchical CKM matrix elements and quark and charged-lepton masses. This is in contrast with the rather anarchic pattern of the neutrino masses and PMNS matrix elements. The lack of an explanation, within the SM, for these features of the flavor sector constitutes the so-called SM flavor puzzle.

- **The hierarchy problem:** Contrary to fermions and gauge bosons, the mass of the Higgs boson, being a scalar particle, is very sensitive to possible NP extensions of the SM. In the presence of such NP, the Higgs mass would receive radiative corrections proportional to the new energy scale, and one would have to introduce a tunning in order to keep its value at the EW scale.

- **Grand Unification:** In quantum field theory, the couplings vary with the energy at which they are measured. An interesting feature of the SM is that if we evolve the gauge couplings of each of its three gauge groups, one can see that they become approximately equal at a very high energy. This might be indicating that, just as it happens with the weak and the electromagnetic forces, the SM forces unify, therefore hinting at an underlying NP sector around the unification scale. Beyond SM theories based on this idea of force unification receive the name of Grand Unified Theories.

- **Gravity:** The SM does not include any effect concerning gravity. Therefore the SM *must* be extended in order to provide for a description of quantum gravity. These effects can be added to the SM by using effective field theory techniques as long as one is restricted to energies below the Planck mass. However, beyond that scale one should rely on a full theory of quantum gravity.

On the other hand, in spite of the enormous phenomenological success of the SM, there are experimental observations that cannot be accounted for in this theory and hint at the presence of physics beyond the SM:

- **Neutrino masses and mixings:** Neutrinos are massless particles in the SM. However, neutrino oscillation experiments have shown that neutrinos do have masses. Though the SM can be easily extended to account for neutrino masses, there are different mechanisms available to accommodate them. Moreover, related to this question, it is unclear whether neutrinos are Majorana or Dirac particles. What is the extension of the SM chosen by nature to explain neutrino masses remains as one of the open questions in Particle Physics.

- **The flavor anomalies:** The LHCb, Belle and Babar experimental collaborations have reported a set of tantalizing anomalies involving several observables in the decays of the B meson (see Chapter 5 for a detailed discussion). Though these measurements are still not significant enough to claim the discovery of NP, they seem to show a rather coherent pattern of deviations. Taken at face value, these experimental anomalies imply a large violation of lepton-flavor universality that cannot be accounted for in the SM.

- **Matter-antimatter asymmetry:** The SM predicts that matter and antimatter should be created in the early universe in almost the same amount. However, the observed universe is mostly made of matter. To explain this asymmetry the SM needs to be extended.

- **Dark Matter and dark energy:** According to cosmological observations, the SM only accounts for 5% of the energy in the universe. Of the remaining energy, 26% should correspond to new colorless matter that does not interact electromagnetically, the so-called DM. The rest (69%) should consist on dark energy, whose nature is still under debate.

In this thesis we will try to tackle some of these problems. In particular in Chapter 2 we will discuss possible extensions of the scalar sector of the SM, which may be of interest for the explanation of the matter-antimatter asymmetry or for DM. The aim of Chapter 3 is to introduce the Strong CP problem and present a mechanism able to solve it while later, in Chapter 8, we will present explicit models that extend the minimal framework to include additional features. In the lack of a clear indication of the particular underlying theory that might extend the SM, it is very useful to make use of effective descriptions that parametrize this possible new dynamics in a model-independent way. We introduce these techniques in Chapter 4, and in Chapter 6 we extend those techniques to the one-loop order. Finally, in Chapter 5 we present the flavor anomalies in more detail, while Chapter 7 is dedicated to the study of possible explanations of the anomalies from an extended gauge sector.

Bibliography

[1] S. L. Glashow, Nucl. Phys. **22** (1961) 579.

[2] S. Weinberg, Phys. Rev. Lett. **19** (1967) 1264.

[3] A. Salam, Conf. Proc. C **680519** (1968) 367.

[4] S. L. Glashow, J. Iliopoulos and L. Maiani, Phys. Rev. D **2** (1970) 1285.

[5] A. Pich, *18th European School (ESHEP 2010): Raseborg, Finland, June 20-July 3, 2010*, [arXiv:1201.0537 [hep-ph]].

[6] D. J. Gross and F. Wilczek, Phys. Rev. Lett. **30** (1973) 1343.

[7] H. D. Politzer, Phys. Rev. Lett. **30** (1973) 1346.

[8] S. R. Coleman and D. J. Gross, Phys. Rev. Lett. **31** (1973) 851.

[9] L. D. Faddeev and V. N. Popov, Phys. Lett. **25B** (1967) 29.

[10] G. 't Hooft, Nucl. Phys. B **33** (1971) 173.

[11] F. Englert and R. Brout, Phys. Rev. Lett. **13** (1964) 321.

[12] P. W. Higgs, Phys. Rev. Lett. **13** (1964) 508.

[13] J. Goldstone, Nuovo Cim. **19** (1961) 154.

[14] G. Aad *et al.* [ATLAS Collaboration], Phys. Lett. B **716** (2012) 1 [arXiv:1207.7214 [hep-ex]].

[15] S. Chatrchyan *et al.* [CMS Collaboration], Phys. Lett. B **716** (2012) 30 [arXiv:1207.7235 [hep-ex]].

[16] G. Aad *et al.* [ATLAS and CMS Collaborations], JHEP **1608** (2016) 045 [arXiv:1606.02266 [hep-ex]].

[17] G. Aad *et al.* [ATLAS and CMS Collaborations], Phys. Rev. Lett. **114** (2015) 191803 [arXiv:1503.07589 [hep-ex]].

[18] L. Wolfenstein, Phys. Rev. Lett. **51** (1983) 1945.

[19] J. Charles *et al.* [CKMfitter Group], Eur. Phys. J. C **41** (2005) no.1, 1 [hep-ph/0406184].

[20] A. Hocker, H. Lacker, S. Laplace and F. Le Diberder, Eur. Phys. J. C **21** (2001) 225 [hep-ph/0104062].

[21] M. Bona *et al.* [UTfit Collaboration], JHEP **0507** (2005) 028 [hep-ph/0501199].

[22] M. Bona *et al.* [UTfit Collaboration], JHEP **0803** (2008) 049 [arXiv:0707.0636 [hep-ph]].

[23] R. Foot, Mod. Phys. Lett. A **6** (1991) 527.

[24] X. G. He, G. C. Joshi, H. Lew and R. R. Volkas, Phys. Rev. D **44** (1991) 2118.

[25] R. Foot, X. G. He, H. Lew and R. R. Volkas, Phys. Rev. D **50** (1994) 4571 [hep-ph/9401250].

[26] T. Araki, J. Heeck and J. Kubo, JHEP **1207** (2012) 083 [arXiv:1203.4951 [hep-ph]].

[27] G. D'Ambrosio, G. F. Giudice, G. Isidori and A. Strumia, Nucl. Phys. B **645** (2002) 155 [hep-ph/0207036].

[28] V. Cirigliano, B. Grinstein, G. Isidori and M. B. Wise, Nucl. Phys. B **728** (2005) 121 [hep-ph/0507001].

[29] T. Feldmann, M. Jung and T. Mannel, Phys. Rev. D **80** (2009) 033003 [arXiv:0906.1523 [hep-ph]].

[30] B. Grinstein, M. Redi and G. Villadoro, JHEP **1011** (2010) 067 [arXiv:1009.2049 [hep-ph]].

[31] M. E. Albrecht, T. Feldmann and T. Mannel, JHEP **1010** (2010) 089 [arXiv:1002.4798 [hep-ph]].

[32] R. Alonso, M. B. Gavela, G. Isidori and L. Maiani, JHEP **1311** (2013) 187 [arXiv:1306.5927 [hep-ph]].

[33] R. Alonso, E. Fernandez Martinez, M. B. Gavela, B. Grinstein, L. Merlo and P. Quilez, JHEP **1612** (2016) 119 [arXiv:1609.05902 [hep-ph]].

CHAPTER

2 The Two-Higgs-doublet model

> "Would you tell me, please, which way I ought to go from here?" "That depends a good deal on where you want to get to," said the Cat. "I don't much care where -" said Alice. "Then it doesn't matter which way you go," said the Cat. "- so long as I get SOMEWHERE," Alice added as an explanation. "Oh, you're sure to do that," said the Cat, "if you only walk long enough."
>
> — *Lewis Carroll*, Alice in Wonderland

The recent discovery by the ATLAS [1] and CMS [2] collaborations of a Higgs particle with a mass around 125 GeV represents one of the greatest achievements of Physics in the last decades and constitutes an indisputable success of the SM. So far, all the measurements of this particle properties are consistent with it being the Higgs boson of the SM.[1] However, as we saw in the previous chapter, the scalar sector remains as one of the least understood parts of the SM. It may thus be possible that NP manifests in this sector. Indeed, there are several theoretical reasons to extend the scalar content of the SM: for instance Supersymmetric models [3], several DM models [4,5], theories of spontaneous CP-violation [6–8], models of electroweak baryogenesis to explain the baryon asymmetry of the Universe [9–11], as well as most solutions to the Strong CP problem [12,13]; they all require an enlarged scalar sector.

Extensions of the scalar content of the SM generically receive a very strong constraint from the measurements of the ρ parameter, defined in Eq. (1.16), whose experimental value is very close to the SM prediction to a good accuracy [14]. Among the possible extensions, the ones with extra Higgs doublets and/or singlets are particularly interesting because they do not modify the ρ parameter at tree level [15], therefore allowing these extra fields to appear at much lower energies yielding a more appealing phenomenology. Other extensions with large $\mathrm{SU(2)_L}$ multiplets, scalars with small or null vev, and models with a custodial SU(2) global symmetry, could also evade this bound but they tend to be rather complex [16]. Contrary to the

[1] The latest results on measurements of the Higgs properties can by found at:

`https://twiki.cern.ch/twiki/bin/view/AtlasPublic/HiggsPublicResults` (ATLAS)

`https://twiki.cern.ch/twiki/bin/view/CMSPublic/PhysicsResultsHIG` (CMS)

scalar singlets, models with extra Higgs doublets have the additional feature that they may have Yukawa couplings to fermions, introducing some interesting effects that are absent in the singlet case and that, perhaps, could help us elucidate something about the flavor structure of the SM. The 2HDM provides one of the most economical of such extensions, offering a simple, yet comprehensive and rich, framework [17–19]. This class of models was proposed by T. D. Lee in 1973 [6] in order to achieve spontaneous CP violation. However it was not until the 1990s that its exploration intensified. Nowadays they are widely studied both from the theoretical and the experimental side given that they can lead to a very rich phenomenology that is being and will be probed at LHC; see for instance Refs. [20–22].

2.1 The 2HDM Lagrangian

The scalar sector of the 2HDM contains two complex $\mathrm{SU}(2)_\mathrm{L}$ doublets of hypercharge $Y = 1/2$ that we generically parameterize as

$$\phi_j = \begin{pmatrix} \varphi_j^+ \\ \varphi_j^0 \end{pmatrix}, \quad j = 1, 2\,. \tag{2.1}$$

The corresponding charge-conjugated fields $\widetilde{\phi}_j = i\tau^2\phi_j$, with τ^2 the Pauli matrix, are also $\mathrm{SU}(2)_\mathrm{L}$ doublets but with hypercharge $Y = -1/2$. The 2HDM Lagrangian takes the following generic form

$$\mathcal{L}_{\mathrm{2HDM}} = \mathcal{L}_{\mathrm{g+f}}^{\mathrm{SM}} + \mathcal{L}_H + \mathcal{L}_Y\,. \tag{2.2}$$

Here $\mathcal{L}_{\mathrm{g+f}}^{\mathrm{SM}}$ denotes the SM Lagrangian for gauge bosons and fermions that was introduced in Chapter 1, see Eq. (1.6), $\mathcal{L}_H = \mathcal{L}_{\mathrm{Kin}} - V$ contains the scalar kinetic terms and potential, and $\mathcal{L}_Y$ describes the Yukawa interactions among fermions and scalars. The most general kinetic term one can build is given by

$$\mathcal{L}_{\mathrm{Kin}} = (D_\mu\phi_1)^\dagger\, D^\mu\phi_1 + (D_\mu\phi_2)^\dagger\, D^\mu\phi_2 + \left[\kappa\,(D_\mu\phi_1)^\dagger\, D^\mu\phi_2 + h.c.\right], \tag{2.3}$$

with the covariant derivative being the same as in Eq. (1.9). Without loss of generality, we can take $\kappa = 0$ since a Langrangian with $\kappa \neq 0$ can be reduced to the former type by means of a non-unitary transformation of the fields [23]. Once the kinetic term is reduced to its canonical form one is still able to perform a global $\mathrm{U}(2)$ transformation of the scalar fields. This transformation, commonly denoted as weak-basis transformation, allows us to rotate along different weak bases. Though the physical observables should be independent of the choice of basis, as we will see later there are certain bases which result more useful in particular cases.

The different implementations of 2HDMs are determined by the choice of the Higgs potential and Yukawa couplings. The most general renormalizable scalar

potential for a 2HDM contains 14 parameters

$$\begin{aligned} V(\phi_1,\phi_2) = & m_1^2\left(\phi_1^\dagger\phi_1\right) + m_2^2\left(\phi_2^\dagger\phi_2\right) + \left[m_{12}^2\left(\phi_1^\dagger\phi_2\right) + h.c.\right] + \frac{\lambda_1}{2}\left(\phi_1^\dagger\phi_1\right)^2 \\ & + \frac{\lambda_2}{2}\left(\phi_2^\dagger\phi_2\right)^2 + \lambda_3\left(\phi_1^\dagger\phi_1\right)\left(\phi_2^\dagger\phi_2\right) + \lambda_4\left(\phi_1^\dagger\phi_2\right)\left(\phi_2^\dagger\phi_1\right) \\ & + \left\{\frac{\lambda_5}{2}\left(\phi_1^\dagger\phi_2\right)^2 + \lambda_6\left(\phi_1^\dagger\phi_1\right)\left(\phi_1^\dagger\phi_2\right) + \lambda_7\left(\phi_2^\dagger\phi_2\right)\left(\phi_1^\dagger\phi_2\right) + h.c.\right\}, \end{aligned} \tag{2.4}$$

where the hermiticity of the potential requires all parameters to be real except for m_{12}, λ_5, λ_6 and λ_7. The presence of new complex parameters leads to the appearance of possible sources of CP violation other than the phase of the CKM matrix. The potential parameters in Eq. (2.4) depend on the choice of weak basis. However, the physical quantities are independent of such choice. For this reason, it is in many cases convenient to find invariants constructed as combinations of parameters that are independent of the weak-basis transformations [23, 24]. These invariants are particularly useful in the determination of CP violating sources. One can show that the freedom in the choice of weak basis allows one to remove three of the 14 parameters.[2] Still, the large number of free parameters in the scalar potential considerably complicates its analytical treatment. Several symmetries are typically imposed in the scalar sector that reduces the number of free parameters in the scalar potential. For instance the following discrete symmetry

$$\mathbb{Z}_2: \qquad \phi_1 \to \phi_1\,, \qquad \phi_2 \to -\phi_2\,, \tag{2.5}$$

forbids the terms λ_6, λ_7 and m_{12}. This condition is too strict since it excludes the possibility of having CP violation other than from the CKM mixing matrix. One can relax this constraint by assuming that the symmetry is softly broken by the presence of m_{12}, which can be either real or complex.[3] In this case it is possible to have explicit and spontaneous CP violation. A more restrictive scenario is obtained when one imposes a U(1) symmetry in the scalar sector, this is done for example in the Peccei-Quinn model that we will present in Section 3.2. The U(1) symmetry additionally forbids the term λ_5 in the potential. In this case, one typically expects the appearance of a Goldstone boson after spontaneous symmetry breaking. However, one can give a mass to this boson by introducing the U(1)-soft-breaking term m_{12} in the scalar potential. In Refs. [25, 26] it was shown that there are six types of family and CP symmetries that can be imposed without producing accidental symmetries.

Electroweak symmetry breaking takes place if the global minimum of the potential appears at non-zero vev for the Higgs fields. The conditions for the extrema of

[2]The counting goes as follows: as already mentioned the basis reparametrization consist on a U(2) transformation of the scalar fields. This can be decomposed as $\mathrm{U}(2) = \mathrm{SU}(2) \times \mathrm{U}(1)$, where the U(1) corresponds to a global hypercharge transformation that has no effect on the potential parameters. As a result one has the freedom to remove three parameters from the three degrees of freedom contained in a SU(2) rotation.

[3]A symmetry is defined as softly-broken when all the terms that explicitly break the symmetry are of dimension lower than four. This way the symmetry is approximately restored at scales much larger than those of the symmetry breaking terms.

the potential are

$$\left.\frac{\partial V}{\partial \phi_1}\right|_{\phi_{1,2}=\langle\phi_{1,2}\rangle} = 0\,, \qquad \left.\frac{\partial V}{\partial \phi_2}\right|_{\phi_{1,2}=\langle\phi_{1,2}\rangle} = 0\,. \tag{2.6}$$

The potential in Eq. (2.4) can have CP-conserving, CP-violating and charge-violating minima. We will assume that the potential parameters are such that the scalar doublets acquire a vev along the charge conserving direction.[4] In general both doublets can acquire a vev, i.e.

$$\langle 0|\phi_j|0\rangle = \frac{1}{\sqrt{2}}\begin{pmatrix} 0 \\ v_j\, e^{i\theta_j}\end{pmatrix}, \quad j=1,2\,. \tag{2.7}$$

Here $v_1 > 0$ and $v_2 > 0$, $v \equiv \sqrt{v_1^2+v_2^2} = \left(\sqrt{2}G_F\right)^{-1/2}$, generate the quark and gauge boson masses. Therefore, after spontaneous symmetry breaking the Higgs doublets can be parameterized as

$$\phi_j = e^{i\theta_j}\begin{pmatrix} \varphi_j^+ \\ \frac{1}{\sqrt{2}}\left(v_j+\rho_j+i\eta_j\right)\end{pmatrix}, \quad j=1,2\,, \tag{2.8}$$

with ρ_j and η_j being real scalar fields, and φ_j^+ a complex scalar field. By an appropriate rephasing of the scalar fields we can set $\theta_1 = 0$ and $\theta_2 \equiv \theta$ without loss of generality. The 2HDM model contains eight real scalar degrees of freedom. After spontaneous symmetry breaking these are the three would-be Goldstone bosons that become the longitudinal components of the W and the Z, $G^\pm$ and G^0, a charged Higgs, $H^\pm$, and three neutral scalars, which in the CP-conserving limit correspond to two CP-even and one CP-odd fields. This can be more easily seen in the so-called Higgs basis, where the Goldstone bosons associated with the longitudinal components of the W and the Z, are singled out and only one Higgs doublet acquires a non-vanishing vev

$$\Phi_1 = \begin{pmatrix} G^+ \\ \frac{1}{\sqrt{2}}\left(v+H^0+iG^0\right)\end{pmatrix}, \qquad \Phi_2 = \begin{pmatrix} H^+ \\ \frac{1}{\sqrt{2}}\left(R+iI\right)\end{pmatrix}. \tag{2.9}$$

To relate the Higgs basis with the one in Eq. (2.8), we perform the following weak-basis transformation

$$\begin{pmatrix}\Phi_1 \\ \Phi_2\end{pmatrix} = \begin{pmatrix}\cos\beta & \sin\beta \\ -\sin\beta & \cos\beta\end{pmatrix}\begin{pmatrix}\phi_1 \\ e^{-i\theta}\phi_2\end{pmatrix}, \tag{2.10}$$

where we have defined $\tan\beta \equiv v_2/v_1$. Note however that in many cases all weak bases are physically equivalent and therefore the angle β is unphysical. The situation is different when one of the weak bases is special because of the presence of a symmetry.

Finally, as a result of having an additional Higgs doublet the Yukawa Lagrangian is extended to the following form

$$-\mathcal{L}_{\rm Y} = \overline{Q_L^0}\left[\Delta_1\,\widetilde{\phi}_1 + \Delta_2\,\widetilde{\phi}_2\right]u_R^0 + \overline{Q_L^0}\,\left[\Gamma_1\,\phi_1+\Gamma_2\,\phi_2\right]d_R^0 + \overline{\ell_L^0}\,\left[\Sigma_1\,\phi_1+\Sigma_2\,\phi_2\right]e_R^0 + \text{h.c.}\,, \tag{2.11}$$

[4] It can be shown that if there is a local minimum that is neutral, any possible charge-breaking extrema of the potential would correspond to a saddle point [27, 28].

where $\tilde{\Phi}_j = i\tau^2\Phi_j^*$. Expanding the Yukawa Lagrangian in the Higgs basis one obtains

$$\begin{aligned}-\mathcal{L}_{\rm Y} \supset\ & \frac{1}{v}\Big\{\overline{u_L^0}\left[vM_u + M_u H^0 + N_u^0 R - iN_u^0 I\right] u_R^0 \\ & + \overline{d_L^0}\left[vM_d + M_d H^0 + N_d^0 R + iN_d^0 I\right] d_R^0 \\ & + \overline{e_L^0}\left[vM_e + M_e H^0 + N_e^0 R + iN_e^0 I\right] e_R^0 \\ & + \sqrt{2}H^+\left(\overline{u_L^0}\, N_d^0\, d_R^0 - \overline{u_R^0}\, N_u^{0\dagger}\, d_L^0 + \overline{\nu_L^0}\, N_e^0\, e_R^0\right) + \text{h.c.}\Big\}\,.\end{aligned} \tag{2.12}$$

The matrices M_f and N_f^0 ($f = u, d, e$) encode the flavor structure of the 2HDM, these are given by

$$\begin{gathered}M_u = \frac{1}{\sqrt{2}}\left(v_1\Delta_1 + v_2 e^{-i\theta}\Delta_2\right)\,, \quad M_d = \frac{1}{\sqrt{2}}\left(v_1\Gamma_1 + v_2 e^{i\theta}\Gamma_2\right)\,, \\ M_e = \frac{1}{\sqrt{2}}\left(v_1\Sigma_1 + v_2 e^{i\theta}\Sigma_2\right)\,,\end{gathered} \tag{2.13}$$

and

$$\begin{aligned}N_u^0 &= \frac{1}{\sqrt{2}}\left(v_2\Delta_1 - v_1 e^{-i\theta}\Delta_2\right) = \frac{v_2}{v_1}M_u - \frac{v_2}{\sqrt{2}}\left(\frac{v_2}{v_1} + \frac{v_1}{v_2}\right)e^{-i\theta}\Delta_2\,, \\ N_d^0 &= \frac{1}{\sqrt{2}}\left(v_2\Gamma_1 - v_1 e^{i\theta}\Gamma_2\right) = \frac{v_2}{v_1}M_d - \frac{v_2}{\sqrt{2}}\left(\frac{v_2}{v_1} + \frac{v_1}{v_2}\right)e^{i\theta}\Gamma_2\,, \\ N_e^0 &= \frac{1}{\sqrt{2}}\left(v_2\Sigma_1 - v_1 e^{i\theta}\Sigma_2\right) = \frac{v_2}{v_1}M_e - \frac{v_2}{\sqrt{2}}\left(\frac{v_2}{v_1} + \frac{v_1}{v_2}\right)e^{i\theta}\Sigma_2\,.\end{aligned} \tag{2.14}$$

The mass matrices M_f determine the Yukawa couplings of the scalar field H^0 while the matrices N_f^0 determine the Yukawa couplings of the scalar R, the pseudoscalar I, and the charged scalar H^+. The mass matrices can be diagonalized through the bi-unitary transformations in Eq. (1.21). As it happens in the SM with the Higgs, these transformations guarantee diagonal quark couplings for H^0 but, in general,

$$\begin{gathered}N_u = U_{uL}^\dagger N_u^0 U_{uR} \neq \text{diag}\,, \quad N_d = U_{dL}^\dagger N_d^0 U_{dR} \neq \text{diag}\,, \\ N_e = U_{eL}^\dagger N_e^0 U_{eR} \neq \text{diag}\,,\end{gathered} \tag{2.15}$$

so that R and I have flavor violating couplings at tree-level. As we will see in the next section, this interesting feature has important phenomenological implications for this class of models. Note that the fields $\{H^0, R, I\}$ are not mass eigenstates in general, the physical neutral scalar bosons will correspond to a linear combination of these fields. The physical states can be obtained by performing an orthogonal transformation that diagonalizes the mass matrix of the neutral scalars, which is fixed by the scalar potential. If the potential is CP-conserving, then only H_0 and R mix, and I is a physical eigenstate. In this case the physical fields, $\{h, H\}$, in terms of $\{H^0, R\}$ read

$$\begin{pmatrix} h \\ H \end{pmatrix} = \begin{pmatrix} \cos(\alpha-\beta) & \sin(\alpha-\beta) \\ -\sin(\alpha-\beta) & \cos(\alpha-\beta) \end{pmatrix}\begin{pmatrix} H^0 \\ R \end{pmatrix}\,, \tag{2.16}$$

where, by convention, h is identified with the lightest field and the value of α depends on the potential parameters. In the basis of Eq. (2.8) this relation reads

$$\begin{pmatrix} h \\ H \end{pmatrix} = \begin{pmatrix} \cos\alpha & \sin\alpha \\ -\sin\alpha & \cos\alpha \end{pmatrix} \begin{pmatrix} \rho_1 \\ \rho_2 \end{pmatrix} . \tag{2.17}$$

The 2HDM receives interesting bounds from both theoretical considerations and experimental limits. For instance certain theoretical restrictions have to be imposed to the scalar potential to guarantee vacuum stability [27, 29–31] as well as perturbativity and perturbative unitarity [32, 33]. Moreover, this class of models should satisfy the constraints from precision measurements of the oblique parameters [34–36] and from direct searches at colliders [21]. One of the most severe constraints that the 2HDM has to face comes from the Yukawa sector of the theory and has to do with the presence of tree-level sources of dangerous FCNC. For instance, assuming couplings of the same size as the b-quark Yukawa, one can set a bound on the mass of the neutral scalars from their contribution to $K - \overline{K}$ mixing which is of the order of 10 TeV [37, 38]. This leads to the so-called 2HDM flavor problem that we discuss in the next section.

2.2 Solutions to the 2HDM flavor problem

As we saw in the previous section, the introduction of more than one scalar doublet in the SM gives rise to unwanted FCNC interactions, which have to be suppressed in order to avoid conflict with experimental data. A possible way out is to assume that an underlying symmetry is forbidding the dangerous FCNCs, leaving open the possibility of additional scalar fields at the electroweak scale. The most common solution to this problem is the NFC condition. This scenario is nothing more than the requirement of simultaneous diagonalization of M_f and N_f^0, or equivalently, the simultaneous diagonalization of the Yukawa matrices in each sector. In the two Higgs doublet model the NFC condition can be implemented in two ways:

- Through a discrete or continuous symmetry which restricts the number of Yukawas in each sector to one [39, 40].
- Using the Yukawa alignment condition, where the Yukawa matrices in the same sector have the same flavor structure up to an overall factor [41]. This can be seen as an effective theory of a larger model with the first condition imposed at the UV level [42]. It can also be seen as a first order expansion in a minimal flavor violating scenario [43–45].

There exists, however, a different scenario where NFC is only imposed in one sector and FCNCs present in the other sector are under control, this is known as the Branco–Grimus–Lavoura model [46]. Finally, it could also happen that there is no symmetry protecting the FCNCs but the model is in a decoupling regime where either the extra scalar fields are heavy or their couplings to the SM particles appear sufficiently suppressed, making them harmless.

Model	u_R	d_R	e_R
Type I	$-$	$-$	$-$
Type II	$-$	$+$	$+$
Lepton-specific	$-$	$-$	$+$
Flipped	$-$	$+$	$-$

Table 2.1: *Different implementations of the $\mathbb{Z}_2$ charge to right-handed fermions in the NFC hypothesis.*

2.2.1 Natural flavor conservation and Yukawa alignment

As mentioned earlier, one solution to the 2HDM flavor problem consist on forbidding the presence of tree-level FCNCs. Glashow and Weinberg [39], and independently Paschos [40], showed that a necessary and sufficient condition for the absence of FCNCs is that all fermions with the same charges couple exclusively to one Higgs doublet. Then from Eqs. (2.13) and (2.14) it is clear than M_f and N_f^0 ($f = u, d, e$) are proportional and therefore they get simultaneously diagonalized by the transformation of Eq. (1.21). This requirement can be achieved by the imposition of a global $\mathbb{Z}_2$ discrete symmetry where the left-handed quarks and one of the scalar doublets are even and the other doublet is odd, i.e.

$$\begin{aligned} \mathbb{Z}_2: \qquad & \phi_1 \to \phi_1\,, \qquad \phi_2 \to -\phi_2\,, \\ & Q_L \to Q_L\,, \qquad \ell_L \to \ell_L\,, \end{aligned} \tag{2.18}$$

while the symmetry transformation for the right-handed quarks can be implemented in different ways, see Table 2.1, yielding four different implementations of the NFC condition:

- **Type I:** In this implementation, initially introduced in Ref. [47], all the fermions couple to ϕ_2 only. An interesting limit of this scenario, denoted as fermiophobic limit, is obtained when $\alpha = \pi/2$ (see Eq. (2.17)) where the lightest neutral scalar does not couple to fermions at tree-level [48–50]. Another interesting scenario is the so-called Inert Doublet Model where the $\mathbb{Z}_2$ is exactly realized in the scalar potential and the vev of ϕ_1 is set to zero [5,51]. In this case, the $\mathbb{Z}_2$ symmetry remains unbroken even after SSB and the SM-like Higgs does not mix with the extra scalars. In this scenario the lightest of the extra neutral scalars can play the role of DM [4, 5].

- **Type II:** Here all down-type fermions couple to ϕ_1 and up-type fermions couple to ϕ_2. This model was initially discussed in Refs. [47, 52], and it is by far the most studied scenario in the literature, since its structure is the same present in supersymmetric models. However, some of the constraints present in the scalar sector of the MSSM are relaxed in this implementation, offering a richer phenomenology.

- **Lepton-specific:** This model, where quarks couple only to ϕ_1 and leptons to ϕ_2, was first discussed in Refs. [53, 54]. This implementation share the same structure in the quark sector as the type I model, and therefore many of its bounds also apply to the lepton-specific scenario. This scenario has recently

Model	ς_u	ς_d	ς_e
Type I	$\cot\beta$	$\cot\beta$	$\cot\beta$
Type II	$\cot\beta$	$-\tan\beta$	$-\tan\beta$
Lepton-specific	$\cot\beta$	$\cot\beta$	$-\tan\beta$
Flipped	$\cot\beta$	$-\tan\beta$	$\cot\beta$
Inert	0	0	0

Table 2.2: *Values of the alignment parameters, $\varsigma_{u,d,e}$, that reduce the A2HDM to the different NFC scenarios.*

received some attention as a possible explanation to several lepton-related anomalies, such the $g-2$ or the cosmic positron excess [55].

- **Flipped:** In this case the up-quark and the leptons are coupled to ϕ_1 while the down-quark receives its mass from ϕ_2 [56]. This model has received little attention in the literature.

A generalization of the NFC hypothesis is provided by the so-called A2HDM [41]. In this class of models one allows the fermions to couple to both doublets but assumes that the Yukawa couplings of ϕ_1 and ϕ_2 are proportional in each sector, i.e.

$$M_u = \varsigma_u^* N_u^0 \,, \qquad M_d = \varsigma_d N_d^0 \,, \qquad M_e = \varsigma_e N_e^0 \,. \tag{2.19}$$

Here the flavor-universal quantities $\varsigma_{u,d,e}$ are free complex parameters of the model that are commonly denoted as alignment parameters. With this condition, the diagonalization of the mass matrices in Eq. (2.13) automatically diagonalizes scalar-fermion interactions in Eq. (2.14). This way the Yukawa alignment condition leads to the absence of tree-level FCNCs at the time that introduces new sources of CP violation in the Yukawa sector through the phases of $\varsigma_{u,d,e}$. Another interesting feature of the A2HDM is that it contains each of the four NFC scenarios based on $\mathbb{Z}_2$ symmetries discussed above. These are obtained from the A2HDM by choosing specific values for the alignment parameters, see Table 2.2. Therefore the A2HDM offers a general framework for the phenomenological analysis of NFC 2HDMs, such as the one performed in Ref. [20]. However, contrary to the NFC models based on $\mathbb{Z}_2$ symmetries, more general Yukawa alignment conditions are not imposed by any symmetry and therefore the proportionality of the Yukawas is only stable under RGE for the cases in Table 2.2 [57, 58]. In any other case, the proportionality of the matrices in Eq. (2.19) gets broken at one loop, situation that was studied in Refs. [57, 59–61], where it was shown that the FCNCs associated to this effect appear sufficiently suppressed to avoid the stringent experimental bounds. Several UV completions to the A2HDM have been proposed in the literature [62–65]. In Section 8.1 we will present a particular model implementation that leads to Yukawa alignment at low energies and provides a solution to the Strong CP problem.

2.2.2 The Branco-Grimus-Lavoura model

There is an special solution to the 2HDM flavor problem where tree-level FCNCs are allowed in one sector but they are exactly related to off-diagonal CKM matrix

elements, and therefore sufficiently controlled. This is the so-called BGL model [46].[5] Such unique feature is achieved by the imposition of a horizontal Abelian symmetry such as

$$\mathcal{S}: \qquad q_{L3} \to e^{i\,\theta} q_{L3}, \qquad u_{R3} \to e^{i\,2\theta} u_{R3}\,, \qquad \phi_2 \to e^{i\,\theta}\phi_2\,. \tag{2.20}$$

This can be implemented as a continuous or as a discrete symmetry; if the latter, the extra condition $\theta \neq 0, \pi$ should be satisfied so the symmetry does not become trivial or a $\mathbb{Z}_2$. However as we will comment later, even the discrete symmetry implementation leads to an accidental U(1) symmetry in the full Lagrangian. The imposition of the BGL symmetry gives rise to a special class of Yukawa textures

$$\begin{aligned} \Gamma_1^{\rm BGL} &= \begin{pmatrix} \times & \times & \times \\ \times & \times & \times \\ 0 & 0 & 0 \end{pmatrix}, \quad \Gamma_2^{\rm BGL} = \begin{pmatrix} 0 & 0 & 0 \\ 0 & 0 & 0 \\ \times & \times & \times \end{pmatrix}, \\ \Delta_1^{\rm BGL} &= \begin{pmatrix} \times & \times & 0 \\ \times & \times & 0 \\ 0 & 0 & 0 \end{pmatrix}, \quad \Delta_2^{\rm BGL} = \begin{pmatrix} 0 & 0 & 0 \\ 0 & 0 & 0 \\ 0 & 0 & \times \end{pmatrix}. \end{aligned} \tag{2.21}$$

The above implementation is usually known as the top-BGL, since it singles out the top quark. This Yukawa structure has the special property that the flavor matrices responsible for the FCNCs take the form

$$\begin{aligned} \left(N_d^{\rm BGL}\right)_{ij} &= \frac{v_2}{v_1}\left(D_d\right)_{ij} - \left(\frac{v_2}{v_1} + \frac{v_1}{v_2}\right)(V^\dagger)_{i3}(V)_{3j}(D_d)_{jj}\,, \\ N_u^{\rm BGL} &= \frac{v_2}{v_1}{\rm diag}(m_u, m_c, 0) - \frac{v_1}{v_2}{\rm diag}(0, 0, m_t)\,, \end{aligned} \tag{2.22}$$

with $V = U_{uL}^\dagger U_{dL}$ the CKM quark mixing matrix. As we can see, this simple implementation introduces no FCNC effects in the up-quark sector while, in the down-quark sector, one has tree-level FCNCs, parameterized by $N_d^{\rm BGL}$, which are suppressed by:

- The down-type quark masses.
- The off-diagonal CKM matrix elements.

This symmetry suppression of the FCNCs allows this class of models to avoid the strong experimental constraints even when the new scalars remain light. Indeed, a full phenomenological analysis of the model was performed in Refs. [67–70] where it was shown that scalars with masses of $\mathcal{O}\,(100$ GeV) remain viable for the top-BGL implementation. Other implementations of the BGL symmetry, resulting on up-down or flavor permutations of the Yukawa textures in Eq. (2.21), are also possible. It was also shown in Refs. [71, 72] that this implementation is unique, up to the aforementioned permutations, in models with Abelian symmetries. Moreover, and contrary to what happened with the Yukawa alignment solution, since the Yukawa

[5] In this section we focus in the BGL implementation for the quark sector. Possible extensions of this solution to the lepton sector have been discussed in Ref. [66].

structure is imposed through a symmetry, this solution is stable under radiative corrections.

Although the BGL model presents several unique features, it still suffers from a few problems. The first problem is present in the scalar potential of the model. While the Abelian flavor symmetry used to get the desired textures can be implemented through a discrete group, the scalar sector will exhibit an accidental global U(1) symmetry leading to a Goldstone boson after spontaneous symmetry breaking [46]. Alternatives to eliminate the accidental global symmetry have been discussed in Ref. [46]; adding soft breaking terms to the scalar potential or extending the scalar sector with gauge singlet fields could protect the model against the phenomenologically dangerous Goldstone modes. On the other hand, the strong CP problem is not addressed in this scenario. While there are no large contributions to electric dipole moments in the BGL model [73], this is based on the assumption of a vanishing or very small $\overline{\theta}$ term [74].

In Chapter 8 we will see that these apparent problems of the BGL model can be solved in an unified way if the required Yukawa textures are imposed by a global U(1) chiral symmetry that acts as a Peccei-Quinn symmetry, offering a solution to the Strong CP problem and leading to the appearance a flavored axion. Another interesting approach which will be discussed in Chapter 7 consists on promoting the accidental U(1) symmetry to a local one, giving rise to a new flavored gauge boson and bringing some advantages we will discuss in the subsequent chapters. For these solutions it is interesting to analyze which is the most general U(1) symmetry compatible with the BGL Yukawa textures.

The $\mathbf{U(1)_{BGL}}$ symmetry

As previously stated, the BGL symmetry leads to an accidental U(1) symmetry in the scalar sector. It is interesting to determine which are the most general $\mathrm{U(1)_{BGL}}$ charge conditions that can impose the BGL Yukawa textures. This can be done by finding the Abelian generators under which the fields must transform, i.e.

$$q_L^0 \to \mathcal{S}_L\, q_L^0\,, \quad d_R^0 \to \mathcal{S}_R^d\, d_R^0\,, \quad u_R^0 \to \mathcal{S}_R^u\, u_R^0\,, \tag{2.23}$$

with

$$\begin{aligned} \mathcal{S}_L =& \mathrm{diag}(e^{iX_{uL}\,\theta}, e^{iX_{cL}\,\theta}, e^{iX_{tL}\,\theta})\,, \quad \mathcal{S}_R^d = \mathrm{diag}(e^{iX_{dR}\,\theta}, e^{iX_{sR}\,\theta}, e^{iX_{bR}\,\theta})\,, \\ \mathcal{S}_R^u =& \mathrm{diag}(e^{iX_{uR}\,\theta}, e^{iX_{cR}\,\theta}, e^{iX_{tR}\,\theta})\,, \end{aligned} \tag{2.24}$$

and

$$\Phi \to \mathcal{S}_\Phi\, \Phi\,, \tag{2.25}$$

where

$$\mathcal{S}_\Phi = \mathrm{diag}(e^{iX_{\Phi 1}\,\theta}, e^{iX_{\Phi 2}\,\theta})\,. \tag{2.26}$$

These field transformations will induce the following constraints[6]

$$\begin{aligned} \mathcal{S}_L^\dagger\, \Gamma_k\, \mathcal{S}_R^d\, (\mathcal{S}_\Phi)_{kk} &= \Gamma_k\,, \\ \mathcal{S}_L^\dagger\, \Delta_k\, \mathcal{S}_R^u\, (\mathcal{S}_\Phi^*)_{kk} &= \Delta_k\,, \end{aligned} \tag{2.27}$$

[6] In the following we drop the BGL superscript in the Yukawa matrices for notational convenience.

with $k = 1, 2$. The Yukawa texture patterns are dictated by the way the fermion fields transform, the Higgs field transformation will only select one of the allowed textures [44, 71–73]. The best way to find these fermion transformations is to study the Hermitian combinations $\Gamma_k \Gamma_k^\dagger$ and $\Gamma_k^\dagger \Gamma_k$ (and similarly for Δ_k). The symmetry constraints on these combinations give

$$\begin{aligned} \mathcal{S}_L^\dagger \left\{ \Gamma_k \Gamma_k^\dagger \, , \Delta_k \Delta_k^\dagger \right\} \mathcal{S}_L &= \left\{ \Gamma_k \Gamma_k^\dagger \, , \Delta_k \Delta_k^\dagger \right\} , \\ \mathcal{S}_R^{(d,u)\dagger} \left\{ \Gamma_k^\dagger \Gamma_k \, , \Delta_k^\dagger \Delta_k \right\} \mathcal{S}_R^{(d,u)} &= \left\{ \Gamma_k^\dagger \Gamma_k \, , \Delta_k^\dagger \Delta_k \right\} . \end{aligned} \tag{2.28}$$

The above equations are nothing more than the commutation of a diagonal matrix $\mathcal{S}_{L,R}$ with a Hermitian matrix. In order for these matrices to commute $\mathcal{S}_{L,R}$ must share the same eigenvectors as the Hermitian combination, or have degenerate eigenvalues for the non-shared eigenvectors. We then get three scenarios:

i) The matrix $\mathcal{S}_{L,R}$ has only one phase. The Hermitian combination has no restriction;

ii) The matrix $\mathcal{S}_{L,R}$ has two different phases. The Hermitian combination must be block diagonal, with the 2×2 block in the same sector as the degeneracy in $\mathcal{S}_{L,R}$;

iii) The matrix $\mathcal{S}_{L,R}$ has three different phases. The Hermitian combination must be diagonal.

For definiteness we focus in what follows on the top-BGL implementation given in Eq. (2.21), since the other implementations can be simply obtained by appropriate flavor and/or up-down permutations. From Eq. (2.21) we see that the Δ_j Yukawa textures are block diagonal in the up-charm sector. The hermitian combinations $\Delta_k \Delta_k^\dagger$ and $\Delta_k^\dagger \Delta_k$ will also share the same form. This in turn implies that the symmetry generators for the left- and right-handed fields must belong to case *ii*), i.e. the Abelian generators have only two different phases

$$\mathcal{S}_L = \text{diag}\left(1, 1, e^{i X_{tL}\, \theta}\right) , \quad \mathcal{S}_R^u = \text{diag}\left(e^{i X_{uR}\, \theta}, e^{i X_{uR}\, \theta}, e^{i X_{tR}\, \theta}\right) , \tag{2.29}$$

where we set one of the charges to zero using a global phase transformation. Notice that the charges should satisfy the conditions

$$\text{Condition A:} \quad X_{tL} \neq 0 \qquad \text{and} \qquad X_{uR} \neq X_{tR} \, , \tag{2.30}$$

in order to stay in the scenario *ii*). When the left-handed quark doublet and the right-handed up-type quark transform under this symmetry, the phases appearing in the matrix elements of the up-quark Yukawas are

$$\Theta_u \equiv \theta \begin{pmatrix} X_{uR} & X_{uR} & X_{tR} \\ X_{uR} & X_{uR} & X_{tR} \\ X_{uR} - X_{tL} & X_{uR} - X_{tL} & X_{tR} - X_{tL} \end{pmatrix} , \tag{2.31}$$

with the additional condition

$$\text{Condition B:} \quad X_{tL} \neq -(X_{uR} - X_{tR}) \, . \tag{2.32}$$

We denote the matrix Θ_u as the up-quark phase transformation matrix. The generators in Eq. (2.29), together with the conditions A and B are the complete and minimal set of required conditions in order to have available the BGL textures for the up sector. In order to pick the desired textures we now have to attribute the correct charges to the Higgs fields. Remembering that in the up-quark sector we have the $\tilde{\Phi}_i$ field coupling, we choose for the scalar fields

$$\mathcal{S}_\Phi^{\text{up}} = \text{diag}\left(e^{iX_{uR}\,\theta}, e^{i(X_{tR}-X_{tL})\,\theta}\right) . \tag{2.33}$$

This choice makes $\tilde{\Phi}_j$ associated with the Δ_j of Eq. (2.21). We can now build the phase transformation matrix for the down-quark sector. The left-handed transformation is the same, since it is shared by the two sectors. Concerning the right-handed generator of Γ_j (see Eq. (2.21)), it belongs to the case i) and, therefore, has the form

$$\mathcal{S}_R^d = e^{iX_{dR}\theta}\,\mathbb{1}\,. \tag{2.34}$$

Similarly, the phases appearing in the down-quark Yukawas after a symmetry transformation of the fermion fields, which we denote as down-quark transformation matrix, are

$$\Theta_d \;\equiv\; \theta \begin{pmatrix} X_{dR} & X_{dR} & X_{dR} \\ X_{dR} & X_{dR} & X_{dR} \\ X_{dR}-X_{tL} & X_{dR}-X_{tL} & X_{dR}-X_{tL} \end{pmatrix} . \tag{2.35}$$

Eqs. (2.29) and (2.34) together with the first part of condition A are the minimal set of required conditions necessary to obtain the BGL textures in the down sector. In order to pick the desired textures we would need the scalar transformation

$$\mathcal{S}_\Phi^{\text{down}} = \text{diag}\left(e^{-iX_{dR}\,\theta}, e^{i(X_{tL}-X_{dR})\,\theta}\right) . \tag{2.36}$$

To make the BGL textures in the up and down sectors compatible without introducing additional textures that spoil the nice features of the BGL-type models we need to impose some extra charge conditions, we call them *texture matching conditions*. They guarantee that the only non-BGL textures present in the Yukawa sector are the null textures,

$$X_{dR} \neq -X_{tR}, \quad X_{tL} \neq X_{uR}+X_{dR}, \quad X_{tL} \neq X_{tR}+X_{dR}, \quad X_{tL} \neq \frac{1}{2}\left(X_{uR}+X_{dR}\right). \tag{2.37}$$

Finally, we have to require an additional texture matching condition indicating how the up and down sectors match. In the original BGL formulation it is crucial that the Higgs doublet coupling to the Γ_1^{BGL} and Δ_1^{BGL} textures is the same, the other possible implementation would violate one of the texture matching conditions in Eq. (2.37). This automatically leads to $X_{dR} = -X_{uR}$. As a result the most general BGL symmetry consistent with the Yukawa structure in Eq. (2.21) is characterized by the following set of charges

$$\begin{aligned} \mathcal{X}^\Phi &= \frac{1}{2}\text{diag}\,\left(X_{uR}-X_{dR}, X_{tR}-X_{dR}\right) , \\ \mathcal{X}_L^q &= \frac{1}{2}\left[\text{diag}\left(X_{uR}, X_{uR}, X_{tR}\right) + X_{dR}\,\mathbb{1}\right] , \\ \mathcal{X}_R^u &= \text{diag}\left(X_{uR}, X_{uR}, X_{tR}\right) , \\ \mathcal{X}_R^d &= X_{dR}\,\mathbb{1}\,, \end{aligned} \tag{2.38}$$

where X_{uR}, X_{tR} and X_{dR} remain as free charges with the texture matching condition $X_{uR} \neq X_{tR}$. The charge conditions for the other BGL implementations are obtained from these of Eq. (2.38) by simply applying the appropriate up-down and/or flavor permutations to the charges.

2.2.3 Decoupling scenarios

In the absence of a flavor symmetry that forbids or protects the dangerous FCNCs, the 2HDM should enter in a decoupling scenario where the effects of the extra scalar fields are small. This can be achieved in two ways:

- **The decoupling limit** [75, 76]: where one of the Higgs doublets becomes much heavier than the electroweak scale and decouples from the other. In the decoupling limit the dangerous tree-level FCNCs are naturally suppressed by the heavy mass scale. This limit can be made explicit by taking the most general scalar potential in the weak basis where m_{12} is zero,[7] i.e.

$$\begin{aligned} V\left(\phi_H, \phi_L\right) = & m_H^2 \left(\phi_H^\dagger \phi_H\right) + m_L^2 \left(\phi_L^\dagger \phi_L\right) + \frac{\lambda_1}{2}\left(\phi_H^\dagger \phi_H\right)^2 + \frac{\lambda_2}{2}\left(\phi_L^\dagger \phi_L\right)^2 \\ & + \lambda_3 \left(\phi_H^\dagger \phi_H\right)\left(\phi_L^\dagger \phi_L\right) + \lambda_4 \left(\phi_H^\dagger \phi_L\right)\left(\phi_L^\dagger \phi_H\right) + \left\{ \frac{\lambda_5}{2}\left(\phi_H^\dagger \phi_L\right)^2 \right. \\ & \left. + \left[\lambda_6 \left(\phi_H^\dagger \phi_H\right) + \lambda_7 \left(\phi_L^\dagger \phi_L\right)\right]\left(\phi_H^\dagger \phi_L\right) + h.c. \right\}, \end{aligned} \tag{2.39}$$

  and imposing that $m_L \sim v << m_H$. In this limit, ϕ_L becomes the SM Higgs doublet up to corrections of $\mathcal{O}\left(v^2/m_H^2\right)$ while the extra scalars become quasi-degenerate and have a heavy mass of $\mathcal{O}(m_H)$, given that they mostly correspond to the fields in the ϕ_H multiplet. The low-energy implications of this limit are more conveniently described using EFTs, that we will introduce in Chapter 4. The tree-level EFT for this framework was obtained in Ref. [77]; its extension to one-loop order is currently under investigation.

- **The alignment limit** [76]: This is not to be confused with the Yukawa alignment scenario presented in Section 2.2.1. It is defined as the limit where the mass mixing between H^0 and the rest of the neutral scalars goes to zero. In the CP-conserving case this corresponds to the limit $\alpha - \beta \to \pi/2$, see Eq. (2.16). The same condition appears naturally in the decoupling limit. However, contrary to the decoupling limit, the extra scalars need not to be heavy in the alignment limit. There is another possibility that cannot be realized in the decoupling limit in which the heavier CP-even Higgs boson, R, is SM-like. This situation is sometimes denoted as reverse alignment and is realized in the CP-conserving case when $\alpha - \beta \to 0, \pi$. A recent phenomenological analysis of the alignment limit in the CP-conserving case can be found in Refs. [20, 78, 79]

The decoupling scenarios would be of particular interest if no deviations from the SM prediction are found in the properties of the Higgs-like particle discovered at LHC.

[7] Note that, in general, this basis does not coincide with the Higgs basis introduced in Eq. (2.9). The exact coincidence between these two bases for a general potential happens in the limit where the heavy mass goes to infinity.

Given their different phenomenological implications these two limiting cases could in principle be distinguished. The most straightforward way would be to discover additional scalar states whose masses lie around the electroweak scale, but one may also be able to distinguish between the two by searching for small deviations in the SM-like Higgs couplings.

Bibliography

[1] G. Aad *et al.* [ATLAS Collaboration], Phys. Lett. B **716** (2012) 1 [arXiv:1207.7214 [hep-ex]].

[2] S. Chatrchyan *et al.* [CMS Collaboration], Phys. Lett. B **716** (2012) 30 [arXiv:1207.7235 [hep-ex]].

[3] H. P. Nilles, Phys. Rept. **110** (1984) 1.

[4] L. Lopez Honorez, E. Nezri, J. F. Oliver and M. H. G. Tytgat, JCAP **0702** (2007) 028 [hep-ph/0612275].

[5] R. Barbieri, L. J. Hall and V. S. Rychkov, Phys. Rev. D **74** (2006) 015007 [hep-ph/0603188].

[6] T. D. Lee, Phys. Rev. D **8** (1973) 1226.

[7] G. C. Branco, Phys. Rev. Lett. **44** (1980) 504.

[8] G. C. Branco, Phys. Rev. D **22** (1980) 2901.

[9] N. Turok and J. Zadrozny, Nucl. Phys. B **358** (1991) 471.

[10] G. W. Anderson and L. J. Hall, Phys. Rev. D **45** (1992) 2685.

[11] J. M. Cline, K. Kainulainen and A. P. Vischer, Phys. Rev. D **54** (1996) 2451 [hep-ph/9506284].

[12] R. D. Peccei and H. R. Quinn, Phys. Rev. Lett. **38** (1977) 1440.

[13] R. D. Peccei and H. R. Quinn, Phys. Rev. D **16** (1977) 1791.

[14] K. A. Olive *et al.* [Particle Data Group], Chin. Phys. C **38** (2014) 090001.

[15] P. Langacker, Phys. Rept. **72** (1981) 185.

[16] H. S. Tsao, AIP Conf. Proc. **72** (1981) 523.

[17] G. C. Branco, L. Lavoura and J. P. Silva, Int. Ser. Monogr. Phys. **103** (1999) 1.

[18] G. C. Branco, P. M. Ferreira, L. Lavoura, M. N. Rebelo, M. Sher and J. P. Silva, Phys. Rept. **516** (2012) 1 [arXiv:1106.0034 [hep-ph]].

[19] I. P. Ivanov, arXiv:1702.03776 [hep-ph].

[20] A. Celis, V. Ilisie and A. Pich, JHEP **1312** (2013) 095 [arXiv:1310.7941 [hep-ph]].

[21] S. Dawson *et al.*, *2013 Community Summer Study on the Future of U.S. Particle Physics: Snowmass on the Mississippi (CSS2013): Minneapolis, MN, USA, July 29-August 6, 2013*, [arXiv:1310.8361 [hep-ex]].

[22] N. Craig, F. D'Eramo, P. Draper, S. Thomas and H. Zhang, JHEP **1506** (2015) 137 [arXiv:1504.04630 [hep-ph]].

[23] I. F. Ginzburg and M. Krawczyk, Phys. Rev. D **72** (2005) 115013 [hep-ph/0408011].

[24] S. Davidson and H. E. Haber, Phys. Rev. D **72** (2005) 035004 Erratum: [Phys. Rev. D **72** (2005) 099902] [hep-ph/0504050].

[25] I. P. Ivanov, Phys. Rev. D **75** (2007) 035001 Erratum: [Phys. Rev. D **76** (2007) 039902] [hep-ph/0609018].

[26] P. M. Ferreira, H. E. Haber, M. Maniatis, O. Nachtmann and J. P. Silva, Int. J. Mod. Phys. A **26** (2011) 769 [arXiv:1010.0935 [hep-ph]].

[27] P. M. Ferreira, R. Santos and A. Barroso, Phys. Lett. B **603** (2004) 219 Erratum: [Phys. Lett. B **629** (2005) 114] [hep-ph/0406231].

[28] A. Barroso, P. M. Ferreira and R. Santos, Phys. Lett. B **632** (2006) 684 [hep-ph/0507224].

[29] N. G. Deshpande and E. Ma, Phys. Rev. D **18** (1978) 2574.

[30] S. Nie and M. Sher, Phys. Lett. B **449** (1999) 89 [hep-ph/9811234].

[31] S. Kanemura, T. Kasai and Y. Okada, Phys. Lett. B **471** (1999) 182 [hep-ph/9903289].

[32] B. W. Lee, C. Quigg and H. B. Thacker, Phys. Rev. Lett. **38** (1977) 883.

[33] B. W. Lee, C. Quigg and H. B. Thacker, Phys. Rev. D **16** (1977) 1519.

[34] H. J. He, N. Polonsky and S. f. Su, Phys. Rev. D **64** (2001) 053004 [hep-ph/0102144].

[35] W. Grimus, L. Lavoura, O. M. Ogreid and P. Osland, Nucl. Phys. B **801** (2008) 81 [arXiv:0802.4353 [hep-ph]].

[36] H. E. Haber and D. O'Neil, Phys. Rev. D **83** (2011) 055017 [arXiv:1011.6188 [hep-ph]].

[37] B. McWilliams and L. F. Li, Nucl. Phys. B **179** (1981) 62.

[38] O. U. Shanker, Nucl. Phys. B **206** (1982) 253.

[39] S. L. Glashow and S. Weinberg, Phys. Rev. D **15** (1977) 1958.

[40] E. A. Paschos, Phys. Rev. D **15** (1977) 1966.

[41] A. Pich and P. Tuzon, Phys. Rev. D **80** (2009) 091702 [arXiv:0908.1554 [hep-ph]].

[42] K. J. Bae, Phys. Rev. D **82** (2010) 055004 [arXiv:1003.5869 [hep-ph]].

[43] A. J. Buras, P. Gambino, M. Gorbahn, S. Jager and L. Silvestrini, Phys. Lett. B **500** (2001) 161 [hep-ph/0007085].

[44] F. J. Botella, G. C. Branco and M. N. Rebelo, Phys. Lett. B **687** (2010) 194 [arXiv:0911.1753 [hep-ph]].

[45] A. J. Buras, M. V. Carlucci, S. Gori and G. Isidori, JHEP **1010** (2010) 009 [arXiv:1005.5310 [hep-ph]].

[46] G. C. Branco, W. Grimus and L. Lavoura, Phys. Lett. B **380** (1996) 119 [hep-ph/9601383].

[47] H. E. Haber, G. L. Kane and T. Sterling, Nucl. Phys. B **161** (1979) 493.

[48] A. Stange, W. J. Marciano and S. Willenbrock, Phys. Rev. D **49** (1994) 1354 [hep-ph/9309294].

[49] M. A. Diaz and T. J. Weiler, hep-ph/9401259.

[50] V. D. Barger, N. G. Deshpande, J. L. Hewett and T. G. Rizzo, *Workshop on Physics at Current Accelerators and the Supercollider Argonne, Illinois, June 2-5, 1993*, [hep-ph/9211234].

[51] E. Ma, Phys. Rev. D **73** (2006) 077301 [hep-ph/0601225].

[52] J. F. Donoghue and L. F. Li, Phys. Rev. D **19** (1979) 945.

[53] R. M. Barnett, G. Senjanovic, L. Wolfenstein and D. Wyler, Phys. Lett. **136B** (1984) 191.

[54] R. M. Barnett, G. Senjanovic and D. Wyler, Phys. Rev. D **30** (1984) 1529.

[55] M. Aoki, S. Kanemura, K. Tsumura and K. Yagyu, Phys. Rev. D **80** (2009) 015017 [arXiv:0902.4665 [hep-ph]].

[56] V. D. Barger, J. L. Hewett and R. J. N. Phillips, Phys. Rev. D **41** (1990) 3421.

[57] P. M. Ferreira, L. Lavoura and J. P. Silva, Phys. Lett. B **688** (2010) 341 [arXiv:1001.2561 [hep-ph]].

[58] J. Bijnens, J. Lu and J. Rathsman, JHEP **1205** (2012) 118 [arXiv:1111.5760 [hep-ph]].

[59] A. Pich, Nucl. Phys. Proc. Suppl. **209** (2010) 182 [arXiv:1010.5217 [hep-ph]].

[60] M. Jung, A. Pich and P. Tuzon, JHEP **1011** (2010) 003 [arXiv:1006.0470 [hep-ph]].

[61] C. B. Braeuninger, A. Ibarra and C. Simonetto, Phys. Lett. B **692** (2010) 189 [arXiv:1005.5706 [hep-ph]].

[62] H. Serôdio, Phys. Lett. B **700** (2011) 133 [arXiv:1104.2545 [hep-ph]].

[63] I. de Medeiros Varzielas, Phys. Lett. B **701** (2011) 597 [arXiv:1104.2601 [hep-ph]].

[64] G. Cree and H. E. Logan, Phys. Rev. D **84** (2011) 055021 [arXiv:1106.4039 [hep-ph]].

[65] A. Celis, J. Fuentes-Martín and H. Serôdio, Phys. Lett. B **737** (2014) 185 [arXiv:1407.0971 [hep-ph]].

[66] F. J. Botella, G. C. Branco, M. Nebot and M. N. Rebelo, JHEP **1110** (2011) 037 [arXiv:1102.0520 [hep-ph]].

[67] G. Bhattacharyya, D. Das, P. B. Pal and M. N. Rebelo, JHEP **1310** (2013) 081 [arXiv:1308.4297 [hep-ph]].

[68] G. Bhattacharyya, D. Das and A. Kundu, Phys. Rev. D **89** (2014) 095029 [arXiv:1402.0364 [hep-ph]].

[69] F. J. Botella, G. C. Branco, A. Carmona, M. Nebot, L. Pedro and M. N. Rebelo, JHEP **1407** (2014) 078 [arXiv:1401.6147 [hep-ph]].

[70] F. J. Botella, G. C. Branco, M. Nebot and M. N. Rebelo, Eur. Phys. J. C **76** (2016) no.3, 161 [arXiv:1508.05101 [hep-ph]].

[71] P. M. Ferreira and J. P. Silva, Phys. Rev. D **83** (2011) 065026 [arXiv:1012.2874 [hep-ph]].

[72] H. Serôdio, Phys. Rev. D **88** (2013) no.5, 056015 [arXiv:1307.4773 [hep-ph]].

[73] F. J. Botella, G. C. Branco and M. N. Rebelo, Phys. Lett. B **722** (2013) 76 [arXiv:1210.8163 [hep-ph]].

[74] H. Y. Cheng, Phys. Rept. **158** (1988) 1.

[75] H. E. Haber and Y. Nir, Nucl. Phys. B **335** (1990) 363.

[76] J. F. Gunion and H. E. Haber, Phys. Rev. D **67** (2003) 075019 [hep-ph/0207010].

[77] J. de Blas, M. Chala, M. Perez-Victoria and J. Santiago, JHEP **1504** (2015) 078 [arXiv:1412.8480 [hep-ph]].

[78] N. Craig, J. Galloway and S. Thomas, arXiv:1305.2424 [hep-ph].

[79] M. Carena, I. Low, N. R. Shah and C. E. M. Wagner, JHEP **1404** (2014) 015 [arXiv:1310.2248 [hep-ph]].

CHAPTER

3 The Strong CP problem and the invisible axion

> "What makes the desert beautiful," said the little prince, "is that somewhere it hides a well..."
>
> — *Antoine de Saint-Exupéry*, The Little Prince

The SM of particle physics stands out as a great success story. The Higgs boson discovery and the lack of significant deviations from direct searches at LHC, or in EW precision tests at LEP, reinforces its role as the theory of EW and strong interactions. However, in spite of its phenomenological success, the SM presents several unanswered questions which might be a hint of physics beyond this framework. One of such open questions is the so-called Strong CP problem [1–3].

3.1 The $U(1)_A$ and the strong CP problems

The Strong CP problem is tightly related to an old problem of QCD termed as the $U(1)_A$ problem. Given that the light quark masses are significantly smaller than the scale at which QCD becomes non-perturbative, i.e. $m_{u,d,s} \ll \Lambda_{\rm QCD}$, it is reasonable to apply the massless limit for these quarks. In this limit, the QCD Lagrangian presents an approximate global chiral symmetry: $U(3)_L \times U(3)_R \equiv SU(3)_V \times SU(3)_A \times U(1)_B \times U(1)_A$, where V (A) stands for vector (axial-vector) and $U(1)_B$ denotes the symmetry associated to baryon number. It is well established that the chiral symmetry gets spontaneously broken by the formation of quark condensates: $\langle \bar{u}u \rangle = \langle \bar{d}d \rangle = \langle \bar{s}s \rangle \neq 0$, leading to an unbroken $SU(3)_V \times U(1)_B$. This breaking of the chiral symmetry should give rise to a spectrum of nine pseudo-Goldstone bosons, one for every broken generator [4–6]. However, experimental measurements showed that one of those bosons, the η', has a significantly higher mass than the rest of the bosons associated to the spontaneous symmetry breaking. This suggests that the $U(1)_A$ symmetry should be broken or not realized in nature and led to an apparent contradiction between theory and experiment that was termed as the $U(1)_A$ problem [7]. The solution to this issue came from the realization by t'Hooft that the QCD vacuum is non-trivial and non-perturbative QCD effects explicitly break the axial-vector symmetry [8].

Indeed, a possible solution to the $U(1)_A$ problem seems to be given by the fact that the axial-vector current

$$J_5^\mu = \bar{q}\gamma_5\gamma^\mu q\,, \tag{3.1}$$

suffers from chiral anomalies [9–11]. As a result, its divergence gives

$$\partial_\mu J_5^\mu = \sum_{q=u,d,s} 2im_q\,\bar{q}\gamma_5 q + \frac{3g_s^2}{32\pi^2} G^\alpha_{\mu\nu}\widetilde{G}^{\mu\nu\,\alpha}\,, \tag{3.2}$$

where g_s is the strong coupling constant and $G^\alpha_{\mu\nu}$ and $\widetilde{G}^\alpha_{\mu\nu} \equiv \frac{1}{2}\epsilon_{\mu\nu\rho\sigma}G^{\rho\sigma\,\alpha}$ are the QCD field-strength tensor and its dual, respectively. Therefore this divergence is non-zero even in the massless limit. This implies that, even though the QCD action in the massless limit is invariant under $\mathrm{U(1)_A}$ at the classical level, an axial-vector transformation,

$$q \to e^{i\alpha\gamma_5/2} q\,, \tag{3.3}$$

would modify the action in the following way

$$\delta S = \alpha \int d^4x\,\partial_\mu J_5^\mu = \alpha \frac{3g_s^2}{32\pi^2}\int d^4x\, G^\alpha_{\mu\nu}\widetilde{G}^{\mu\nu\,\alpha}\,, \tag{3.4}$$

introducing an explicit breaking of the axial-vector symmetry and potentially solving the $\mathrm{U(1)_A}$ puzzle. Nonetheless, using the Bardeen identity [12] the anomaly term can be written as a total derivative

$$G^\alpha_{\mu\nu}\widetilde{G}^{\mu\nu\,\alpha} = \partial_\mu K^\mu\,, \tag{3.5}$$

with $K^\mu = \epsilon^{\mu\nu\rho\sigma}A^\alpha_\nu\left(G^\alpha_{\rho\sigma} - \frac{g_s}{3}f_{\alpha\beta\gamma}A^\beta_\rho A^\gamma_\sigma\right)$ the Chern-Simons current. In a topologically trivial theory this term would yield a null contribution and therefore the axial-vector charge would be conserved in the massless limit even in the presence of the anomalous term. Interestingly, there are special configurations, termed as *instanton solutions*, where the gauge field, A^α_μ, does not vanish at infinity but instead it goes to a pure gauge, i.e. a gauge transformation of the null-field configuration. These solutions explicitly break the $\mathrm{U(1)_A}$ symmetry through the anomaly term and therefore provide a natural explanation for the η' mass [8].

However, the topological properties of QCD possess other implications. The instanton configurations appear as the result of the non-trivial vacuum structure of QCD, characterized by the presence of an infinite number of vacua with minimal classical energy, usually called n-vacua and denoted by $|n\rangle$. Tunneling transitions between different n-vacua correspond to the instanton solutions, see Figure 3.1, that are characterized by their topological charge

$$n = \frac{g_s^2}{32\pi^2}\int d^4x\, G^\alpha_{\mu\nu}\widetilde{G}^{\mu\nu\,\alpha}\,, \tag{3.6}$$

where $n \in \mathbb{N}$ is denoted as the winding number and labels the transition between vacua given by the instantons. There are gauge transformations that cannot be generated infinitesimally, often called large gauge transformations, which carry a winding number. Under those transformations, the n-vacua transform as

$$T_{n'}|n\rangle = |n + n'\rangle\,. \tag{3.7}$$

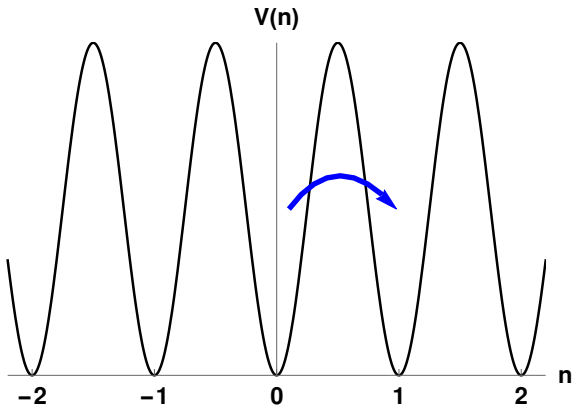

Figure 3.1: *Illustration of the non-trivial nature of the QCD vacuum. The arrow represents an instanton transition between different n-vacua.*

Large gauge transformations commute with the Hamiltonian and therefore they should map the vacuum to itself up to a phase. This invariance requires the definition of the correct vacuum of QCD, the θ-vacuum, defined by

$$|\theta\rangle = \sum_{n=-\infty}^{\infty} e^{-in\theta}|n\rangle\,, \tag{3.8}$$

which presents the correct behavior under large gauge transformations

$$T_{n'}|\theta\rangle = \sum_{n=-\infty}^{\infty} e^{-in\theta}\, T_{n'}|n\rangle = e^{in'\theta}|\theta\rangle\,. \tag{3.9}$$

In a complete theory one should use the non-perturbative physical vacuum, the θ-vacuum, instead of the naive perturbative vacuum, $|0\rangle$. This modification can be mimicked by an "effective term" in the QCD Lagrangian

$$\begin{aligned} {}_+\langle\theta|\theta\rangle_- &= \sum_{n=-\infty}^{\infty} e^{in\theta} \sum_{m=-\infty}^{\infty} {}_+\langle n+m|m\rangle_- \\ &= \frac{1}{Z}\sum_{n=-\infty}^{\infty}\int \mathcal{D}\left[A,n\right] e^{iS[A]}\, e^{in\theta}\,, \end{aligned} \tag{3.10}$$

where $S\left[A\right]$ is the QCD action and Z a normalization factor. Using Eq. (3.6) we get

$${}_+\langle\theta|\theta\rangle_- = \frac{1}{Z}\sum_{n=-\infty}^{\infty}\int \mathcal{D}\left[A,n\right] e^{\,i\int d^4x\left(\mathcal{L}_{\rm QCD}[A]+\theta\frac{g_s^2}{32\pi^2}G^{\alpha}_{\mu\nu}\widetilde{G}^{\mu\nu\,\alpha}\right)}\,, \tag{3.11}$$

and therefore we have obtained that, when considering the topological properties of QCD, a new term appears in the Lagrangian

$$\mathcal{L}_{\rm strongCP} \equiv \theta\,\frac{g_s^2}{32\pi^2}G^{\alpha}_{\mu\nu}\widetilde{G}^{\mu\nu\,\alpha}\,. \tag{3.12}$$

If along with QCD the EW sector is introduced, one should also take into account that quark masses are complex in general. Therefore to get the Lagrangian in the

physical basis, a chiral $U(1)_A$ transformation should be performed. As a result, the QCD vacuum angle in Eq. (3.12) is substituted in the full theory by $\bar{\theta}$ defined as

$$\bar{\theta} = \theta + \text{Arg}\,(\text{Det}\,M)\ , \tag{3.13}$$

with M being the quark mass matrix. For $\bar{\theta} \neq 0$, Eq. (3.12) introduces a violation of P and T but not C and consequently a violation of CP, and therefore it would induce a neutron dipole moment. However, the present bound on the neutron dipole moment, $|d_n| < 2.9 \times 10^{-26}$ e cm [13], sets a stringent bound on this angle $|\bar{\theta}| \lesssim 10^{-11}$ [14]. The reason why this parameter, coming from the strong and the EW sectors, is so small is unknown and gives rise to the Strong CP problem.

3.2 The Peccei-Quinn solution and the axion

A simple solution to the Strong CP problem consists in the introduction of a chiral symmetry that rotates the $\bar{\theta}$ angle away and makes it unphysical.[1] This solution, commonly referred as the PQ mechanism [19], consists in the introduction of a global chiral $U(1)_{PQ}$ symmetry with mixed anomalies with QCD, that gets spontaneously broken. This way the PQ mechanism effectively replaces the CP-violating phase by a CP-odd field, the so-called axion, which corresponds to the pseudo-Goldstone boson resulting from the spontaneous breaking of the PQ symmetry [20, 21]. As a result the axion, a, presents a shift transformation under this symmetry

$$a \to a + c f_a\,, \tag{3.14}$$

with f_a being the axion decay constant, and c an arbitrary complex number. Since making the SM invariant under the PQ symmetry implies an extension of the SM Lagrangian that includes axion interactions,

$$\mathcal{L}^{\text{eff}}_{\text{axion}} = \mathcal{L}_{\text{SM}} + \left(\bar{\theta} + C_{ag}\frac{a}{f_a}\right)\frac{g_s^2}{32\pi^2}G^{\alpha}_{\mu\nu}\widetilde{G}^{\mu\nu\,\alpha} + \frac{1}{2}\partial_\mu a\,\partial^\mu a + \mathcal{L}_{a\gamma\gamma} + \mathcal{L}_{a\bar{\psi}\psi}\,, \tag{3.15}$$

then by a shift in a one can eliminate $\bar{\theta}$. Here the terms $\mathcal{L}_{a\gamma\gamma}$ and $\mathcal{L}_{a\bar{\psi}\psi}$ are, respectively, the axion interaction to photons and to matter, and the quantity C_{ag} is determined by the chiral color anomaly of the current associated with the $U(1)_{PQ}$ transformation [10],

$$C_{ag} \equiv \sum_{i=\text{colored}} (X_{\psi_{iR}} - X_{\psi_{iL}})\ , \tag{3.16}$$

where $X_{\psi_{iL(R)}}$ denotes the PQ charge of the corresponding fermions. In a more formal way, the color anomaly term in the above Lagrangian induces a potential for the axion field that is periodic in the effective vacuum angle [19]

$$V_{\text{axion}} \simeq -\Lambda^4_{\text{QCD}}\cos\left(\bar{\theta} + C_{ag}\frac{a}{f_a}\right)\ , \tag{3.17}$$

[1] Indeed, the Strong CP problem would find a trivial solution if the bare mass of one of the quarks, say the up-quark mass, was zero [15, 16]. Nevertheless current algebra computations and lattice QCD results show that this possibility is excluded [17, 18].

and whose minimum appears at $\langle a \rangle = -\bar{\theta} f_a / C_{ag}$, therefore providing a dynamical solution to the Strong CP problem.

The PQ symmetry yields an elegant solution to the Strong CP problem. Nevertheless, it appears unnatural to introduce a symmetry that is exact at the classical level but intrinsically broken by QCD anomalies. Indeed, PQ invariance is not even an approximate symmetry since instanton effects cannot be treated as a small perturbation. This issue can be resolved by considering the modified PQ symmetry, $\mathrm{U}(1)'_{\mathrm{PQ}}$, defined as an anomaly-free combination of the PQ and the axial-vector currents [22]. Actually, strictly speaking the axion is the pseudo-Goldstone boson associated to the spontaneous symmetry breaking of $\mathrm{U}(1)'_{\mathrm{PQ}}$ and not $\mathrm{U}(1)_{\mathrm{PQ}}$. Contrary to the PQ symmetry, the modified PQ symmetry is an exact symmetry in the massless quark limit and therefore it can be considered as an approximate symmetry of Nature, explicitly broken by the small masses of the light quarks. These small masses give both the pion and the axion a mass. Given that $\mathrm{U}(1)'_{\mathrm{PQ}}$ is spontaneously broken by the quark condensate, $\langle \bar{q} q \rangle$, and explicitly broken by the quark masses, the axion mass squared is given by

$$m_a^2 \sim \frac{m_q \langle \bar{q} q \rangle}{f_a^2} \,, \tag{3.18}$$

while from current algebra one can obtain the following relation for the pion mass [23][2]

$$m_\pi^2 f_\pi^2 = -\langle m_u \, \bar{u} u + m_d \, \bar{d} d \rangle \,, \tag{3.19}$$

where $m_\pi \simeq 135$ MeV and $f_\pi \simeq 92$ MeV are the pion mass and decay constant, respectively. Therefore, we have the following relation between the two masses

$$m_a \sim \frac{m_\pi f_\pi}{f_a} \,. \tag{3.20}$$

Indeed, using current algebra methods one can obtain the following expression for the axion mass [20],[3]

$$\begin{aligned} m_a &= \frac{m_\pi f_\pi |C_{ag}|}{f_a} \left[\frac{m_u \, m_d \, m_s}{(m_u + m_d) \, (m_u \, m_d + m_u \, m_s + m_d \, m_s)} \right]^{1/2} \\ &= \frac{m_\pi f_\pi |C_{ag}|}{f_a} \left[\frac{z}{(1+z) \, (1+z+w)} \right]^{1/2} , \end{aligned} \tag{3.21}$$

which agrees with our previous expectations based on the modified PQ symmetry considerations. Here, the parameters z and w denote the quark mass ratios $z = m_u/m_d \simeq 0.56$ and $w = m_u/m_s \simeq 0.029$. Note that while in the language of the modified PQ current both the axion and the pion acquire a mass through the same mechanism, the axion would become a true Goldstone if any of the light quark masses is taken to zero while the pion would only become massless when both m_u and m_d are set to zero, as expected from symmetry considerations. It is however

[2] See also Section 19.4 of Ref. [24] for more details.

[3] The next-to-leading order correction to the axion mass has been computed recently in Ref. [25].

misleading to think that the axion mass has nothing to do with instanton effects. Indeed, if instanton effects are neglected then the PQ symmetry becomes exact, while the axial-vector symmetry is explicitly broken by the quark masses. In this case, the axion corresponds to the Goldstone of $\mathrm{U}(1)_{\mathrm{PQ}}$, which acquires a mass only when instanton effects play a role.

Given that the axion is the pseudo-Goldstone boson associated to $\mathrm{U}(1)'_{\mathrm{PQ}}$, the axion-matter interactions, described by $\mathcal{L}_{a\bar{\psi}\psi}$, are given by

$$\mathcal{L}_{a\bar{\psi}\psi} = \frac{\partial_\mu a}{f_a} j^\mu_{\mathrm{PQ}'} - \partial^\mu a \partial_\mu a \,, \tag{3.22}$$

where the modified PQ current reads

$$j^\mu_{\mathrm{PQ}'} = j^\mu_{\mathrm{PQ}} - \frac{1}{2}\,\frac{C_{ag}}{1+z+w}\left(\bar{u}\gamma^\mu\gamma_5 u + z\,\bar{d}\gamma^\mu\gamma_5 d + w\,\bar{s}\gamma^\mu\gamma_5 s\right) , \tag{3.23}$$

which, by construction, is anomaly free. In the case where all fermions have family-universal charges, the PQ current is flavor-conserving and takes the following generic form in the mass-diagonal basis

$$j^\mu_{\mathrm{PQ}} = f_a \partial_\mu a + \frac{1}{2}\sum_i g_{\psi_i}\,\bar{\psi}_i\gamma_\mu\gamma_5\psi_i \,, \tag{3.24}$$

with $g_{\psi_i} \equiv X_{\psi_{iR}} - X_{\psi_{iL}}$. A more general case, where axion charges are non-universal will be discussed Chapter 8. From Eq. (3.22) it follows that quark- and lepton-axion interactions are given by

$$\begin{aligned}\mathcal{L}_{a\bar{\psi}\psi} = \frac{1}{2}\frac{\partial_\mu a}{f_a}\ \big[&g_e\,\bar{e}\gamma^\mu\gamma_5\ e + g_u\ \bar{u}\gamma^\mu\gamma_5\,u + g_d\,\bar{d}\gamma^\mu\gamma_5\,d + g_s\,\bar{s}\gamma^\mu\gamma_5\,s \\ &-\eta\,C_{ag}\left(\bar{u}\gamma^\mu\gamma_5 u + z\bar{d}\gamma^\mu\gamma_5 d + w\bar{s}\gamma^\mu\gamma_5 s\right)\big] + \ldots ,\end{aligned} \tag{3.25}$$

with $\eta = (1+z+w)^{-1}$ and where the ellipsis stands for interactions with neutrinos, and heavy quarks, leptons and scalars. Below the chiral symmetry breaking scale, i.e. $\Lambda_{\mathrm{QCD}} \simeq 1$ GeV, it is more convenient to describe the axion interactions with quarks in terms of mesons and baryons. Once the effect of the light-quark masses is considered, the axion mixes with the η and the π^0,[4]

$$a_{\mathrm{phys}} \simeq a + \xi_\pi\,\pi^0 + \xi_\eta\,\eta \,. \tag{3.26}$$

Using standard techniques, one can obtain from Eq. (3.25) the following mixing angles [27]

$$\begin{aligned}\xi_\pi &\simeq -\frac{1}{2}\,\frac{f_\pi}{f_a}\left[C_{ag}\frac{1-z}{1+z+w} - g_u + g_d\right] , \\ \xi_\eta &\simeq -\frac{1}{2\sqrt{3}}\,\frac{f_\pi}{f_a}\left[C_{ag}\frac{1+z-2w}{1+z+w} - g_u + g_d\right] .\end{aligned} \tag{3.27}$$

[4]The effect of the η' was considered in Ref. [26], where it was shown to give negligible corrections to the axion low-energy dynamics.

On the other hand, the axion-nucleon interactions can be parametrized by

$$\mathcal{L}_{\rm aN} = \frac{1}{2}\,\frac{\partial_\mu a}{f_a}\,\overline{N}(g^0 + g^3\sigma_3)\gamma^\mu\gamma_5\,N\,, \tag{3.28}$$

with σ_3 the Pauli matrix in isospin space and $N = (p,\, n)^T$ the nucleon doublet. The isoscalar and isovector couplings are given in Refs. [28,29]. The couplings to protons and neutrons are given in terms of those by

$$\begin{aligned} g_p \equiv g^0 + g^3 =& (g_u - 2\eta\, C_{ag})\Delta u + (g_d - 2\eta z\, C_{ag})\Delta d + (g_s - 2\eta w\, C_{ag})\Delta s\,, \\ g_n \equiv g^0 - g^3 =& (g_u - 2\eta\, C_{ag})\Delta d + (g_d - 2\eta z\, C_{ag})\Delta u + (g_s - 2\eta w\, C_{ag})\Delta s\,, \end{aligned} \tag{3.29}$$

with $\Delta u = 0.841 \pm 0.020$, $\Delta d = -0.426 \pm 0.020$ and $\Delta s = -0.085 \pm 0.015$ [30].

Apart from its interactions to matter, the axion is also characterized by its coupling to photons,

$$\mathcal{L}_{a\gamma\gamma} = C_{a\gamma}^{\rm eff} C_{ag}\,\frac{a}{f_a}\frac{\alpha}{8\pi}\,F_{\mu\nu}\widetilde{F}^{\mu\nu}\,. \tag{3.30}$$

Here $\alpha = e^2/4\pi \simeq 1/137$, $F_{\mu\nu}$ is the electromagnetic field-strength tensor and $\widetilde{F}_{\mu\nu}$ its dual tensor. The effective factor $C_{a\gamma}^{\rm eff}$ takes the form [28]:

$$C_{a\gamma}^{\rm eff} = \frac{C_{a\gamma}}{C_{ag}} - \frac{2}{3}\frac{4+z+w}{1+z+w}, \tag{3.31}$$

where the second term is a model-independent quantity that comes from the mixing of the axion with the π^0 and the η while $C_{a\gamma}$ is a model-dependent quantity associated to the electromagnetic anomaly with the PQ current. This is determined in terms of the fermion charges by

$$C_{a\gamma} = 2\sum_{i=\text{charged}} (X_{\psi_{iR}} - X_{\psi_{iL}})\,Q_i^2\,. \tag{3.32}$$

3.2.1 The original axion model

The implementation of the PQ mechanism requires the extension of the matter content of the SM. In its original formulation, the scalar sector is enlarged to a 2HDM to make the SM invariant under a new chiral transformation, and the PQ charges are chosen so that they enforce NFC [31]. This way the severe experimental constraints from FCNCs [32] are avoided (see Section 2.2.1). Using the same notation as in Chapter 2, the scalar potential of the model is the same as in Eq. (2.4) with $m_{12} = \lambda_5 = \lambda_6 = \lambda_7 = 0$, and the Yukawa interactions are given by

$$\mathcal{L}_Y = \overline{q_L}\,\Gamma_u\tilde{\phi}_1\,u_R + \overline{q_L}\,\Gamma_d\phi_2\,d_R + \overline{\ell_L}\,\Gamma_e\phi_i\,e_R\,, \tag{3.33}$$

where $i = 1, 2$ correspond, respectively, to the type II and flipped scenarios in Section 2.2.1.[5] In this model the scalars and fermions carry the following PQ charges

$$q_{Lp} \to e^{iX_q\theta}q_{Lp}, \qquad\qquad \ell_{Lp} \to e^{iX_\ell\theta}\ell_{Lp},$$

[5] If the scalar field that couples to leptons is neither ϕ_1 nor ϕ_2 there is a Goldstone, denoted as the arion [33–35], which does not receive mass from instanton effects. We will not consider this possibility here.

$$u_{Rp} \to e^{iX_u\,\theta} u_{Rp}, \qquad e_{Rp} \to e^{iX_e\,\theta} e_{Rp}, \tag{3.34}$$
$$d_{Rp} \to e^{iX_d\,\theta} d_{Rp}, \qquad \phi_i \to e^{iX_i\,\theta} \phi_i,$$

where $p = 1, 2, 3$ is a flavor index. Note that the above choice for the PQ charges is not unique. Indeed the Lagrangian will remain invariant if we redefine the PQ charges by performing a vectorial transformation in the quark and lepton sectors, which allows us to set $X_q = X_\ell = 0$ without loss of generality. The invariance of the Yukawa Lagrangian in Eq. (3.33) implies the following charge constraints

$$X_u = X_1, \qquad X_d = -X_2, \qquad X_e = -X_i\,, \tag{3.35}$$

with $i = 1, 2$. In this model, the anomalous $\mathrm{U(1)_{PQ}}$ and the $\mathrm{U(1)_Y}$ symmetries are spontaneously broken by the vacuum expectation values (vev) of the doublets. This will lead to two Goldstone bosons: the one that becomes the longitudinal component of the Z, G^0, and the axion, a,

$$G^0 = \frac{1}{v}\left(v_1\,\eta_1 + v_2\,\eta_2\right)\,, \qquad a = \frac{1}{f_a}\left(X_1 v_1\,\eta_1 + X_2 v_2\,\eta_2\right)\,, \tag{3.36}$$

where v_i is the vev of the corresponding doublet with $v \equiv (v_1^2 + v_2^2)^{1/2} = (\sqrt{2} G_F)^{-1/2}$, and η_i are the neutral components of the imaginary part of the Higgs doublets (see Eq. (2.8)). The axion decay constant reads

$$f_a = \sqrt{X_1^2 v_1^2 + X_2^2 v_2^2}\,. \tag{3.37}$$

Requiring that the PQ symmetry does not overlap with $\mathrm{U(1)_Y}$, impose the condition

$$X_1 v_1^2 + X_2 v_2^2 = 0\,, \tag{3.38}$$

which fixes the charges of the scalar doublets[6]

$$X_1 = \frac{v_2}{v_1}\,, \qquad X_2 = -\frac{v_1}{v_2}\,, \tag{3.39}$$

as well as the axion decay constant, $f_a = v$. This choice of charges also fixes the color anomaly coefficient

$$C_{ag} = N_f \left(\frac{v_1}{v_2} + \frac{v_2}{v_1}\right)\,, \tag{3.40}$$

where $N_f = 3$ is the number of fermion families, and therefore the axion mass for the original PQ model reads (see Eq. (3.21))

$$m_a \simeq \left(\frac{v_1}{v_2} + \frac{v_2}{v_1}\right) \times 75 \text{ keV}\,. \tag{3.41}$$

[6]Note that this choice for the charges is not unique, since a global rescaling of the scalar charges would not spoil the orthogonality condition in Eq. (3.38). However, this rescaling would also change the axion decay constant (see Eq. (3.37)) such that all the physical quantities are independent of the absolute magnitude of the PQ charges.

As we can see, the original axion is characterized by having a sizable mass and presents large couplings to matter. As a result and in spite of elegantly solving the Strong CP problem, this formulation was soon ruled out by experimental data. For example, using the axion-pion and axion-eta mixing angles from Eq. (3.27) one can estimate the $K^+ \to \pi^+ a$ branching ratio to be [27]

$$\mathrm{Br}\left(K^+ \to \pi^+ a\right) \simeq 2 \times 10^{-6} \left(\frac{v_1}{v_2} + \frac{v_2}{v_1}\right) , \tag{3.42}$$

which is well above the current experimental limit set by the E787 Collaboration: $\mathrm{Br}\left(K^+ \to \pi^+ a\right) \leq 4.5 \times 10^{-11}$ at 90% CL [36].

3.3 Invisible axion models

Even though the original axion is ruled out, the PQ solution still constitutes an appealing idea for the solution of the Strong CP problem. Indeed, the presence of the tight experimental constraints from axion searches is simply the result of having related two a priori independent scales: the PQ and the EW symmetry breaking scales. In fact, one can easily evade all the experimental bounds by assuming that these two scales are very far apart, which can be achieved by the introduction of a scalar singlet acquiring a vev that breaks the PQ symmetry at a scale much higher than the EW scale. As a result, these models present a very large axion decay constant, i.e. $f_a \gg v$, and therefore, the mass and the couplings of the axion are heavily suppressed. Models of this type are generically denoted as invisible axion models and, apart from evading current bounds from axion searches, they possess several interesting features. For instance, the invisible axion is a promising candidate for cold dark matter [37]. Additionally, the type I seesaw mechanism [38] can be naturally implemented in these models allowing for the possibility to explain the smallness of the active neutrino masses and providing a dynamical origin to the heavy seesaw scale [39].

3.3.1 Benchmark invisible axion models

There are two benchmark invisible axion models: the KSVZ [40,41] and the DFSZ [42, 43] models. In the KSVZ model the SM fields carry no PQ charge and one adds to the SM particle content a heavy color triplet vector-like quark and a complex scalar gauge singlet. On the other hand, in the DFSZ model one introduces an additional Higgs doublet and a complex scalar gauge singlet and fixes the PQ symmetry by enforcing NFC, just like in the original PQ model. Both benchmark models are characterized by having flavor-universal interactions. In Chapter 8 we will discuss other invisible axion implementations with non-trivial flavor structures.

The KSVZ model

The first invisible axion model was proposed by Kim [40] and independently by Shifman, Vainshtein and Zakharov [41]. In this model it is assumed that the SM particles are singlets under the PQ symmetry. To implement the PQ mechanism,

this model introduces a heavy fermion, Q, which is vector-like under the SM gauge group and a scalar SM singlet, S. Additionally, a discrete symmetry is enforced to forbid a bare-mass term for the heavy fermion $m\,\overline{Q}Q$

$$R: \qquad Q_L \to -Q_L\,, \qquad Q_R \to Q_R\,, \qquad S \to -S\,, \tag{3.43}$$

while all the SM model fields remain invariant under this symmetry. Then, the most general Lagrangian one can write for the new fields compatible with the discrete symmetry

$$\mathcal{L} = y\,S\,\overline{Q_L}Q_R + y\,S^*\,\overline{Q_R}Q_L + V\left(\phi, S\right)\,, \tag{3.44}$$

is invariant under a $\mathrm{U(1)_A}$ transformation

$$S \to e^{-i\theta}S\,, \qquad Q \to e^{i\theta\gamma_5/2}Q\,, \tag{3.45}$$

which can be used as a PQ symmetry provided Q is charged under $\mathrm{SU(3)_c}$. It is then assumed that the scalar singlet acquires a very large vev $\langle S\rangle = v_{\mathrm{PQ}} \gg v$ spontaneously breaking the accidental $\mathrm{U(1)_A}$ symmetry and giving rise to an invisible axion. The same expressions given in Section 3.2 for the axion mass and couplings also apply to the KSVZ axion but in this case $f_a \simeq v_{\mathrm{PQ}}$. The resulting axion mass for this model is then given by

$$m_a = \frac{f_\pi m_\pi}{v_{\mathrm{PQ}}}\left[\frac{z}{(1+z)\,(1+z+w)}\right]^{1/2} \simeq 6\ \mathrm{meV} \times \left(\frac{10^9\ \mathrm{GeV}}{v_{\mathrm{PQ}}}\right)\,, \tag{3.46}$$

and is therefore small for $v_{\mathrm{PQ}} \gg v$. Here we have taken into consideration that, in the KSVZ model, $C_{ag} = 1$.

The couplings of the axion to matter and to photons are also suppressed by a factor of $1/f_a \simeq 1/v_{\mathrm{PQ}}$. The most stringent bound on the KSVZ axion comes from its coupling to photons; assuming that Q is a color triplet of electric charge X_Q^{em}, the KSVZ invisible axion has the following effective coupling to photons (see Eq. (3.31))

$$C_{a\gamma}^{\mathrm{eff}} = 6\,X_Q^{em} - \frac{2}{3}\,\frac{4+z+w}{1+z+w}. \tag{3.47}$$

On the other hand, the presence of the R symmetry in Eq. (3.43) forbids axion couplings to the SM fermions at tree-level. However, the vev of S spontaneously breaks the R symmetry and therefore they will appear at higher order (see Ref. [28] for more details). Even though the tree-level couplings of the KSVZ axion to quarks are protected by the R symmetry, the axion still has substantial coupling to nucleons due to the contribution from the anomaly (see Eq. (3.29)).

The DFSZ model

This axion model was originally proposed by Zhitnitsky [42]. However, this work was overlooked in the literature and was later independently proposed by Dine, Fischler and Srednicki [43]. The model is identical to the one presented in Section 3.2.1, except for the fact that it is supplemented with an additional scalar field S, singlet

under the SM group but charged under the PQ symmetry, that develops an arbitrarily large vev. This way the breaking of the PQ symmetry is decoupled from the EW scale and can occur at much higher energies. The Yukawa Lagrangian of the model is the same as in Eq. (3.33) and the PQ charges of the model follow the same structure as in Eq. (3.34) with the singlet field transforming as

$$S \to e^{i\theta X_S} S\,, \tag{3.48}$$

and where the same charge conditions as in Eq. (3.35) are enforced. Additionally, in order to avoid the presence of dangerous Goldstone bosons, the scalar charges should satisfy one of the following restrictions

$$X_1 - X_2 = \pm X_S\,, \qquad \text{or} \qquad X_1 - X_2 = \pm 2X_S\,. \tag{3.49}$$

In what follows we will take the same condition as in the original implementation, i.e. $X_1 - X_2 = 2X_S$, and assume $X_S = 1$. The most general scalar potential compatible with this symmetry reads

$$\begin{aligned} V(\phi_1,\phi_2,S) = {} & m_1^2\left(\phi_1^\dagger\phi_1\right) + m_2^2\left(\phi_2^\dagger\phi_2\right) + \frac{\lambda_1}{2}\left(\phi_1^\dagger\phi_1\right)^2 + \frac{\lambda_2}{2}\left(\phi_2^\dagger\phi_2\right)^2 \\ & + \lambda_3\left(\phi_1^\dagger\phi_1\right)\left(\phi_2^\dagger\phi_2\right) + \lambda_4\left(\phi_1^\dagger\phi_2\right)\left(\phi_2^\dagger\phi_1\right) + m_s\left|S\right|^2 \\ & + \frac{\lambda_S}{2}\left|S\right|^4 + \delta_1\left(\phi_1^\dagger\phi_1\right)\left|S\right|^2 + \delta_2\left(\phi_2^\dagger\phi_2\right)\left|S\right|^2 \\ & + \left[\delta_3\left(\phi_1^\dagger\phi_2\right)S^2 + \delta_3\left(\phi_2^\dagger\phi_1\right)S^{*\,2}\right]\,, \end{aligned} \tag{3.50}$$

where, without loss of generality, the parameter δ_3 is chosen to be real by an appropriate rephasing of S. It is assumed that the parameters in the scalar potential are such that the scalar fields acquire a vev in the following directions

$$\langle\phi_i\rangle = \frac{v_i}{\sqrt{2}}\,, \qquad \langle S\rangle = \frac{v_{\rm PQ}}{\sqrt{2}}\,, \tag{3.51}$$

with $v_{\rm PQ} \gg v$. As with the original PQ model, we have two Golstone bosons: one associated to the axion, $\tilde{a}$, and the other related to the longitudinal component of the Z boson, G^0,

$$G^0 = \frac{1}{v}\left(v_1\,\eta_1 + v_2\,\eta_2\right)\,, \qquad \tilde{a} = \frac{1}{f_a}\left(X_1 v_1\,\eta_1 + X_2\,v_2\,\eta_2 + v_{\rm PQ}\,\eta_s\right)\,, \tag{3.52}$$

where η_s corresponds to the imaginary part of S and where we took $X_S = 1$. It is convenient to define the physical axion such that it does not overlap with G^0

$$a = \tilde{a} - \frac{v}{f_a}\,X\,G^0\,, \tag{3.53}$$

where the coefficient X is given by

$$X = \frac{v_1^2}{v^2}\,X_1 + \frac{v_2^2}{v^2}\,X_2\,. \tag{3.54}$$

This shift in the axion field implies the following redefinition of the scalar PQ charges

$$X_i' = X_i - X\,. \tag{3.55}$$

Given the large hierarchy among the vevs, the DFSZ axion is mostly given by the imaginary part of the complex singlet, η_s, and $f_a \simeq v_{\rm PQ}$. As it happened in the KSVZ model, the large vev of the scalar singlet also yields a very small mass for the axion,

$$m_a = \frac{f_\pi m_\pi |C_{ag}|}{v_{\rm PQ}} \left[\frac{z}{(1+z)\,(1+z+w)}\right]^{1/2} \simeq 6\ {\rm meV} \times \left(\frac{10^9\ {\rm GeV}}{v_{\rm PQ}/|C_{ag}|}\right)\,, \tag{3.56}$$

where the color anomaly coefficient in the DFSZ model takes the value

$$C_{ag} = \sum_{i={\rm colored}} X_{\psi_{iR}} - X_{\psi_{iL}} = 2N_f = 6\,. \tag{3.57}$$

As it happened with the KSVZ axion, the couplings of the DFSZ axion to matter and to photons are suppressed by $1/f_a \simeq 1/v_{\rm PQ}$ and hence they are sufficiently small to evade the experimental bounds. In this model the effective coupling to photons is completely fixed and reads (see Eqs. (3.31) and (3.32))

$$C_{a\gamma}^{\rm eff} = \frac{8}{3} - \frac{2}{3}\,\frac{4+z+w}{1+z+w}, \tag{3.58}$$

while the couplings to nucleons and to electrons can be directly read from Eqs. (3.25) and (3.29), respectively, by using the appropriate values for the charges given by Eq. (3.55).

3.3.2 Axion domain walls

During the evolution of the Universe the PQ symmetry gets broken in different ways. In the early Universe the PQ symmetry is spontaneously broken by the expectation value of the S field. At this stage the potential has the mexican-hat shape, the angular part of the field becomes a Goldstone boson and the Lagrangian remains global phase invariant. As the Universe cools down non-perturbative instanton effects at the QCD scale take place and the PQ symmetry gets explicitly broken by the QCD gluon anomaly $[{\rm SU}(3)_C]^2 \times {\rm U}(1)_{\rm PQ}$ [20,21]. However QCD instantons only break the symmetry down to a discrete $\mathcal{Z}_N$ subgroup. This can be easily seen from Eq. (3.12) and the fact that the θ term is invariant under the shift $\bar\theta \to \bar\theta + 2\pi k$. While before the QCD scale the shift $a \to a + \alpha\, v_{\rm PQ}$ was allowed for any α, the presence of the axion coupling to gluons restricts the phase to the values $\alpha_k = 2\pi k/|C_{ag}|$ (with $k = 0, 1, \ldots, |C_{ag}| - 1$), which just reflects the original $\bar\theta$ periodicity. Therefore, the order N of the discrete group is given by the color instantons effects to be $N = |C_{ag}|$. As pointed out by Sikivie [44], these models will have $N_{\rm DW}$ degenerate disconnected vacua. This in turn leads to an unwanted domain wall structure in the early universe [44–46].

In general, the domain wall number, $N_{\rm DW}$, coincides with the order of the discrete group, i.e. $N_{\rm DW} = N = |C_{ag}|$. Nonetheless, in some cases only a subgroup of $\mathcal{Z}_N$

acts non-trivially on the vacuum. To examine the vacuum structure one should analyze the gauge invariant order parameters of the theory. In this way the domain wall number will coincide with the dimension of the higher order subgroup of $\mathcal{Z}_N$ which acts non-trivially on at least one of the order parameters. For the models we will discuss in this thesis, it suffices to notice that for the singlet condensate

$$\langle S\rangle_k \to \exp\left[\frac{2\pi k}{N/X_S}\right]\langle S\rangle_0 \ , \tag{3.59}$$

as we set $X_S = 1$ the vacuum periodicity is N, i.e. all elements of the residual $\mathcal{Z}_N$ act non-trivially on the vacuum. As a result, we have $N_{\rm DW} = |C_{ag}|$ for the class of models that will be studied here.[7]

Many axion models suffer from the domain wall problem. In particular, the DFSZ invisible axion model has a domain wall number $N_{\rm DW} = 2N_f$ or $N_{\rm DW} = N_f$ depending on the scalar potential implementation, with N_f the number of quark families. On the other hand, in implementations where $N_{\rm DW} = 1$, such as the KSVZ invisible axion model, the resulting domain wall structure is harmless [47].

Even for $N_{\rm DW} \neq 1$, some solutions to the domain wall problem can be found in the literature. It is possible to avoid the domain wall problem by assuming that inflation has occurred after the PQ symmetry breaking. In this case, one can derive limits on the inflationary scale based on the observation of isocurvature fluctuations in the cosmic microwave background [48]. Also, there have been several attempts to introduce an explicit breaking of the PQ symmetry that also breaks the $\mathcal{Z}_N$ discrete group in such a way that the PQ solution to the Strong CP problem is protected [44,49]. This explicit breaking could come from gravity, giving rise to Planck scale suppressed operators [50,51]. However, it was argued that this solution would give rise to long lived domain walls which introduce cosmological problems [52]. Additionally, gravity violations of the PQ symmetry should be controlled in order not to spoil the PQ solution [53–59]. This issue will be considered in the next section.

3.3.3 Protecting the axion from gravity

Until now we have discussed axion models where an ad hoc PQ symmetry is imposed. However, the presence of semi-classical gravitational effects can potentially violate global symmetries [50, 51], spoiling the strong CP solution [53–59]. As we saw in Section 3.2, in the absence of gravity, the axion potential coming from the instanton contributions can be written as [19]

$$V_{\rm axion} \simeq -\Lambda^4_{\rm QCD}\,\cos\frac{a_{\rm phys}}{v_{\rm PQ}}\,, \tag{3.60}$$

which has a minimum at $\langle a_{\rm phys}\rangle = \bar\theta = 0$ and where the estimated axion mass is $m_a \simeq \Lambda^2_{\rm QCD}/v_{\rm PQ}$. On the other hand, when including gravitational effects, the axion

[7] Considering higher dimensional order parameters such as $\left\langle \Phi_i^\dagger \Phi_j \right\rangle$ or $\langle \overline{q_{L\alpha}} q_{R\alpha}\rangle$ would not change the periodicity of the full vacuum, since in our choice of normalization the residual discrete group always acts non trivially in $\langle S\rangle$.

potential will change. For example in our invisible axion model, we should expect higher dimensional PQ violating terms of the type

$$\frac{1}{M_{\rm Pl}^{n-2}}\Phi_i^\dagger\Phi_j S^n\,, \quad \frac{1}{M_{\rm Pl}^{n-4}}S^n\,, \quad \cdots \tag{3.61}$$

with the Planck scale denoted by $M_{\rm Pl}$. Let us consider, for simplicity, the second term in the above equation. By introducing this term in the Lagrangian the axion potential gets modified and takes the form [57]

$$\widetilde{V}_{\rm axion} \simeq -\Lambda_{\rm QCD}\,\cos\frac{a_{\rm phys}}{v_{\rm PQ}} - \frac{c\,v_{\rm PQ}^n}{M_{\rm Pl}^{n-4}}\,\cos\left[\frac{a_{\rm phys}}{v_{\rm PQ}}+\delta\right]\,. \tag{3.62}$$

The parameter c is just a coupling constant and δ a CP violating phase. The problem with this new axion potential is that the minimum is no longer at $\langle a_{\rm phys}\rangle = 0$, but rather at

$$\bar\theta = \frac{\langle a_{\rm phys}\rangle}{v_{\rm PQ}} \simeq c\,\sin\delta\frac{v_{\rm PQ}^n}{M_{\rm Pl}^{n-4}\Lambda_{\rm QCD}^4}\,, \tag{3.63}$$

which in general will be far from zero. The axion mass will also be affected by these gravitational effects, taking the form

$$m_a^2 \simeq \frac{\Lambda_{\rm QCD}^4}{v_{\rm PQ}^2} + c\frac{v_{\rm PQ}^{n-2}}{M_{\rm Pl}^{n-4}}\,. \tag{3.64}$$

Therefore, in this simple scenario we see that gravitational effects will in general spoil the strong CP solution coming from the PQ symmetry.

Over the years several solutions to this problem have emerged, which allow us to preserve the PQ solution of the strong CP problem. GUT motivated models [56, 57], extra dimensional [60] ones and even models having neutrinos playing a big role in gravity protection [61] can be found in the literature. However, many of these solutions need a significant extension of the original PQ model. One of such solutions is the use of gauge discrete symmetries to protect the PQ solution against gravity [62]. This solution has the interesting feature that the low energy spectrum of the theory does not need to be extended. Gauge discrete symmetries, which arise through the spontaneous symmetry breaking of a gauge symmetry, are not broken by gravity and can provide natural suppression to the harmful gravitational effects. The idea proposed is to have a large discrete Abelian symmetry $\mathcal{Z}_P$ forbidding, up to a given order, these unwanted terms [63, 64]. For example, if the symmetry only allows terms of the form $S^m/M_{\rm Pl}^{m-4}$ for $m \geq 13$, we will just get irrelevant contributions to the axion mass and its vev [65]. In Section 8.2.4 we will treat this solution in more detail for specific model implementations.

3.3.4 Experimental searches on the invisible axion

Given its small couplings to matter and radiation, the search for invisible axions is a complicated task.[8] One of the most promising approaches in the search for this type

[8] In this section we will focus on some of the most constraining axion limits, for a more exhaustive discussion on axion searches we refer the reader to the PDG review on this topic [66].

of axion comes from its coupling to photons. As we saw in Section 3.2, the axion couples to photons through the dimension 5 operator in Eq. (3.30). For practical convenience, it is useful to define the axion-photon coupling constant as

$$g_{a\gamma} = \frac{\alpha}{2\pi v_{\rm PQ}} C_{ag} C_{a\gamma}^{\rm eff} \,. \tag{3.65}$$

In various extensions of the SM, weakly coupled light pseudoscalar particles emerge naturally. However, the axion possesses (due to QCD effects) an inherent correlation between the photon coupling and its mass

$$(m_a/1\,{\rm eV}) \simeq 0.5\,\xi\, g_{10}\,, \tag{3.66}$$

where $g_{10} = |g_{a\gamma}| \times 10^{10}$ GeV and $\xi = 1/|C_{a\gamma}^{\rm eff}|$. The dimensionless coefficient ξ is in many axion models of order 1. In the DFSZ (type II and flipped) and KSVZ models ξ takes the approximate values 1.4 (0.8) and 0.5, respectively.[9]

Axion emission through its coupling to photons introduces a non-standard mechanism for stellar energy losses that could affect the stellar evolution. A strong bound to this process can be derived from globular-cluster stars [67]. These are homogeneous gravitationally bound systems of stars formed around the same time, allowing for detailed tests of stellar-evolution theory. The actual experimental bound gives $g_{10} \lesssim 1$ for axion masses up to 30 keV. The analysis of the evolution of massive stars lead to the bound $g_{10} \lesssim 0.8$, based on the fact that Cepheid variable stars exist [68]. An even more stringent bound from an updated analysis of 39 Galactic Globular Clusters has been reported [69], setting the limit $g_{10} \lesssim 0.66$ at 95% CL.

Instead of using stellar energy losses to constrain the axion, one can also directly search for axion fluxes coming from the Sun (helioscopes) or from galactic halos (haloscopes). Several helioscope and haloscopes experiments are currently involved in probing the $g_{a\gamma}$ coupling. The most powerful axion helioscope experiment is CAST, which searches for solar axions via axion-photon conversion using a dipole magnet directed towards the sun. CAST achieved the limit $g_{10} \lesssim 0.88$ for $m_a \lesssim 0.02\,{\rm eV}$, while slightly weaker bounds were obtained for heavier axions [70]. Still the astrophysical bounds represent a slight improvement over CAST results. It is expected that the next generation of axion helioscope experiments, such as the IAXO [71], will provide better bounds on the axion-photon couplings in the future. Microwave cavity haloscopes, including the ADMX, exclude a window for the axion around a few μeV [72–74]. These experiments search for cold dark matter axions in the local galactic dark matter halo.

On the other hand, the axion also receives interesting bounds from its coupling to electrons. Here, we define the axion-electron coupling constant as $h_{aee} = |g_e| m_e / v_{\rm PQ}$, with g_e given in Eq. (3.25). The axion-electron coupling is bounded from astrophysical sources. In globular clusters, energy losses in red-giant stars due to axion emission would delay helium-ignition and make the red-giant branch extend to brighter stars. This places the following upper bound on the axion-electron coupling, $h_{aee} \lesssim 3 \times 10^{-13}$ [75]. A more restrictive bound comes from white-dwarf cooling due

[9] For the KSVZ model we have taken the benchmark of $X_Q^{em} = 0$, with X_Q^{em} denoting the electric charge of the exotic color triplet Q.

to axion losses [67, 76],

$$h_{aee} < 1.3 \times 10^{-13} \quad \Rightarrow \quad v_{\rm PQ} > |g_e| \times (4 \times 10^9\,{\rm GeV})\,. \tag{3.67}$$

The bounds that can be extracted on the PQ symmetry breaking scale, or alternatively, on the axion mass, are very model dependent for this observable. The value of g_e not only depends on the particular charge assignments of the model considered but also on the vevs of the scalar fields. In some regions of the parameter space it is even possible to obtain $g_e \simeq 0$ so that white-dwarf cooling arguments would not place a strong bound on the axion mass, this is the case for instance for the tree-level value of g_e in the KSVZ model.[10] Taking the benchmark point $|g_e|/C_{ag} = 10^{-1}$ for example, implies the upper bound $m_a \lesssim 15$ meV. This bound together with the ones from CAST, IAXO and ADMX are shown in Figure 3.2.

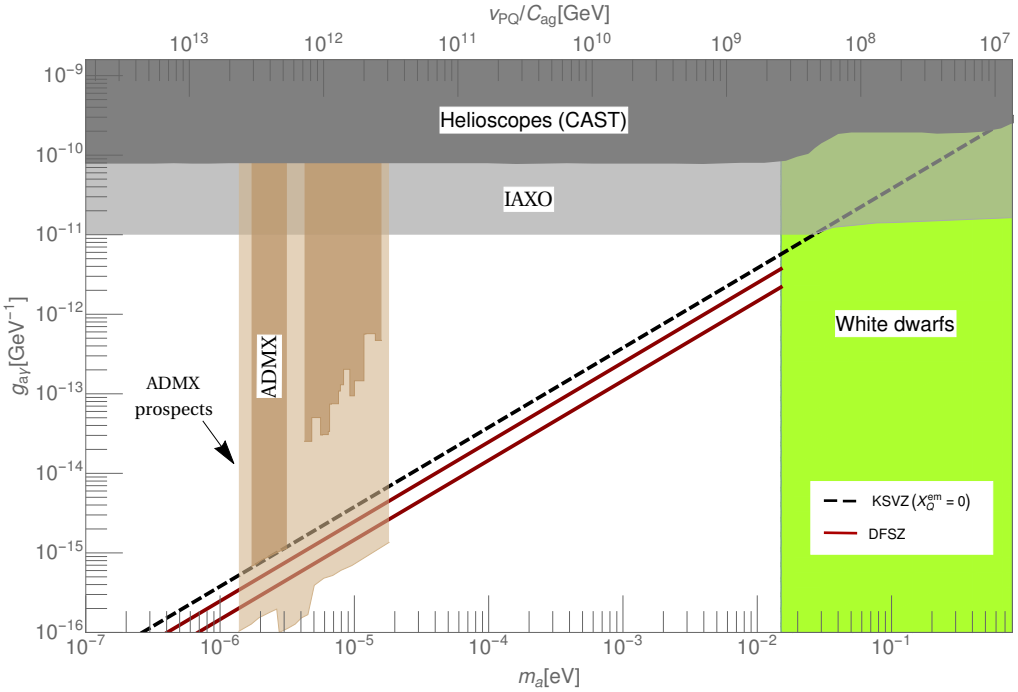

Figure 3.2: *Constraints on the DFSZ type II (flipped) and KSVZ invisible axions where searches axion-photon conversion and astrophysical considerations are considered. Also shown are the constraints from white-dwarfs cooling for the benchmark point* $|g_e|/C_{ag} = 10^{-1}$. *Figure adapted from Ref.* [77]

Finally, axion-nucleon interactions are constrained by the requirement that the neutrino signal of the supernova SN 1987A is not excessively shortened by axion losses [67, 78]. This constraint is typically of the same size as the one coming from white-dwarf cooling arguments. However, the SN 1987A limit involves many uncertainties which are not easy to quantify [67]. The axion couplings to matter can also be tested in terrestrial laboratories, with promising prospects of probing unexplored regions of the axion parameter space. Dark matter axions can cause transitions between atomic states that differ in energy by an amount equal to the axion mass. By

[10] For a very small axion-electron coupling one should also include the one loop contributions [28].

tuning the atomic states energy using the Zeeman effect it is possible in principle to detect axion dark matter candidates in the 10^{-4} eV mass range [79]. The axion can also be tested in dedicated laboratory experiments looking for oscillating nucleon EDMs [80–82], and, oscillating parity- and time reversal-violating effects in atoms and molecules [81, 82]. The proposed CASPEr for example, could cover the entire range of axion dark matter masses $m_a \lesssim \mu$eV by looking for oscillating EDMs in a nuclear magnetic resonance solid-state experiment [83].

Bibliography

[1] H. Y. Cheng, Phys. Rept. **158** (1988) 1.

[2] R. D. Peccei, Lect. Notes Phys. **741** (2008) 3 [hep-ph/0607268].

[3] J. E. Kim and G. Carosi, Rev. Mod. Phys. **82** (2010) 557 [arXiv:0807.3125 [hep-ph]].

[4] Y. Nambu, Phys. Rev. **117** (1960) 648.

[5] J. Goldstone, Nuovo Cim. **19** (1961) 154.

[6] J. Goldstone, A. Salam and S. Weinberg, Phys. Rev. **127** (1962) 965.

[7] S. Weinberg, Phys. Rev. D **11** (1975) 3583.

[8] G. 't Hooft, Phys. Rev. Lett. **37** (1976) 8.

[9] J. S. Bell and R. Jackiw, Nuovo Cim. A **60** (1969) 47.

[10] S. L. Adler, Phys. Rev. **177** (1969) 2426.

[11] W. A. Bardeen, Phys. Rev. **184** (1969) 1848.

[12] W. A. Bardeen, Nucl. Phys. B **75** (1974) 246.

[13] C. A. Baker *et al.*, Phys. Rev. Lett. **97** (2006) 131801 [hep-ex/0602020].

[14] V. Baluni, Phys. Rev. D **19** (1979) 2227.

[15] G. 't Hooft, Phys. Rev. D **14** (1976) 3432 Erratum: [Phys. Rev. D **18** (1978) 2199].

[16] D. B. Kaplan and A. V. Manohar, Phys. Rev. Lett. **56** (1986) 2004.

[17] J. Gasser and H. Leutwyler, Phys. Rept. **87** (1982) 77.

[18] D. R. Nelson, G. T. Fleming and G. W. Kilcup, Phys. Rev. Lett. **90** (2003) 021601 [hep-lat/0112029].

[19] R. D. Peccei and H. R. Quinn, Phys. Rev. Lett. **38** (1977) 1440.

[20] S. Weinberg, Phys. Rev. Lett. **40** (1978) 223.

[21] F. Wilczek, Phys. Rev. Lett. **40** (1978) 279.

[22] W. A. Bardeen and S.-H. H. Tye, Phys. Lett. **74B** (1978) 229.

[23] M. Gell-Mann, R. J. Oakes and B. Renner, Phys. Rev. **175** (1968) 2195.

[24] S. Weinberg, "The quantum theory of fields. Vol. 2: Modern applications", Cambridge University Press, New York (1996)

[25] G. Grilli di Cortona, E. Hardy, J. Pardo Vega and G. Villadoro, JHEP **1601** (2016) 034 [arXiv:1511.02867 [hep-ph]].

[26] K. Choi, K. Kang and J. E. Kim, Phys. Lett. B **181** (1986) 145.

[27] I. Antoniadis and T. N. Truong, Phys. Lett. **109B** (1982) 67.

[28] M. Srednicki, Nucl. Phys. B **260** (1985) 689.

[29] M. Hindmarsh and P. Moulatsiotis, Phys. Rev. D **56** (1997) 8074 [hep-ph/9708281].

[30] J. Beringer *et al.* [Particle Data Group], Phys. Rev. D **86** (2012) 010001.

[31] S. L. Glashow and S. Weinberg, Phys. Rev. D **15** (1977) 1958.

[32] M. Bona *et al.* [UTfit Collaboration], JHEP **0803** (2008) 049 [arXiv:0707.0636 [hep-ph]].

[33] A. A. Anselm and N. G. Uraltsev, Phys. Lett. **114B** (1982) 39.

[34] A. A. Anselm, JETP Lett. **36** (1982) 55.

[35] A. A. Anselm, CERN-TH-4349/86.

[36] S. S. Adler *et al.* [E787 Collaboration], Phys. Lett. B **537** (2002) 211 [hep-ex/0201037].

[37] J. Preskill, M. B. Wise and F. Wilczek, Phys. Lett. **120B** (1983) 127.

[38] P. Minkowski, Phys. Lett. **67B** (1977) 421.

[39] Y. Chikashige, R. N. Mohapatra and R. D. Peccei, Phys. Lett. **98B** (1981) 265.

[40] J. E. Kim, Phys. Rev. Lett. **43** (1979) 103.

[41] M. A. Shifman, A. I. Vainshtein and V. I. Zakharov, Nucl. Phys. B **166** (1980) 493.

[42] A. R. Zhitnitsky, Sov. J. Nucl. Phys. **31** (1980) 260 [Yad. Fiz. **31** (1980) 497].

[43] M. Dine, W. Fischler and M. Srednicki, Phys. Lett. **104B** (1981) 199.

[44] P. Sikivie, Phys. Rev. Lett. **48** (1982) 1156.

[45] Y. B. Zeldovich, I. Y. Kobzarev and L. B. Okun, Zh. Eksp. Teor. Fiz. **67** (1974) 3 [Sov. Phys. JETP **40** (1974) 1].

[46] A. Vilenkin, Phys. Rept. **121** (1985) 263.

[47] S. M. Barr, K. Choi and J. E. Kim, Nucl. Phys. B **283** (1987) 591.

[48] D. H. Lyth, Phys. Lett. B **236** (1990) 408.

[49] B. Holdom, Phys. Rev. D **27** (1983) 332.

[50] L. F. Abbott and M. B. Wise, Nucl. Phys. B **325** (1989) 687.

[51] T. Banks, Physicalia Mag. **12** (1990) 19.

[52] T. Hiramatsu, M. Kawasaki, K. Saikawa and T. Sekiguchi, JCAP **1301** (2013) 001 [arXiv:1207.3166 [hep-ph]].

[53] S. Ghigna, M. Lusignoli and M. Roncadelli, Phys. Lett. B **283** (1992) 278.

[54] R. Holman, S. D. H. Hsu, T. W. Kephart, E. W. Kolb, R. Watkins and L. M. Widrow, Phys. Lett. B **282** (1992) 132 [hep-ph/9203206].

[55] M. Kamionkowski and J. March-Russell, Phys. Lett. B **282** (1992) 137 [hep-th/9202003].

[56] H. M. Georgi, L. J. Hall and M. B. Wise, Nucl. Phys. B **192** (1981) 409.

[57] S. M. Barr and D. Seckel, Phys. Rev. D **46** (1992) 539.

[58] R. Kallosh, A. D. Linde, D. A. Linde and L. Susskind, Phys. Rev. D **52** (1995) 912 [hep-th/9502069].

[59] B. A. Dobrescu, Phys. Rev. D **55** (1997) 5826 [hep-ph/9609221].

[60] K. w. Choi, Phys. Rev. Lett. **92** (2004) 101602 [hep-ph/0308024].

[61] G. Dvali, S. Folkerts and A. Franca, Phys. Rev. D **89** (2014) no.10, 105025 [arXiv:1312.7273 [hep-th]].

[62] T. Banks and M. Dine, Phys. Rev. D **45** (1992) 1424 [hep-th/9109045].

[63] K. S. Babu, I. Gogoladze and K. Wang, Phys. Lett. B **560** (2003) 214 [hep-ph/0212339].

[64] A. G. Dias, V. Pleitez and M. D. Tonasse, Phys. Rev. D **67** (2003) 095008 [hep-ph/0211107].

[65] A. G. Dias, A. C. B. Machado, C. C. Nishi, A. Ringwald and P. Vaudrevange, JHEP **1406** (2014) 037 [arXiv:1403.5760 [hep-ph]].

[66] C. Patrignani *et al.* [Particle Data Group], Chin. Phys. C **40** (2016) no.10, 100001.

[67] G. G. Raffelt, Lect. Notes Phys. **741** (2008) 51 [hep-ph/0611350].

[68] A. Friedland, M. Giannotti and M. Wise, Phys. Rev. Lett. **110** (2013) no.6, 061101 [arXiv:1210.1271 [hep-ph]].

[69] A. Ayala, I. Domínguez, M. Giannotti, A. Mirizzi and O. Straniero, Phys. Rev. Lett. **113** (2014) no.19, 191302 [arXiv:1406.6053 [astro-ph.SR]].

[70] K. Zioutas *et al.* [CAST Collaboration], Phys. Rev. Lett. **94** (2005) 121301 [hep-ex/0411033].

[71] I. G. Irastorza *et al.*, JCAP **1106** (2011) 013 [arXiv:1103.5334 [hep-ex]].

[72] S. De Panfilis *et al.*, Phys. Rev. Lett. **59** (1987) 839.

[73] S. J. Asztalos *et al.* [ADMX Collaboration], Phys. Rev. D **69** (2004) 011101 [astro-ph/0310042].

[74] G. Carosi, A. Friedland, M. Giannotti, M. J. Pivovaroff, J. Ruz and J. K. Vogel, arXiv:1309.7035 [hep-ph].

[75] G. Raffelt and A. Weiss, Phys. Rev. D **51** (1995) 1495 [hep-ph/9410205].

[76] M. M. Miller Bertolami, B. E. Melendez, L. G. Althaus and J. Isern, JCAP **1410** (2014) no.10, 069 [arXiv:1406.7712 [hep-ph]].

[77] A. Celis, J. Fuentes-Martin and H. Serodio, Phys. Lett. B **741** (2015) 117 [arXiv:1410.6217 [hep-ph]].

[78] W. Keil, H. T. Janka, D. N. Schramm, G. Sigl, M. S. Turner and J. R. Ellis, Phys. Rev. D **56** (1997) 2419 [astro-ph/9612222].

[79] P. Sikivie, Phys. Rev. Lett. **113** (2014) no.20, 201301 [arXiv:1409.2806 [hep-ph]].

[80] P. W. Graham and S. Rajendran, Phys. Rev. D **84** (2011) 055013 [arXiv:1101.2691 [hep-ph]].

[81] Y. V. Stadnik and V. V. Flambaum, Phys. Rev. D **89** (2014) no.4, 043522 [arXiv:1312.6667 [hep-ph]].

[82] B. M. Roberts, Y. V. Stadnik, V. A. Dzuba, V. V. Flambaum, N. Leefer and D. Budker, Phys. Rev. D **90** (2014) no.9, 096005 [arXiv:1409.2564 [hep-ph]].

[83] D. Budker, P. W. Graham, M. Ledbetter, S. Rajendran and A. Sushkov, Phys. Rev. X **4** (2014) no.2, 021030 [arXiv:1306.6089 [hep-ph]].

CHAPTER

4 Effective Field Theories

> "We demand rigidly defined areas of doubt and uncertainty!"
>
> — *Douglas Adams*, The Hitchhiker's Guide to the Galaxy

When one aims for the description of a particular phenomenon, it is useful to isolate those degrees of freedom that give the most relevant effects, allowing us to obtain a simplified framework without the need to know every aspect of its dynamics. This is the philosophy behind EFTs [1–4], which essentially consists in considering that the dynamics of the systems at low energies cannot depend on the details at high energies. Notice that whenever we are talking about low or high energies, we are setting a scale and, at the same time, establishing a range of validity for the effective theory. As long as we remain within its range of applicability, i.e. at energies below the high-energy scale, the EFT gives a complete and unitary description of the physical phenomena [5]. This way, low-energy physics can be described by an effective Lagrangian which only contains the degrees of freedom that are relevant at the low-energy scale, while additional degrees of freedom, that are more important at higher energies, are removed from the effective description and their effects are encoded as an expansion weighted by inverse powers of the high-energy scale. Eliminating these degrees of freedom produces a great simplification in our physical description, which can be systematically improved by adding higher-order terms in the effective expansion.

An interesting feature of EFTs is that one does not need to know what is the fundamental theory behind the effective one. When this happens, EFTs could be a useful tool not only to describe the low-energy dynamics but also to extract useful information about any possible more fundamental theory. The standard procedure in the construction of an EFT when the high-energy theory is unknown is first to determine the relevant degrees of freedom of the theory, the symmetries of the system, and the power counting for the effective expansion (related to the range of validity of the theory). Once we know that, the most general local Lagrangian containing these fields and respecting these symmetries is constructed order by order in this expansion. It is expected that possible heavy NP that decouples at low energies manifests as a specific pattern on the low-energy couplings of the expansion, i.e. the WCs of the EFT. We can analyze the marks of the underlying high-energy theory upon comparison with the low-energy scale phenomenology, and in this way obtain information on the NP dynamics. This is the approach one typically uses

when obtaining constraints on NP scenarios from the SMEFT or from the WET, both of which will be introduced in Section 4.2. While this approach is completely independent of the NP model, it is interesting to compare the results obtained in the EFT with those one would expect from a given UV model. For this, it is important to have general techniques that allow us to connect, in a simple manner, an arbitrary UV model to its corresponding effective description.

There are two equivalent approaches for the construction of EFTs from a more fundamental theory. The most employed one amounts to matching in the full theory and in the EFT the diagrammatic computation of given Green functions with light-particle external legs. This is done at energies below the high-energy scale, where the EFT description of the dynamics remains valid. Another approach, which is of more interest for this thesis, consists in performing the functional integration of the heavy states without being concerned with specific Green Functions, and later extract the local contributions that are relevant for the description of the low-energy dynamics of the light fields. Functional integration techniques have obvious advantages over the matching procedure as, for instance, one does not need to handle Feynman diagrams nor symmetry factors, and one obtains directly the whole set of EFT operators together with their matching conditions, i.e. no prior knowledge about the specifics of the EFT operator structure, symmetries, etc., is required. In the next section we will show how this method can be applied at tree level while we leave the discussion about the extension of this technique to one-loop order to Chapter 6.

4.1 Effective Field Theories from the path integral

The physical information of a given field theory is contained in its Green functions. The *Feynman path integral* [6–10] provides a useful tool to handle this information since it provides a closed expression for the generating functional of the Green functions, which is given by the partition function

$$Z\left[J_L, J_H\right] = \mathcal{N} \int \mathcal{D}\eta_L \, \mathcal{D}\eta_H \, \exp\left\{ i \int d^d x \, \left(\mathcal{L}\left[\eta_L, \eta_H\right] + J_L \, \eta_L + J_H \, \eta_H \right) \right\} , \quad (4.1)$$

in terms of the Lagrangian of the theory $\mathcal{L}\left[\eta_L, \eta_H\right]$. Here we have explicitly separated the fields of the theory, $\eta = (\eta_H, \eta_L)$, into those that we consider heavy, η_H, and the ones we treat as light fields, that we denote as η_L. On the other hand J_L (J_H) denote external sources for the light (heavy) fields, $\mathcal{D}\eta_{L,H}$ is the path integral measure for the corresponding fields and $\mathcal{N}$ is a normalization factor. In what follows, we set to zero the external current for the heavy fields since, for the calculation of the EFT, the Green functions that we need are those with only light-particles in the external legs.

Our aim is to remove the heavy fields from the theory in favor of an effective description in terms of only light fields, for which we need to "integrate out" the heavy fields from the path integral. Before we do that, it is convenient to use the BFM [11–18]. This method consists in separating the fields into a background field

configuration, $\hat{\eta}_{L,H}$, which satisfies the classical EOMs,

$$\frac{\delta\mathcal{L}}{\delta\eta_L}\left[\hat{\eta}_L,\hat{\eta}_H\right]+J_L=0\,,\qquad \frac{\delta\mathcal{L}}{\delta\eta_H}\left[\hat{\eta}_L,\hat{\eta}_H\right]=0\,, \tag{4.2}$$

with the *variational derivative* acting on the Lagrangian, and quantum fluctuations, i.e. we write

$$\eta_L\to\hat{\eta}_L+\eta_L\,,\qquad \eta_H\to\hat{\eta}_H+\eta_H\,. \tag{4.3}$$

Diagrammatically, the background configuration corresponds to tree lines in Feynman graphs while lines inside loops arise from the quantum fields; this means that terms higher than quadratic in the quantum fields yield vertices that can only appear in diagrams at higher loop orders. This separation is particularly useful for several reasons: on the one hand, it allows for the quantization of the fields in a way that preserves explicit gauge invariance of the background fields, even after having included the gauge-fixing and ghost terms; on the other hand, it allows us to rewrite the Lagrangian plus source terms as an expansion in the number of quantum fields

$$\mathcal{L}\left[\eta\right]+J_L\,\eta_L=\mathcal{L}[\hat{\eta}]+J_L\,\hat{\eta}_L+\mathcal{L}^{(\eta^2)}[\hat{\eta},\eta]+\mathcal{O}\left(\eta^3\right)\,, \tag{4.4}$$

where the zeroth order term, $\mathcal{L}[\hat{\eta}]$, depends only on the classical field configurations and yields the tree-level effective action (as we will see later). Linear terms in η in the expansion around the background fields are, up to a total derivative, proportional to the EOMs and thus vanish. The term quadratic in the quantum fields, $\mathcal{L}^{(\eta^2)}$, contains all the one-loop contributions and will be further analyzed in Chapter 6, while terms with three or more quantum fields yield higher-order loops and are not of interest for this thesis.

We can rewrite the partition function in Eq. (4.1) as

$$Z\left[J_L,J_H=0\right]\simeq\mathcal{N}\int\mathcal{D}\eta_L\,\mathcal{D}\eta_H\,\exp\left\{i\int d^dx\left(\mathcal{L}[\hat{\eta}]+J_L\,\hat{\eta}_L+\mathcal{L}^{(\eta^2)}\left[\hat{\eta},\eta\right]\right)\right\}, \tag{4.5}$$

where we removed the terms contributing beyond one-loop order. The corresponding effective action is obtained from a Legendre transform of the partition function and reads

$$iS\left[\hat{\eta}\right]=\ln\,Z\left[J_L,J_H=0\right]-i\int d^dx\,J_L\hat{\eta}_L\,, \tag{4.6}$$

which, using the expression in Eq. (4.5), simply gives

$$e^{iS[\hat{\eta}]}\simeq\mathcal{N}\int\mathcal{D}\eta_L\,\mathcal{D}\eta_H\,\exp\left\{i\int d^dx\,\left(\mathcal{L}[\hat{\eta}]+\mathcal{L}^{(\eta^2)}\left[\hat{\eta},\eta\right]\right)\right\}\,. \tag{4.7}$$

The term $\mathcal{L}[\hat{\eta}]$ is independent of the quantum fields and can be taken out of the path integral yielding the result

$$S\left[\hat{\eta}\right]\simeq\int d^dx\,\mathcal{L}\left[\hat{\eta}\right]+S^{1\text{loop}}\left[\hat{\eta}\right]\,, \tag{4.8}$$

where we defined the one-loop effective action as

$$e^{iS^{1\text{loop}}[\hat{\eta}]} = \mathcal{N} \int \mathcal{D}\eta_L \, \mathcal{D}\eta_H \, \exp\left\{ i \int d^d x \, \mathcal{L}^{(\eta^2)} \left[\hat{\eta}, \eta\right] \right\} . \tag{4.9}$$

A systematic method to obtain the one-loop EFT from the one-loop effective action will be discussed in Chapter 6. Here we simply ignore this contribution and focus on the tree-level EFT, which is obtained from $\mathcal{L}[\hat{\eta}]$ upon removing the background heavy fields; these can be written in terms of the light fields by using their EOMs, given in the second equation in (4.2). The resulting effective action will be a non-local function of the light fields

$$S^{\text{tree}}\left[\hat{\eta}_L\right] = \int d^d x \, \mathcal{L}\left[\hat{\eta}_L, \hat{\eta}_H[\hat{\eta}_L]\right] . \tag{4.10}$$

At energies much lower than the mass of the heavy fields, m_H, we can solve pertubatively their EOMs, in an expansion in inverse powers of m_H. This allows us to expand the expression in the r.h.s in a series of local (effective) operators, $\mathcal{O}_i$, which finally leads to the effective Lagrangian

$$S^{\text{tree}}_{\text{EFT}}[\hat{\eta}_L] = \int d^d x \, \mathcal{L}^{\text{tree}}_{\text{EFT}}[\hat{\eta}_L] = \int d^d x \sum_i c_i(m_H) \, \mathcal{O}_i[\hat{\eta}_L] , \tag{4.11}$$

where the corresponding WCs, $c_i(m_H)$, will appear as a polynomial expansion in powers of m_H.

In the next section we will provide examples of EFTs within the SM framework. These are of great importance in the analysis of possible NP that extends the SM at high energies. In particular, in Section 4.2.2 we will provide an explicit example of the application of the method to obtain the Fermi Lagrangian.

4.2 Effective field theories within the SM

The SM is an extremely successful theory that yields accurate predictions for the outcome of a wide range of high-energy experiments at both the intensity and energy frontiers. However, as we have already commented, the lack of an explanation within the SM to several theoretical and experimental problems makes this theory incomplete. On the other hand, the SM has been tested to very high accuracy over the last decades. This has strong implications for the possible NP scenarios, which are typically required to involve high-mass scales, and most manifestations of NP are expected to show up above the TeV scale. This situation makes EFTs particularly useful to describe the possible NP extensions. Indeed following the EFT philosophy, the SM can be seen as the lowest contribution of an EFT whose higher-order operators parametrize the effects of any possible underlying NP theory that decouples at low energies. This is the so-called SMEFT, whose major features will be outlined in Section 4.2.1.

The masses of the SM particles span several orders of magnitude. When one aims to describe the dynamics at lower energies it is useful to "integrate out" those

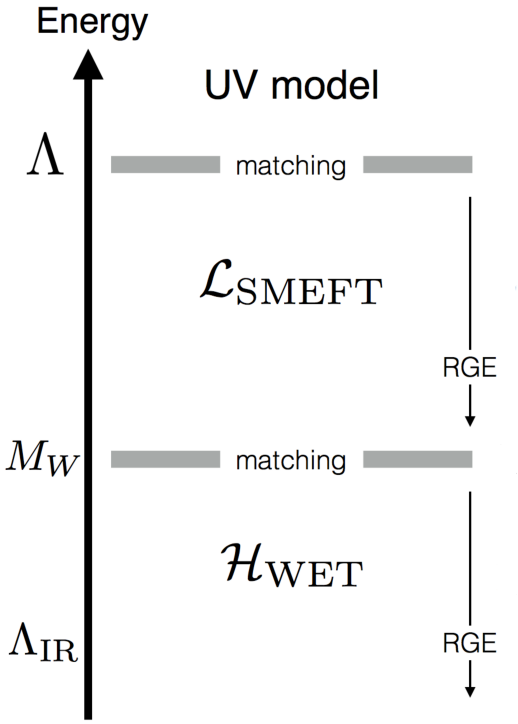

Figure 4.1: *Illustration of the matching and running procedures in the SMEFT and the WET. Figure taken from Ref. [19]*

particles that, being heavier, appear suppressed in the dynamics of the problem. For this reason it is convenient to trade the full-theory top, higgs, and weak gauge bosons contributions by effective operators in order to describe the physics at the b-mass scale which, as we will see in Chapter 7, is a region of great phenomenological interest. The resulting EFT is often called WET. It is crucial for the WET to include one-loop effects since many of its features that do not appear at tree-level happen at one loop. This is because, as we commented in Section 1.2, FCNCs only appear in the SM at one loop. For a coherent description of the one-loop dynamics it is also necessary to perform the running of the WCs of the SMEFT down to the matching scale of the WET (i.e. around the W mass) and of the WET WCs to the b-mass scale or any other low-energy scale of phenomenological interest. This whole procedure is illustrated in Figure 4.1. The complete RGE of the WCs of the SMEFT were calculated in Refs. [20–23] while the matching and running of these operators in the WET was performed in Ref. [24].[1] These results can be used in an automated way with the Mathematica package DsixTools [19].

4.2.1 The Standard Model Effective Theory

The great number of NP theories and the lack for a clear guiding principle that could tell us which of them (if any) provides a true description of Nature makes necessary the use of model-independent techniques. In this sense, if we assume that the NP that extends the SM decouples at low energies, we can embed the SM in a EFT framework where any possible heavy degrees of freedom have been integrated

[1] See also Ref. [25] for the matching between the SMEFT and the WET at one loop, and Refs. [26–36] for the anomalous dimension in the SM operator basis, i.e. not including the effects of the SMEFT dimension-six operators.

out. In this way the SM appears as the lowest-order terms in an effective expansion where NP effects are encoded in the WCs of an expansion of higher-dimensional local operators, which depend only on SM fields, suppressed by the high energy scale. The SMEFT gives the most general low-energy description compatible with the SM fields and gauge symmetry[2]

$$\mathcal{L} = \mathcal{L}_{\rm SM} + \frac{1}{\Lambda}\sum_k C_k^{(5)} Q_k^{(5)} + \frac{1}{\Lambda^2}\sum_k C_k^{(6)} Q_k^{(6)} + \mathcal{O}\left(\frac{1}{\Lambda^3}\right), \tag{4.12}$$

where Λ denotes the new physics scale, typically associated with the mass of a heavy particle or set of particles, which is assumed to be much larger than the electroweak scale. The SM Lagrangian only contains dimension-two and -four operators. There is only one dimension-five operator, the Weinberg operator, that gives a Majorana mass term for the neutrinos after EW symmetry breaking [41]. A complete list of dimension-six operators was first presented in Ref. [42]. However, it was shown in Refs. [43–46] that some of the operators in this list were redundant, since they can be related by using the EOMs [14, 47–50]. A non-redundant basis of dimension-six operators was introduced in Ref. [51] and is commonly known as the *Warsaw basis*. Ignoring flavor indices and assuming baryon number conservation, the dimension-six basis has 59 operators, of which some are non-Hermitian and therefore have complex WCs. This leads to a total of 76 real WCs. If we also take into account flavor indices, the dimension-six basis contains 1350 CP-even and 1149 CP-odd operators, resulting in a total of 2499 hermitian operators [22]. The complete set of independent dimension-six baryon-number-violating operators was identified in Ref. [52], and barring flavor indices it is formed by four operators.

4.2.2 The Weak Effective Theory

Except for the top quark, the SM fermions have a mass which is much lower than the ones of the weak gauge bosons, the W and the Z. For this reason, it is convenient to describe the low-energy dynamics of the weak interactions in an EFT framework where those degrees of freedom that are much heavier than the b quark have been integrated out. Following the approach in Section 4.1, the first step to construct this EFT is to evaluate the SM Lagrangian in the background fields, i.e $\mathcal{L}_{\rm SM}[\hat{\eta}_L, \hat{\eta}_H]$. In this expression η_H corresponds to the heavy fields we want to integrate, i.e. $\eta_H = W, Z, h, t$, and η_L to the light ones, which in this case are given by the rest of SM fields. At energies much lower than the mass of the heavy fields, this expression is then expanded in powers of the heavy masses, yielding the corresponding EFT for the weak interactions.

Since we are mostly interested in flavor violating transitions in this thesis, let us perform as an example the tree-level integration of the W up to $\mathcal{O}\left(M_W^{-2}\right)$, whose

[2]By construction the SMEFT does not include any possible light NP such as light right-handed neutrinos, axions or axion-like particles (see for example Ref. [37,38] for an EFT framework where axion-like particles have been included). Moreover, the SMEFT assumes that the electroweak symmetry breaking is triggered, as in the SM, by a Higgs doublet; a more general EFT that considers a generic non-linear realization of the electroweak symmetry breaking has been considered for instance in Refs. [39, 40].

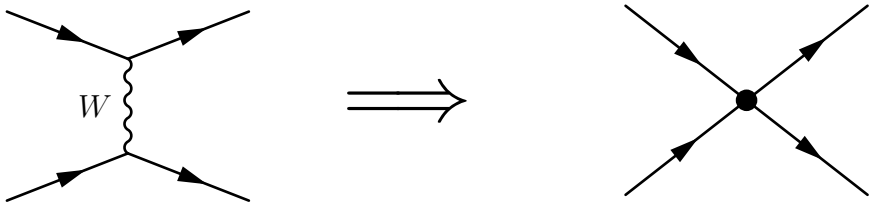

Figure 4.2: *Illustration of the procedure of integrating out the W boson. At low energies, the lowest order effects of the W-exchange are reduced to a four-fermion interaction.*

result is the so-called Fermi theory. In this case we only have to obtain the W background configuration, $\hat{W}$, in terms of the background light fields. From the EOM of $\hat{W}$ we get

$$\frac{\delta \mathcal{L}_{\rm SM}}{\delta W_\mu^\dagger}\left[\hat{\eta}_L, \hat{\eta}_H\right] = M_W^2\, \hat{W}^\mu + \frac{g}{\sqrt{2}}\left(\overline{\hat{u}_L}\gamma^\mu\, V \hat{d}_L + \overline{\hat{\nu}_L}\gamma^\mu \hat{e}_L\right) + \cdots = 0\,, \tag{4.13}$$

where we have omitted the contributions from the kinetic term of the W and terms with two or more heavy fields, which would yield higher-order terms in the expansion in M_W^{-1}. From this equation one immediately obtains the value of $\hat{W}$ in terms of the background light fields

$$\hat{W}_\mu = -\frac{g}{\sqrt{2} M_W^2}\, \mathcal{J}_\mu + \mathcal{O}\left(M_W^{-4}\right)\,, \tag{4.14}$$

where the fermion current is defined as

$$\mathcal{J}_\mu \equiv \overline{\hat{u}_L}\gamma_\mu V \hat{d}_L + \overline{\hat{\nu}_L}\gamma_\mu \hat{e}_L\,. \tag{4.15}$$

Inserting the expression in Eq. (4.14) into the SM Lagrangian and expanding up to $\mathcal{O}\left(M_W^{-2}\right)$, it is straightforward to get the following effective Lagrangian for the W interactions

$$\mathcal{L}_{\rm Fermi} = -\frac{4\, G_F}{\sqrt{2}}\, \mathcal{J}_\mu{}^\dagger \mathcal{J}^\mu\,, \tag{4.16}$$

with the Fermi coupling constant defined as

$$\frac{G_F}{\sqrt{2}} \equiv \frac{g^2}{8\, M_W^2}\,. \tag{4.17}$$

As we see, the effects of the W at lowest order are reduced to an effective four-fermion interaction, situation that is depicted in Figure 4.2. The corresponding WCs for these four-fermion interactions receive a suppression of $\mathcal{O}\left(M_W^{-2}\right)$ through the Fermi constant, showing that the effects of these interactions decouple when M_W is taken to infinity. Expanding further in Eqs. (4.13) and (4.14) we would get operators of higher dimension that would yield higher-order corrections to the interactions in Eq. (4.16).

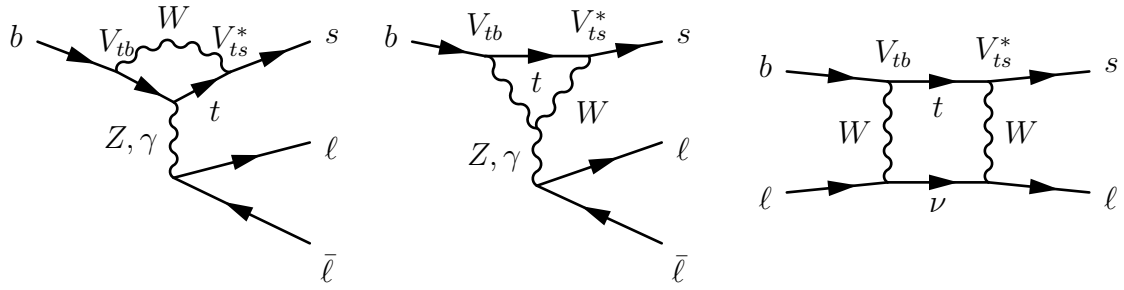

Figure 4.3: *Diagrams contributing to $\mathcal{O}^\ell_{9,10}$ in the SM. Leaving the photon leg unattached in the first two diagrams we get the corresponding contributions to $\mathcal{O}_7$.*

Integrating out the Z in the SM would give a similar result but in this case the corresponding four-fermion interactions would be flavor conserving. This result is expected, since as we discussed in Section 1.2, the SM has no tree-level FCNCs. The situation changes at one loop and FCNCs appear through transitions like the ones shown in Figure 4.3. Since one-loop corrections introduce completely new effects, these are crucial in the description of low-energy phenomena in terms of the WET. Given that $b \to s\ell^+\ell^-$ transitions are of special interest for some of the topics addressed in this thesis, we show explicitly the part of the WET related to these transitions [53–55][3]

$$\mathcal{H}_{\rm WET} \supset -\frac{4G_F}{\sqrt{2}}\,\frac{e^2}{16\pi^2}\,V_{tb}V_{ts}^*\sum_{i,\ell}\Big[C_i^\ell\,\mathcal{O}_i^\ell + h.c.\Big] + \mathcal{H}_{\rm eff}^{b\to s\gamma}\,, \tag{4.18}$$

where the operators

$$\begin{aligned}
\mathcal{O}_9^\ell &= (\bar{s}\gamma_\mu P_L b)\left(\bar{\ell}\gamma^\mu\ell\right)\,, & \mathcal{O}_{9'}^\ell &= (\bar{s}\gamma_\mu P_R b)\left(\bar{\ell}\gamma^\mu\ell\right)\,,\\
\mathcal{O}_{10}^\ell &= (\bar{s}\gamma_\mu P_L b)\left(\bar{\ell}\gamma^\mu\gamma_5\ell\right)\,, & \mathcal{O}_{10'}^\ell &= (\bar{s}\gamma_\mu P_R b)\left(\bar{\ell}\gamma^\mu\gamma_5\ell\right)\,,\\
\mathcal{O}_S^\ell &= m_b(\bar{s}P_R b)(\bar{\ell}\ell)\,, & \mathcal{O}_{S'}^\ell &= m_b(\bar{s}P_L b)(\bar{\ell}\ell)\,,\\
\mathcal{O}_P^\ell &= m_b(\bar{s}P_R b)(\bar{\ell}\gamma_5\ell)\,, & \mathcal{O}_{P'}^\ell &= m_b(\bar{s}P_L b)(\bar{\ell}\gamma_5\ell)\,,
\end{aligned} \tag{4.19}$$

with $\ell = e,\mu,\tau$ and $P_{L,R} = 1/2(1 \mp \gamma_5)$, constitute a complete basis for the four-fermion operators involving the $b \to s\ell^+\ell^-$ interaction. The piece $\mathcal{H}_{\rm eff}^{b\to s\gamma}$ gives the effective Hamiltonian for the radiative transitions including dipole operators [56]

$$\mathcal{O}_7 = \frac{m_b}{e}\,(\bar{s}\,\sigma_{\mu\nu}\,P_R\,b)\;F^{\mu\nu}, \qquad \mathcal{O}_{7'} = \frac{m_b}{e}\,(\bar{s}\,\sigma_{\mu\nu}\,P_L\,b)\;F^{\mu\nu}. \tag{4.20}$$

In the SM only the C_7, C_9^ℓ and C_{10}^ℓ WCs receive non-negligible contributions, through diagrams like the ones showed in Figure 4.3 (see e.g. Refs. [57,58] for the numerical

[3]For historical reasons it is common to use a Hamiltonian instead of a Lagrangian in this case. The only difference is a global sign in the interactions. Also, given that all the fields appearing in the EFT are classical and there is no room for confusion, in what follows we omit the hat in the fields for notational simplicity.

values including next-to-leading-order QCD corrections). At the b-quark mass scale C_9^ℓ and C_{10}^ℓ satisfy the approximate relation in the SM: $C_9^{\mathrm{SM}\,\ell}(m_b) \simeq -C_{10}^{\mathrm{SM}\,\ell}(m_b) \simeq 4.2$, which is lepton-family universal. However NP interactions could modify these WCs and/or induce other WCs that are not present in the SM alone. As we will see in the next chapter, there are several experimental anomalies that hint that this indeed might be the case for the WCs of some of the operators in Eq. (4.19).

Bibliography

[1] H. Georgi, Ann. Rev. Nucl. Part. Sci. **43** (1993) 209.

[2] A. V. Manohar, Lect. Notes Phys. **479** (1997) 311 [hep-ph/9606222].

[3] J. Wudka, Int. J. Mod. Phys. A **9** (1994) 2301 [hep-ph/9406205].

[4] A. Pich, *Summer School in Theoretical Physics, NATO Advanced Study Institute, 68th session, Les Houches, France, July 28-September 5, 1997*, [hep-ph/9806303].

[5] S. Weinberg, Physica A **96** (1979) 327.

[6] R. P. Feynman, Rev. Mod. Phys. **20** (1948) 367.

[7] J. S. Schwinger, Proc. Nat. Acad. Sci. **37** (1951) 452.

[8] R.P. Feynman and A.R. Hibbs, "Quantum Mechanics and Path Integrals", McGraw-Hill, New York, USA (1965)

[9] G. Roepstorff, "Path integral approach to quantum physics: An Introduction," Springer, Berlin, Germany (1994)

[10] M. Bohm, A. Denner and H. Joos, "Gauge theories of the strong and electroweak interaction," Teubner, Stuttgart, Germany (2001)

[11] B. S. DeWitt, Phys. Rev. **162** (1967) 1195.

[12] G. 't Hooft, Acta Universitatis Wratislavensis **368** (1976) 345.

[13] H. Kluberg-Stern and J. B. Zuber, Phys. Rev. D **12** (1975) 482.

[14] H. Kluberg-Stern and J. B. Zuber, Phys. Rev. D **12** (1975) 3159.

[15] B. Berg, Phys. Lett. **104B** (1981) 475.

[16] C. F. Hart, Phys. Rev. D **28** (1983) 1993.

[17] L. F. Abbott, Nucl. Phys. B **185** (1981) 189.

[18] L. F. Abbott, Acta Phys. Polon. B **13** (1982) 33.

[19] A. Celis, J. Fuentes-Martin, A. Vicente and J. Virto, arXiv:1704.04504 [hep-ph], https://dsixtools.github.io.

[20] E. E. Jenkins, A. V. Manohar and M. Trott, JHEP **1310** (2013) 087 [arXiv:1308.2627 [hep-ph]].

[21] E. E. Jenkins, A. V. Manohar and M. Trott, JHEP **1401** (2014) 035 [arXiv:1310.4838 [hep-ph]].

[22] R. Alonso, E. E. Jenkins, A. V. Manohar and M. Trott, JHEP **1404** (2014) 159 [arXiv:1312.2014 [hep-ph]].

[23] R. Alonso, H. M. Chang, E. E. Jenkins, A. V. Manohar and B. Shotwell, Phys. Lett. B **734** (2014) 302 [arXiv:1405.0486 [hep-ph]].

[24] J. Aebischer, M. Fael, C. Greub and J. Virto, arXiv:1704.06639 [hep-ph].

[25] J. Aebischer, A. Crivellin, M. Fael and C. Greub, JHEP **1605** (2016) 037 doi:10.1007/JHEP05(2016)037 [arXiv:1512.02830 [hep-ph]].

[26] A. J. Buras, M. Jamin, M. E. Lautenbacher and P. H. Weisz, Nucl. Phys. B **400** (1993) 37 doi:10.1016/0550-3213(93)90397-8 [hep-ph/9211304].

[27] M. Ciuchini, E. Franco, G. Martinelli and L. Reina, Nucl. Phys. B **415** (1994) 403 doi:10.1016/0550-3213(94)90118-X [hep-ph/9304257].

[28] M. Misiak and M. Munz, Phys. Lett. B **344** (1995) 308 doi:10.1016/0370-2693(94)01553-O [hep-ph/9409454].

[29] K. G. Chetyrkin, M. Misiak and M. Munz, Phys. Lett. B **400** (1997) 206 Erratum: [Phys. Lett. B **425** (1998) 414] doi:10.1016/S0370-2693(97)00324-9 [hep-ph/9612313].

[30] K. G. Chetyrkin, M. Misiak and M. Munz, Nucl. Phys. B **520** (1998) 279 doi:10.1016/S0550-3213(98)00131-X [hep-ph/9711280].

[31] K. G. Chetyrkin, M. Misiak and M. Munz, Nucl. Phys. B **518** (1998) 473 doi:10.1016/S0550-3213(98)00122-9 [hep-ph/9711266].

[32] C. Bobeth, M. Misiak and J. Urban, Nucl. Phys. B **574** (2000) 291 doi:10.1016/S0550-3213(00)00007-9 [hep-ph/9910220].

[33] P. Gambino, M. Gorbahn and U. Haisch, Nucl. Phys. B **673** (2003) 238 doi:10.1016/j.nuclphysb.2003.09.024 [hep-ph/0306079].

[34] M. Gorbahn and U. Haisch, Nucl. Phys. B **713** (2005) 291 doi:10.1016/j.nuclphysb.2005.01.047 [hep-ph/0411071].

[35] M. Gorbahn, U. Haisch and M. Misiak, Phys. Rev. Lett. **95** (2005) 102004 doi:10.1103/PhysRevLett.95.102004 [hep-ph/0504194].

[36] M. Czakon, U. Haisch and M. Misiak, JHEP **0703** (2007) 008 doi:10.1088/1126-6708/2007/03/008 [hep-ph/0612329].

[37] H. Georgi, D. B. Kaplan and L. Randall, Phys. Lett. **169B** (1986) 73.

[38] I. Brivio, M. B. Gavela, L. Merlo, K. Mimasu, J. M. No, R. del Rey and V. Sanz, arXiv:1701.05379 [hep-ph].

[39] G. Buchalla and O. Cata, JHEP **1207** (2012) 101 [arXiv:1203.6510 [hep-ph]].

[40] G. Buchalla, O. Catà and C. Krause, Nucl. Phys. B **880** (2014) 552 Erratum: [Nucl. Phys. B **913** (2016) 475] [arXiv:1307.5017 [hep-ph]].

[41] S. Weinberg, Phys. Rev. Lett. **43** (1979) 1566.

[42] W. Buchmuller and D. Wyler, Nucl. Phys. B **268** (1986) 621.

[43] B. Grzadkowski, Z. Hioki, K. Ohkuma and J. Wudka, Nucl. Phys. B **689** (2004) 108 [hep-ph/0310159].

[44] P. J. Fox, Z. Ligeti, M. Papucci, G. Perez and M. D. Schwartz, Phys. Rev. D **78** (2008) 054008 [arXiv:0704.1482 [hep-ph]].

[45] J. A. Aguilar-Saavedra, Nucl. Phys. B **812** (2009) 181 [arXiv:0811.3842 [hep-ph]].

[46] J. A. Aguilar-Saavedra, Nucl. Phys. B **821** (2009) 215 [arXiv:0904.2387 [hep-ph]].

[47] H. D. Politzer, Nucl. Phys. B **172** (1980) 349.

[48] C. Grosse-Knetter, Phys. Rev. D **49** (1994) 6709 [hep-ph/9306321].

[49] C. Arzt, Phys. Lett. B **342** (1995) 189 [hep-ph/9304230].

[50] H. Simma, Z. Phys. C **61** (1994) 67 [hep-ph/9307274].

[51] B. Grzadkowski, M. Iskrzynski, M. Misiak and J. Rosiek, JHEP **1010** (2010) 085 [arXiv:1008.4884 [hep-ph]].

[52] L. F. Abbott and M. B. Wise, Phys. Rev. D **22** (1980) 2208.

[53] B. Grinstein, R. P. Springer and M. B. Wise, Phys. Lett. B **202** (1988) 138.

[54] G. Buchalla, A. J. Buras and M. E. Lautenbacher, Rev. Mod. Phys. **68** (1996) 1125 [hep-ph/9512380].

[55] A. J. Buras, *Summer School in Theoretical Physics, NATO Advanced Study Institute, 68th session, Les Houches, France, July 28-September 5, 1997*, [hep-ph/9806471].

[56] A. J. Buras, F. De Fazio and J. Girrbach, JHEP **1302** (2013) 116 [arXiv:1211.1896 [hep-ph]].

[57] M. Misiak, Nucl. Phys. B **393** (1993) 23 Erratum: [Nucl. Phys. B **439** (1995) 461]. doi:10.1016/0550-3213(95)00029-R, 10.1016/0550-3213(93)90235-H

[58] A. J. Buras and M. Munz, Phys. Rev. D **52** (1995) 186 doi:10.1103/PhysRevD.52.186 [hep-ph/9501281].

CHAPTER

5 Flavor anomalies in B decays

> Without change something sleeps inside us, and seldom awakens. The sleeper must awaken.
>
> — *Frank Herbert*, Dune

Low-energy experiments have been crucial in the development of the EW sector of the SM, based on the gauge group $\mathrm{SU}(2)_L \times \mathrm{U}(1)_Y$. The EW structure of the SM was beautifully revealed by a large variety of experimental observations at low energy, together with requirements of a proper high-energy behavior of the theory. In particular, the intermediate vector bosons $W^{\pm}, Z$ were predicted theoretically before their experimental discovery. Precision experiments at low energies continue providing important information about the possible UV completions of the SM, and NP might be revealed again first at the precision frontier.

Indeed, there are currently two sets of interesting tensions in B-physics data that seem to point to large violations of lepton-flavor universality:

- The LHCb Collaboration has reported deviations from the SM prediction in the theoretically-clean ratios $R_{K^{(*)}} = \mathrm{Br}(B \to K^{(*)}\mu^+\mu^-)/\mathrm{Br}(B \to K^{(*)}e^+e^-)$ [1, 2]. These discrepancies are supported by other not-so-clean deviations in the angular observables of $B \to K^*\mu^+\mu^-$ [3, 4] and in the branching ratio of $B_s \to \phi\mu^+\mu^-$ [5, 6], which are compatible with the same NP explanation under the assumption of small NP couplings to electrons. These are the so-called $b \to s\ell^+\ell^-$ anomalies.

- The BaBar, Belle and LHCb collaborations have measured departures from lepton universality at the 25% level in the exclusive semileptonic $b \to c\ell\nu$ decays, through a measurement of the ratios $R(D^{(*)}) = \mathrm{Br}(B \to D^{(*)}\tau\nu)/\mathrm{Br}(B \to D^{(*)}\ell\nu)$ [7–12], with $\ell = e, \mu$.

In this chapter we will briefly review the current status of these experimental anomalies, and outline several ideas that have been proposed in the recent literature to account for them from NP extensions of the SM. In doing so, we will separate the discussion for each set of anomalies since, while they share some features, they are of different nature.

5.1 The $b \to s\ell^+\ell^-$ anomalies

While most flavor observables agree very well with the SM, current data in $b \to s\ell^+\ell^-$ transitions show an intriguing pattern of deviations. In 2013 using the $1\,\text{fb}^{-1}$ dataset, the LHCb Collaboration reported the measurement of angular observables in the $B \to K^*\mu\mu$ decay [3]. In this analysis, the optimized observable P_5' [13] showed a discrepancy of $3.7\,\sigma$ with respect to the SM prediction in one of the bins, the so-called P_5' anomaly [14]. In 2015, LHCb confirmed the anomaly with more statistics ($3\,\text{fb}^{-1}$) and a finer binning [4], reporting a deviation in two adjacent bins of P_5' with a significance of $3\,\sigma$ for each of them. LHCb has also observed a deficit in the branching ratios of other decays, such as $B_s \to \phi\mu^+\mu^-$ [5, 6], whose value differs $3.1\,\sigma$ from the SM prediction, or $B \to K^{(*)}\mu^+\mu^-$ [15]. Recent analyses by the Belle Collaboration [16,17] provided an independent confirmation of the P_5' anomaly, showing a $2.6\,\sigma$ deviation from the SM prediction consistent with the LHCb measurement, though with larger errors. The ATLAS [18] and CMS [19] Collaborations also presented at Moriond EW 2017 their preliminary analyses of the angular observables with the full Run I dataset. The compatibility of all these measurements was studied in Ref. [20], confirming the presence of a sizable discrepancy with the SM prediction.

These experimental anomalies have led to the reassessment of the possible theoretical uncertainties in these observables due to form factors [21–24] and non-factorisable hadronic effects [25–28]. In this regard, the measurement of $b \to s\ell^+\ell^-$ observables that are free from hadronic uncertainties is particularly important. Interestingly enough, the LHCb Collaboration has also found discrepancies in the ratio

$$R_K^{[q^2_{\text{min}},q^2_{\text{max}}]} = \frac{\int_{q^2_{\text{min}}}^{q^2_{\text{max}}} d\Gamma(B \to K\mu^+\mu^-)}{\int_{q^2_{\text{min}}}^{q^2_{\text{max}}} d\Gamma(B \to Ke^+e^-)}\,, \tag{5.1}$$

that provides a very clean theoretical prediction since, in the absence of large NP LFUV, hadronic uncertainties cancel to a very good approximation in the ratio and appear suppressed by m_μ^2/m_b^2 [29].[1] In particular, in 2014 LHCb reported the measurement of R_K in the dilepton-invariant-mass region $q^2 \in [1, 6]$ GeV^2 [1]

$$R_K^{[1,6]} = 0.745^{+0.090}_{-0.074} \pm 0.036\,, \tag{5.2}$$

that implies a deviation from the SM prediction [29–31],

$$R_K^{[1,6]}\Big|_{\text{SM}} = 1.00 \pm 0.01\,, \tag{5.3}$$

at the $2.6\,\sigma$ level and hints for large LFUV. Also recently, the Belle Collaboration found slight differences between the electron and muon channels in their lepton-flavor-dependent angular analysis of $B \to K^*\ell^+\ell^-$ [17], in particular in the measurement of the clean observables Q_4 and Q_5 [32]. Very recently, the LHCb Collaboration has reported the measurement of the ratio R_{K^*} [2], analogous to R_K but

[1] The impact of radiative electromagnectic corrections was evaluated in Refs. [30, 31], where it was found that the associated theory error is at the level of $\mathcal{O}(1\%)$. It is also important to note that, when NP LFUV is included, hadronic uncertainties are not suppressed by m_μ^2/m_b^2, but only by $(1 - R_{K^{(*)}}|_{\text{SM+NP}})$.

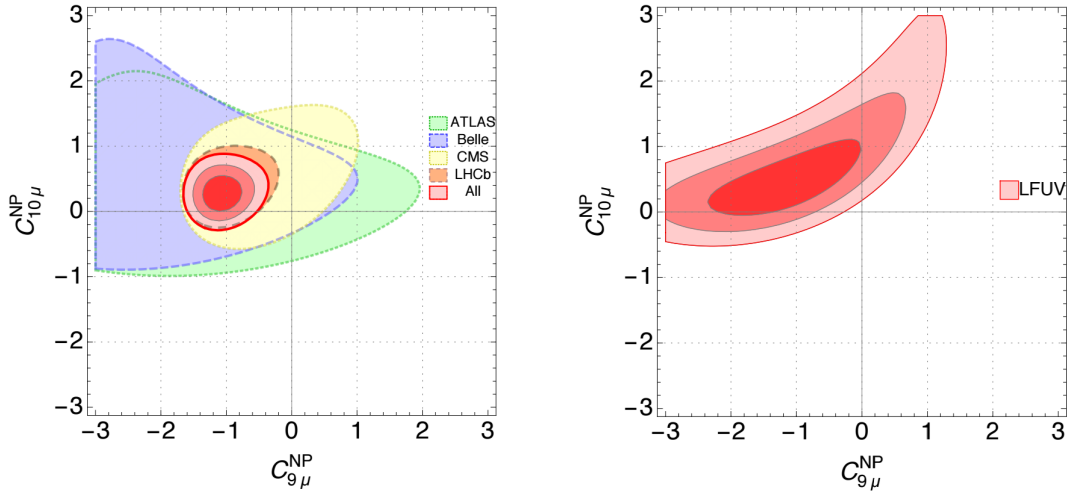

Figure 5.1: *Global fit to $b \to s\ell\ell$ data in the $\left(C_{9\mu}^{\rm NP}, C_{10\mu}^{\rm NP}\right)$ plane for the corresponding two-dimensional hypothesis, using all available data (left) and only LFUV ratios (right). Figures taken from Ref. [34].*

with different final-state meson. This measurement has been performed in two q^2 bins

$$\begin{aligned} R_{K^*}^{[0.045,1.1]} &= 0.660^{+0.110}_{-0.070} \pm 0.024\,, \\ R_{K^*}^{[1.1,6.0]} &= 0.685^{+0.113}_{-0.069} \pm 0.047\,, \end{aligned} \tag{5.4}$$

and, when compared to the SM predictions [33],

$$\begin{aligned} R_{K^*}^{[0.045,1.1]}\Big|_{\rm SM} &= 0.92 \pm 0.02\,, \\ R_{K^*}^{[1.1,6.0]}\Big|_{\rm SM} &= 1.00 \pm 0.01\,, \end{aligned} \tag{5.5}$$

it shows a deviation of $2.2\,\sigma$ for the low-q^2 region (i.e. $q^2 \in [0.045, 1.1]$ GeV^2), and $2.4\,\sigma$ in the central-q^2 region (i.e $q^2 \in [1.1, 6.0]$ GeV^2). Although the individual discrepancies are not statistically significant to claim the discovery of LFUV, in combination they yield an intriguing set of anomalies.

Global fits to $b \to s\ell^+\ell^-$ data, using the WET introduced in Section 4.2.2, show a good overall agreement and obtain a consistent NP explanation of these departures from the SM (at the level of -25% of the SM prediction) with significances at the $4-5\sigma$ level [34–38], depending on the statistical methods used and the treatment of hadronic uncertainties. Four symmetry-based solutions (taking into account at most two non-zero WCs) give a very good fit to data: NP in $C_9^{{\rm NP}\mu}$ only, $C_9^{{\rm NP}\mu} = -C_{10}^{{\rm NP}\mu}$, $C_9^{{\rm NP}\mu} = -C_{9'}^{\mu}$ and $C_9^{{\rm NP}\mu} = -3\,C_9^{{\rm NP}e}$. Interestingly, global fits including only the LFUV ratios already give a discrepancy with the SM at the $3-4$ sigma level. It is encouraging that the independent global fits to $b \to s\mu\mu$ data and to the LFUV ratios prefer similar regions for the NP Wilson coefficients (assuming no NP in the electron sector); this can be seen in Figure 5.1 where the results of the global fit from Ref. [34] for a particular NP scenario is presented. A complementary analysis

in terms of the SMEFT was presented in Ref. [39], where it was shown that the dimension-six effective operators of the SMEFT,

$$\left[C_{\ell q}^{(1)}\right]_{2223} = \left(\bar{\ell}_2\gamma_\mu\ell_2\right)\left(\bar{q}_2\gamma^\mu q_3\right) , \qquad \left[C_{\ell q}^{(3)}\right]_{2223} = \left(\bar{\ell}_2\gamma_\mu\tau^a\ell_2\right)\left(\bar{q}_2\gamma^\mu\tau^a q_3\right) , \tag{5.6}$$

generated either at tree-level or at one loop through RGE operator-mixing effects, play a crucial role in the explanation of the anomalies. This can be seen in Figure 5.2, where the individual constraints from the different LFUV ratios as well as the global fits only to LFUV ratios and to all $b \to s\ell\ell$ data are shown. An important implication of the R_{K^*} measurement is that if offers a complementary direction in the test for NP with respect to R_K. Indeed, as noted in Refs. [40, 41], left- and right-handed $b \to s$ contributions appear in almost orthogonal combinations for R_K and R_{K^*} in the central-q^2 region; as can also be seen in Figure 5.2. This implies that the double ratio $\hat{R}_{K^*} = R_{K^*}/R_K$ is mostly sensitive to only right-handed currents [40]. Given that the measured values of R_K and R_{K^*} in the central-q^2 region are comparable, the recent measurement of R_{K^*} disfavors the presence of large right-handed $b \to s$ contributions when considering only the LFUV ratios [41]. Finally, it is interesting to comment that, given the current experimental error, the measured q^2 dependence of R_{K^*} is compatible with NP in the form of WCs from the WET. However, the measured central value of R_{K^*} in the low-q^2 bin is hard to accommodate through NP of this type. This is because the branching ratio is dominated in the low-q^2 region by the photon pole, making NP contributions from the WET to this observable to appear more suppressed. One should note, though, that with the values of the WCs preferred by the other observables, the tension in the low-q^2 bin gets lowered with respect to that of the SM. Moreover, as already commented, the hadronic uncertainties could be larger in the presence of NP since the cancellation in the branching ratio is not as strong as in the SM. It is well possible that the current experimental value of R_{K^*} in this bin is partly due to a downward statistical fluctuation. However, the presence of significant discrepancies in future measurements could imply the existence of a new light mediator with a mass around or below the low-q^2 region, whose effects cannot be encoded in the effective description of the WET.

A considerable amount of effort has been devoted to provide ultraviolet-complete models that can explain the anomalies. Models that supplement the SM with leptoquarks [42–49] or with an extended gauge sector [50–68] are among the most popular ones. Explanations of the anomalies with a massive resonance from a strong sector [69–72] or with Kaluza-Klein excitations [73–75] have also been considered in the literature. Alternatively, models with extra scalars and fermions that induce the required interactions at the one-loop level have been studied in Refs. [76, 77]. In Refs. [78, 79] it was found that the MSSM with R-parity cannot explain the anomalies. In this thesis we will focus on explanations of the anomalies from gauge extended models. Extensions of the SM gauge group by an additional $\mathrm{U}(1)'$ factor are among the simplest NP scenarios that could explain these deviations. The corresponding Z' should couple to quarks and have LFUV couplings to leptons. As we saw in Section 1.3, the only anomaly-free symmetry one can gauge with the SM matter content and just one Higgs is one of the combinations of family-specific lepton numbers, $L_\alpha - L_\beta$ (with $\alpha, \beta = e, \mu, \tau$ and $\alpha \neq \beta$). Since the resulting Z' boson couples

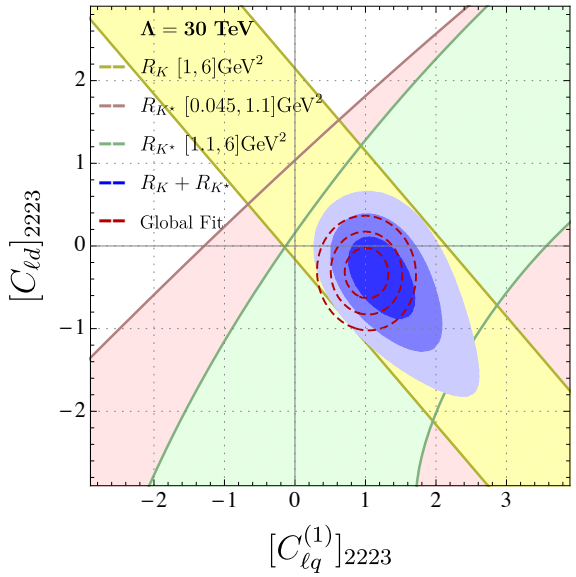

Figure 5.2: *Constraints on the SMEFT Wilson coefficients $C^{(1)}_{\ell q}$ and $C_{\ell d}$ with $\Lambda = 30$ TeV, assuming no NP in the electron modes. The constraints are the same for the $(C^{(3)}_{\ell q}, C_{\ell d})$ plane. The individual constraints from R_K and R_{K^*} at the 3σ level are represented by filled bands. The combined fit to R_K and R_{K^*} is shown in blue (1,2 and 3 σ contours). The result of a global fit with all $b \to s\ell^+\ell^-$ data included in [34] is shown in a similar way as red dashed contours. Taken from Ref. [39].*

only to leptons, these cannot accommodate the anomalies and have been discussed mostly in the context of neutrino phenomenology, usually considering the $L_\mu - L_\tau$ symmetry [80]. A way to circumvent this problem is by introducing additional fermions (vector-like quarks) that induce the required couplings to quarks through mixing effects once the $\mathrm{U}(1)'$ symmetry gets broken [50, 51, 65]. A similar idea was used in Ref. [53] to explain the anomalies from a dark sector, while providing a dark matter candidate; see also Refs. [55, 60, 61, 64, 65] for other models that explore the interplay between the flavor anomalies and dark matter. One can avoid vector-like fermions if the $\mathrm{U}(1)'$ involve both quarks and leptons and is flavor-nonuniversal. However, such a non-trivial flavor symmetry in the quark sector requires the extension of the scalar sector in order to accommodate the quark masses and mixing angles [81], typically by adding an additional Higgs doublet. For instance, Ref. [52] gave an explanation based on the gauge symmetry $\mathrm{U}(1)' \subset \mathrm{U}(1)_{\mu-\tau} \times \mathrm{U}(1)_q$, where $\mathrm{U}(1)_q$ is the symmetry associated to $B_1 + B_2 - 2\,B_3$ with B_i the individual baryon family numbers. As we will see in Section 7.2 (see also Ref. [62]), the $\mathrm{U}(1)_{\mu-\tau} \times \mathrm{U}(1)_q$ can appear naturally from the sequential breaking of the flavor symmetry introduced in Eq. (1.31). Other horizontal symmetries have been explored in Refs. [64, 66, 67]. In Section 7.1 (see also Ref. [54]) we will present in detail a model with a gauged horizontal symmetry, based on the $\mathrm{U}(1)_{\mathrm{BGL}}$ introduced in Section 2.2.2, characterized by being anomaly-free with SM fermion content alone and by having all the FCNCs exactly related to the quark mixing matrix. Larger gauge groups and their possible connections to other anomalies (see next section) have also been explored in the literature; see for instance Refs. [57–59]. In Section 7.3 we will present one of such extensions, based on the works in Refs. [58, 59].

5.2 Anomalies in $b \to c\ell\nu$ transitions

Measurements of $b \to c\ell\nu$ transitions for different final-state leptons can also be used to test lepton-flavor universality to a great precision given the cancellation of

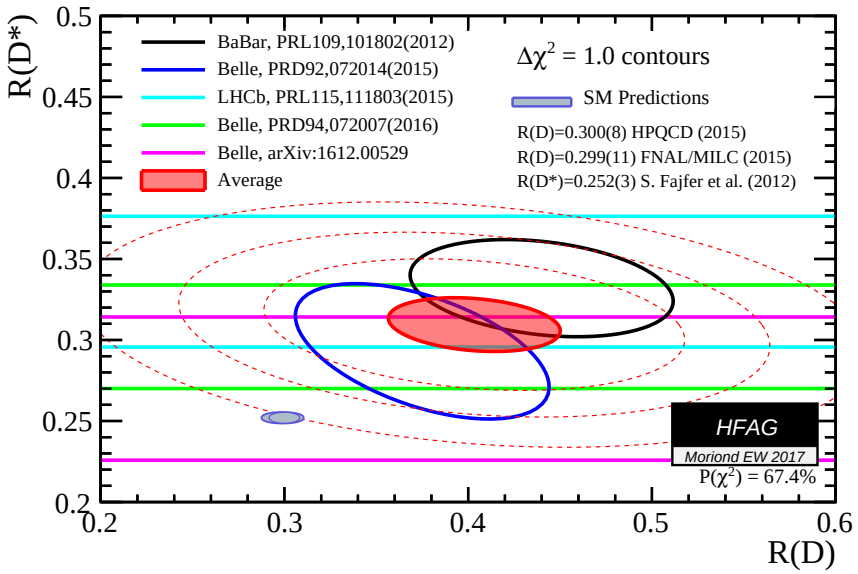

Figure 5.3: *Experimental measurements of $R(D)$ and $R(D^*)$ together with their average (dashed lines indicate the $2, 3$ and $4\,\sigma$ contours) and the SM prediction. Figure taken from [82].*

many sources of theoretical uncertainties occurring in ratios such as

$$R(D) = \frac{\Gamma(B \to D\tau\nu)}{\Gamma(B \to D\ell\nu)}\,, \qquad R(D^*) = \frac{\Gamma(B \to D^*\tau\nu)}{\Gamma(B \to D^*\ell\nu)}\,, \tag{5.7}$$

which in the SM model are predicted to take the values $R(D) = 0.300 \pm 0.008$ [83–85] (see also Ref. [86]) and $R(D^*) = 0.252 \pm 0.003$ [87]. Interestingly, the measurement of these observables can also be interpreted as a hint for lepton-flavor nonuniversality. In 2012 the BaBar Collaboration reported the measured values of these ratios, $R(D) = 0.440 \pm 0.072$ and $R(D^*) = 0.332 \pm 0.030$ [7], which show an excess with respect to the SM prediction of $2.0\,\sigma$ and $2.7\,\sigma$ respectively [87, 88]. The Belle Collaboration also measured these ratios in 2015 showing a slight enhancement with respect to the SM, $R(D) = 0.375 \pm 0.069$ and $R(D^*) = 0.293 \pm 0.041$ [10]. The LHCb Collaboration also reported the measurement $R(D^*) = 0.336 \pm 0.040$ [9], representing a deviation from the SM at the $\sim 2\,\sigma$ level. Recently, the Belle Collaboration has presented a new independent determination of $R(D^*)$ [11] which is $1.6\,\sigma$ above the SM and is compatible with all the previous measurements: $R(D^*) = 0.302 \pm 0.032$. Yet another measurement of $R(D^*)$, also including for the first time the measurement of the τ polarization, was recently reported by the Belle Collaboration: $R(D^*) = 0.270 \pm 0.035^{+0.028}_{-0.025}$ [12], which is compatible with the SM prediction. The latest average of BaBar, Belle and LHCb measurements for these processes is $R(D) = 0.403 \pm 0.047$ and $R(D^*) = 0.310 \pm 0.017$, implying a combined deviation

from the SM of 3.9σ [82] (see also Ref. [89]). All these results are summarized in Figure 5.3.[2]

While the $b \to s\ell^+\ell^-$ transitions are mediated by neutral currents, which in the SM appear at one-loop, the $R(D^{(*)})$ anomalies involve charged current contributions that are mediated by a tree-level W exchange in the SM. This makes its explanation within a NP framework typically more involved, since one needs to account for a large NP contribution while evading other experimental bounds. The $R(D^{(*)})$ anomalies have been explained with charged scalars [91–99], leptoquarks (or with R-parity violating supersymmetry) [100–107], or a W' boson [108]. Effects due to the presence of light sterile neutrinos have also been explored in Refs. [109, 110]. The impact of direct searches on these explanations using the 8 TeV and 13 TeV LHC data was studied in Refs. [111, 112].

Unified explanations of both sets of anomalies are scarcer. This is due to the difficulty of accounting for deviations of similar size in processes that take place in the SM at different orders: loop level for $b \to s\ell^+\ell^-$ and tree-level for $R(D^{(*)})$. A simultaneous explanation of the $b \to c\tau\nu$ and $b \to s\ell^+\ell^-$ anomalies has been initially discussed in Ref. [113] within an EFT point of view, building on the idea of Ref. [114] that nonuniversality in R_K could be due to NP coupling predominantly to the third generation. This EFT approach was followed later in a series of works [43,44,115,116] and some observations about the relevance of quantum effects have been given in Ref. [117]. We can also find models based on leptoquarks [43, 46, 47, 118–121], or strongly-interacting models [122]. In Section 7.3 we will present a UV complete model aimed for the simultaneous explanation of both set of anomalies from a SU(2)-extended gauge sector. One should note however that these models typically receive strong constraints from LHC searches in the $\tau^+\tau^-$ channel [111, 112] and/or their contributions to $B \to K^{(*)}\bar{\nu}\nu$. One can elude these bounds if there are more than one mediators involved in the explanation of the anomalies and a (partial) cancellation in their contributions to the dangerous observables takes place; see for instance Refs. [48, 122].

[2]The LHCb Collaboration has very recently presented a new measurement of $R(D^*)$: $R(D^*) = 0.285 \pm 0.019(stat) \pm 0.025(syst)$ [90], which is compatible with the SM at 1σ, pulling down a bit the world average for this measurement, but slightly increasing the discrepancy with the SM due to a reducction of the error.

Bibliography

[1] R. Aaij *et al.* [LHCb Collaboration], Phys. Rev. Lett. **113** (2014) 151601 [arXiv:1406.6482 [hep-ex]].

[2] R. Aaij *et al.* [LHCb Collaboration], arXiv:1705.05802 [hep-ex].

[3] R. Aaij *et al.* [LHCb Collaboration], Phys. Rev. Lett. **111** (2013) 191801 [arXiv:1308.1707 [hep-ex]].

[4] R. Aaij *et al.* [LHCb Collaboration], JHEP **1602** (2016) 104 [arXiv:1512.04442 [hep-ex]].

[5] R. Aaij *et al.* [LHCb Collaboration], JHEP **1307** (2013) 084 [arXiv:1305.2168 [hep-ex]].

[6] R. Aaij *et al.* [LHCb Collaboration], JHEP **1509** (2015) 179 [arXiv:1506.08777 [hep-ex]].

[7] J. P. Lees *et al.* [BaBar Collaboration], Phys. Rev. Lett. **109** (2012) 101802 [arXiv:1205.5442 [hep-ex]].

[8] J. P. Lees *et al.* [BaBar Collaboration], Phys. Rev. D **88** (2013) no.7, 072012 [arXiv:1303.0571 [hep-ex]].

[9] R. Aaij *et al.* [LHCb Collaboration], Phys. Rev. Lett. **115** (2015) no.11, 111803 Erratum: [Phys. Rev. Lett. **115** (2015) no.15, 159901] [arXiv:1506.08614 [hep-ex]].

[10] M. Huschle *et al.* [Belle Collaboration], Phys. Rev. D **92** (2015) no.7, 072014 [arXiv:1507.03233 [hep-ex]].

[11] Y. Sato *et al.* [Belle Collaboration], Phys. Rev. D **94** (2016) no.7, 072007 [arXiv:1607.07923 [hep-ex]].

[12] S. Hirose *et al.* [Belle Collaboration], arXiv:1612.00529 [hep-ex].

[13] S. Descotes-Genon, T. Hurth, J. Matias and J. Virto, JHEP **1305** (2013) 137 [arXiv:1303.5794 [hep-ph]].

[14] S. Descotes-Genon, J. Matias and J. Virto, Phys. Rev. D **88** (2013) 074002 [arXiv:1307.5683 [hep-ph]].

[15] R. Aaij *et al.* [LHCb Collaboration], JHEP **1406** (2014) 133 [arXiv:1403.8044 [hep-ex]].

[16] A. Abdesselam *et al.* [Belle Collaboration], arXiv:1604.04042 [hep-ex].

[17] S. Wehle *et al.* [Belle Collaboration], Phys. Rev. Lett. **118** (2017) no.11, 111801 [arXiv:1612.05014 [hep-ex]].

[18] The ATLAS collaboration [ATLAS Collaboration], ATLAS-CONF-2017-023.

[19] CMS Collaboration [CMS Collaboration], CMS-PAS-BPH-15-008.

[20] W. Altmannshofer, C. Niehoff, P. Stangl and D. M. Straub, arXiv:1703.09189 [hep-ph].

[21] S. Jäger and J. Martin Camalich, JHEP **1305** (2013) 043 [arXiv:1212.2263 [hep-ph]].

[22] S. Jäger and J. Martin Camalich, Phys. Rev. D **93** (2016) no.1, 014028 [arXiv:1412.3183 [hep-ph]].

[23] S. Descotes-Genon, L. Hofer, J. Matias and J. Virto, JHEP **1412** (2014) 125 [arXiv:1407.8526 [hep-ph]].

[24] B. Capdevila, S. Descotes-Genon, L. Hofer and J. Matias, JHEP **1704** (2017) 016 [arXiv:1701.08672 [hep-ph]].

[25] J. Lyon and R. Zwicky, arXiv:1406.0566 [hep-ph].

[26] M. Ciuchini, M. Fedele, E. Franco, S. Mishima, A. Paul, L. Silvestrini and M. Valli, JHEP **1606** (2016) 116 [arXiv:1512.07157 [hep-ph]].

[27] M. Ciuchini, M. Fedele, E. Franco, S. Mishima, A. Paul, L. Silvestrini and M. Valli, PoS ICHEP **2016** (2016) 584 [arXiv:1611.04338 [hep-ph]].

[28] V. G. Chobanova, T. Hurth, F. Mahmoudi, D. Martinez Santos and S. Neshatpour, arXiv:1702.02234 [hep-ph].

[29] G. Hiller and F. Kruger, Phys. Rev. D **69** (2004) 074020 [hep-ph/0310219].

[30] A. Guevara, G. López Castro, P. Roig and S. L. Tostado, Phys. Rev. D **92** (2015) no.5, 054035 [arXiv:1503.06890 [hep-ph]].

[31] M. Bordone, G. Isidori and A. Pattori, Eur. Phys. J. C **76** (2016) no.8, 440 [arXiv:1605.07633 [hep-ph]].

[32] B. Capdevila, S. Descotes-Genon, J. Matias and J. Virto, JHEP **1610** (2016) 075 [arXiv:1605.03156 [hep-ph]].

[33] S. Descotes-Genon, L. Hofer, J. Matias and J. Virto, JHEP **1606** (2016) 092 [arXiv:1510.04239 [hep-ph]].

[34] B. Capdevila, A. Crivellin, S. Descotes-Genon, J. Matias and J. Virto, arXiv:1704.05340 [hep-ph].

[35] W. Altmannshofer, P. Stangl and D. M. Straub, arXiv:1704.05435 [hep-ph].

[36] G. D'Amico, M. Nardecchia, P. Panci, F. Sannino, A. Strumia, R. Torre and A. Urbano, arXiv:1704.05438 [hep-ph].

[37] L. S. Geng, B. Grinstein, S. Jäger, J. Martin Camalich, X. L. Ren and R. X. Shi, arXiv:1704.05446 [hep-ph].

[38] M. Ciuchini, A. M. Coutinho, M. Fedele, E. Franco, A. Paul, L. Silvestrini and M. Valli, arXiv:1704.05447 [hep-ph].

[39] A. Celis, J. Fuentes-Martin, A. Vicente and J. Virto, arXiv:1704.05672 [hep-ph].

[40] G. Hiller and M. Schmaltz, JHEP **1502** (2015) 055 [arXiv:1411.4773 [hep-ph]].

[41] G. Hiller and I. Nisandzic, arXiv:1704.05444 [hep-ph].

[42] I. de Medeiros Varzielas and G. Hiller, JHEP **1506** (2015) 072 [arXiv:1503.01084 [hep-ph]].

[43] R. Alonso, B. Grinstein and J. Martin Camalich, JHEP **1510** (2015) 184 [arXiv:1505.05164 [hep-ph]].

[44] L. Calibbi, A. Crivellin and T. Ota, Phys. Rev. Lett. **115** (2015) 181801 [arXiv:1506.02661 [hep-ph]].

[45] H. Päs and E. Schumacher, Phys. Rev. D **92** (2015) no.11, 114025 [arXiv:1510.08757 [hep-ph]].

[46] S. Fajfer and N. Košnik, Phys. Lett. B **755** (2016) 270 [arXiv:1511.06024 [hep-ph]].

[47] R. Barbieri, G. Isidori, A. Pattori and F. Senia, Eur. Phys. J. C **76** (2016) no.2, 67 [arXiv:1512.01560 [hep-ph]].

[48] A. Crivellin, D. Müller and T. Ota, arXiv:1703.09226 [hep-ph].

[49] D. Bečirević and O. Sumensari, arXiv:1704.05835 [hep-ph].

[50] W. Altmannshofer, S. Gori, M. Pospelov and I. Yavin, Phys. Rev. D **89** (2014) 095033 [arXiv:1403.1269 [hep-ph]].

[51] A. Crivellin, G. D'Ambrosio and J. Heeck, Phys. Rev. Lett. **114** (2015) 151801 [arXiv:1501.00993 [hep-ph]].

[52] A. Crivellin, G. D'Ambrosio and J. Heeck, Phys. Rev. D **91** (2015) no.7, 075006 [arXiv:1503.03477 [hep-ph]].

[53] D. Aristizabal Sierra, F. Staub and A. Vicente, Phys. Rev. D **92** (2015) no.1, 015001 [arXiv:1503.06077 [hep-ph]].

[54] A. Celis, J. Fuentes-Martin, M. Jung and H. Serodio, Phys. Rev. D **92** (2015) no.1, 015007 [arXiv:1505.03079 [hep-ph]].

[55] G. Bélanger, C. Delaunay and S. Westhoff, Phys. Rev. D **92** (2015) 055021 [arXiv:1507.06660 [hep-ph]].

[56] A. Falkowski, M. Nardecchia and R. Ziegler, JHEP **1511** (2015) 173 [arXiv:1509.01249 [hep-ph]].

[57] C. W. Chiang, X. G. He and G. Valencia, Phys. Rev. D **93** (2016) no.7, 074003 [arXiv:1601.07328 [hep-ph]].

[58] S. M. Boucenna, A. Celis, J. Fuentes-Martin, A. Vicente and J. Virto, Phys. Lett. B **760** (2016) 214 [arXiv:1604.03088 [hep-ph]].

[59] S. M. Boucenna, A. Celis, J. Fuentes-Martin, A. Vicente and J. Virto, JHEP **1612** (2016) 059 [arXiv:1608.01349 [hep-ph]].

[60] A. Celis, W. Z. Feng and M. Vollmann, Phys. Rev. D **95** (2017) no.3, 035018 [arXiv:1608.03894 [hep-ph]].

[61] W. Altmannshofer, S. Gori, S. Profumo and F. S. Queiroz, JHEP **1612** (2016) 106 [arXiv:1609.04026 [hep-ph]].

[62] A. Crivellin, J. Fuentes-Martin, A. Greljo and G. Isidori, Phys. Lett. B **766** (2017) 77 [arXiv:1611.02703 [hep-ph]].

[63] D. Bhatia, S. Chakraborty and A. Dighe, JHEP **1703** (2017) 117 [arXiv:1701.05825 [hep-ph]].

[64] J. M. Cline, J. M. Cornell, D. London and R. Watanabe, arXiv:1702.00395 [hep-ph].

[65] P. Ko, T. Nomura and H. Okada, arXiv:1702.02699 [hep-ph].

[66] P. Ko, Y. Omura, Y. Shigekami and C. Yu, arXiv:1702.08666 [hep-ph].

[67] R. Alonso, P. Cox, C. Han and T. T. Yanagida, arXiv:1704.08158 [hep-ph].

[68] J. F. Kamenik, Y. Soreq and J. Zupan, arXiv:1704.06005 [hep-ph].

[69] B. Gripaios, M. Nardecchia and S. A. Renner, JHEP **1505** (2015) 006 [arXiv:1412.1791 [hep-ph]].

[70] C. Niehoff, P. Stangl and D. M. Straub, JHEP **1601** (2016) 119 [arXiv:1508.00569 [hep-ph]].

[71] A. Carmona and F. Goertz, Phys. Rev. Lett. **116** (2016) no.25, 251801 [arXiv:1510.07658 [hep-ph]].

[72] R. Barbieri, C. W. Murphy and F. Senia, Eur. Phys. J. C **77** (2017) no.1, 8 [arXiv:1611.04930 [hep-ph]].

[73] E. Megias, G. Panico, O. Pujolas and M. Quiros, JHEP **1609** (2016) 118 [arXiv:1608.02362 [hep-ph]].

[74] I. Garcia Garcia, JHEP **1703** (2017) 040 [arXiv:1611.03507 [hep-ph]].

[75] E. Megias, M. Quiros and L. Salas, arXiv:1703.06019 [hep-ph].

[76] B. Gripaios, M. Nardecchia and S. A. Renner, JHEP **1606** (2016) 083 [arXiv:1509.05020 [hep-ph]].

[77] P. Arnan, L. Hofer, F. Mescia and A. Crivellin, JHEP **1704** (2017) 043 [arXiv:1608.07832 [hep-ph]].

[78] W. Altmannshofer and D. M. Straub, Eur. Phys. J. C **73** (2013) 2646 [arXiv:1308.1501 [hep-ph]].

[79] F. Mahmoudi, S. Neshatpour and J. Virto, Eur. Phys. J. C **74** (2014) no.6, 2927 [arXiv:1401.2145 [hep-ph]].

[80] P. Binetruy, S. Lavignac, S. T. Petcov and P. Ramond, Nucl. Phys. B **496** (1997) 3 [hep-ph/9610481].

[81] M. Leurer, Y. Nir and N. Seiberg, Nucl. Phys. B **398** (1993) 319 [hep-ph/9212278].

[82] Heavy Flavor Averaging Group (HFAG), "Average of $R(D)$ and $R(D^*)$ for Moriod EW 2017", http://www.slac.stanford.edu/xorg/hfag/semi/moriond17/RDRDs.html

[83] J. A. Bailey *et al.* [MILC Collaboration], Phys. Rev. D **92** (2015) no.3, 034506 [arXiv:1503.07237 [hep-lat]].

[84] H. Na *et al.* [HPQCD Collaboration], Phys. Rev. D **92** (2015) no.5, 054510 Erratum: [Phys. Rev. D **93** (2016) no.11, 119906] [arXiv:1505.03925 [hep-lat]].

[85] S. Aoki *et al.*, Eur. Phys. J. C **77** (2017) no.2, 112 [arXiv:1607.00299 [hep-lat]].

[86] D. Bigi and P. Gambino, Phys. Rev. D **94** (2016) no.9, 094008 [arXiv:1606.08030 [hep-ph]].

[87] S. Fajfer, J. F. Kamenik and I. Nisandzic, Phys. Rev. D **85** (2012) 094025 [arXiv:1203.2654 [hep-ph]].

[88] J. F. Kamenik and F. Mescia, Phys. Rev. D **78** (2008) 014003 [arXiv:0802.3790 [hep-ph]].

[89] Y. Amhis *et al.*, arXiv:1612.07233 [hep-ex].

[90] Guy Wormser on behalf of the LHCb Collaboration, Seminar at Flavor Physics & CP Violation 2017, Prague, Czech Republic, 5-9 Jun 2017.

[91] A. Crivellin, C. Greub and A. Kokulu, Phys. Rev. D **86** (2012) 054014 [arXiv:1206.2634 [hep-ph]].

[92] A. Celis, M. Jung, X. Q. Li and A. Pich, JHEP **1301** (2013) 054 [arXiv:1210.8443 [hep-ph]].

[93] J. A. Bailey *et al.*, Phys. Rev. Lett. **109** (2012) 071802 [arXiv:1206.4992 [hep-ph]].

[94] P. Ko, Y. Omura and C. Yu, JHEP **1303** (2013) 151 [arXiv:1212.4607 [hep-ph]].

[95] A. Crivellin, J. Heeck and P. Stoffer, Phys. Rev. Lett. **116** (2016) no.8, 081801 [arXiv:1507.07567 [hep-ph]].

[96] J. M. Cline, Phys. Rev. D **93** (2016) no.7, 075017 [arXiv:1512.02210 [hep-ph]].

[97] M. Freytsis, Z. Ligeti and J. T. Ruderman, Phys. Rev. D **92** (2015) no.5, 054018 [arXiv:1506.08896 [hep-ph]].

[98] S. Nandi, S. K. Patra and A. Soni, arXiv:1605.07191 [hep-ph].

[99] A. Celis, M. Jung, X. Q. Li and A. Pich, arXiv:1612.07757 [hep-ph].

[100] S. Fajfer, J. F. Kamenik, I. Nisandzic and J. Zupan, Phys. Rev. Lett. **109** (2012) 161801 [arXiv:1206.1872 [hep-ph]].

[101] N. G. Deshpande and A. Menon, JHEP **1301** (2013) 025 [arXiv:1208.4134 [hep-ph]].

[102] M. Tanaka and R. Watanabe, Phys. Rev. D **87** (2013) no.3, 034028 [arXiv:1212.1878 [hep-ph]].

[103] Y. Sakaki, M. Tanaka, A. Tayduganov and R. Watanabe, Phys. Rev. D **88** (2013) no.9, 094012 [arXiv:1309.0301 [hep-ph]].

[104] I. Doršner, S. Fajfer, N. Košnik and I. Nišandžić, JHEP **1311** (2013) 084 [arXiv:1306.6493 [hep-ph]].

[105] C. Hati, G. Kumar and N. Mahajan, JHEP **1601** (2016) 117 [arXiv:1511.03290 [hep-ph]].

[106] J. Zhu, H. M. Gan, R. M. Wang, Y. Y. Fan, Q. Chang and Y. G. Xu, Phys. Rev. D **93** (2016) no.9, 094023 [arXiv:1602.06491 [hep-ph]].

[107] X. Q. Li, Y. D. Yang and X. Zhang, JHEP **1608** (2016) 054 [arXiv:1605.09308 [hep-ph]].

[108] X. G. He and G. Valencia, Phys. Rev. D **87** (2013) no.1, 014014 [arXiv:1211.0348 [hep-ph]].

[109] A. Abada, A. M. Teixeira, A. Vicente and C. Weiland, JHEP **1402** (2014) 091 [arXiv:1311.2830 [hep-ph]].

[110] G. Cvetic and C. S. Kim, Phys. Rev. D **94** (2016) no.5, 053001 Erratum: [Phys. Rev. D **95** (2017) no.3, 039901] [arXiv:1606.04140 [hep-ph]].

[111] D. A. Faroughy, A. Greljo and J. F. Kamenik, Phys. Lett. B **764** (2017) 126 [arXiv:1609.07138 [hep-ph]].

[112] A. Greljo and D. Marzocca, arXiv:1704.09015 [hep-ph].

[113] B. Bhattacharya, A. Datta, D. London and S. Shivashankara, Phys. Lett. B **742** (2015) 370 [arXiv:1412.7164 [hep-ph]].

[114] S. L. Glashow, D. Guadagnoli and K. Lane, Phys. Rev. Lett. **114** (2015) 091801 [arXiv:1411.0565 [hep-ph]].

[115] A. Greljo, G. Isidori and D. Marzocca, JHEP **1507** (2015) 142 [arXiv:1506.01705 [hep-ph]].

[116] M. Bordone, G. Isidori and S. Trifinopoulos, arXiv:1702.07238 [hep-ph].

[117] F. Feruglio, P. Paradisi and A. Pattori, Phys. Rev. Lett. **118** (2017) no.1, 011801 [arXiv:1606.00524 [hep-ph]].

[118] M. Bauer and M. Neubert, Phys. Rev. Lett. **116** (2016) no.14, 141802 [arXiv:1511.01900 [hep-ph]].

[119] C. Hati, Phys. Rev. D **93** (2016) no.7, 075002 [arXiv:1601.02457 [hep-ph]].

[120] F. F. Deppisch, S. Kulkarni, H. Päs and E. Schumacher, Phys. Rev. D **94** (2016) no.1, 013003 [arXiv:1603.07672 [hep-ph]].

[121] D. Das, C. Hati, G. Kumar and N. Mahajan, Phys. Rev. D **94** (2016) 055034 [arXiv:1605.06313 [hep-ph]].

[122] D. Buttazzo, A. Greljo, G. Isidori and D. Marzocca, JHEP **1608** (2016) 035 [arXiv:1604.03940 [hep-ph]].

Part II

Scientific Research

CHAPTER

6 One-loop matching of Effective Field Theories

> "You know my methods. Apply them, and it will be instructive to compare results."
>
> — *Arthur Conan Doyle*, The Sign of Four

Although the rationale and procedure for the use of EFTs has been well developed long ago in the literature (see Chapter 4 for a brief review), the integration at next-to-leading order in the upper theory, that is to say at one loop, is undergoing lately an intense debate [1–6] that, as we put forward in this chapter, still allows for simpler alternatives.[1] One of the issues recently arisen involves the widely used technique to perform the functional integration of the heavy fields set up more than thirty years ago by the works of Aitchison and Fraser [10–13], Chan [14, 15], Gaillard [16] and Cheyette [17]. As implemented by Refs. [1, 2], this technique did not include all the one-loop contributions from the integration, in particular those where heavy and light field quantum fluctuations appear in the same loop. This fact was noticed in Ref. [3], and fixed later on in Refs. [5, 6], by the use of variants of the functional approach which require additional ingredients in order to subtract the parts of the heavy-light loops which are already accounted for by the one-loop EFT contribution.

Here we would like to introduce a more direct method to obtain the one-loop effective theory that builds upon the works of Refs. [8,9], and that uses the technique of "expansion by regions" [18–20] to read off the one-loop matching coefficients from the full theory computation, thus bypassing the need of subtracting any infrared contribution. In short, the determination of the one-loop EFT in the approach we propose reduces to the calculation of the *hard* part of the determinant of $\widetilde{\Delta}_H$, where $\widetilde{\Delta}_H$ arises from the diagonalization of the quadratic term in the expansion of the full theory Lagrangian around the classical field configurations, and the determinant is just the result of the Gaussian integration over the heavy quantum fluctuations. In this way, the terms that mix light and heavy spectra inside the loop get disentangled by means of a field transformation in the path integral that brings the quadratic fluctuation into diagonal form: The part involving only the light quantum fields remains untouched by the transformation and all heavy particle effects in the loops are shifted to the modified heavy quadratic form $\widetilde{\Delta}_H$. This provides a conceptually

[1] The contents of this chapter are based in the publication in Ref. [7].

simple and straightforward technique to obtain all the one-loop local EFT couplings from an underlying theory that can contain arbitrary interactions between the heavy and the light degrees of freedom. A diagrammatic formulation of this technique has been recently put forward in Ref. [21].

The contents of this chapter are the following. The general outline of the method is given in Section 6.1, where we describe the transformation that diagonalizes the quadratic fluctuation which defines $\widetilde{\Delta}_H$, and then discuss how to extract the contributions from $\widetilde{\Delta}_H$ that are relevant for determining the one-loop EFT. In Section 6.2 we compare our procedure with those proposed recently by [1, 5] and [2, 6]. The virtues of our method are better seen through examples: first we consider a simple scalar toy model in Section 6.3, where we can easily illustrate the advantages of our procedure with respect the conventional matching approach; then we turn to an extension of the SM with a heavy real scalar triplet, that has been used as an example in recent papers. We conclude with Section 6.4. Additional material concerning the general formulae for dimension-six operators, and the expression of the fluctuation operator in the SM case is provided in the appendices.

6.1 The method

In Section 4.1 we outlined the functional method to determine the EFT Lagrangian describing the dynamics of the full-theory at energies much smaller than m_H, the typical mass of a heavy particle, or set of particles. In this section we present the extension of this functional method to the one-loop level. The application of the method to specific examples is postponed to Section 6.3.

Let us consider a general theory whose field content can be split into heavy, η_H, and light, η_L, degrees of freedom, that we collect generically in $\eta = (\eta_H\,, \eta_L)$. For charged degrees of freedom, the field and its complex conjugate enter as separate components in η_H and η_L. As described in Section 4.1, the one-loop effective action is obtained, after applying the BFM, from the quadratic term in the quantum fluctuations in the expansion of Eq. (4.4) (see also Eq. (4.9)). The latter is given in terms of the Lagrangian of the full-theory by

$$\mathcal{L}^{(\eta^2)} = \frac{1}{2}\eta^\dagger \frac{\delta^2 \mathcal{L}}{\delta\eta^*\,\delta\eta}\bigg|_{\eta=\hat{\eta}} \eta \equiv \frac{1}{2}\eta^\dagger\,\mathcal{O}\,\eta\,. \tag{6.1}$$

From this expression we identify the fluctuation operator $\mathcal{O}$, with generic form

$$\mathcal{O} = \begin{pmatrix} \Delta_H & X_{LH}^\dagger \\ X_{LH} & \Delta_L \end{pmatrix}\,, \tag{6.2}$$

and which depends only on the classical fields $\hat{\eta}$.

The one-loop effective action is simply obtained by Gaussian integration of the path integral in Eq. (4.9). Our aim is to compute the one-loop heavy particle effects in the Green functions of the light fields as an expansion in the heavy mass scale m_H. In terms of Feynman diagrams, the latter corresponds to computing all one-loop diagrams involving heavy lines and expanding them in $1/m_H$. This can be formally achieved by doing the functional integration over the fields η_H.

However, the presence of mixing terms among heavy and light quantum fields in $\mathcal{L}^{(\eta^2)}$ (equivalently, of one-loop diagrams with both heavy and light lines inside the loop), makes it necessary to first rewrite the fluctuation operator in Eq. (6.2) in an equivalent block-diagonal form. A way of achieving this is by performing shifts (with unit Jacobian determinant) in the quantum fields, which can be done in different ways. We choose a field transformation that shifts the information about the mixing terms X_{LH} in the fluctuation operator into a redefinition of the heavy-particle block Δ_H, while leaving Δ_L untouched. This has the advantage that all heavy particle effects in the one-loop effective action are thus obtained through the computation of the determinant that results from the path integral over the heavy fields. This shifting procedure was actually used in Refs. [8,9] for integrating out the Higgs field in the SU(2) gauge theory and in the SM. An alternative shift, which is implicitly used in Ref. [5], will be discussed in Section 6.2.

The explicit form of the field transformation that brings $\mathcal{O}$ into the desired block-diagonal form reads

$$P = \begin{pmatrix} I & 0 \\ -\Delta_L^{-1} X_{LH} & I \end{pmatrix} , \tag{6.3}$$

and one immediately obtains

$$P^\dagger \mathcal{O} P = \begin{pmatrix} \widetilde{\Delta}_H & 0 \\ 0 & \Delta_L \end{pmatrix} , \tag{6.4}$$

with

$$\widetilde{\Delta}_H = \Delta_H - X_{LH}^\dagger \Delta_L^{-1} X_{LH} \, . \tag{6.5}$$

The functional integration over the heavy fields η_H can now be carried out easily,

$$e^{iS^{1\text{loop}}} = \left(\det \widetilde{\Delta}_H\right)^{-c} \mathcal{N} \int \mathcal{D}\eta_L \, \exp\left[i \int dx \, \frac{1}{2} \eta_L^\dagger \Delta_L \eta_L \right] , \tag{6.6}$$

with $c = 1/2, -1$ depending on the bosonic or fermionic nature of the heavy fields. For simplicity, we assume that all degrees of freedom in the heavy sector are either bosons or fermions. In the case of mixed statistics, one needs to further diagonalize $\widetilde{\Delta}_H$ to decouple the bosonic and fermionic blocks. The remaining Gaussian integration in Eq. (6.6) reproduces the one-loop contributions with light particles running inside the loop, and heavy fields can appear only as tree-level lines through the dependence of Δ_L in $\hat{\eta}_H$. We thus define the part of the one-loop effective action coming from loops involving heavy fields as

$$S_H = i \, c \, \ln \det \widetilde{\Delta}_H \, . \tag{6.7}$$

In order to compute the determinant of $\widetilde{\Delta}_H$ we use standard techniques developed in the literature [14, 22]. First it is rewritten as

$$S_H = i \, c \, \mathrm{Tr} \ln \widetilde{\Delta}_H , \tag{6.8}$$

where Tr denotes the full trace of the operator, also in coordinate space. It is convenient for our purposes to rewrite the functional trace using momentum eigenstates defined in d dimensions as

$$\begin{aligned} S_H &= i\,c\,\mathrm{tr}\int\frac{d^dp}{(2\pi)^d}\,\langle p|\ln\widetilde{\Delta}_H|p\rangle \\ &= i\,c\,\mathrm{tr}\int d^dx\int\frac{d^dp}{(2\pi)^d}\,e^{-ipx}\ln\left(\widetilde{\Delta}_H\left(x,\partial_x\right)\right)e^{ipx} \\ &= i\,c\,\mathrm{tr}\int d^dx\int\frac{d^dp}{(2\pi)^d}\,\ln\left(\widetilde{\Delta}_H\left(x,\partial_x+ip\right)\right)\mathbb{1}\,. \end{aligned} \tag{6.9}$$

The derivatives in $\widetilde{\Delta}_H$ yields factors of ip upon acting on the exponentials[2]. The symbol tr denotes the trace over internal degrees of freedom only. Since $\widetilde{\Delta}_H$ contains the kinetic term of the heavy fields, in the case of scalar fields it has the generic form

$$\widetilde{\Delta}_H = -\hat{D}^2 - m_H^2 - U\,, \tag{6.10}$$

with $\hat{D}_\mu$ denoting the covariant derivative for the heavy fields with background gauge fields. Performing the shift $\partial_x \to \partial_x + ip$ we find

$$S_H = \frac{i}{2}\,\mathrm{tr}\int d^dx\int\frac{d^dp}{(2\pi)^d}\,\ln\left(p^2 - m_H^2 - 2ip\hat{D} - \hat{D}^2 - U\left(x,\partial_x+ip\right)\right)\mathbb{1}\,. \tag{6.11}$$

For fermions, the same formula, Eq. (6.11), applies but with an overall minus sign and with U replaced by

$$U_{\text{ferm.}} = -\frac{i}{2}\sigma^{\mu\nu}\left[\hat{D}_\mu,\hat{D}_\nu\right] - i\left[\hat{\not{D}},\Sigma_e\right] + i\left\{\hat{\not{D}},\Sigma_o\right\} + 2m_H\Sigma_e + \Sigma\left(\Sigma_e - \Sigma_o\right)\,. \tag{6.12}$$

Here $\Sigma \equiv \Sigma_e + \Sigma_o$ is defined by $\widetilde{\Delta}_H = i\hat{\not{D}} - m_H - \Sigma$, and Σ_e (Σ_o) contains an even (odd) number of gamma matrices. Finally, we can Taylor expand the logarithm to get

$$S_H = \mp\frac{i}{2}\int d^dx\sum_{n=1}^{\infty}\frac{1}{n}\int\frac{d^dp}{(2\pi)^d}\,\mathrm{tr}\left\{\left(\frac{2ip\hat{D}+\hat{D}^2+U\left(x,\partial_x+ip\right)}{p^2-m_H^2}\right)^n\mathbb{1}\right\}\,, \tag{6.13}$$

where we have dropped an irrelevant constant term, and the negative (positive) global sign corresponds to the integration of boson (fermion) heavy fields.

The effective action Eq. (6.13) generates all one-loop amplitudes with at least one heavy particle propagator in the loop. One-loop diagrams with n heavy propagators are reproduced from the n-th term in the expansion of Eq. (6.13). In addition

[2]Note that $\widetilde{\Delta}_H$ can also depend in $\partial_x^{\intercal}$. Transpose derivatives are defined from the adjoint operator, which acts on the function at the left, and can be replaced by $-\partial_x$, the difference being a total derivative term. The identity $\mathbb{1}$ in Eq. (6.9) serves as a reminder that derivatives at the rightmost disappear after acting on the exponential.

the diagram can contain light propagators, that arise upon expanding the term $X_{LH}^\dagger \Delta_L^{-1} X_{LH}$ in $\widetilde{\Delta}_H$ using

$$\Delta_L^{-1} = \sum_{n=0}^{\infty} (-1)^n \left(\widetilde{\Delta}_L^{-1} X_L\right)^n \widetilde{\Delta}_L^{-1}, \tag{6.14}$$

which corresponds to the Neumann series expansion of Δ_L^{-1}, and we have made the separation $\Delta_L = \widetilde{\Delta}_L + X_L$, with $\widetilde{\Delta}_L$ corresponding to the the fluctuations coming from the kinetic terms, i.e. $\widetilde{\Delta}_L^{-1}$ is the light field propagator. From the definition of the fluctuation operator $\mathcal{O}$, Eq. (6.2), the terms in $\widetilde{\Delta}_L$ are part of the diagonal components of $\mathcal{O}$. At the practical level, for the calculation of Δ_L^{-1} using Eq. (6.14) it is simpler to define $\widetilde{\Delta}_L$ directly as the whole diagonal of $\mathcal{O}$.

Loops with heavy particles receive contributions from the region of *hard* loop momenta $p \sim m_H$, and from the *soft* momentum region, where the latter is set by the low-energy scales in the theory, either $p \sim m_L$ or any of the light-particle external momenta, $p_i \ll m_H$. In dimensional regularization the two contributions can be computed separately by using the so-called "expansion by regions" [18–20]. In this method the contribution of each region is obtained by expanding the integrand into a Taylor series with respect to the parameters that are small there, and then integrating every region over the full d-dimensional space of the loop momenta. In the hard region, all the low-energy scales are expanded out and only m_H remains in the propagators. The resulting integrand yields local contributions in the form of a polynomial in the low-energy momenta and masses, with factors of $1/m_H$ to adjust the dimensions. This part is therefore fully determined by the short-distance behavior of the full theory and has to be included into the EFT Lagrangian in order to match the amplitudes in the full and effective theories. Indeed, the coefficients of the polynomial terms from the hard contribution of a given (renormalized) amplitude provide the one-loop matching coefficients of corresponding local terms in the effective theory. This can be understood easily since the soft part of the amplitude results upon expanding the vertices and propagators according to $p \sim m_L \ll m_H$, with p the loop momentum. This expansion, together with the one-loop terms with light particles that arise from the Gaussian integral of Δ_L in Eq. (6.6), yields the same one-loop amplitude as one would obtain using the Feynman rules of the effective Lagrangian for the light fields obtained by tree-level matching, equivalently the Feynman rules from $\mathcal{L}^{\text{tree}}$ in Eq. (4.4) where the background heavy field $\hat{\eta}_H$ has been eliminated in favor of $\hat{\eta}_L$ using the classical EOM. Therefore, in the difference of the full-theory and EFT renormalized amplitudes at one-loop only the hard part of the full-theory amplitude remains, and one can read off the one-loop matching coefficients directly from the computation of the latter. Let us finally note that in the conventional matching approach, the same infrared regularization has to be used in the full and EFT calculations, in order to guarantee that the infrared behavior of both theories is identical. This is of course fulfilled in the approach suggested here, since the one-loop EFT amplitude is defined implicitly by the full theory result. Likewise, the ultraviolet (UV) divergences of the EFT are determined by UV divergences in the soft part, that are regulated in d dimensions in our approach. For the renormalization of the amplitudes, we shall use the $\overline{\text{MS}}$ scheme.

Translated into the functional approach, the preceding discussion implies that the EFT Lagrangian at one-loop is then determined as

$$\int d^d x \, \mathcal{L}_{\rm EFT}^{\rm 1loop} = S_H^{\rm hard} \,, \tag{6.15}$$

where $S_H^{\rm hard}$, containing only the hard part of the loops, can be obtained from the representation (6.13) by expanding the integrand in the hard loop-momentum limit, $p \sim m_H \gg m_L, \partial_x$. In order to identify the relevant terms in this expansion, it is useful to introduce the counting

$$p_\mu, \, m_H \sim \zeta \,, \tag{6.16}$$

and determine the order ζ^{-k}, $k > 0$, of each term in the integrand of Eq. (6.13). For a given order in ζ only a finite number of terms in the expansion contributes because U is at most $\mathcal{O}(\zeta)$ and the denominator is $\mathcal{O}(\zeta^2)$.[3] For instance, to obtain the dimension-six effective operators, i.e. those suppressed by $1/m_H^2$, it is enough to truncate the expansion up to terms of $\mathcal{O}\left(\zeta^{-2}\right)$, which means computing U up to $\mathcal{O}\left(\zeta^{-4}\right)$ (recall that $d^4 p \sim \zeta^4$). Though it was phrased differently, this prescription is effectively equivalent to the one used in Refs. [8, 9] to obtain the non-decoupling effects (i.e. the $\mathcal{O}(m_H^0)$ terms) introduced by a SM-like heavy Higgs.

Finally we recall that, although the covariance of the expansion in Eq. (6.13) is not manifest, the symmetry of the functional trace guarantees that the final result can be rearranged such that all the covariant derivatives appear in commutators [15, 23]. As a result, one can always rearrange the expansion of Eq. (6.13) in a manifestly covariant way in terms of traces containing powers of U, field-strength tensors and covariant derivatives acting on them. As noted in Refs. [16, 22, 23], this rearrangement can be easily performed when U does not depend on derivatives, as it is the case when only heavy particles enter in the loop.[4] However, for the case where $U = U\left(x, \partial_x + ip\right)$, as it happens in general in theories with heavy-light loops, the situation is more involved and the techniques developed in Refs. [16, 22, 23] cannot be directly applied. In this more general case it is convenient to separate U into momentum-dependent and momentum-independent pieces, i.e. $U = U_H(x) + U_{LH}\left(x, \partial_x + ip\right)$ which, at the diagrammatic level, typically corresponds to a separation into pure heavy loops and heavy-light loops.[5] This separation presents two major advantages: first, the power counting for U_H and U_{LH} is generically different, with U_H at most $\mathcal{O}\left(\zeta\right)$ and U_{LH} at most $\mathcal{O}\left(\zeta^0\right)$, both for bosons and fermions, which allows for a different truncation of the series in Eq. (6.13) for

[3] The part of the operator U coming from Δ_H arises from interaction terms with at least three fields. If all three fields are bosons, the dimension-4 operator may contain a dimensionful parameter $\sim \zeta$ or a derivative, giving rise to a term in U of $\mathcal{O}(\zeta)$. If two of the fields are fermions the operator is already of dimension 4 and then $\Sigma \sim \zeta^0$, which yields a contribution in U of $\mathcal{O}(\zeta)$ upon application of Eq. (6.12). Contributions from $X_{LH}^\dagger \Delta_L^{-1} X_{LH}$, in the following referred as heavy-light, appear from the product of two interaction terms and a light-field propagator and hence they generate terms in U of $\mathcal{O}(\zeta^0)$.

[4] With the exception of theories with massive vector fields and derivative couplings among two heavy and one light fields.

[5] This diagrammatic interpretation is not valid for theories with vector fields containing derivative couplings with two heavy and one light fields.

the terms involving only pure heavy contributions and those involving at least one power of U_{LH}. Second, universal expansions of Eq. (6.13) in a manifestly covariant form for $U = U_H(x)$ have been derived in the literature up to $\mathcal{O}(\zeta^{-2})$, i.e. for the case of dimension-six operators [1,22,24,25], that we reproduce in Eq. (6.A.2). The evaluation of the remaining piece, corresponding to terms containing at least one power of U_{LH} can be done explicitly from Eq. (6.15).

Let us end the section by summarizing the steps required to obtain the one-loop matching coefficients in our method:

1. We collect all field degrees of freedom in $\mathcal{L}$, light and heavy, in a field multiplet $\eta = (\eta_H, \eta_L)$, where η_i and $(\eta_i)^*$ must be written as separate components for charged fields. We split the fields into classical and quantum part, i.e $\eta \to \hat{\eta}+\eta$, and identify the fluctuation operator $\mathcal{O}$ from the second order variation of $\mathcal{L}$ with respect to η^* and η evaluated at the classical field configuration, see Eqs. (6.1) and (6.2),

$$\mathcal{O}_{ij} = \left.\frac{\partial^2 \mathcal{L}}{\partial \eta_i^* \, \partial \eta_j}\right|_{\eta=\hat{\eta}} . \tag{6.17}$$

2. We then consider $U(x, \partial_x)$, given in Eqs. (6.10) and (6.12), with $\widetilde{\Delta}_H$ defined in Eq. (6.5) in terms of the components of $\mathcal{O}$. Derivatives in U must be shifted as $\partial_x \to \partial_x + ip$. The computation of U requires the inversion of Δ_L: A general expression for the latter is provided in Eq. (6.14). The operator $U(x, \partial_x + ip)$ has to be expanded up to a given order in ζ, with the counting given by $p, m_H \sim \zeta \gg m_L, \partial_x$. For deriving the dimension-six EFT operators, the expansion of U must be taken up to $\mathcal{O}(\zeta^{-4})$.

3. The final step consists on the evaluation of the traces of $U(x, \partial_x + ip)$ in Eq. (6.13) up to the desired order – $\mathcal{O}(\zeta^{-2})$ for the computation of the one-loop dimension-six effective Lagrangian –. For this computation it is convenient to make the separation $U(x, \partial_x + ip) = U_H(x) + U_{LH}(x, \partial_x + ip)$ and apply the standard formulas for the traces of $U_H(x)$, see Eq. (6.A.2). The remaining contributions consist in terms involving at least one power of $U_{LH}(x, \partial_x + ip)$: A general formula for the case of dimension-six operators can be found in Eq. (6.A.3). Their computation only requires trivial integrals of the form:

$$\int \frac{d^d p}{(2\pi)^d} \frac{p_{\mu_1} \dots p_{\mu_{2k}}}{(p^2)^\alpha \, (p^2 - m_H^2)^\beta} = \frac{(-1)^{\alpha+\beta+k} \, i}{(4\pi)^{\frac{d}{2}}} \frac{\Gamma\left(\frac{d}{2} + k - \alpha\right) \Gamma\left(-\frac{d}{2} - k + \alpha + \beta\right)}{\Gamma(\beta) \, \Gamma\left(\frac{d}{2} + k\right)} \times \frac{g_{\mu_1 \dots \mu_{2k}}}{2^k} \, m_H^{d+2k-2\alpha-2\beta} , \tag{6.18}$$

where $g_{\mu_1 \dots \mu_{2k}}$ is the totally symmetric tensor with $2k$ indices constructed from $g_{\mu\nu}$ tensors.

Terms containing open covariant derivatives, i.e. derivatives acting only at the rightmost of the traces, should be kept throughout the computation and will either vanish or combine in commutators, yielding gauge-invariant terms with field strength tensors. A discussion about such terms can be found in Appendix 6.A.

6.2 Comparison with previous approaches

In Ref. [5], a procedure to obtain the one-loop matching coefficients also using functional integration has been proposed. We wish to highlight here the differences of that method, in the following referred as HLM, with respect to the one presented in this manuscript.

The first difference is how Ref. [5] disentangles contributions from heavy-light loops from the rest. In the HLM method the determinant of the fluctuation operator $\mathcal{O}$ which defines the complete one-loop action S is split using an identity (see their Appendix B) that is formally equivalent in our language to performing a field transformation of the form

$$P_{\rm HLM} = \begin{pmatrix} I & -\Delta_H^{-1} X_{LH}^\dagger \\ 0 & I \end{pmatrix} , \tag{6.19}$$

that block-diagonalizes the fluctuation operator as:

$$P_{\rm HLM}^\dagger \, \mathcal{O} P_{\rm HLM} = \begin{pmatrix} \Delta_H & 0 \\ 0 & \widetilde{\Delta}_L \end{pmatrix} , \tag{6.20}$$

where now

$$\widetilde{\Delta}_L = \Delta_L - X_{LH} \Delta_H^{-1} X_{LH}^\dagger \, . \tag{6.21}$$

The functional determinant is then separated in the HLM framework into two terms: The determinant of Δ_H, that corresponds to the loops with only heavy particles, and the determinant of $\widetilde{\Delta}_L$, containing both the loops with only light propagators and those with mixed heavy and light propagators. The former contributes directly to U_H, and provides part of the one-loop matching conditions (namely those denoted as "heavy" in Ref. [5]), upon using the universal formula valid for U not depending in derivatives, Eq. (6.A.2), up to a given order in the expansion in $1/m_H$. On the other hand, to obtain the matching conditions that arise from $\widetilde{\Delta}_L$ (called "mixed" contributions in the HLM terminology), one has to subtract those contributions already contained in the one-loop terms from the EFT theory matched at tree-level. To perform that subtraction without computing both the determinant of $\widetilde{\Delta}_L$ and that of the quadratic fluctuation of $\mathcal{L}_{\rm EFT}^{\rm tree}$, HLM argues that one has to subtract to the heavy propagators that appear in the computation of $\det \widetilde{\Delta}_L$ the expansion of the heavy propagator to a given order in the limit $m_H \to \infty$. According to HLM, the subtracted piece builds up the terms ("local counterparts") that match the loops from $\mathcal{L}_{\rm EFT}^{\rm tree}$. These "local counterparts" have to be identified for each order in the EFT, and then dropped prior to the evaluation of the functional traces. This prescription resembles the one used in Ref. [25] to obtain the one-loop effective Lagrangian from integrating out a heavy scalar singlet added to the SM.

While we do not doubt the validity of the HLM method, which the authors of Ref. [5] have shown through specific examples, we believe the framework presented in this manuscript brings some important simplifications. Let us note first that in the method of Ref. [5], contributions from heavy-light loops are incorporated into $\det \widetilde{\Delta}_L$, which results from the functional integration over the light fields. If the light

sector contains both bosonic and fermonic degrees of freedom that interact with the heavy sector (as it is the case in most extensions of the SM), a further diagonalization of $\widetilde{\Delta}_L$ into bosonic and fermionic blocks is required in order to perform the Gaussian integral over the light fields. That step is avoided in our approach, where we shift all heavy particle effects into $\widetilde{\Delta}_H$ and we only need to perform the path integral over the heavy fields. Secondly, our method provides a closed formula (up to trivial integrations which depend on the structure of U_{LH}) valid for any given model, from which the matching conditions of all EFT operators of a given dimension are obtained. In this sense it is more systematic than the subtraction prescription of the HLM method, which requires some prior identification of the subtraction terms for the heavy particle propagators in the model of interest. Furthermore, in the HLM procedure the light particle mass in the light field propagators is not expanded out in the computation of the functional traces, and intermediate results are therefore more involved. In particular, non-analytic terms in the light masses can appear in intermediate steps of the calculation, and cancellations of such terms between different contributions have to occur to get the infrared-finite matching coefficients at one loop. Given the amount of algebra involved in the computation of the functional traces, automation is a prerequisite for integrating out heavy particles in any realistic model. In our method, such automation is straightforward (and indeed has been used for the heavy real scalar triplet example given in Section 6.3). From the description of Ref. [5], it seems to us that is harder to implement the HLM method into an automated code that does not require some manual intervention.

An alternative framework to obtain the one-loop effective Lagrangian through functional integration, that shares many similarities with that of HLM, has been suggested in Ref. [6]. The authors of Ref. [6] have also introduced a subtraction procedure that involves the truncation of the heavy particle propagator. Their result for the dimension-6 effective Lagrangian in the case that the heavy-light quadratic fluctuation is derivative-independent has been written in terms of traces of manifestly gauge-invariant operators depending on the quadratic fluctuation $U(x)$, times coefficients where the EFT contributions have been subtracted. Examples on the calculation of such subtracted coefficients, which depend on the ultraviolet model, are provided in this reference. The approach is however limited, as stated by the authors, by the fact that it cannot be applied to cases where the heavy-light interactions contain derivative terms. That is the case, for instance, in extensions of the SM where the heavy fields have interactions with the SM gauge bosons (see the example we provide in Section 6.3.2). Let us also note that the general formula provided in the framework of Ref. [6] is written in terms of the components of the original fluctuation operator where no diagonalization to separate heavy- and light-field blocks has been performed. This implies that its application to models with mixed statistics in the part of the light sector that interacts with the heavy one, and even to models where the heavy and light degrees of freedom have different statistics, must require additional steps that are not discussed in Ref. [6].

6.3 Examples

In this section we perform two practical applications of the framework that we have developed above. The first one is a scalar toy model simple enough to allow a comparison of our method with the standard matching procedure. Through this example we can also illustrate explicitly that matching coefficients arise from the hard region of the one-loop amplitudes in the full theory. The second example corresponds to a more realistic case where one integrates out a heavy real scalar triplet that has been added to the SM.

6.3.1 Scalar toy model

Let us consider a model with two real scalar fields, φ with mass m and ϕ with mass M, whose interactions are described by the Lagrangian

$$\mathcal{L}(\varphi,\phi) = \frac{1}{2}\left(\partial_\mu\phi\,\partial^\mu\phi - M^2\,\phi^2\right) + \frac{1}{2}\left(\partial_\mu\varphi\,\partial^\mu\varphi - m^2\,\varphi^2\right) - \frac{\kappa}{4!}\,\varphi^4 - \frac{\lambda}{3!}\,\varphi^3\,\phi\,. \quad (6.22)$$

Assuming $M \gg m$ we wish to determine the effective field theory resulting from integrating out the ϕ field: $\mathcal{L}_{\rm EFT}(\hat\varphi)$. We perform the calculation up to and including $1/M^2$-suppressed operators in the EFT. Within this model this implies that we have to consider up to six-point Green functions. This same model has also been considered in Ref. [5].

At tree level we solve for the equation of motion of the ϕ field and we obtain

$$\hat\phi = -\frac{\lambda}{6M^2}\,\hat\varphi^3 + \mathcal{O}(M^{-4})\,, \quad (6.23)$$

that, upon substituting in Eq. (6.22), gives the tree-level effective Lagrangian

$$\mathcal{L}^{\rm tree}_{\rm EFT} = \frac{1}{2}\left(\partial_\mu\hat\varphi\,\partial^\mu\hat\varphi - m^2\,\hat\varphi^2\right) - \frac{\kappa}{4!}\,\hat\varphi^4 + \frac{\lambda^2}{72M^2}\,\hat\varphi^6\,. \quad (6.24)$$

To proceed at one loop we use the background field method as explained in Section 6.1: $\phi \to \hat\phi + \phi$ and $\varphi \to \hat\varphi + \varphi$. We have $\eta = (\phi,\varphi)^\intercal$ and we consider the same counting as in Eq. (6.16): $p_\mu, M \sim \zeta$. The fluctuation operator in Eq. (6.2) is given by

$$\begin{aligned} \Delta_H &= -\partial^2 - M^2\,,\\ \Delta_L &= -\partial^2 - m^2 - \frac{\kappa}{2}\,\hat\varphi^2 - \lambda\,\hat\varphi\,\hat\phi\,,\\ X_{LH} &= -\frac{\lambda}{2}\,\hat\varphi^2\,, \end{aligned} \quad (6.25)$$

that only depends on the classical field configurations. In order to construct $\widetilde{\Delta}_H(x,\partial_x + ip)$ in Eq. (6.5) we need to determine $\Delta_L^{-1}(x,\partial_x+ip)$ up to, and including, terms of order ζ^{-4}:

$$\begin{aligned} \Delta_L(x,\partial_x+ip) &= p^2 - m^2 - 2i\,p_\mu\,\partial^\mu - \partial^2 - \frac{\kappa}{2}\,\hat\varphi^2 - \lambda\,\hat\varphi\,\hat\phi\,,\\ \Delta_L^{-1}(x,\partial_x+ip) &= \frac{1}{p^2}\left(1+\frac{m^2}{p^2}\right) + \frac{1}{p^4}\left(2i\,p_\mu\partial^\mu + \partial^2 + \frac{\kappa}{2}\hat\varphi^2\right) - 4\,\frac{p_\mu p_\nu}{p^6}\,\partial^\mu\partial^\nu + \mathcal{O}(\zeta^{-5})\,. \end{aligned} \quad (6.26)$$

Using this result we get $U(x, \partial_x + ip)$ from Eq. (6.10)

$$U(x,\partial_x+ip) = \frac{\lambda^2}{4}\,\hat{\varphi}^2\,\left[\frac{1}{p^2}\left(1+\frac{m^2}{p^2}\right)+\frac{1}{p^4}\left(2i\,p_\mu\partial^\mu+\partial^2+\frac{\kappa}{2}\hat{\varphi}^2\right)-4\,\frac{p_\mu p_\nu}{p^6}\,\partial^\mu\partial^\nu\right]\,\hat{\varphi}^2 + \mathcal{O}(\zeta^{-5})\,. \tag{6.27}$$

Inserting this operator in Eq. (6.13), we notice that at the order we are considering only the $n = 1$ term contributes, with

$$\mathcal{L}_{\rm EFT}^{\rm 1loop} \;=\; -\frac{i}{2}\int\frac{d^dp}{(2\pi)^d}\,\frac{U(x,\partial_x+ip)}{p^2-M^2}\,. \tag{6.28}$$

The momentum integration can be readily performed: In the $\overline{\rm MS}$ regularization scheme with $\mu = M$ we finally obtain

$$\mathcal{L}_{\rm EFT}^{\rm 1loop} \;=\; \frac{\lambda^2}{16(16\pi^2)}\left[2\left(1+\frac{m^2}{M^2}\right)\hat{\varphi}^4-\frac{1}{M^2}\hat{\varphi}^2\partial^2\hat{\varphi}^2+\frac{\kappa}{M^2}\hat{\varphi}^6\right]\,. \tag{6.29}$$

Let us recover now this result through the usual matching procedure between the full theory $\mathcal{L}(\varphi,\phi)$ in Eq. (6.22) and the effective theory without the heavy scalar field ϕ. Our goal is to further clarify the discussion given in Section 6.1 on the hard origin of the matching coefficients of the effective theory by considering this purely academic case. In order to make contact with the result obtained in Eq. (6.29) using the functional approach, we perform the matching off-shell and we use the $\overline{\rm MS}$ regularization scheme with $\mu = M$. We do not consider in the matching procedure one-loop diagrams with only light fields, since they are present in both the full-theory and the effective theory amplitudes and, accordingly, cancel out in the matching.

For the model under discussion there is no contribution to the two- and three-point Green functions involving heavy particles in the loop. The diagrams contributing to the matching of the four-point Green function are given by

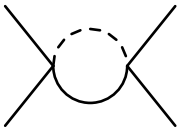

$$= \frac{i}{16\pi^2}\,\lambda^2\left[3+3\,\frac{m^2}{M^2}+\frac{s+t+u}{2M^2}\right]\Bigg|_{\rm hard} + \frac{i}{16\pi^2}\,\lambda^2\left[-3\,\frac{m^2}{M^2}+3\,\frac{m^2}{M^2}\ln\left(\frac{m^2}{M^2}\right)\right]\Bigg|_{\rm soft}+\mathcal{O}(M^{-4}),$$

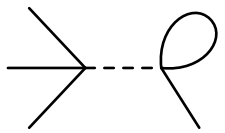

$$= \frac{i}{16\pi^2}\,\lambda^2\left[-2\,\frac{m^2}{M^2}+2\,\frac{m^2}{M^2}\ln\left(\frac{m^2}{M^2}\right)\right]\Bigg|_{\rm soft}+\mathcal{O}(M^{-4}), \tag{6.30}$$

where we have explicitly separated the contributions from the hard and soft loop-momentum regions. Note that a non-analytic term in m can only arise from the

soft region, since in the hard region the light mass and the external momenta are expanded out from the propagators. For the corresponding EFT computation we need the effective Lagrangian matched at one-loop:

$$\mathcal{L}_{\rm EFT} = \mathcal{L}_{\rm EFT}^{\rm tree} + \frac{\alpha}{4!}\,\hat{\varphi}^4 \,+\, \frac{\beta}{4!M^2}\,\hat{\varphi}^2\partial^2\hat{\varphi}^2 + \frac{\gamma}{6!M^2}\,\hat{\varphi}^6\,, \tag{6.31}$$

which now includes the dimension-6 operator with four light fields, and the one-loop matching coefficient for the 4- and 6-light field operators already present in $\mathcal{L}_{\rm EFT}^{\rm tree}$. The EFT contributions to the four-point Green function read

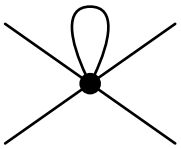

$$= \frac{i}{16\pi^2}\,\lambda^2\left[-5\,\frac{m^2}{M^2} + 5\,\frac{m^2}{M^2}\ln\left(\frac{m^2}{M^2}\right)\right] + \mathcal{O}(M^{-4})\,,$$

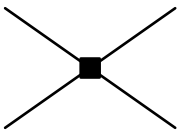

$$= i\,\alpha \,-\, i\,\frac{\beta}{3M^2}\,(s+t+u)\,. \tag{6.32}$$

We see that the soft components of the full-theory amplitude match the one-loop diagram in the effective theory, and the matching coefficients of the φ^4 operators get thus determined by the hard part of the one-loop full-theory amplitude:

$$\alpha \,=\, \frac{3}{16\pi^2}\,\lambda^2\left(1+\frac{m^2}{M^2}\right) \quad , \qquad \beta \,=\, -\,\frac{3}{16\pi^2}\,\frac{\lambda^2}{2}\,. \tag{6.33}$$

in agreement with the result for the φ^4 terms in Eq. (6.29).

The next contribution to the one-loop effective theory comes from the six-point Green function. The full theory provides two diagrams for the matching:

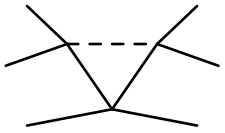

$$= \frac{i}{16\pi^2}\,45\,\frac{\kappa\,\lambda^2}{M^2}\bigg|_{\rm hard} + \frac{i}{16\pi^2}\,45\,\frac{\kappa\,\lambda^2}{M^2}\ln\left(\frac{m^2}{M^2}\right)\bigg|_{\rm soft} + \mathcal{O}(M^{-4}),$$

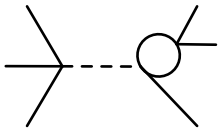

$$= \frac{i}{16\pi^2}\,30\,\frac{\kappa\,\lambda^2}{M^2}\ln\left(\frac{m^2}{M^2}\right)\bigg|_{\rm soft} + \mathcal{O}(M^{-4}), \tag{6.34}$$

where once more we have explicitly separated the hard and soft contributions from each diagram. The six-point effective theory amplitude gives

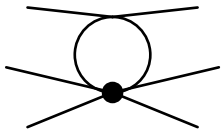

$$= \frac{i}{16\pi^2}\,75\,\frac{\kappa\,\lambda^2}{M^2}\ln\left(\frac{m^2}{M^2}\right) + \mathcal{O}(M^{-4})\,,$$

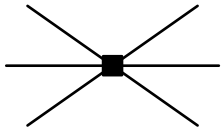

$$= i\frac{\gamma}{M^2}\,. \tag{6.35}$$

Again, we note that the soft terms of the full theory are reproduced by the one-loop diagram in the effective theory. The local contribution is determined by the hard part of the full theory amplitude and thus reads

$$\gamma \;=\; \frac{45}{16\pi^2}\,\kappa\,\lambda^2\,, \tag{6.36}$$

that matches the result found in Eq. (6.29) for the $\hat{\varphi}^6$ term.

6.3.2 Heavy real scalar triplet extension

As a second example, we consider an extension of the SM with an extra scalar sector comprised by a triplet of heavy scalars with zero hypercharge, $\Phi^a, a = 1, 2, 3$, which interacts with the light Higgs doublet [26]. A triplet of scalars are ubiquitous in many extensions of the SM, see for instance Refs. [27–32]. However, we are not interested here in the phenomenology of the model but in how to implement our procedure in order to integrate out, at one loop, the extra scalar sector of the theory, assumed it is much heavier than the rest of the spectrum. Partial results for the dimension-6 operators involving the light Higgs doublet that are generated from this model have been provided in the functional approaches of Refs. [5, 6].

The Lagrangian of the model is given by

$$\mathcal{L} = \mathcal{L}_{\rm SM} + \frac{1}{2}D_\mu\Phi^a D^\mu\Phi^a - \frac{1}{2}M^2\Phi^a\Phi^a - \frac{\lambda_\Phi}{4}\left(\Phi^a\Phi^a\right)^2 + \kappa\,\left(\phi^\dagger\tau^a\phi\right)\Phi^a - \eta\left(\phi^\dagger\phi\right)\Phi^a\Phi^a, \tag{6.37}$$

Here ϕ is the SM Higgs doublet and the covariant derivative acting on the triplet is defined as $D_\mu\Phi^a \equiv D^{ac}_\mu\,\Phi^c = \left(\partial_\mu\,\delta^{ac} + g\varepsilon^{abc}W^b_\mu\right)\Phi^c$. Within the background field method we split the fields into their classical (with hat) and quantum components: $\Phi^a \to \hat{\Phi}^a + \Phi^a$, $\phi \to \hat{\phi} + \phi$ and $W^a_\mu \to \hat{W}^a_\mu + W^a_\mu$. Given as an expansion in inverse powers of its mass, the classical field of the scalar triplet reads

$$\hat{\Phi}^a = \frac{\kappa}{M^2}\left(\hat{\phi}^\dagger\tau^a\hat{\phi}\right) - \frac{\kappa}{M^4}\left[\hat{D}^2 + 2\eta\left(\hat{\phi}^\dagger\hat{\phi}\right)\right]\left(\hat{\phi}^\dagger\tau^a\hat{\phi}\right) + \mathcal{O}\left(\frac{\kappa}{M^6}\right). \tag{6.38}$$

Following the procedure described in the Section 6.1 we divide the fields into heavy and light, respectively, as $\eta_H = \Phi^a$ and $\eta_L = \{\phi, \phi^*, W^a_\mu\}$. The fluctuation matrix is readily obtained from Eqs. (6.1) and (6.2),

$$\begin{aligned}
\Delta_H &= \Delta^{ab}_{\Phi\Phi}\,,\\
X^\dagger_{LH} &= \left(\left(X^a_{\phi^*\Phi}\right)^\dagger\;\left(X^a_{\phi^*\Phi}\right)^\intercal\;\left(X^{\nu\,da}_{W\Phi}\right)^\intercal\right),\\
\Delta_L &= \begin{pmatrix}
\Delta_{\phi^*\phi} & X^\dagger_{\phi\phi} & \left(X^{\nu\,d}_{W\phi}\right)^\dagger\\
X_{\phi\phi} & \Delta^\intercal_{\phi^*\phi} & \left(X^{\nu\,d}_{W\phi}\right)^\intercal\\
X^{\mu\,c}_{W\phi} & \left(X^{\mu\,c}_{W\phi}\right)^* & \Delta^{\mu\nu\,cd}_W
\end{pmatrix},
\end{aligned} \tag{6.39}$$

with

$$\begin{aligned}
\Delta_W^{\mu\nu\,ab} &= \left(\Delta_W^{\mu\nu\,ab}\right)_{\rm SM} + g^2\, g_{\mu\nu}\,\epsilon^{acm}\epsilon^{bdm}\,\hat{\Phi}^c\hat{\Phi}^d,\\
\Delta_{\phi^*\phi} &= (\Delta_{\phi^*\phi})_{\rm SM} + \kappa\,\tau^a\hat{\Phi}^a - \eta\,\hat{\Phi}^a\hat{\Phi}^a,\\
\Delta_{\Phi\Phi}^{ab} &= -\,\hat{D}^2_{ab} + \delta_{ab}\left[-M^2 - \lambda_\Phi\hat{\Phi}^c\hat{\Phi}^c - 2\eta\left(\hat{\phi}^\dagger\hat{\phi}\right)\right] - 2\lambda_\Phi\hat{\Phi}^a\hat{\Phi}^b\,,\\
X_{W\Phi}^{\mu\,ab} &= g\epsilon^{abc}\left(\hat{D}^\mu\hat{\Phi}^c\right) + g\epsilon^{acd}\,\hat{\Phi}^c\hat{D}^{\mu\,db},\\
X_{\phi^*\Phi}^{a} &= \kappa\,\tau^a\,\hat{\phi} - 2\eta\,\hat{\phi}\,\hat{\Phi}^a,
\end{aligned} \tag{6.40}$$

and the rest of fluctuations in Δ_L involving only the light fields are contained in the quadratic piece of the SM Lagrangian, which we provide in Eqs. (6.B.2) and (6.B.4). The quadratic term containing all fluctuations related to the heavy triplet is given by our formula (6.5),

$$\widetilde{\Delta}_{\Phi\Phi} = \Delta_{\Phi\Phi} - X_{LH}^\dagger\Delta_L^{-1}X_{LH}\,. \tag{6.41}$$

The expansion in inverse powers of the heavy mass of the triplet requires a counting analogous to the one in Eq. (6.16), i.e. $p_\mu \sim \zeta$ and $M \sim \zeta$. For the counting of the dimensionful parameter κ we choose $\kappa \sim \zeta$ and then, from Eq. (6.38) we have $\hat{\Phi}^a \sim \zeta^{-1}$. As we are interested in dimension-six effective operators we can neglect contributions $\mathcal{O}\left(\zeta^{-5}\right)$ and smaller. This is because in Eq. (6.13) the propagator in the heavy particle provides an extra power ζ^{-2}. Hence we only need the numerator up to $\mathcal{O}(\zeta^{-4})$.

For practical reasons we choose to work in the Landau gauge for the quantum fluctuations, i.e. the renormalizable gauge with $\xi_W = 0$ in Eqs. (6.B.5) and (6.B.8). The computation is much simpler in this gauge because the inverse of the propagators are transverse. Rearranging the expression in Eq. (6.41), we can write

$$\begin{aligned}
\widetilde{\Delta}_{\Phi\Phi}^{ab} = \Delta_{\Phi\Phi}^{ab} &- \left[\left(X_{\phi^*\Phi}^a\right)^\dagger\overline{\Delta}_{\phi^*\phi}^{\;-1}X_{\phi^*\Phi}^b + \left(X_{\phi^*\Phi}^a\right)^\intercal\overline{X}_{\phi\phi}X_{\phi^*\Phi}^b + c.c.\right]\\
&- \left(\overline{X}_{W\Phi}^{\mu\,ca}\right)^\intercal\left(\Delta_W^{\mu\nu\,cd}\right)^{-1}\overline{X}_{W\Phi}^{\nu\,db} + \mathcal{O}\left(\zeta^{-5}\right)\,,
\end{aligned} \tag{6.42}$$

where *c.c.* is short for complex conjugation and we have used the following definitions:

$$\begin{aligned}
\overline{\Delta}_{\phi^*\phi}^{\;-1} &= \Delta_{\phi^*\phi}^{-1} + \Delta_{\phi^*\phi}^{-1}X_{\phi\phi}^\dagger\left(\Delta_{\phi^*\phi}^{-1}\right)^\intercal X_{\phi\phi}\Delta_{\phi^*\phi}^{-1}\,,\\
\overline{X}_{\phi\phi} &= -\left(\Delta_{\phi^*\phi}^{-1}\right)^\intercal X_{\phi\phi}\,\Delta_{\phi^*\phi}^{-1}\,,\\
\overline{X}_{W\Phi}^{\mu\,ab} &= X_{W\Phi}^{\mu\,ab} - \left(X_{W\phi}^{\mu\,a}\Delta_{\phi^*\phi}^{-1}X_{\phi^*\Phi}^b + c.c.\right)\,.
\end{aligned} \tag{6.43}$$

To proceed we now come back to Eq. (6.13) (with negative sign), with $m_H = M$ and $U = -\hat{D}^2 - M^2 - \widetilde{\Delta}_{\Phi\Phi}$. Remember that the hat on the covariant derivatives indicates that only the classical field configuration for the gauge bosons is involved. Then by computing Eq. (6.42) up to $\mathcal{O}(\zeta^{-4})$ one can obtain the one-loop effective theory that derives from the model specified in Eq. (6.37) upon integrating out the triplet of heavy scalars.

We do not intend here to provide the complete result of the generated dimension-six operators. As a simple example and for illustrative purposes, we provide details on the computation of the heavy-light contributions arising from the quantum fluctuations of the electroweak gauge bosons. The latter provide the matching contributions to the dimension-six operators with Higgs fields and no field strength tensors proportional to g^2, which were not obtained with the functional approach in Ref. [6] due to the presence of "open" covariant derivatives. The computation of such contributions was also absent in the approach of Ref. [5]. The relevant term in $U(x, \partial_x + ip)$ for this calculation is

$$\left[\left(\overline{X}^{\mu\, ca}_{W\Phi}\right)^{\intercal}\left(\Delta^{\mu\nu\, cd}_{W}\right)^{-1}\overline{X}^{\nu\, db}_{W\Phi}\right](x, \partial_x + ip)\ . \tag{6.44}$$

The first operator in Eq. (6.44) simply reads

$$\begin{aligned}
\overline{X}^{\mu\, ab}_{W\Phi}(x, \partial_x + ip) = &-ig\,\epsilon^{abc}\,\hat{\Phi}^c p^\mu + \frac{\kappa}{p^2}\,ig\,\epsilon^{abc}\left(\hat{\phi}^\dagger\tau^c\hat{\phi}\right)p_\mu \\
&+ g\epsilon^{abc}\left(\hat{D}^\mu\hat{\Phi}^c\right) + g\epsilon^{acd}\,\hat{\Phi}^c\hat{D}^{\mu\, db} - \frac{1}{p^2}\,g\kappa\left\{-\frac{i}{2}\left[\left(\hat{D}_\mu\hat{\phi}\right)^\dagger\tau^a\tau^b\,\hat{\phi}\right]\right. \\
&\left.+\frac{i}{2}\left(\hat{\phi}^\dagger\tau^a\tau^b\hat{D}_\mu\hat{\phi}\right) + \frac{i}{2}\left(\hat{\phi}^\dagger\tau^a\tau^d\hat{\phi}\right)\hat{D}^{db}_\mu + c.c.\right\} + \mathcal{O}\left(\zeta^{-2}\right) \\
= &\ g\,\epsilon^{abc}\left(\hat{D}^\mu\hat{\Phi}^c\right) - \frac{g\kappa}{p^2}\,i\,\delta_{ab}\left(\hat{\phi}^\dagger\overset{\leftrightarrow}{\hat{D}}_\mu\hat{\phi}\right) \\
&- g\,\frac{p^2 - M^2}{p^2}\,\epsilon^{acd}\,\hat{\Phi}^d\left(\hat{D}^{cb}_\mu + ip_\mu\,\delta^{cb}\right) + \mathcal{O}\left(\zeta^{-2}\right)\ ,
\end{aligned} \tag{6.45}$$

where, in the last line, we used the EOM for the heavy triplet, Eq. (6.38), and we defined the hermitian derivative terms

$$\left(\phi^\dagger\overset{\leftrightarrow}{D}_\mu\phi\right) \equiv \left(\phi^\dagger D_\mu\phi\right) - \left[\left(D_\mu\phi\right)^\dagger\phi\right]\ , \tag{6.46}$$

with the covariant derivative acting on the Higgs field as specified in Eq. (1.9). The contributions from the heavy triplet to the fluctuation Δ_W, see Eq. (6.40), do not affect the computation of $\Delta_W^{-1}(x, \partial_x + ip)$ at leading order, and we can take the expression given in Eq. (6.B.8) (with $\xi_W = 0$) for the latter. As a result we obtain

$$\begin{aligned}
\left[\left(\overline{X}^{\mu\, ca}_{W\Phi}\right)^{\intercal}\left(\Delta^{\mu\nu\, cd}_{W}\right)^{-1}\overline{X}^{\nu\, db}_{W\Phi}\right](x, \partial_x + ip) = g^2\left[-\frac{g^{\mu\nu}}{p^2} + \frac{p^\mu p^\nu}{p^4}\right]\left[\delta_{ab}\left(\hat{D}_\mu\hat{\Phi}^c\right)\left(\hat{D}_\nu\hat{\Phi}^c\right)\right. \\
- \delta_{ab}\frac{\kappa^2}{p^4}\left(\hat{\phi}^\dagger\overset{\leftrightarrow}{\hat{D}}_\mu\hat{\phi}\right)\left(\hat{\phi}^\dagger\overset{\leftrightarrow}{\hat{D}}_\nu\hat{\phi}\right) \\
\left.- \left(\hat{D}_\mu\hat{\Phi}^a\right)\left(\hat{D}_\nu\hat{\Phi}^b\right)\right] + \mathcal{O}\left(\zeta^{-5}\right)\ ,
\end{aligned} \tag{6.47}$$

and we dropped the terms proportional to $(p^2 - M^2)$ since they yield a null contribution in the momentum integration, as explained below.

Only the first term of the series in Eq. (6.13) contributes in this case:

$$\mathcal{L}^{1\text{loop}}_{\text{EFT}}\big|_W = -\frac{i}{2}\int\frac{d^dp}{(2\pi)^d}\,\frac{\left[\left(\overline{X}^{\mu\, ca}_{W\Phi}\right)^{\intercal}\left(\Delta^{\mu\nu\, cd}_{W}\right)^{-1}\overline{X}^{\nu\, da}_{W\Phi}\right](x, \partial_x + ip)}{p^2 - M^2}\ . \tag{6.48}$$

From Eq. (6.48) it is clear that terms proportional to $(p^2 - M^2)$ yield scaleless terms that are set to zero in dimensional regularization, which justifies having dropped them in Eq. (6.47). After evaluating the integral in the $\overline{\text{MS}}$ regularization scheme, using the heavy triplet EOMs and rearranging the result through partial integration we finally get for $\mu = M$

$$\mathcal{L}_{\text{EFT}}^{\text{1loop}}\big|_W = \frac{1}{16\pi^2}\frac{g^2\kappa^2}{M^4}\left[-\frac{25}{16}\left(\hat{\phi}^\dagger\hat{\phi}\right)\partial^2\left(\hat{\phi}^\dagger\hat{\phi}\right) + \frac{5}{4}\left[\left(\hat{\phi}^\dagger\hat{\phi}\right)\left(\hat{\phi}^\dagger\hat{D}^2\hat{\phi}\right) + h.c.\right] - \frac{5}{4}\left|\hat{\phi}^\dagger\hat{D}_\mu\hat{\phi}\right|^2\right]. \tag{6.49}$$

In order to compare this result with previous calculations done in the literature, we focus on the heavy triplet contributions to $Q_{\phi D} = \left|\phi^\dagger D^\mu\phi\right|^2$. From the result in Eq. (6.49) we find for its one-loop matching coefficient

$$C_{\phi D}(\mu = M)\Big|_{\mathcal{O}(g^2)} = -\frac{1}{16\pi^2}\frac{\kappa^2}{M^4}\frac{5}{4}g^2\,, \tag{6.50}$$

which agrees with the result given in Ref. [3] for the term proportional to g^2. The remaining contributions to $C_{\phi D}(\mu = M)$ have also been calculated with our method. However their computation is lengthy and does not provide any new insight on the method. The final result reads

$$C_{\phi D}(\mu = M) = \frac{\kappa^2}{M^4}\left[-2 + \frac{1}{16\pi^2}\left(5\frac{\kappa^2}{M^2} - \frac{5}{4}g^2 + 16\eta - 3\lambda - 20\lambda_\Phi\right)\right]. \tag{6.51}$$

In Eq. (6.51) we have also included the term arising from the redefinition of ϕ that absorbs the one-loop contribution to the kinetic term, $\phi \to \left(1 - 3\kappa^2/64\pi^2M^2\right)\phi$. This result is in agreement with the one provided in Ref. [3] once we account for the different convention in the definition of λ: our λ equals 2λ in that reference.

6.4 Conclusions

The search for new physics in the next run at LHC stays as a powerful motivation for a systematic scrutiny of the possible extensions of the SM. The present status that engages both collider and precision physics has, on the theoretical side, a robust tool in the construction, treatment and phenomenology of effective field theories that are the remains of ultraviolet completions of the SM upon integration of heavy spectra.

Though, traditionally, there are two essential procedures to construct those effective field theories, namely functional methods and matching schemes, the latter have become the most frequently used. Recently there has been a rediscovery of the functional methods, initiated by the work of Henning et al. [1]. The latter work started a discussion regarding the treatment of the terms that mix heavy and light quantum fluctuations, that was finally clarified but which, in our opinion, was already settled in the past literature on the subject. In this chapter we have addressed this issue and we have provided a framework that further clarifies the treatment of the heavy-light contributions and simplifies the technical modus operandi.

The procedure amounts to a particular diagonalization of the quadratic form in the path integral of the full theory that leaves untouched the part that entails the light fields. In this way we can integrate, at one loop, contributions with only heavy fields inside the loop and contributions with mixed components of heavy and light fields, with a single computation and following the conventional method employed to carry out the first ones only. We have also showed that in the resulting determinant containing the heavy particle effects only the *hard* components are needed to derive the one-loop matching coefficients of the effective theory. Within dimensional regularization these hard contributions are obtained by expanding out the low-energy scales with respect the hard loop momentum which has to be considered of the same order as the mass of the heavy particle. In this way, our determination of the EFT local terms that reproduce the heavy-particle effects does not require the subtraction of any one-loop contributions from the EFT, as opposed to the conventional (diagrammatic) matching approach or to the recently proposed methods that use functional techniques. We have included two examples in Section 6.3: A scalar toy model, that nicely illustrates the simplicity of our approach as compared to the diagrammatic approach, and a heavy real scalar triplet extension of the SM, which shows that our method can be applied also to more realistic cases.

Appendices

6.A General expressions for dimension-six operators

In this appendix we workout $\mathcal{L}_{\rm EFT}^{\rm 1loop}$ for the case of dimension-six operators. Following the guidelines in Section 6.1, we make the separation $U(x,\partial_x+ip) = U_H(x) + U_{LH}(x,\partial_x+ip)$ and expand Eq. (6.13) up to $\mathcal{O}(\zeta^{-2})$. The Lagrangian $\mathcal{L}_{\rm EFT}^{\rm 1loop}$ then consists of two pieces:

$$\mathcal{L}_{\rm EFT}^{\rm 1loop} = \mathcal{L}_{\rm EFT}^{\rm 1loop}\Big|_{\rm H} + \mathcal{L}_{\rm EFT}^{\rm 1loop}\Big|_{\rm LH} \,. \tag{6.A.1}$$

The first term comes from contributions involving $U_H(x)$ only and, since $U_H(x)$ is momentum independent, it can be obtained from the universal formula provided in the literature [1,22,24,25] (see also [2] for the case when several scales are involved) which, for completeness, we reproduce here:

$$\begin{aligned}
\mathcal{L}_{\rm EFT}^{\rm 1loop}\Big|_{\rm H} = \frac{c_s}{16\pi^2}\Bigg\{ & m_H^2\left(1+\ln\frac{\mu^2}{m_H^2}\right)\mathrm{tr}\left\{U_H\right\} \\
& + \Big[\frac{1}{2}\ln\frac{\mu^2}{m_H^2}\,\mathrm{tr}\left\{U_H^2\right\} + \frac{1}{12}\ln\frac{\mu^2}{m_H^2}\,\mathrm{tr}\left\{\hat{F}_{\mu\nu}\hat{F}^{\mu\nu}\right\}\Big] \\
& + \frac{1}{m_H^2}\Big[-\frac{1}{6}\mathrm{tr}\left\{U_H^3\right\} + \frac{1}{12}\mathrm{tr}\left\{(\hat{D}_\mu U_H)^2\right\} - \frac{1}{12}\mathrm{tr}\left\{U_H\hat{F}^{\mu\nu}\hat{F}_{\mu\nu}\right\} \\
& \qquad + \frac{1}{60}\mathrm{tr}\left\{(\hat{D}_\mu\hat{F}^{\mu\nu})^2\right\} - \frac{1}{90}\mathrm{tr}\left\{\hat{F}^{\mu\nu}\hat{F}_{\nu\rho}\hat{F}^{\rho}{}_{\mu}\right\}\Big] \\
& + \frac{1}{m_H^4}\Big[\frac{1}{24}\mathrm{tr}\left\{U_H^4\right\} - \frac{1}{12}\mathrm{tr}\left\{U_H(\hat{D}_\mu U_H)^2\right\} + \frac{1}{60}\mathrm{tr}\left\{\hat{F}_{\mu\nu}(\hat{D}^\mu U_H)(\hat{D}^\nu U_H)\right\} \\
& \qquad + \frac{1}{120}\mathrm{tr}\left\{(\hat{D}^2U_H)^2\right\} + \frac{1}{40}\mathrm{tr}\left\{U_H^2\hat{F}_{\mu\nu}\hat{F}^{\mu\nu}\right\} + \frac{1}{60}\mathrm{tr}\left\{(U_H\hat{F}_{\mu\nu})^2\right\}\Big] \\
& + \frac{1}{m_H^6}\Big[-\frac{1}{60}\mathrm{tr}\left\{U_H^5\right\} + \frac{1}{20}\mathrm{tr}\left\{U_H^2(\hat{D}_\mu U_H)^2\right\} + \frac{1}{30}\mathrm{tr}\left\{(U_H\hat{D}_\mu U_H)^2\right\}\Big] \\
& + \frac{1}{m_H^8}\frac{1}{120}\mathrm{tr}\left\{U_H^6\right\} + \mathcal{O}\left(\zeta^{-3}\right) \,,
\end{aligned} \tag{6.A.2}$$

where $c_s = 1/2, -1/2$ depending, respectively, on the bosonic or fermionic nature of the heavy fields. Here $F_{\mu\nu} \equiv [D_\mu, D_\nu]$ and the momentum integrals are regulated in d dimensions, with the divergences subtracted in the $\overline{\rm MS}$ scheme. The second term in Eq. (6.A.1) is built from pieces containing at least one power of U_{LH}. Given that U_H is at most $\mathcal{O}(\zeta)$ and U_{LH} at most $\mathcal{O}(\zeta^0)$ in our power counting, the series in Eq. (6.13) has to be expanded up to $n=5$ for the contributions to dimension-six operators

$$\begin{aligned}
\mathcal{L}_{\rm EFT}^{\rm 1loop}\Big|_{\rm LH} = -ic_s\int\frac{d^dp}{(2\pi)^d}\Bigg\{ & \frac{1}{p^2-m_H^2}\,\mathrm{tr_s}\left\{U\right\} + \frac{1}{2}\frac{1}{\left(p^2-m_H^2\right)^2}\,\mathrm{tr_s}\left\{U^2\right\} \\
& + \frac{1}{3}\frac{1}{\left(p^2-m_H^2\right)^3}\left[\mathrm{tr_s}\left\{U^3\right\} + \mathrm{tr_s}\left\{U\hat{D}^2U\right\} + 2ip^\mu\,\mathrm{tr_s}\left\{U\hat{D}_\mu U\right\}\right]
\end{aligned}$$

$$
\begin{aligned}
&+\frac{1}{4}\frac{1}{(p^2-m_H^2)^4}\Big[\mathrm{tr_s}\left\{U^4\right\}+2ip^\mu\,\mathrm{tr_s}\left\{U^2\hat{D}_\mu U\right\}+2ip^\mu\,\mathrm{tr_s}\left\{U\hat{D}_\mu U^2\right\}\\
&\qquad+\mathrm{tr_s}\left\{U^2\hat{D}^2U\right\}+\mathrm{tr_s}\left\{U\hat{D}^2U^2\right\}\\
&\qquad-4\,p^\mu p^\nu\,\mathrm{tr_s}\left\{U\hat{D}_\mu\hat{D}_\nu U\right\}+2ip^\mu\,\mathrm{tr_s}\left\{U\hat{D}^2\hat{D}_\mu U\right\}\\
&\qquad+2ip^\mu\,\mathrm{tr_s}\left\{U\hat{D}_\mu\hat{D}^2U\right\}+\mathrm{tr_s}\left\{U(\hat{D}^2)^2\,U\right\}\Big]\\
&+\frac{1}{5}\frac{1}{(p^2-m_H^2)^5}\Big[\mathrm{tr_s}\left\{U^5\right\}+2ip^\mu\,\mathrm{tr_s}\left\{U^3\hat{D}_\mu U\right\}+2ip^\mu\,\mathrm{tr_s}\left\{U^2\hat{D}_\mu U^2\right\}\\
&\qquad+2ip^\mu\,\mathrm{tr_s}\left\{U\hat{D}_\mu U^3\right\}-4p^\mu p^\nu\,\mathrm{tr_s}\left\{U^2\hat{D}_\mu\hat{D}_\nu U\right\}\\
&\qquad-4p^\mu p^\nu\,\mathrm{tr_s}\left\{U\hat{D}_\mu U\hat{D}_\nu U\right\}-4p^\mu p^\nu\,\mathrm{tr_s}\left\{U\hat{D}_\mu\hat{D}_\nu U^2\right\}\\
&\qquad-8i\,p^\mu p^\nu p^\rho\,\mathrm{tr_s}\left\{U\hat{D}_\mu\hat{D}_\nu\hat{D}_\rho U\right\}\Big]\Big\}\\
&+\mathcal{L}^F_{\rm EFT}+\mathcal{O}\left(\zeta^{-3}\right)\,.
\end{aligned}
\tag{6.A.3}
$$

We have introduced a subtracted trace which is defined as

$$
\mathrm{tr_s}\left\{f(U,D_\mu)\right\}\equiv\mathrm{tr}\left\{f(U,D_\mu)-f(U_H,D_\mu)-\Theta_f\right\}\,,
\tag{6.A.4}
$$

where f is an arbitrary function of U and covariant derivatives, and Θ_f generically denotes all the terms with covariant derivatives at the rightmost of the trace (i.e. open covariant derivative terms) contained in the original trace. The terms involving only U_H that are subtracted from the trace were already included in Eq. (6.A.2) while all open derivative terms from the different traces are collected in $\mathcal{L}^F_{\rm EFT}$. The latter combine into gauge invariant pieces with field-strength tensors, although the manner in which this occurs is not easily seen and involves the contribution from different orders in the expansion.

With the purpose of illustration, we compute $\mathcal{L}^F_{\rm EFT}$ that results from the integration of the real scalar triplet extension of the SM presented in Section 6.3.2. In this case, gauge invariance of the final result guarantees that the leading order contribution to $\mathcal{L}^F_{\rm EFT}$ should contain at least four covariant derivatives, as terms with two covariant derivatives cannot be contracted to yield a gauge invariant term. As it is clear from Eq. (6.13), traces with j derivatives and a number k of U operators have a power suppression of $\mathcal{O}\left(\zeta^{4-j-2k}\right)$ (we recall that $d^dp\sim\zeta^4$). The expansion of the operator U_{LH} can yield in addition ℓ covariant derivatives, and each of these receives a further suppression of ζ^{-1} because they are accompanied with a light-field propagator, see Eq. (6.A.6). Since U_{LH} is at most $\mathcal{O}(\zeta^0)$ we then find that, in general, terms with k insertions of U_{HL} and a total number of $j+\ell$ derivatives have a power counting of at most $\mathcal{O}(\zeta^{4-j-\ell-2k})$. As a result, the only gauge invariant object involving U_{LH} and four derivatives that one can construct at $\mathcal{O}(\zeta^{-2})$ includes only one power of U_{LH} (i.e. $j+\ell=4$ and $k=1$). Moreover, since U_{LH} has to be evaluated at leading order, the only relevant piece from U_{LH} for the computation of $\mathcal{L}^F_{\rm EFT}$ reads

$$
U^F_{LH}=X^{(1)\,\dagger}_{LH}\,\Delta_L^{-1}\big|_{\hat{\eta}=0}\,X^{(1)}_{LH}\,.
\tag{6.A.5}
$$

Here $X_{LH}^{(1)}$ is defined as the part of X_{LH} that is $\mathcal{O}(\zeta)$, and we remind that $\hat{\eta}$ stands for the classical field configurations. Using the expressions in Eqs. (6.39) and (6.40) we have

$$\begin{aligned} U_{LH}^{F}(x,\partial_x+ip) \subset \frac{\kappa^2}{p^2}\sum_{m=0}^{4}\Bigg[& \hat{\phi}^\dagger\tau^a\left(\frac{2ip\hat{D}+\hat{D}^2}{p^2}\right)^m\tau^b\hat{\phi} \\ & +\hat{\phi}^{\intercal}(\tau^a)^{\intercal}\left(\frac{2ip\hat{D}^*+\hat{D}^{*\,2}}{p^2}\right)^m(\tau^b)^*\hat{\phi}^*\Bigg]\,, \end{aligned} \tag{6.A.6}$$

where the covariant derivatives have to be expanded by applying the identities

$$\begin{aligned} D_\mu\tau^a\phi &= \tau^a\left(D_\mu\phi\right)+\tau^c\phi\,D_\mu^{ca}\,, \\ D_\mu^*\left(\tau^a\right)^*\phi^* &= \left(\tau^a\right)^*\left(D_\mu\phi\right)^*+\left(\tau^c\right)^*\phi^*\,D_\mu^{ca}\,, \end{aligned} \tag{6.A.7}$$

with D_μ denoting the Higgs field covariant derivative, see Eq. (1.9), and with D_μ^{ca} as defined in Section 6.1. For the computation of $\mathcal{L}_{\rm EFT}^{F}$ up to $\mathcal{O}(\zeta^{-2})$ we need to isolate the terms in Eq. (6.13) with up to four open covariant derivatives and just one power of U_{LH}^{F}. These are given by

$$\begin{aligned} \mathcal{L}_{\rm EFT}^{F} \subset -\frac{i}{2}\int\frac{d^dp}{(2\pi)^d}\frac{1}{p^2-M^2}\sum_{n=0}^{4}\sum_{k=0}^{n}\frac{1}{n+1} \\ \times\,\mathrm{tr}\left\{\left(\frac{2ip\hat{D}+\hat{D}^2}{p^2-M^2}\right)^{n-k}U_{LH}^{F}(x,\partial_x+ip)\left(\frac{2ip\hat{D}+\hat{D}^2}{p^2-M^2}\right)^{k}\right\}\,, \end{aligned} \tag{6.A.8}$$

and using the cyclic property of the trace we get[6]

$$\mathcal{L}_{\rm EFT}^{F} \subset -\frac{i}{2}\int\frac{d^dp}{(2\pi)^d}\frac{1}{p^2-M^2}\sum_{n=0}^{4}\mathrm{tr}\left\{U_{LH}^{F}(x,\partial_x+ip)\left(\frac{2ip\hat{D}+\hat{D}^2}{p^2-M^2}\right)^{n}\right\}\,. \tag{6.A.9}$$

Finally, keeping only terms with up to four covariant derivatives, performing the momentum integration (see Eq. (6.18)) and evaluating the $SU(2)$ trace we arrive at the final result

$$\begin{aligned} \mathcal{L}_{\rm EFT}^{F} = \frac{1}{16\pi^2}\frac{\kappa^2}{M^4}\Bigg[& -\frac{g^2}{3}\left(\hat{\phi}^\dagger\hat{\phi}\right)\hat{W}^{\mu\nu\,a}\hat{W}^{a}_{\mu\nu}+g\left(\hat{\phi}^\dagger\,i\overleftrightarrow{\hat{D}^a_\mu}\,\hat{\phi}\right)\left(\hat{D}_\nu\,\hat{W}^{\mu\nu}\right)^a \\ & -\frac{gg'}{2}\left(\hat{\phi}^\dagger\tau^a\hat{\phi}\right)\hat{W}^{a}_{\mu\nu}\hat{B}^{\mu\nu}\Bigg]\,, \end{aligned} \tag{6.A.10}$$

[6]The use of the cyclic property when derivative terms are involved is only justified for the functional trace, that we denoted in this chapter as Tr. However, as noted in Refs. [15, 22], in the evaluation of the functional determinant, which is a gauge invariant object, the trace over internal degrees of freedom 'tr' can be recast into the full trace through the use of the identity (we recall that $S=\int d^dx\,\mathcal{L}$)

$$\mathrm{Tr}\{f(\hat{x})\}=\int d^dx\;\mathrm{tr}\{\langle x|f(\hat{x})|x\rangle\}=\int d^dx\;\mathrm{tr}\{f(x)\}\,\delta^d(0)\,,$$

and then reverted to a trace over internal degrees of freedom after the application of the cyclic property.

with the field-strength tensors defined in Eq. (1.7) and

$$\left(\phi^\dagger\, i\overset{\leftrightarrow}{D}{}^a_\mu \phi\right) = i\left(\phi^\dagger\, \tau^a D_\mu \phi\right) - i\left[(D_\mu\phi)^\dagger\, \tau^a \phi\right]. \tag{6.A.11}$$

6.B The fluctuation operator of the SM

In this appendix we provide the fluctuation operator for the SM Lagrangian, which was introduced in Chapter 1. Following the same procedure as in Section 6.1, we separate the fields into background, $\hat{\eta}$, and quantum field configurations, η, and expand the SM Lagrangian to second order in the quantum fluctuation:

$$\mathcal{L}_{\rm SM} = \mathcal{L}^{\rm tree}_{\rm SM}(\hat{\eta}) + \mathcal{L}^{(\eta^2)}_{\rm SM} + \mathcal{O}\left(\eta^3\right), \tag{6.B.1}$$

where $\mathcal{L}^{\rm tree}_{\rm SM}$ is the tree-level SM effective Lagrangian, and $\mathcal{L}^{(\eta^2)}_{\rm SM}$ is computed using Eq. (6.1):

$$\mathcal{L}^{(\eta^2)}_{\rm SM} = \frac{1}{2}\left(\phi^\dagger\ \phi^\intercal\ A^{a\,\intercal}_\mu\ \overline{\psi}\ \psi^\intercal\right)\begin{pmatrix} \Delta_{\phi^*\phi} & X^\dagger_{\phi\phi} & \left(X^{\nu\,b}_{A\phi}\right)^\dagger & \overline{X}_{\bar{\psi}\phi} & -X^\intercal_{\bar{\psi}\phi^*} \\ X_{\phi\phi} & \Delta^\intercal_{\phi^*\phi} & \left(X^{\nu\,b}_{A\phi}\right)^\intercal & \overline{X}_{\bar{\psi}\phi^*} & -X^\intercal_{\bar{\psi}\phi} \\ X^{\mu\,a}_{A\phi} & \left(X^{\mu\,a}_{A\phi}\right)^* & \Delta^{\mu\nu\,ab}_A & \overline{X}^{\mu\,a}_{\bar{\psi}A} & -\left(X^{\mu\,a}_{\bar{\psi}A}\right)^\intercal \\ X_{\bar{\psi}\phi} & X_{\bar{\psi}\phi^*} & X^{\nu\,b}_{\bar{\psi}A} & \Delta_{\bar{\psi}\psi} & 0 \\ -\overline{X}^\intercal_{\bar{\psi}\phi^*} & -\overline{X}^\intercal_{\bar{\psi}\phi} & -\left(\overline{X}^{\nu\,b}_{\bar{\psi}A}\right)^\intercal & 0 & -\Delta^\intercal_{\bar{\psi}\psi} \end{pmatrix}\begin{pmatrix} \phi \\ \phi^* \\ A^b_\nu \\ \psi \\ \overline{\psi}^\intercal \end{pmatrix} + \mathcal{L}^{(\eta^2)}_{\rm ghost}, \tag{6.B.2}$$

with $A^a_\mu = \left(G^\alpha_\mu\ W^a_\mu\ B_\mu\right)^\intercal$ denoting the gauge fields and

$$\Delta^{\mu\nu\,ab}_A = \begin{pmatrix} \Delta^{\mu\nu\,\alpha\beta}_G & 0 & 0 \\ 0 & \Delta^{\mu\nu\,ab}_W & \Delta^{\mu\nu\,a}_{BW} \\ 0 & \Delta^{\mu\nu\,a}_{BW} & \Delta^{\mu\nu}_B \end{pmatrix} \quad , \quad X^{\mu\,a}_{A\phi} = \begin{pmatrix} 0 \\ X^{\mu\,a}_{W\phi} \\ X^\mu_{B\phi} \end{pmatrix} \quad , \quad \overline{X}^{\mu\,a}_{\bar{\psi}A} = \begin{pmatrix} \overline{X}^{\mu\,\alpha}_{\bar{\psi}G} \\ \overline{X}^{\mu\,a}_{\bar{\psi}W} \\ \overline{X}^\mu_{\bar{\psi}B} \end{pmatrix}, \tag{6.B.3}$$

where, generically, $\overline{X} = X^\dagger\gamma^0$. The pieces in the quadratic fluctuation are defined as

$$\begin{aligned}
\Delta_{\phi^*\phi} &= -\hat{D}^2 - m^2_\phi - \lambda\left(\hat{\phi}^\dagger\hat{\phi}\right) - \lambda\hat{\phi}\hat{\phi}^\dagger, \\
\Delta^{\mu\nu\,\alpha\beta}_G &= \delta_{\alpha\beta}\left[g^{\mu\nu}\hat{D}^2 + \frac{1-\xi_G}{\xi_G}\hat{D}^\mu\hat{D}^\nu\right] - g_c\epsilon_{\alpha\beta\gamma}\hat{G}^{\mu\nu\,\gamma}, \\
\Delta^{\mu\nu\,ab}_W &= \delta_{ab}\left\{g^{\mu\nu}\left[\hat{D}^2 + \frac{1}{2}g^2\left(\hat{\phi}^\dagger\hat{\phi}\right)\right] + \frac{1-\xi_W}{\xi_W}\hat{D}^\mu\hat{D}^\nu\right\} - g\epsilon_{abc}\hat{W}^{\mu\nu\,c}, \\
\Delta^{\mu\nu}_B &= g^{\mu\nu}\left[\partial^2 + \frac{1}{2}g'^2\left(\hat{\phi}^\dagger\hat{\phi}\right)\right] + \frac{1-\xi_B}{\xi_B}\partial^\mu\partial^\nu, \\
\Delta^{\mu\nu\,a}_{BW} &= \frac{1}{2}gg'g_{\mu\nu}\left(\hat{\phi}^\dagger\tau^a\hat{\phi}\right),
\end{aligned}$$

$$
\begin{aligned}
\Delta_{\bar{\psi}\psi} &= i\hat{\not{D}} - \left[\left(i\tau_2\,\hat{\phi}^*\,y_{Lu}\,P_u + \hat{\phi}\,y_{Ld}\,P_d + \hat{\phi}\,y_{Le}\,P_e\right)P_R + \begin{pmatrix} h.c. \\ R\to L\end{pmatrix}\right], \\
X_{\phi\phi} &= -\,\lambda\,\hat{\phi}^*\hat{\phi}^\dagger\,, \\
X^{\mu\,a}_{W\phi} &= \frac{1}{2}ig\left[\hat{\phi}^\dagger\tau^a\hat{D}^\mu - \left(\hat{D}^\mu\hat{\phi}\right)^\dagger\tau^a\right], \\
X^{\mu}_{B\phi} &= \frac{1}{2}ig'\left[\hat{\phi}^\dagger\hat{D}^\mu - \left(\hat{D}^\mu\hat{\phi}\right)^\dagger\right], \\
X^{\mu\,\alpha}_{\bar{\psi}G} &= \frac{1}{2}g_c\,\lambda^\alpha P_q\,\gamma^\mu\hat{\psi}\,, \\
X^{\mu\,a}_{\bar{\psi}W} &= \frac{1}{2}g\,\tau^a\,\gamma^\mu P_L\hat{\psi}\,, \\
X^{\mu}_{\bar{\psi}B} &= g'\gamma^\mu Y_\psi\,\hat{\psi}\,, \\
X_{\bar{\psi}\phi} &= -\overleftarrow{P}_u P_L y_u^\dagger\,\hat{\psi}^t\,i\tau_2 - y_d\,P_d P_R\,\hat{\psi}\,, \\
X_{\bar{\psi}\phi^*} &= -\,i\tau^2\,y_u P_u P_R\hat{\psi} - \overleftarrow{P}_d P_L y_d^\dagger\hat{\psi}^t\,.
\end{aligned}
\tag{6.B.4}
$$

Here $P_q = P_u + P_d$, the operators $P_{u,d,e}$ project over the corresponding fermion, and the superscript t in the fermion fields denotes transposition in isospin space. Additionally, we have fixed the gauge of the quantum fields using the *background field gauge*, which ensures that the theory remains invariant under gauge transformations of the background fields. This choice corresponds to the following gauge-fixing Lagrangian:

$$
\mathcal{L}_{\rm GF} = -\,\frac{1}{2\xi_G}\left(\hat{D}_\mu G^{\mu\,\alpha}\right)^2 - \frac{1}{2\xi_W}\left(\hat{D}_\mu W^{\mu\,a}\right)^2 - \frac{1}{2\xi_B}\left(\partial_\mu B^\mu\right)^2\,. \tag{6.B.5}
$$

Our choice of gauge-fixing Lagrangian also fixes the ghost term, $\mathcal{L}_{\rm ghost}$, which at the one-loop level remains unaffected with all our manipulations and therefore does not play any role in the discussion.

Finally we also provide the expansion for the inverse operators $\Delta_X\,(x, \partial_x + ip)^{-1}$, with $X = \{\phi^*\phi,\, B,\, W\}$, when $p_\mu \sim \zeta$. We have:

$$
\begin{aligned}
\Delta_{\phi^*\phi}\,(x,\partial_x+ip) &= p^2 - m_\phi^2 - 2ip\hat{D} - \hat{D}^2 - \lambda\left(\hat{\phi}^\dagger\hat{\phi}\right) - \lambda\hat{\phi}\hat{\phi}^\dagger\,, \\
\Delta_W^{\mu\nu\,ab}\,(x,\partial_x+ip) &= \delta_{ab}\left[-g^{\mu\nu}p^2 - \frac{1-\xi_W}{\xi_W}p^\mu p^\nu\right] + \mathcal{O}\,(\zeta)\,, \\
\Delta_B^{\mu\nu}\,(x,\partial_x+ip) &= -g^{\mu\nu}p^2 - \frac{1-\xi_B}{\xi_B}p^\mu p^\nu + \mathcal{O}\,(\zeta)\,.
\end{aligned}
\tag{6.B.6}
$$

from where, and defining

$$
\Omega \;=\; \hat{D}^2 + \lambda\left(\hat{\phi}^\dagger\hat{\phi}\right) + \lambda\,\hat{\phi}\hat{\phi}^\dagger\,, \tag{6.B.7}
$$

it is straightforward to get

$$
\Delta_{\phi^*\phi}\,(x,\partial_x+ip)^{-1} = \frac{1}{p^2}\left(1 + \frac{m_\phi^2}{p^2} + \frac{m_\phi^4}{p^4}\right) + 2i\,\frac{p_\mu}{p^4}\left(1 + 2\frac{m_\phi^2}{p^2}\right)\,\hat{D}^\mu
$$

$$
\begin{aligned}
&+\frac{1}{p^4}\left(1+2\frac{m_\phi^2}{p^2}\right)\,\Omega\,-4\,\frac{p_\mu p_\nu}{p^6}\left(1+3\frac{m_\phi^2}{p^2}\right)\,\hat{D}^\mu\hat{D}^\nu\\
&+2i\,\frac{p_\mu}{p^6}\,\left\{\hat{D}^\mu\,\Omega\,+\,\Omega\,\hat{D}^\mu\right\}\,+\,\frac{1}{p^6}\,\Omega^2\\
&-8i\,\frac{p_\mu p_\nu p_\rho}{p^8}\,\hat{D}^\mu\hat{D}^\nu\hat{D}^\rho\,+16\,\frac{p_\mu p_\nu p_\rho p_\sigma}{p^{10}}\,\hat{D}^\mu\hat{D}^\nu\hat{D}^\rho\hat{D}^\sigma\\
&-4\,\frac{p_\mu p_\nu}{p^8}\left\{\hat{D}^\mu\hat{D}^\nu\,\Omega\,+\,\Omega\,\hat{D}^\mu\hat{D}^\nu+\,\hat{D}^\mu\,\Omega\,\hat{D}^\nu\right\}+\mathcal{O}\left(\zeta^{-7}\right),
\end{aligned}
$$

$$
\Delta_B^{\mu\nu}\,(x,\partial_x+ip)^{-1}=-\frac{g^{\mu\nu}}{p^2}+(1-\xi_B)\,\frac{p^\mu p^\nu}{p^4}+\mathcal{O}\left(\zeta^{-3}\right)\,,
$$

$$
\Delta_W^{\mu\nu\,ab}\,(x,\partial_x+ip)^{-1}=\delta_{ab}\left[-\frac{g^{\mu\nu}}{p^2}+(1-\xi_W)\,\frac{p^\mu p^\nu}{p^4}\right]+\mathcal{O}\left(\zeta^{-3}\right)\,, \tag{6.B.8}
$$

and analogously for $\Delta_G^{\mu\nu\,\alpha\beta}\,(x,\partial_x+ip)^{-1}$. The inverse operator $[\Delta^*_{\phi^*\phi}\,(x,\partial_x+ip)]^{-1}$ can be obtained from $\Delta_{\phi^*\phi}\,(x,\partial_x+ip)^{-1}$ by making the substitution $\hat{D}_\mu\,\rightarrow\,\hat{D}^*_\mu$ while $[\Delta^\intercal_{\phi^*\phi}\,(x,\partial_x+ip)]^{-1}$ and $[\Delta^*_{\phi^*\phi}\,(x,\partial_x+ip)]^{-1}$ share the same expression, up to a total derivative term.

Bibliography

[1] B. Henning, X. Lu and H. Murayama, JHEP **1601** (2016) 023 [arXiv:1412.1837 [hep-ph]].

[2] A. Drozd, J. Ellis, J. Quevillon and T. You, JHEP **1603** (2016) 180 [arXiv:1512.03003 [hep-ph]].

[3] F. del Aguila, Z. Kunszt and J. Santiago, Eur. Phys. J. C **76** (2016) no.5, 244 [arXiv:1602.00126 [hep-ph]].

[4] M. Boggia, R. Gomez-Ambrosio and G. Passarino, JHEP **1605** (2016) 162 [arXiv:1603.03660 [hep-ph]].

[5] B. Henning, X. Lu and H. Murayama, arXiv:1604.01019 [hep-ph].

[6] S. A. R. Ellis, J. Quevillon, T. You and Z. Zhang, Phys. Lett. B **762** (2016) 166 [arXiv:1604.02445 [hep-ph]].

[7] J. Fuentes-Martin, J. Portoles and P. Ruiz-Femenia, JHEP **1609** (2016) 156 [arXiv:1607.02142 [hep-ph]].

[8] S. Dittmaier and C. Grosse-Knetter, Phys. Rev. D **52** (1995) 7276 [hep-ph/9501285].

[9] S. Dittmaier and C. Grosse-Knetter, Nucl. Phys. B **459** (1996) 497 [hep-ph/9505266].

[10] C. M. Fraser, Z. Phys. C **28** (1985) 101.

[11] I. J. R. Aitchison and C. M. Fraser, Phys. Lett. **146B** (1984) 63.

[12] I. J. R. Aitchison and C. M. Fraser, Phys. Rev. D **31** (1985) 2605.

[13] I. J. R. Aitchison and C. M. Fraser, Phys. Rev. D **32** (1985) 2190.

[14] L. H. Chan, Phys. Rev. Lett. **54** (1985) 1222 Erratum: [Phys. Rev. Lett. **56** (1986) 404].

[15] L. H. Chan, Phys. Rev. Lett. **57** (1986) 1199.

[16] M. K. Gaillard, Nucl. Phys. B **268** (1986) 669.

[17] O. Cheyette, Phys. Rev. Lett. **55** (1985) 2394.

[18] M. Beneke and V. A. Smirnov, Nucl. Phys. B **522** (1998) 321 [hep-ph/9711391].

[19] V. A. Smirnov, Springer Tracts Mod. Phys. **177** (2002) 1.

[20] B. Jantzen, JHEP **1112** (2011) 076 [arXiv:1111.2589 [hep-ph]].

[21] Z. Zhang, arXiv:1610.00710 [hep-ph].

[22] R. D. Ball, Phys. Rept. **182** (1989) 1.

[23] O. Cheyette, Nucl. Phys. B **297** (1988) 183.

[24] J. Caro and L. L. Salcedo, Phys. Lett. B **309** (1993) 359.

[25] M. S. Bilenky and A. Santamaria, Nucl. Phys. B **420** (1994) 47 [hep-ph/9310302].

[26] Z. U. Khandker, D. Li and W. Skiba, Phys. Rev. D **86** (2012) 015006 [arXiv:1201.4383 [hep-ph]].

[27] M. Magg and C. Wetterich, Phys. Lett. **94B** (1980) 61. doi:10.1016/0370-2693(80)90825-4

[28] T. P. Cheng and L. F. Li, Phys. Rev. D **22** (1980) 2860. doi:10.1103/PhysRevD.22.2860

[29] J. Schechter and J. W. F. Valle, Phys. Rev. D **22** (1980) 2227. doi:10.1103/PhysRevD.22.2227

[30] R. N. Mohapatra and G. Senjanovic, Phys. Rev. D **23** (1981) 165. doi:10.1103/PhysRevD.23.165

[31] G. B. Gelmini and M. Roncadelli, Phys. Lett. **99B** (1981) 411.

[32] G. Lazarides, Q. Shafi and C. Wetterich, Nucl. Phys. B **181** (1981) 287. doi:10.1016/0550-3213(81)90354-0

CHAPTER 7

Flavor anomalies in B decays from extended gauge sectors

> The only thing that makes life possible is permanent, intolerable uncertainty: not knowing what comes next.
>
> — *Ursula K. Le Guin*, The Left Hand of Darkness

We saw in Chapter 5 that there are several interesting tensions in B-physics data. These can be classified in two sets according to their nature: the ones involving $b \to s\ell^+\ell^-$ data, and those related to the $b \to c\ell\nu$ transitions. As we outlined in that section, there are several attempts from different extensions of the SM to explain these tensions, either focusing in just one set of anomalies or considering both together. In this section we will present in detail three particular examples of these extensions, all of them based on an enlarged gauge sector. In particular, we will present two models that are able to accommodate the anomalies in $b \to s\ell^+\ell^-$ transitions: In Section 7.1 we will introduce a minimal class of Z' models characterized by having all of its couplings completely determined by the gauge symmetry and the CKM matrix (with no need for extra fermions); while in Section 7.2 we will present a more elaborated framework, based on the hypothesis of dynamical Yukawa couplings, that offers for a possible explanation to the basic features of quark and leptons masses and mixings. Finally, in Section 7.3 we will address the possibility of explaining simultaneously the anomalies in $b \to s\ell^+\ell^-$ and $b \to c\ell\nu$ data from an extended SU(2) gauge symmetry. The phenomenology of each these models, together with their predictions, will be addressed in detail in each of the corresponding sections.

Note added: While this thesis was being completed, several new experimental measurements concerning the $b \to s\ell^+\ell^-$ anomalies have been reported. Of those, the most relevant for the present discussion is the measurement of R_{K^*} in two bins by the LHCb Collaboration [1] (see Chapter 5 for a brief discussion). Because of time constraints, in this chapter we will not include the new measurements in the phenomenological discussion of the models, or use the global fits to flavor observables that incorporate them. However we note that, given that all the models presented in this chapter predict the approximate relation $R_K|_{q^2\in[1,6]\ \mathrm{GeV}^2} \simeq R_{K^*}|_{q^2\in[1.1,6]\ \mathrm{GeV}^2}$, the inclusion of the new measurements would not modify the overall picture and, in any case, would contribute to improve the global significance of these models

with respect to the SM prediction. We will also not discuss the phenomenological implications of the recent dilepton resonance search performed by ATLAS at 13 TeV with 36.1 fb^{-1} of data [2].

7.1 Non-universal Z' models with protected flavor-changing interactions

In this section, based on the publication in Ref. [3], we present a class of models that extends the SM gauge symmetry with an extra $\text{U}(1)'$ such that *all* the fermion couplings to the new gauge bosons are related *exactly* to elements of the CKM matrix. We achieve this by gauging the BGL symmetry introduced in Section 2.2.2. As we saw in this section, while the BGL model can be implemented through an Abelian discrete symmetry, this always yields an accidental continuous Abelian symmetry which introduces an undesired Goldstone boson into the theory [4]. Several solutions to this problem have already been proposed in the literature [4–6] and discussed in this thesis (see Section 8.2); in the following we provide a new solution: promoting the BGL symmetry to a local one. In this gauged BGL framework ($\text{U}(1)' \equiv \text{U}(1)_{\text{BGL}}$), the properties of the BGL models are transferred to the gauge boson sector: we obtain FCNC mediated at tree-level by the neutral scalar and massive gauge vector bosons of the theory, all suppressed by off-diagonal CKM elements and/or fermion masses, and therefore naturally suppressed. This class of models necessarily exhibits deviations from lepton universality due to its gauge structure. Note that this form of flavor suppression in the down-quark sector also appears in certain 3-3-1 models [7, 8]. However, in our framework this is not a choice, but a consequence of the gauge symmetry.

This section is organized as follows: We formulate the gauged $\text{U}(1)_{\text{BGL}}$ models in Section 7.1.1. In Section 7.1.2 we discuss the constraints from flavor and collider data, testing the strong correlations present in these models, specifically with respect to the deviations observed by LHCb. We conclude in Section 7.1.5. The appendices 7.A and 7.B include technical details on anomaly cancellation and the scalar sector.

7.1.1 Gauged BGL symmetry

The aim of this section is to study the necessary conditions required to promote the $\text{U}(1)_{\text{BGL}}$ introduced in Section 2.2.2 to a local symmetry. As we are dealing with a chiral symmetry, one should pay special attention to the cancellation of anomalies when gauging the BGL symmetry.[1] In Section 8.2.1 (see also Refs. [5,6]) we showed that BGL 2HDM are automatically free of color anomalies, i.e. $\text{U}(1)'[\text{SU}(3)_\text{c}]^2$. However, we also need to fulfill the anomaly conditions for the following combinations:

$$\begin{aligned} &\text{U}(1)'[\text{SU}(2)_\text{L}]^2\,, \quad \text{U}(1)'[\text{U}(1)_\text{Y}]^2\,, \qquad [\text{U}(1)']^2\text{U}(1)_\text{Y}\,, \\ &[\text{U}(1)']^3\,, \qquad\qquad \text{U}(1)'[\text{Gravity}]^2\,. \end{aligned} \tag{7.1}$$

[1] In this section we consider only symmetries as "good" if all gauge anomalies are canceled. It would be also possible to consider anomalous U(1) extensions in the low-energy theory whose anomaly graphs get canceled via the so-called Green–Schwarz mechanism [9–11].

We find that there is no solution for this system within the quark sector alone with the charge assignments in Eq. (2.38). Satisfying these anomaly conditions is highly non-trivial and requires, in general, additional fermions. However, the implementation of the BGL symmetry as a local symmetry is possible by adding only the SM leptonic sector when allowing for lepton-flavor non-universal couplings. As in the SM, the cancellation of the gauge anomalies then occurs due to a cancellation between quark and lepton contributions; the cancellation will however involve all three fermion generations, contrary to the SM gauge group, for which the anomaly cancellation occurs separately within each fermion generation.

Gauging the BGL symmetry therefore not only removes the unwanted Goldstone boson, which is "eaten" by the Z', but also provides a consistent Z' model without extending the particle content beyond the additional scalars, i.e. no extra fermions are necessary. The flavor structure is extended to the Z' couplings, yielding again strongly suppressed FCNCs in the down-type quark sector, while the up-type-quark couplings remain diagonal. Especially, since the flavored gauge symmetry fixes also the charged-lepton Yukawa matrices to be diagonal, we can obtain large deviations from lepton universality without introducing lepton-flavor violation. Our models provide thereby explicit examples for which the general arguments given in Refs. [12–14] do not hold.

Lepton sector

As emphasized above, the anomaly constraints can be fulfilled by assuming that leptons are also charged under the $\mathrm{U}(1)'$ symmetry. The resulting charge constraints are given in Appendix 7.A.

For $X_{\Phi_2} = 0$ the mixing between the neutral massive gauge bosons is suppressed for large $\tan\beta$. With this choice, we obtain only one possible solution to the anomaly conditions up to lepton-flavor permutations, implying the following charge assignments:

$$\begin{aligned} \mathcal{X}_R^d &= \mathbb{1}\,, & \mathcal{X}_R^u &= \mathrm{diag}\left(-\frac{7}{2}, -\frac{7}{2}, 1\right)\,, \\ \mathcal{X}_L^q &= \mathrm{diag}\left(-\frac{5}{4}, -\frac{5}{4}, 1\right)\,, & \mathcal{X}_L^\ell &= \mathrm{diag}\left(\frac{9}{4}, \frac{21}{4}, -3\right)\,, \\ \mathcal{X}_R^e &= \mathrm{diag}\left(\frac{9}{2}, \frac{15}{2}, -3\right)\,, & \mathcal{X}^\Phi &= \mathrm{diag}\left(-\frac{9}{4}, 0\right)\,. \end{aligned} \tag{7.2}$$

We have normalized all $\mathrm{U}(1)'$ charges by setting $X_{dR} = 1$, thereby fixing also the normalization for the gauge coupling $g_{Z'}$. In addition to the top, this particular model singles out the tau lepton as the only one coupling to Φ_2. Permutations of the charges in $\mathcal{X}_L^\ell$ and $\mathcal{X}_R^e$ give rise to 5 more models.

With the charge transformations in Eq. (7.2), the charged-lepton Yukawa sector takes the form

$$-\mathcal{L}_{\mathrm{Yuk}}^{\text{c-leptons}} = \overline{\ell_L^0}\,\Pi_i\,\Phi_i e_R^0 + \mathrm{h.c.}\,, \tag{7.3}$$

with

$$\Pi_1 = \begin{pmatrix} \times & 0 & 0 \\ 0 & \times & 0 \\ 0 & 0 & 0 \end{pmatrix}, \quad \Pi_2 = \begin{pmatrix} 0 & 0 & 0 \\ 0 & 0 & 0 \\ 0 & 0 & \times \end{pmatrix}, \tag{7.4}$$

while the quark Yukawa sector remains unchanged.

We call to attention that no reference to the neutrino sector has been made in the previous arguments. In this section we are mostly interested in the properties of the quark and charged-lepton sectors in the presence of a new gauge boson, while we leave a detailed discussion of the neutrino sector to future work. For a possible implementation with the SM fermion content we can build the $d = 5$ Weinberg effective operator $(\overline{\ell}\tilde{\Phi}_a)(\tilde{\Phi}_b^T \ell^c)$, which after spontaneous symmetry breaking induces a Majorana mass term for the neutrinos. If this effective operator is invariant under the new flavored gauge symmetry in Eq. (7.2), we are led to a $L_\mu - L_\tau$ symmetric $d = 5$ effective operator and, consequently, Majorana mass term. This structure has been studied in Refs. [15–19], and while it is not capable of fully accommodating the neutrino data, it can serve as a good starting point.

If we want to improve on this scenario while keeping our solution to the anomaly conditions, we may want a mechanism that at the effective level already breaks the accidental $L_\mu - L_\tau$ symmetry. For instance, we may extend the model with 3 right-handed neutrinos, where one of them is not charged while the other two have opposite charges. In this way the anomaly solutions remain unchanged. Choosing the charges of the right-handed neutrinos appropriately, the Dirac mass term for the neutrinos can be made diagonal and the Majorana mass for the right-handed ones $L_\mu - L_\tau$ symmetric. Along the lines of Ref. [20], coupling an additional scalar to the right-handed neutrinos could break the accidental symmetry at the effective level. We can also envisage other mechanisms that do change the anomaly conditions and, therefore, introduce new solutions.

Gauge boson sector

In order to avoid experimental constraints on a Z' boson, the $\mathrm{U}(1)'$ symmetry must be broken at a relatively high scale, rendering the new gauge boson significantly heavier than the SM ones [21]. This can be achieved through the introduction of a complex scalar singlet S, charged under the BGL symmetry with charge X_S, which acquires a vev $|\langle S \rangle| = v_S/\sqrt{2} \gg v$. The charge of the scalar singlet is fixed once the scalar potential is specified, in our case $X_S = -9/8$, see Appendix 7.B for details.

As a consequence of the gauge symmetry breaking, $\mathrm{G_{SM}} \times \mathrm{U}(1)' \to \mathrm{U}(1)_{\mathrm{em}}$, the neutral massive gauge bosons mix, giving rise to a Lagrangian of the form[2]

$$\begin{aligned} \mathcal{L} = & -\frac{1}{4} A_{\mu\nu} A^{\mu\nu} - \frac{1}{4} \hat{Z}_{\mu\nu} \hat{Z}^{\mu\nu} - \frac{1}{4} \hat{Z}'_{\mu\nu} \hat{Z}'^{\mu\nu} + \frac{1}{2} \hat{M}_Z^2 \hat{Z}_\mu \hat{Z}^\mu + \frac{1}{2} \hat{M}_{Z'}^2 \hat{Z}'_\mu \hat{Z}'^\mu \\ & + \Delta^2 \hat{Z}'_\mu \hat{Z}^\mu - J_A^\mu A_\mu - \hat{J}_Z^\mu \hat{Z}_\mu - \hat{J}_{Z'}^\mu \hat{Z}'_\mu \,, \end{aligned} \tag{7.5}$$

[2]We neglect here a possible mixing coming from the gauge kinetic Lagrangian as the mass mixing shows already all relevant qualitative effects [21].

where J_A^μ and $\hat{J}_Z^\mu$ are the SM currents of the photon and the Z, respectively. The fermionic piece of the new current takes the form

$$\hat{J}_{Z'}^\mu \supset g_{Z'}\,\overline{\psi_i}\gamma^\mu\left[\left(\widetilde{\mathcal{X}}_L^\psi\right)_{ij}P_L+\left(\widetilde{\mathcal{X}}_R^\psi\right)_{ij}P_R\right]\psi_j\,, \tag{7.6}$$

with $P_{L,R}=(1\mp\gamma_5)/2$ denoting the usual chiral projectors, $g_{Z'}$ the $\mathrm{U}(1)'$ gauge coupling, and $\widetilde{\mathcal{X}}_X^\psi$ the phase transformation matrices in the fermion mass basis, i.e.

$$\begin{aligned}&\widetilde{\mathcal{X}}_R^\psi=\mathcal{X}_R^\psi\,,\quad \widetilde{\mathcal{X}}_L^u=\mathcal{X}_L^q\,,\quad \widetilde{\mathcal{X}}_L^e=\mathcal{X}_L^\ell\,,\quad \text{and}\\ &\widetilde{\mathcal{X}}_L^d=-\frac{5}{4}\mathbb{1}+\frac{9}{4}\begin{pmatrix}|V_{td}|^2 & V_{ts}V_{td}^* & V_{tb}V_{td}^*\\ V_{td}V_{ts}^* & |V_{ts}|^2 & V_{tb}V_{ts}^*\\ V_{td}V_{tb}^* & V_{ts}V_{tb}^* & |V_{tb}|^2\end{pmatrix}\,.\end{aligned} \tag{7.7}$$

The neutral gauge boson mass and mass-mixing parameters in this model are given by

$$\hat{M}_Z^2=\frac{e^2v^2}{4\hat{s}_W^2\hat{c}_W^2}\,,\quad \hat{M}_{Z'}^2=g_{Z'}^2\left(v_i^2X_{\Phi_i}^2+v_S^2X_S^2\right)\,,\quad \Delta^2=-\frac{e\,g_{Z'}}{2\hat{c}_W\hat{s}_W}X_{\Phi_i}v_i^2\,, \tag{7.8}$$

where $e=\sqrt{4\pi\alpha}$ is the electromagnetic charge and its ratio with the $\mathrm{SU}(2)_\mathrm{L}$ coupling g defines $\hat{\theta}_W\equiv\arcsin(e/g)$, which differs from the experimentally measured weak angle due to mixing effects [22]: $\hat{s}_W\hat{c}_W\hat{M}_Z=s_Wc_WM_Z$, where M_Z is the physical Z mass. We rotate to the physical eigenbasis by performing the following orthogonal transformation:

$$\begin{pmatrix}Z_\mu\\ Z'_\mu\end{pmatrix}=O\begin{pmatrix}\hat{Z}_\mu\\ \hat{Z}'_\mu\end{pmatrix}\,,\quad \text{with}\quad O=\begin{pmatrix}c_\xi & s_\xi\\ -s_\xi & c_\xi\end{pmatrix}\quad\text{and}\quad \tan 2\xi=\frac{2\Delta^2}{\hat{M}_Z^2-\hat{M}_{Z'}^2}\,. \tag{7.9}$$

Since we assume $v\ll v_S$, we obtain $\hat{M}_Z^2,\,\Delta^2\ll\hat{M}_{Z'}^2$ and the resulting mixing angle is small [21]:

$$g_{Z'}\xi\simeq\frac{e}{2\hat{c}_W\hat{s}_W}\frac{X_{\Phi_1}v_1^2+X_{\Phi_2}v_2^2}{X_S^2v_S^2}\simeq-\frac{9e}{8\hat{c}_W\hat{s}_W}\left(\frac{g_{Z'}c_\beta v}{M_{Z'}}\right)^2\,. \tag{7.10}$$

Expanding in this small parameter, we obtain the following leading expression for the hatted weak angle in terms of physical quantities

$$\hat{s}_W^2\simeq s_*^2\equiv s_W^2-\frac{c_W^2s_W^2}{c_W^2-s_W^2}\xi^2\left(\frac{M_{Z'}^2}{M_Z^2}-1\right)\,. \tag{7.11}$$

In the physical basis the neutral gauge boson masses read

$$M_{Z,\,Z'}^2=\frac{1}{2}\left[\hat{M}_{Z'}^2+\hat{M}_Z^2\mp\sqrt{\left(\hat{M}_{Z'}^2-\hat{M}_Z^2\right)^2+4\Delta^4}\right]\,, \tag{7.12}$$

and their fermionic currents are given by

$$J_{Z^{(\prime)}}^\mu\supset\overline{\psi_i}\gamma^\mu\left[\epsilon_{L,ij}^{(\prime)\psi}P_L+\epsilon_{R,ij}^{(\prime)\psi}P_R\right]\psi_j\,, \tag{7.13}$$

with the couplings (up to $\mathcal{O}(\xi^2)$)

$$\begin{aligned}\epsilon^{\psi}_{X,ij} &= \frac{e}{c_W s_W}\left[1+\frac{\xi^2}{2}\left(\frac{M^2_{Z'}}{M^2_Z}-1\right)\right]\left[\left(T_3^{\psi_X}-s_*^2 Q_\psi\right)\mathbb{1}+\xi\frac{g_{Z'}c_W s_W}{e}\widetilde{\mathcal{X}}^{\psi}_X\right]_{ij}\,,\\ \epsilon'^{\psi}_{X,ij} &= \frac{e}{c_W s_W}\left[\frac{g_{Z'}c_W s_W}{e}\widetilde{\mathcal{X}}^{\psi}_X-\xi\left(T_3^{\psi_X}-s_W^2 Q_\psi\right)\mathbb{1}\right]_{ij}\,.\end{aligned} \tag{7.14}$$

Here $T_3^{\psi_L}$ is the third component of weak isospin for the left-handed fields ($T_3^{\psi_R}=0$) and Q_ψ the electric charge. We also define the vector and axial-vector combinations of the $Z^{(\prime)}$ couplings,

$$\epsilon^{(\prime)\,\psi}_{V,ij} \equiv \epsilon^{(\prime)\,\psi}_{L,ij}+\epsilon^{(\prime)\,\psi}_{R,ij}\,, \qquad \epsilon^{(\prime)\,\psi}_{A,ij} \equiv \epsilon^{(\prime)\,\psi}_{R,ij}-\epsilon^{(\prime)\,\psi}_{L,ij}\,. \tag{7.15}$$

The coefficients $\epsilon^{\psi}_{V(A),ij}$ encode corrections to the SM Z couplings due to mixing with the Z' which are proportional to $g_{Z'}\xi$ at leading order in the mixing angle. Such corrections are restricted to be small ($g_{Z'}\xi \lesssim 10^{-4}$) [23, 24]. In addition to our initial assumption, $v_S \gg v$, which already gives a small ξ, we will assume that the mixing angle receives an additional suppression, because $\tan\beta$ is large.[3] This also guarantees that flavor-changing effects mediated by the Z are negligible compared with those of the Z'.

Another important theoretical constraint is obtained when requiring the absence of a low-energy Landau pole, i.e. an energy scale $\Lambda_{\rm LP}$ at which perturbativity is lost. This scale can be found from the renormalization-group running of the $\mathrm{U}(1)'$ coupling, we have:

$$\frac{d\alpha_{Z'}}{d\ln q^2} = b\,\alpha^2_{Z'}+\mathcal{O}(\alpha^3_{Z'})\,, \tag{7.16}$$

where the one-loop beta function b contains the charge information of the model. It reads

$$b = \frac{1}{4\pi}\left[\frac{2}{3}\sum_f X^2_{fL,R}+\frac{1}{3}\left(2\sum_i X^2_{\Phi i}+X^2_S\right)\right]\,, \tag{7.17}$$

with f including all fermion degrees of freedom and $i=1,2$. The Landau pole can be extracted from the pole of $\alpha'(q^2)=g^2_{Z'}(q^2)/4\pi$, we obtain

$$\Lambda_{\rm LP} \simeq M_{Z'}\exp\left[\frac{1}{2\,b\,\alpha_{Z'}(M^2_{Z'})}\right]\,. \tag{7.18}$$

For the charges in our model we have $b \simeq 12.90$, see Eq. (7.2). Taking $M_{Z'} \simeq 4$ TeV, we get a Landau pole at the Planck scale, $\Lambda_{\rm LP} \gtrsim 10^{19}$ GeV, for $g_{Z'} \lesssim 0.12$. Notice that this bound is stronger than the naïve perturbativity bound $\alpha_{Z'}(M^2_{Z'}) \lesssim \mathcal{O}(1/\max\{|X_i|\}^2)$, which in our model gives $g_{Z'} \lesssim 0.47$. We can relax this condition by assuming that additional NP will appear at the see-saw or the Grand Unification scale. This way we obtain $g_{Z'} \lesssim 0.14$ for $\Lambda_{\rm LP} \geq 10^{14}$ GeV and $g_{Z'} \lesssim 0.13$ for $\Lambda_{\rm LP} \geq 10^{16}$ GeV. The extension of the model to these scales is beyond the scope of this thesis.

[3] This limit is quite natural in our model since Φ_2 is coupled to the top quark, while Φ_1 is coupled to the light first two generations. Therefore, the hierarchy $v_2 > v_1$ accommodates well the quark mass spectrum.

Scalar sector

Here we discuss the main features of the Higgs sector of the model, a detailed derivation of these results is given in Appendix 7.B. It consists of two complex Higgs doublets and a complex scalar gauge singlet. Their properties are largely determined by the fact that $v/v_S \ll 1$. The spectrum contains four would-be Goldstone bosons giving mass to the EW gauge vector bosons $\{M_W, M_Z, M_{Z'}\}$, a charged Higgs $H^\pm$ and four neutral scalars (three CP-even $\{H_1, H_2, H_3\}$ and a CP-odd A).

We obtain a decoupling scenario with a light SM-like Higgs boson, $M^2_{H_1} \sim \mathcal{O}(v^2)$, three heavy quasi-degenerate states coming mainly from the scalar doublets $M^2_{H_2} \simeq M^2_A \simeq M^2_{H^\pm} \sim \mathcal{O}(v_S^2)$ and another heavy CP-even Higgs coming mainly from the scalar singlet $M^2_{H_3} \sim \mathcal{O}(v_S^2)$.[4] The Yukawa interactions of the scalar bosons reflect this decoupling. They can be written as

$$\begin{aligned} -\mathcal{L}_Y \supset & \sum_{\varphi=H_k,A} \varphi \left[\overline{d_L}\, Y_d^\varphi\, d_R + \overline{u_L}\, Y_u^\varphi\, u_R + \overline{\ell_L}\, Y_\ell^\varphi\, e_R\right] \\ & + \frac{\sqrt{2}}{v} H^+ \left(\overline{u_L} N_d d_R - \overline{u_R} N_u^\dagger d_L + \overline{\ell_L} N_\ell e_R\right) + \text{h.c.} \end{aligned} \tag{7.19}$$

Neglecting corrections of $\mathcal{O}(v^2/v_S^2)$ we obtain

$$\begin{aligned} Y_f^{H_1} &= \frac{D_f}{v}\,, & Y_f^{H_2} &= -\frac{N_f}{v}\,, \\ Y_u^A &= i\frac{N_u}{v}\,, & Y_{d,\ell}^A &= -i\frac{N_{d,\ell}}{v}\,, \end{aligned} \tag{7.20}$$

with $(f = u, d, \ell)$. Here fermions have been rotated to the mass eigenbasis. The diagonal matrices $D_{f=u,d,\ell}$ contain the fermion masses, and the matrices N_f are given as

$$\begin{aligned} (N_d)_{ij} &= \frac{v_2}{v_1}(D_d)_{ij} - \left(\frac{v_2}{v_1} + \frac{v_1}{v_2}\right)(V^\dagger)_{i3}(V)_{3j}(D_d)_{jj}\,, \\ N_u &= \frac{v_2}{v_1}\text{diag}(m_u, m_c, 0) - \frac{v_1}{v_2}\text{diag}(0, 0, m_t)\,, \\ N_\ell &= \frac{v_2}{v_1}\text{diag}(m_e, m_\mu, 0) - \frac{v_1}{v_2}\text{diag}(0, 0, m_\tau)\,. \end{aligned} \tag{7.21}$$

The couplings of the scalar H_3 to the fermions are additionally suppressed, since they are generated only through mixing with the doublet degrees of freedom: $Y_f^{H_3} \simeq \mathcal{O}(v/v_S)$. The matrix N_d is non-diagonal in flavor space, giving again rise to tree-level FCNCs in the down-quark sector controlled by the CKM matrix V. Furthermore, as shown in Appendix 7.B, the constraints from the $\text{U}(1)'$ symmetry render the scalar potential CP invariant. CP violation in our model is therefore uniquely controlled by the CKM phase, like in the SM.[5]

[4] It is also possible to motivate scenarios that avoid decoupling based on an enhanced Poincaré symmetry protecting the weak scale [25]. These can give rise to a rich scalar sector at the EW scale and a pseudo-Goldstone boson in the spectrum.

[5] We do not consider strong CP violation in this section.

Model variations

As aforementioned, we have six model implementations according to the different lepton flavor permutations of the $\mathrm{U}(1)'$ charges, with identical quark and scalar charges given in Eq. (7.2). These permutations are performed in the basis where the lepton mass matrix is diagonal and the eigenvalues are correctly ordered. This way each permutation corresponds to the simultaneous interchange of the charges of both left- and right-handed leptons. It is straightforward to check that the permutation of just one set of charges, while satisfying the anomaly conditions as well, would give rise to a non-diagonal mass matrix and reduce to one of the six cases considered here after diagonalization.

In order to present the predictions for each of these models, we introduce the generic lepton charges

$$\begin{aligned} X_{1L} &= \frac{9}{4}\,, \qquad X_{2L} = \frac{21}{4}\,, \qquad X_{3L} = -3\,, \\ X_{1R} &= \frac{9}{2}\,, \qquad X_{2R} = \frac{15}{2}\,, \qquad X_{3R} = -3\,, \end{aligned} \tag{7.22}$$

such that each implementation is labeled by $(e,\,\mu,\,\tau) = (i,\,j,\,k)$. For instance, the model presented in Eq. (7.2) is now labeled as (1, 2, 3).

The additional possibilities to implement the quark and neutrino sectors have been discussed in the previous sections.

7.1.2 Discussion

In this section we discuss the phenomenology of the gauged BGL models introduced in the previous section. The phenomenology of a scalar sector with a flavor structure identical to the one of our model has been analyzed in Refs. [26, 27]. Since we are assuming a decoupling scalar sector, we can naturally accommodate a SM-like Higgs at 125 GeV; the heavy scalars are not expected to yield sizable contributions to flavor observables in general. We therefore focus on the phenomenological implications of the Z' boson for this class of models. In the cases where the constraints depend on the choice of lepton charges in our model, we give here the most conservative bound and discuss the differences in the next sections.

Low-energy constraints

Despite the large mass of several TeV, the Z' boson yields potentially significant contributions on flavor observables, due to its flavor-violating couplings in the down-type quark sector. However, because of $M_W^2/M_{Z'}^2 \leq 0.1\%$ and the CKM suppression of the flavor-changing Z' couplings, these contributions can only be relevant when the corresponding SM amplitude has a strong suppression in addition to G_F. This is specifically the case for meson mixing amplitudes and electroweak penguin processes which we will discuss below. Further examples are differences of observables that are small in the SM, for example due to lepton universality or isospin symmetry.

The particular flavor structure of the model implies a strong hierarchy for the size of different flavor transitions: $|V_{ts}^* V_{td}| \sim \lambda^5 \ll |V_{td}^* V_{tb}| \sim \lambda^3 \ll |V_{ts}^* V_{tb}| \sim \lambda^2$ (where

$\lambda \simeq 0.226$). However, since the SM amplitudes often show a similar hierarchy, the relative size of the Z' contribution has to be determined on a case-by-case basis. We obtain for example similar bounds from the mass differences $\Delta m_{d,s}$ in the $B_{d,s}$ systems and ϵ_K. Here we include exemplarily the constraint from B_s mixing, while we leave a detailed phenomenological analysis for future work.

Given the high experimental precision of Δm_s [28], the strength of the corresponding constraint depends completely on our capability to predict the SM value. The limiting factors here are our knowledge of the hadronic quantity $f_{B_s}\sqrt{\hat{B}_s}$ (see Ref. [29–32]) and the relevant CKM elements. Using the corresponding values from Refs. [33] and [34], respectively, we conclude that contributions to Δm_s up to 20% remain possible at 95% CL; from this we obtain the limit $M_{Z'}/g_{Z'} \gtrsim 25$ TeV. Tree-level scalar contributions have been neglected, since their effect cancels to a very good approximation in the decoupling limit considered here [35, 36].

Regarding the input for the CKM parameters, we make the following observations in our models: (i) Charged-current tree-level processes receive negligible contributions. (ii) The mixing phase in $B_{d,s}$ mixing and the ratio $\Delta m_s/\Delta m_d$ remain SM-like. (iii) The additional direct CP violation in $B \to \pi\pi, \rho\pi, \rho\rho$ and $B \to J/\Psi K$ is negligible. These observations imply that in our context the global fits from Refs. [34, 37] remain valid to good approximation.

In our models the Z' boson couples to muons and will contribute to NTP, $\nu_\mu N \to \nu N \mu^+\mu^-$. We expect dominance of the Z' vector current for our models. The NTP cross section normalized to the SM one was calculated in Refs. [38–40]. Using a combination of the latest NTP cross-section measurements we obtain a bound on the parameter combination $M_{Z'}/g_{Z'}$ [41–43], which is however weaker than the one from B_s mixing.

APV measurements also place bounds on additional neutral gauge bosons coupling to electrons and light quarks. In particular, the precise measurement of the ^{133}Cs weak charge from APV experiments is in a reasonable agreement with the prediction of the SM and can be used to set bounds on the Z' boson of our models [44–50]. The bound we obtain on $M_{Z'}/g_{Z'}$ from the latest determination of the ^{133}Cs weak charge is however again weaker than the limit from B_s mixing.

Further potentially strong bounds stem from EDM and the anomalous magnetic moment of the muon. EDMs from the scalar sector occur at the two-loop level; while this alone does not render them necessarily sufficiently small, the additional suppression and cancellations in the decoupling limit imply very small effects [26, 27, 51, 52]. Anomalous magnetic moments can be present at the one loop level, but are again too small in 2HDMs near the decoupling limit [26, 27, 53]. Concerning the new gauge boson, one-loop contributions to EDMs require different phases for left- and right-handed Z' couplings to quarks and/or leptons [54]; this feature is not present in our model, therefore the Z' contributions are again at the two-loop level and sufficiently suppressed, given the large Z' mass. In the case of anomalous magnetic moments we have non-vanishing one-loop contributions, which for the muon read [55, 56]

$$a_\mu^{\rm NP} \simeq \frac{m_\mu^2}{4\pi^2}\frac{g_{Z'}^2}{M_{Z'}^2}\left(\frac{1}{3}X_{\mu V}^2 - \frac{5}{3}X_{\mu A}^2\right), \tag{7.23}$$

where $X_{\mu V} \equiv (X_{\mu L} + X_{\mu R})/2$ and $X_{\mu A} \equiv (X_{\mu R} - X_{\mu L})/2$. Using the bound on $M_{Z'}/g_{Z'}$ from $\bar{B}_s^0 - B_s^0$ mixing, we get $a_\mu^{\rm NP} < 1.3 \times 10^{-11}$ for all charge assignments, which is smaller than the current theory uncertainty in the prediction of $a_\mu^{\rm SM}$ [23].

Direct searches

The obvious way to search directly for a Z' is via a resonance peak in the invariant-mass distribution of its decay products. At the LHC this experimental analysis is usually performed by the ATLAS [57, 58] and CMS [59, 60] collaborations[6] for Z' production in the s-channel in a rather model-independent way, but assuming validity of the NWA, negligible contributions of interference with the SM [65], and flavor-universal Z' couplings to quarks. Under these assumptions, the cross section for $pp \to Z'X \to f\bar{f}X$ takes the simplified form [66, 67]

$$\sigma = \frac{\pi}{48s}\left[c_u^f w_u\left(s,\, M_{Z'}^2\right) + c_d^f w_d\left(s,\, M_{Z'}^2\right)\right] , \tag{7.24}$$

where the functions $w_{u,d}$ are hadronic structure factors that encode the information of the Drell-Yan production processes of the Z' and their QCD corrections (for a precise definition of these functions we refer the reader to Ref. [67]). The model-dependent part of the cross section is contained in the coefficients $c_{u,d}$:

$$\begin{aligned} c_u^f &\simeq g_{Z'}^2\left(X_{uL}^2 + X_{uR}^2\right) \mathrm{Br}\left(Z' \to f\bar{f}\right) , \\ c_d^f &\simeq g_{Z'}^2\left(X_{uL}^2 + X_{dR}^2\right) \mathrm{Br}\left(Z' \to f\bar{f}\right) . \end{aligned} \tag{7.25}$$

While the assumptions for these expressions are not exactly fulfilled in our model, they are applicable when neglecting the small contributions proportional to the off-diagonal CKM matrix elements. The reason is that under this approximation the Z' couplings to the first two generations - which yield the dominant contribution to the Drell-Yan production of the Z' - are universal and flavor conserving in the quark sector, see Eqs. (7.2) and (7.7). Note that $X_{uL} \simeq X_{dL}$ up to small corrections proportional to the off-diagonal CKM matrix elements that we are neglecting.[7]

For high values of $g_{Z'}$ the ratio $\Gamma_{Z'}/M_{Z'}$ can be quite large, spoiling the NWA. The constraint is therefore only applicable for $g_{Z'} \lesssim 0.2$, such that $\Gamma_{Z'}/M_{Z'}$ does not exceed 15%. However, for the mass range accessible so far such a large coupling is typically excluded by the constraint R_K, as will be shown below. Combined exclusion limits on the Z' at 95% CL using the dimuon and dielectron channels have been provided by the CMS collaboration in the (c_u, c_d) plane [59, 60]. Using these bounds together with the constraint from R_K, we find that a Z' boson is excluded in our models for $M_{Z'} \lesssim$ 3-4 TeV, depending on the lepton charge assignments, while $g_{Z'}$ should be $\mathcal{O}(10^{-1})$. These bounds are stronger than those from many Z' benchmark models, for which current LHC data typically give a lower bound of $M_{Z'} \gtrsim$ 2-3 TeV [57–60]. The reason is a combination of a sizable value for $g'/M_{Z'}$

[6] In this section we will not consider the analyses on dilepton resonance searches at 13 TeV [2, 61–63] nor the implications from the high-p_T tails [64] using this data.

[7] Flavor changing Z' couplings between the first two quark generations are suppressed by $|V_{td}V_{ts}^*| \sim \lambda^5$ while violations of universality are suppressed by $|V_{td}|^2 \sim \lambda^6$ and $|V_{ts}|^2 \sim \lambda^4$, with $\lambda \simeq 0.226$.

required by the constraint from R_K and the combination of Z' couplings to fermions appearing in our model, see Eq. (7.25).

When the Z' is too heavy to be produced at a given collider, $M_{Z'}^2 \gg s$, indirect searches can be carried out by looking for effects from contact interactions, i.e. effective operators generated by integrating out the heavy Z'. At the LHC, the corresponding expressions hold for $M_{Z'} \gg 4.5$ TeV, and limits can be extracted e.g. from searches for the contact interactions $(\bar{q}\gamma_\mu P_{L,R} q)(\bar{\ell}\gamma^\mu P_{L,R}\ell)$ [68]. These are presented in terms of benchmark scenarios considering a single operator with a specific chirality structure. From the 95% CL limit provided in Ref. [68] for the operator $(\bar{q}\gamma_\mu P_L q)(\bar{e}\gamma^\mu P_R e)$ we extract $M_{Z'}/g_{Z'} \gtrsim 22$ TeV. Searches for contact interactions of the type $(\bar{e}\gamma_\mu P_{L,R} e)(\bar{f}\gamma^\mu P_{L,R} f)$ were performed at LEP [69]. These are sensitive to a Z'-boson coupling to electrons assuming $M_{Z'} \gg 210$ GeV and the resulting limits are again given for benchmark scenarios. In this case we extract $M_{Z'}/g_{Z'} \gtrsim 25$ TeV from the 95% CL bound on the operator $(\bar{e}\gamma^\alpha P_R e)(\bar{\mu}\gamma_\alpha P_R \mu)$. It is important to note that the extracted bounds from contact interactions using benchmark scenarios do not capture the full dynamics of our models once the Z' boson is integrated out. Interference effects due to operators with different chirality structures will be relevant in general; a detailed analysis of these effects is however beyond the scope of this thesis. These bounds should therefore be taken as a rough guide to the sensitivity of contact interactions searches at LEP and the LHC to the Z' of our models. However, in general they do not put relevant bounds as long as $g_{Z'}$ is not too large.

7.1.3 Discriminating the different models

The constructed class of models has two important features which imply specific deviations from the SM: controlled FCNCs in the down-quark sector and violations of lepton universality. Thanks to the very specific flavor structure, the two are strongly correlated in each of our models. While the flavor-changing couplings are universal in the models we discuss here, the lepton charges differ. Correspondingly the models can be discriminated by processes involving leptons, specifically rare leptonic and semileptonic decays of B mesons, which can test both features.

The effective Hamiltonian describing these $b \to s\ell^+\ell^-$ transitions was introduced in Section 4.2.2. New physics contributions to the $\mathcal{H}_{\text{eff}}^{b\to s\gamma}$ part of this Hamiltonian arise in our models from one-loop diagrams mediated by Z' and Higgs bosons. Both of them are very small due to the assumed mass scale of several TeV [70]. At the b-quark scale, the SM contribution to the remaining part reads $C_9^{\text{SM}} \simeq -C_{10}^{\text{SM}} \simeq 4.2$ and is universal for the three lepton families, while all other contributions are negligible. The chirality-flipped operators $\mathcal{O}_{9',10'}$ receive negligible contributions also in our models since $\epsilon'^d_{R,sb} = 0$, while all others receive contributions from Z' or Higgs exchanges [35, 36, 70]. The Z' contribution to $C_{9,10}^\ell$ is given by

$$\begin{aligned} C_9^{\text{NP}\ell} &\simeq -\frac{\pi v^2}{\alpha V_{ts}^* V_{tb}} \frac{\epsilon'^d_{L,sb}\epsilon'^e_{V,\ell\ell}}{M_{Z'}^2}\,, \\ C_{10}^{\text{NP}\ell} &\simeq -\frac{\pi v^2}{\alpha V_{ts}^* V_{tb}} \frac{\epsilon'^d_{L,sb}\epsilon'^e_{A,\ell\ell}}{M_{Z'}^2}\,, \end{aligned} \tag{7.26}$$

Model	$C_{10}^{\mathrm{NP}\mu}/C_9^{\mathrm{NP}\mu}$	$C_9^{\mathrm{NP}e}/C_9^{\mathrm{NP}\mu}$	$C_{10}^{\mathrm{NP}e}/C_9^{\mathrm{NP}\mu}$	$C_9^{\mathrm{NP}\tau}/C_9^{\mathrm{NP}\mu}$	$C_{10}^{\mathrm{NP}\tau}/C_9^{\mathrm{NP}\mu}$	κ_9^μ
(1,2,3)	3/17	9/17	3/17	−8/17	0	−1.235
(1,3,2)	0	−9/8	−3/8	−17/8	−3/8	0.581
(2,1,3)	1/3	17/9	1/3	−8/9	0	−0.654
(2,3,1)	0	−17/8	−3/8	−9/8	−3/8	0.581
(3,1,2)	1/3	−8/9	0	17/9	1/3	−0.654
(3,2,1)	3/17	−8/17	0	9/17	3/17	−1.235

Table 7.1: *Correlations among the NP contributions to the effective operators $\mathcal{O}_{9,10}^\ell$. Each model is labeled by its lepton charge implementation $(e,\mu,\tau)=(i,j,k)$.*

where $C_i^\ell \equiv C_i^{\mathrm{SM}} + C_i^{\mathrm{NP}\ell}$. In Table 7.1 we show the correlations between the Wilson coefficients $C_{9,10}^{\mathrm{NP}\ell}$ in our models and provide $C_9^{\mathrm{NP}\mu}$ as a function of $g_{Z'}/M_{Z'}$ by introducing a conveniently normalized parameter κ_9^μ:

$$C_9^{\mathrm{NP}\mu} \equiv \kappa_9^\mu \times 10^4 \left(\frac{g_{Z'}v}{M_{Z'}}\right)^2 = \kappa_9^\mu \times 605\ \mathrm{TeV}^2 \left(\frac{g_{Z'}}{M_{Z'}}\right)^2 . \tag{7.27}$$

This allows the direct estimation of $C_{9,10}^{\mathrm{NP}\ell}$ in terms of $g_{Z'}/M_{Z'}$, useful for phenomenological purposes.

The CP-even Higgs H_2 and the CP-odd Higgs A can give sizable contributions to O_S^ℓ and O_P^ℓ, respectively. For muons we have[8]

$$C_S^{\mathrm{NP}\mu} \simeq -C_P^{\mathrm{NP}\mu} \simeq \frac{-2\,\pi\,(t_\beta + t_\beta^{-1})(N_\ell)_{\mu\mu}}{\alpha \bar{M}_H^2} . \tag{7.28}$$

Here we have denoted the quasi-degenerate masses of H_2 and A by $\bar{M}_H \equiv M_{H_2} \simeq M_A$, see Appendix 7.B for details of the scalar sector. The coupling $(N_\ell)_{\mu\mu}$ is again model-dependent: $(N_\ell)_{\mu\mu} = t_\beta m_\mu$ for models $(1,2,3)$, $(2,1,3)$, $(3,1,2)$ and $(3,2,1)$, while $(N_\ell)_{\mu\mu} = -t_\beta^{-1} m_\mu$ for $(1,3,2)$ and $(2,3,1)$. The suppression by the muon mass renders these contributions negligible, apart from observables in which also the SM and Z' contributions receive this suppression, e.g. $B_s \to \mu^+\mu^-$. Higgs contributions to $O_{S',P'}^\ell$ will be additionally suppressed by a factor m_s/m_b compared to the corresponding non-primed operators and are neglected in the following.

The angular distributions of neutral-current semileptonic $b \to s\ell^+\ell^-$ transitions allow for testing these coefficients in global fits. Furthermore, they provide precise tests of lepton universality when considering ratios of the type

$$R_M \equiv \frac{\mathrm{Br}(\bar{B} \to \bar{M}\mu^+\mu^-)}{\mathrm{Br}(\bar{B} \to \bar{M}e^+e^-)} \overset{\mathrm{SM}}{=} 1 + \mathcal{O}(m_\mu^2/m_b^2) , \tag{7.29}$$

with $M \in \{K, K^*, X_s, K_0(1430), \ldots\}$ [72], where many sources of uncertainties cancel when integrating over identical phase-space regions.

[8] The correlation $C_S = -C_P$ was expected given the assumed decoupling in the scalar sector [71].

Additional sensitivity to the dynamics of NP can be obtained via double-ratios [73],

$$\widehat{R}_M \equiv \frac{R_M}{R_K}\,. \tag{7.30}$$

It was shown in Ref. [73] that the dependence on the NP coupling to left-handed quarks cancels out in $\widehat{R}_M$. Since $C^{\ell}_{9',10'} = 0$ in our models we have $\widehat{R}_{K^*} = \widehat{R}_{X_s} = \widehat{R}_{K_0(1430)} = 1$, providing an important test of the flavor structure of our models.[9]

The possible hadronic final states for these ratios yield sensitivity to different NP structures, thereby providing complementary information. The discriminating power of these observables has been shown in Ref. [74] within the framework of leptoquark models and in more general contexts in Refs. [73, 75, 76].

To analyze the deviations from flavor-universality we define $R_M \simeq 1 + \Delta + \Sigma$, where Σ is the pure contribution from NP and Δ the one from the interference with the SM. These quantities are given by

$$\begin{aligned}\Delta &= \frac{2}{|C_9^{\rm SM}|^2 + |C_{10}^{\rm SM}|^2}\left[\mathrm{Re}\left\{C_9^{\rm SM}\left(C_9^{{\rm NP}\mu}\right)^*\right\}\right.\\ &\quad\left.+\,\mathrm{Re}\left\{C_{10}^{\rm SM}\left(C_{10}^{{\rm NP}\mu}\right)^*\right\} - (\mu \to e)\right]\,,\\ \Sigma &= \frac{\left|C_9^{{\rm NP}\mu}\right|^2 + \left|C_{10}^{{\rm NP}\mu}\right|^2}{|C_9^{\rm SM}|^2 + |C_{10}^{\rm SM}|^2} - (\mu \to e)\,,\end{aligned} \tag{7.31}$$

and are valid to a very good approximation given the present experimental uncertainties.

Our models also give clean predictions for the rare decays $B \to M\nu\bar{\nu}$, with $M = K, K^*, X_s$ [70]. Tree-level Z'-boson contributions to these decays are generically expected of the same size as in $b \to s\ell^+\ell^-$ transitions. However, the modes with neutrino final states do not distinguish between our different models, since there is no sensitivity to the neutrino species. We obtain again a universal value for all ratios $R_M^{\nu} = \mathrm{Br}(B \to M\bar{\nu}\nu)/\mathrm{Br}(B \to M\bar{\nu}\nu)|_{\rm SM}$, due to the fact that $\epsilon'^{d}_{R,sb} = 0$. For the same reason the average of the K^* longitudinal polarization fraction in $B \to K^*\nu\bar{\nu}$ is not affected by the Z' exchange contribution [70]. The enhancement of R_M^{ν} turns out to be relatively small, $\mathcal{O}(10\%)$ for $g_{Z'} \sim 0.1$ and $M_{Z'} \sim \mathcal{O}(\mathrm{TeV})$. The reason is again the sum over the different neutrino species: due to the different charges, the Z' contribution interferes with the SM one both constructively and destructively, leaving a net effect that is smaller than in the modes with charged leptons.

The leptonic decays $B^0_{s,d} \to \ell^+\ell^-$ constitute another sensitive probe of small NP effects. Within the SM, these decays arise again at the loop level and are helicity suppressed. Due to the leptonic final state, the theoretical prediction of these processes is very clean. They receive Z'- and Higgs-mediated contributions at tree-level in our model through the operators $\mathcal{O}^{\mu}_{10,S,P}$ [75],

$$\frac{\mathrm{Br}(\bar{B}_s \to \mu^+\mu^-)}{\mathrm{Br}(\bar{B}_s \to \mu^+\mu^-)^{\rm SM}} \simeq \left|1 - 0.24 C_{10}^{{\rm NP}\mu} - y_\mu C_P^{{\rm NP}\mu}\right|^2 + |y_\mu C_S^{{\rm NP}\mu}|^2\,, \tag{7.32}$$

[9] This important prediction of the model is in agreement with the recent measurement of R_{K^*} in the dilepton invariant-mass-squared region $q^2 \in [1.1, 6]$ GeV^2 performed by the the LHCb Collaboration [1]. See note added at the beginning of the chapter.

Model	$\mu_{e/\mu}$	$\mu_{e/\tau}$	$\mu_{\mu/\tau}$
(1,2,3)	45/149	45/32	149/32
(1,3,2)	45/32	45/149	32/149
(2,1,3)	149/45	149/32	45/32
(2,3,1)	149/32	149/45	32/45
(3,1,2)	32/45	32/149	45/149
(3,2,1)	32/149	32/45	149/45

Table 7.2: *Model-dependent predictions for the ratio $\mu_{\ell/\ell'}$. The different models are labeled by their lepton charge implementations, i.e. $(e, \mu, \tau) = (i, j, k)$.*

where $y_\mu \simeq 7.7\, m_b$. For the range of model parameters relevant here, the Z' contribution to $\bar{B}_s \to \mu^+\mu^-$ is very small with respect to the SM, $\sim 1\%$ for $M_{Z'} \sim 5$ TeV and $g_{Z'} \sim 0.1$. Larger contributions are possible due to scalar mediation for the models $(1,2,3)$, $(2,1,3)$, $(3,1,2)$ and $(3,2,1)$, given that $C_S \simeq -C_P \propto t_\beta^2$ in these cases. Taking $\bar{M}_H \sim 10$ TeV and $t_\beta \sim 30$ for example, one obtains a suppression of $\mathrm{Br}(\bar{B}_s \to \mu^+\mu^-)$ of about 10% relative to the SM. In our model the ratio $\mathrm{Br}(\bar{B}_d \to \mu^+\mu^-)/\mathrm{Br}(\bar{B}_s \to \mu^+\mu^-)$ remains unchanged with respect to the SM to a very good approximation.

If a Z' boson is discovered during the next runs of the LHC [77], its decays to leptons can be used to discriminate the models presented here. We define the ratios

$$\mu_{f/f'} \equiv \frac{\sigma(pp \to Z' \to f\bar{f})}{\sigma(pp \to Z' \to f'\bar{f}')}\,, \tag{7.33}$$

where again the dominant sources of uncertainty cancel, rendering them particularly useful to test lepton universality. This possibility has also been discussed in Refs. [78–83]. In our models we have

$$\mu_{b/t} \simeq \frac{X_{bL}^2 + X_{bR}^2}{X_{tL}^2 + X_{tR}^2}\,, \qquad \mu_{\ell/\ell'} \simeq \frac{X_{\ell L}^2 + X_{\ell R}^2}{X_{\ell' L}^2 + X_{\ell' R}^2}\,. \tag{7.34}$$

The first ratio is fixed in our models, $\mu_{b/t} \simeq 1$, while large deviations from $\mu_{\ell/\ell'} = 1$ are possible. The model-specific predictions for the ratio $\mu_{\ell/\ell'}$ are shown in Table 7.2. We note that there is a correlation between R_K and $\mu_{e/\mu}$: an enhancement of R_K (as present in models $(1,3,2)$, $(2,1,3)$ and $(2,3,1)$) implies an enhancement of $\mu_{e/\mu}$ and the other way around. Violations of lepton universality can therefore be tested by complementary measurements of flavor observables at LHCb or Belle II and Z' properties to be measured at ATLAS and CMS.

7.1.4 Interpretation of $b \to s\ell^+\ell^-$ anomalies

The LHCb collaboration has performed two measurements of decays with $b \to s\ell^+\ell^-$ transitions that show a tension with respect to the SM expectations.[10] The first

[10] As already stated, we exclude from the discussion the very recent measurement of R_{K^*} by the LHCb Collaboration [1]. See note added at the beginning of the chapter.

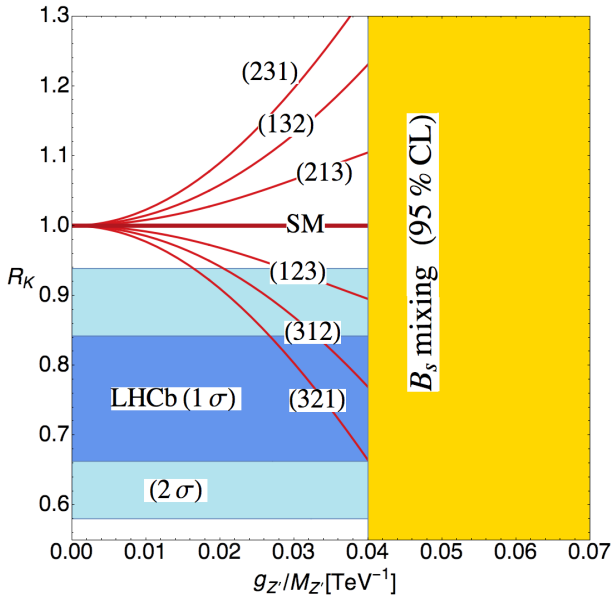

Figure 7.1: *Model-dependent predictions for R_K as a function of $g_{Z'}/M_{Z'}$. The measurement of R_K by the LHCb collaboration is shown at 1σ and 2σ. Constraints from B_s mixing are also shown at 95% CL.*

measurement is that of the ratio R_K introduced in the last section, where LHCb measures [84] $R_K^{\rm LHCb} = 0.745^{+0.090}_{-0.074} \pm 0.036$ for $q^2 \in [1,6]$ GeV^2, a $2.6\,\sigma$ deviation with respect to the SM prediction [72, 85–87]. The second measurement is the angular analysis of $B \to K^* \mu^+ \mu^-$ decays [88], where an excess of 2.9σ is observed for the angular observable P_5' in the bin $q^2 \in [4,6]$ GeV^2,[11] which has been constructed to reduce the influence of form factor uncertainties [89]. Similarly the branching fraction of $B_s \to \phi \mu^+ \mu^-$ also disagrees with the SM prediction [90, 91] by about $3\,\sigma$ [92]

Attributing the measurement of R_K solely to NP, i.e. assuming that it will be confirmed with higher significance in the next run of the LHC and/or by additional R_M measurements, it is the first way to exclude some of our models, since it requires sizable non-universal contributions with a specific sign. The flavor structure in each of our models is fixed, so half of them cannot accommodate $R_K < 1$, namely (1, 3, 2), $(2, 1, 3)$ and (2, 3, 1). This is illustrated in Figure 7.1, where it is additionally seen that a large deviation from $R_K = 1$, as indicated by the present central value and 1σ interval, can actually only be explained in two of the remaining models. This strong impact shows the importance of further measurements of R_M ratios.

In Figure 7.2 we show the constraints from the R_K measurement for the remaining models $(1, 2, 3)$, $(3, 1, 2)$ and $(3, 2, 1)$. The allowed regions are consistent with the constraint from B_s^0-meson mixing. LHC searches for a Z' boson exclude values of $M_{Z'}$ below 3-4 TeV, as discussed in the previous section; the corresponding areas are shown in gray. We also show the theoretical perturbativity bounds obtained from the requirement that the Landau pole for the U(1)$'$ gauge coupling appears beyond the see-saw or the Grand Unification scales, i.e. $\Lambda_{\rm LP} > 10^{14}$ GeV and $\Lambda_{\rm LP} > 10^{16}$ GeV, respectively.

Regarding the angular analysis in $B \to K^* \mu^+ \mu^-$, the situation is more complicated. The wealth of information provided in this and related measurements requires

[11] The bin $q^2 \in [6,8]$ GeV^2 shows nominally a tension with identical significance; however, this bin is considered less theoretically clean, due to the larger influence of charm resonances.

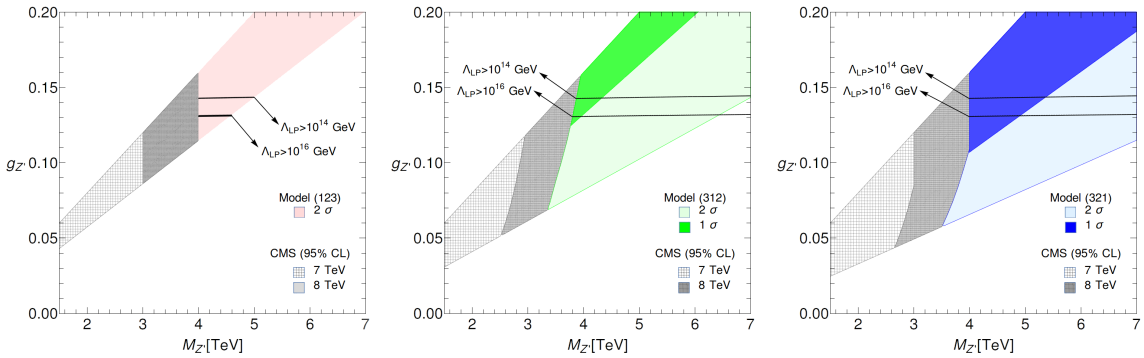

Figure 7.2: *Regions allowed at* 1σ *and* 2σ *by the* R_K *measurement in the* $\{M_{Z'}, g_{Z'}\}$ *plane for the models* $(1,2,3)$, $(3,1,2)$ *and* $(3,2,1)$. *Exclusion limits from* Z' *searches at the LHC are shown in gray. The black lines indicate bounds from perturbativity of* $g_{Z'}$.

a global analysis, which is beyond the scope of this thesis. However, a number of model-independent studies have been carried out [92–99]. These analyses differ in terms of the statistical methods used, treatment of hadronic uncertainties (see also Ref. [100]), and consequently in the significance they find for the NP hypothesis over the SM one. However, they agree that a contribution $C_9^{\mathrm{NP}\mu} \sim -1$ can fit the data for P_5' and $\mathrm{Br}(B_s \to \phi\mu^+\mu^-)$ without conflicting with other observables. Additional contributions from e.g. $C_{10}^{\mathrm{NP}\mu}$ can be present, but are less significant and tend to be smaller. When using Table 7.1 to translate the R_K measurement into a bound on $C_9^{\mathrm{NP}\mu}$ in our models, see Table 7.3, the ranges are perfectly compatible with the values obtained by the global fits to $b \to s\mu\mu$ data, as also observed for other Z' models [92–94, 96, 99]. This is highly non-trivial given the strong correlations in our models and will allow for decisive tests with additional data.

Let us further comment on the implications of the recent measurements of $\bar{B}^0_{d,s} \to \mu^+\mu^-$ decays [101],

$$\begin{aligned} \frac{\mathrm{Br}(\bar{B}_s \to \mu^+\mu^-)^{\mathrm{exp}}}{\mathrm{Br}(\bar{B}_s \to \mu^+\mu^-)^{\mathrm{SM}}} &= 0.76^{+0.20}_{-0.18}\,, \\ \frac{\mathrm{Br}(\bar{B}_d \to \mu^+\mu^-)^{\mathrm{exp}}}{\mathrm{Br}(\bar{B}_d \to \mu^+\mu^-)^{\mathrm{SM}}} &= 3.7^{+1.6}_{-1.4}\,. \end{aligned} \tag{7.35}$$

Both results seem to hint at a deviation from the SM, however in opposite directions. A confirmation of this situation with higher significance would rule out our models which predict these ratios to be equal; however, the uncertainties in the B_d mode are still large.[12] Regarding the B_s mode, which is measured consistent with the SM prediction, it should be noted that the result depends sensitively on the value adopted for $|V_{cb}|$, where the value from inclusive $B \to X_c\ell\nu$ decays was chosen in the SM calculation [103]. In any case, as already discussed, a potential shift could be explained in the context of our models by scalar contributions, which are, however, not directly related to the Z' contributions discussed above.

[12] While this thesis was being completed, the LHCb Collaboration presented a new measurement of these observables in agreement with the SM expectations [102]; this is compatible with our models expectations.

Model	$C_9^{\mathrm{NP}\mu}(1\sigma)$	$C_9^{\mathrm{NP}\mu}(2\sigma)$
(1,2,3)	–	$[-1.20, -0.61]$
(3,1,2)	$[-0.63, -0.43]$	$[-0.63, -0.17]$
(3,2,1)	$[-1.20, -0.53]$	$[-1.20, -0.20]$

Table 7.3: *Model-dependent bound on $C_9^{\mathrm{NP}\mu}$ from the R_K measurement. The constraint from B_s mixing is taken into account.*

The models that accommodate the $b \to s\ell^+\ell^-$ data can be further discriminated using the observables described in the last section, notably using the ratios $\mu_{\ell/\ell'}$, provided a Z' boson is discovered at the LHC.

7.1.5 Conclusions

The class of family-non-universal Z' models presented in this section exhibits FCNCs at tree level that are in accordance with available flavor constraints while still inducing potentially sizable effects in various processes, testable at existing and future colliders. This is achieved by gauging the specific (BGL-)symmetry structure, introduced in Ref. [4], which renders the resulting models highly predictive.

The particle content of the models is minimal in the sense that the extension of the $\mathrm{U}(1)'$ symmetry to the lepton sector allows to restrict the fermion content to the SM one. The only additional particles are then a second Higgs doublet, a scalar singlet and the Z' boson, all of which are heavy after spontaneous symmetry breaking, due to the large mass scale for the singlet. The anomaly conditions largely determine the charge assignments under the $\mathrm{U}(1)'$ symmetry; the remaining freedom is used for two phenomenologically motivated choices, leaving only six possible models which are related by permutations in the lepton sector.

The main phenomenological features of these models can be summarized as follows:

1. FCNCs at tree level in the down-quark sector, which are mediated by heavy Z' gauge bosons and neutral scalars, controlled by combinations of CKM matrix elements and/or fermion mass factors.

2. Non-universal lepton couplings determined by the charges under the additional $\mathrm{U}(1)'$ symmetry.

3. No FCNCs in the charged-lepton or up-quark sectors.

4. Complete determination of the $\mathrm{U}(1)'$ sector up to two real parameters, $M_{Z'}$ and $g_{Z'}$, where all observables at the electroweak scale and below depend only on the combination $g_{Z'}/M_{Z'}$.

Present data already strongly restrict the possible parameter ranges in our models: direct searches exclude Z' masses below $3 - 4$ TeV and the constraint from B mixing implies $M_{Z'}/g_{Z'} \geq 16$ TeV (95% CL). Theoretical bounds from perturbativity give an upper bound on the value of the gauge coupling, e.g. $g_{Z'} \lesssim 0.14$ for a Landau pole beyond the see-saw scale. Nevertheless, three of our models can explain the deviations from SM expectations in $b \to s\ell^+\ell^-$ transitions seen in LHCb measurements [84, 88], while the other three are excluded (at 95% CL) by $R_K < 1$. These findings are illustrated in Figs. 7.1 and 7.2.

Any significant deviation from the SM in an observable with Z' contributions allows for predicting all other observables, for instance the values for $C_{9,10}^{\mathrm{NP}\ell}$ obtained from R_K, see Tables 7.1 and 7.3. Further characteristic predictions in our models include the following:

- The absence of flavor-changing Z' couplings to right-handed quarks implies $\widehat{R}_M = 1$, i.e. all ratios defined in Eq. (7.29) are expected to be equal, $R_K = R_{K^*} = R_{X_s} = \ldots$ The same holds for the ratios R_M^ν in $B \to M\bar{\nu}\nu$ decays.
- If a Z' is discovered at the LHC, measurements of $\sigma(pp \to Z' \to \ell_i\bar{\ell}_i)/\sigma(pp \to Z' \to \ell_j\bar{\ell}_j)$ can be used to discriminate between our models, due to the specific patterns of lepton-non-universality, see Table 7.2.
- Leptonic down-quark FCNC decays are sensitive to the Higgs couplings in our model, specifically $B_{d,s} \to \ell^+\ell^-$. Double ratios of B_s and B_d decays are again expected to equal unity.

In the near future we will therefore be able to differentiate our new class of models from other Z' models as well as its different realizations from each other. This will be possible due to a combination of direct searches/measurements at the LHC and high-precision measurements at low energies, e.g. from Belle II and LHCb. Further progress can come directly from theory, e.g. by more precise predictions for $\Delta m_{d,s}$ or ϵ_K.

As a final remark, we recall that in this minimal implementation of gauged BGL symmetry neutrinos are massless. Additional mechanisms to explain neutrinos masses can introduce new solutions to the anomaly equations; these new variants are subject to future work.

7.2 Flavor anomalies from dynamical Yukawas

In this section, based on the publication in Ref. [104], we analyze the possible interplay between the flavor anomalies in $b \to s\ell^+\ell^-$ transitions and the SM flavor puzzle. As already discussed, the SM flavor puzzle –the lack of explanation for the peculiar structure of fermion masses and mixing angles– with masses spanning several orders of magnitude and very hierarchical mixing in the quark sector in contrast to the anarchical structure in the lepton sector, remains as one of the long-standing questions the SM cannot address. An interesting approach to reproduce the main features of quark and lepton mass matrices is to assume the Yukawa couplings are generated from dynamical fields, whose background values minimize a generic potential invariant under a large non-Abelian flavor symmetry group, such as $[\mathrm{SU}(3)]^5 \times \mathrm{O}(3)$ [105,106] (see Section 1.3). Employing general group theory arguments, the natural extrema of such potential, corresponding to maximally unbroken subgroups, robustly predict large (zero) third (first two) generation quark mass, and a trivial CKM matrix (equal to the identity matrix). In the lepton sector, the same approach leads to a solution with hierarchical charged lepton masses accompanied by at least two degenerate Majorana neutrinos, with potentially large θ_{12} mixing

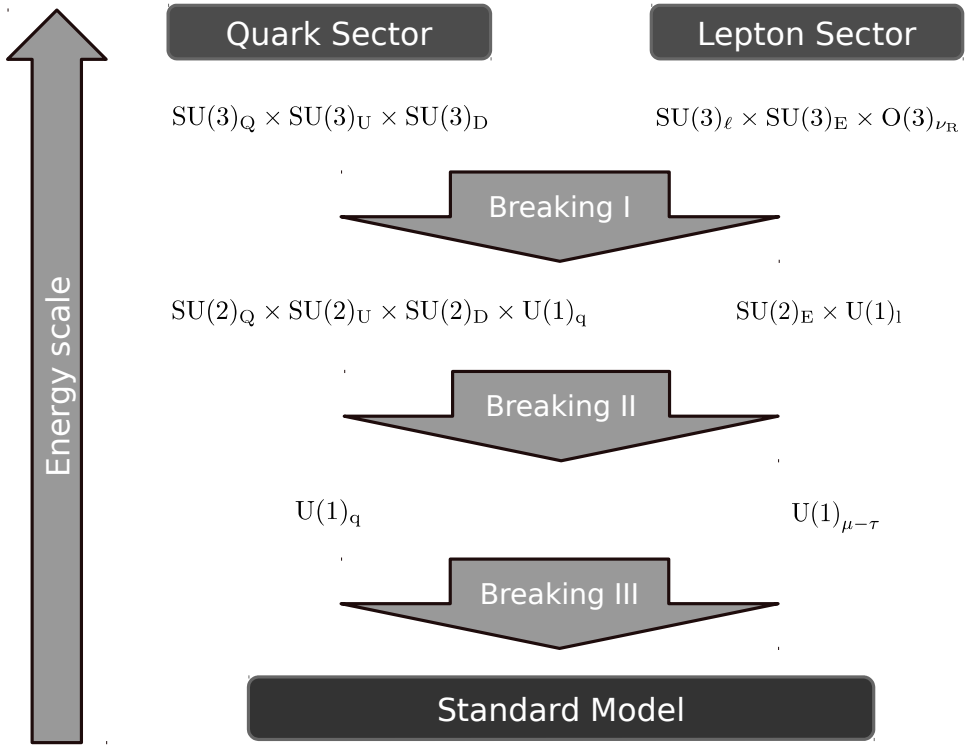

Figure 7.3: *Illustration of the symmetry breaking pattern in the quark and lepton sectors.*

angle, $\theta_{23} = \pi/4$, $\theta_{13} = 0$ and one maximal Majorana phase [107]. Adding small perturbations to this picture, quantitatively reconciles well with observations.

In such framework, in order to avoid massless Goldstone bosons, it is natural to expect that the flavor symmetry is gauged (see e.g. [108–110]). The complete spectrum of the corresponding massive vector bosons is quite complicated and may span several orders of magnitude. However, a large fraction of such states may be irrelevant at low energies. In this section we focus on the phenomenology of the potentially lightest vector states, associated to some of the residual unbroken subgroups. In particular, this setup naturally leads to a gauged $L_\mu - L_\tau$ symmetry [15–18,111–115] in the lepton sector [107] and an independent Abelian symmetry in the quark sector, $U(1)_q$, that may have interesting implications for the observed deviations from the SM in $b \to s\mu^+\mu^-$. Interestingly, gauging a linear combination of the two U(1)'s was already proposed in Ref. [20] as a solution of the LHCb anomalies. While this was purely phenomenologically motivated, here we suggest that such symmetries might be connected with the observed pattern of fermion masses and mixings. In contrast to Ref. [20], the presence of two neutral gauge bosons make the collider signatures of this model quite different, allowing for lighter gauge bosons.

7.2.1 Natural minima perturbations and lowest-lying Z' bosons

Building on Ref. [107], we consider the extension of the SM gauge sector by the maximal flavor symmetry in the limit of vanishing Yukawa couplings and non-vanishing Majorana mass term for the right-handed neutrinos: $\mathcal{G} = \mathrm{SU}(3)_Q \times \mathrm{SU}(3)_D \times \mathrm{SU}(3)_U \times \mathrm{SU}(3)_\ell \times \mathrm{SU}(3)_E \times \mathrm{O}(3)_{\nu_R}$. Here, Q (ℓ) corresponds to the left-handed quarks (leptons) while U (D) and E stand for the right-handed up (down) quarks and charged leptons, respectively. Neutrino masses are accounted for via the see-saw mechanism by introducing three right-handed neutrinos. Natural extrema of a generic Yukawa scalar potential break the flavor symmetry to a maximal subgroup, providing a good first-order explanation of the fermion masses and mixings, both in quark and lepton sectors [107]. In a second step, perturbations are introduced (e.g. via extra scalar fields [116, 117]), breaking the residual flavor symmetry and fitting the observed masses and mixing angles. Below we present a detailed discussion of the sequential breaking patterns for both sectors, identifying the appearance of the two residual U(1) symmetries. Finally, the spectrum and the couplings of the corresponding Z' bosons are discussed. The global picture is illustrated in Figure 7.3.

Quark sector

Step I: Following the approach in Ref. [107], we choose the hierarchical natural minima of the flavon fields in such a way that the following form for the Yukawa couplings is generated:

$$Y_u^{(0)} = \mathrm{diag}\,(0, 0, y_t)\ , \qquad Y_d^{(0)} = \mathrm{diag}\,(0, 0, y_b)\ , \tag{7.36}$$

leading to a diagonal CKM matrix and resulting in the following flavor symmetry breaking pattern

$$\mathrm{SU}(3)_Q \times \mathrm{SU}(3)_U \times \mathrm{SU}(3)_D \to \mathrm{SU}(2)_Q \times \mathrm{SU}(2)_U \times \mathrm{SU}(2)_D \times \mathrm{U}(1)_q\,. \tag{7.37}$$

This solution provides a good starting point for the explanation of fermion masses and mixings. Here $\mathrm{U}(1)_q$ is defined by the subgroup of the flavor symmetry given by

$$\mathrm{U}(1)_q :\ \exp(i\alpha\lambda_8^Q) \times \exp(i\alpha\lambda_8^U) \times \exp(i\alpha\lambda_8^D)\,, \tag{7.38}$$

with λ_8^I denoting the Gell-Mann matrix, which corresponds to the following charge assignments in generation space

$$X_Q = X_U = X_D = \left(-\frac{1}{2}, -\frac{1}{2}, 1\right)\ . \tag{7.39}$$

Step II: Perturbations around this minima are needed to provide the correct description of the observed masses and mixing angles. However, since the natural minima are very stable, it is not possible to induce these perturbations through one-loop corrections and (or) higher dimensional operators including Yukawa fields only [118]. In Ref. [116–118] it was shown that the correct perturbations can be

introduced in a natural way through the inclusion of additional scalars in reducible representations of the flavor group. In this section, we focus on the perturbations yielding the following flavor symmetry breaking pattern

$$\mathrm{SU}(2)_Q \times \mathrm{SU}(2)_U \times \mathrm{SU}(2)_D \times \mathrm{U}(1)_q \to \mathrm{U}(1)_q \,, \tag{7.40}$$

at a very high scale, followed by a subsequent breaking of $\mathrm{U}(1)_q$ around the TeV scale (**Step III**).

Finally, the perturbations to Eq. (7.36) take the form

$$Y^{(1)}_{u(d)} = \begin{pmatrix} \epsilon^{11}_{u(d)} & \epsilon^{12}_{u(d)} & \delta^1_{u(d)} \\ \epsilon^{21}_{u(d)} & \epsilon^{22}_{u(d)} & \delta^2_{u(d)} \\ \sigma^1_{u(d)} & \sigma^2_{u(d)} & 0 \end{pmatrix} \,, \tag{7.41}$$

and the full Yukawa matrix is given by $Y_{u(d)} = Y^{(0)}_{u(d)} + Y^{(1)}_{u(d)}$. The correct masses and mixings are obtained for

$$|\epsilon^{ij}_{u(d)}| \ll |\delta^i_{u(d)}| \ll 1 \,. \tag{7.42}$$

For simplicity, we assume negligible $\sigma^i_{u(d)}$: these terms are not required for fitting the CKM matrix and their absence/smallness is welcome to suppress right-handed FCNCs. In a given model, $\epsilon_{u(d)}$ and $\delta_{u(d)}$ are functions of the vevs of the corresponding extra flavon fields that induce step-II (and III) breaking, and other physical scales involved (see Section 7.2.2 for a specific realization).

Lepton sector

Step I: For leptons, the presence of a Majorana mass term for neutrinos yields a different structure for the natural extrema of the flavon fields [107]

$$Y^{(0)}_e = \mathrm{diag}\,(0,0,y_\tau) \,, \quad Y^{(0)}_\nu = \begin{pmatrix} iy_1 & 0 & 0 \\ 0 & \frac{i}{\sqrt{2}}y_2 & \frac{1}{\sqrt{2}}y_2 \\ 0 & \frac{i}{\sqrt{2}}y_3 & -\frac{1}{\sqrt{2}}y_3 \end{pmatrix} \,, \tag{7.43}$$

that break the flavor group to the maximal subgroup

$$\mathrm{SU}(3)_\ell \times \mathrm{SU}(3)_E \times \mathrm{O}(3)_{\nu_R} \to \mathrm{SU}(2)_E \times \mathrm{U}(1)_l \,, \tag{7.44}$$

where the $\mathrm{U}(1)_l$ subgroup is defined as

$$\mathrm{U}(1)_l : \ \exp(i\alpha\lambda'^{\ell}_3) \times \exp(i\frac{\sqrt{3}}{2}\alpha\lambda^E_8) \times \exp(i\alpha\lambda^{\nu_R}_7) \,, \tag{7.45}$$

with $\lambda'_3 = \mathrm{diag}(0,1,-1)$. Again, the induced Yukawa pattern provides a good starting point for the description of the lepton masses and mixing angles.

Step II: Perturbations will in turn induce additional breaking of the flavor group. Here we assume that the charged lepton Yukawas are generated at very high energies, i.e.

$$Y^{(1)}_e = \mathrm{diag}\,(y_e, y_\mu, 0) \,, \tag{7.46}$$

with $|y_e| \ll |y_\mu| \ll |y_\tau|$, implying the following breaking pattern

$$\mathrm{SU}(2)_E \times \mathrm{U}(1)_l \to \mathrm{U}(1)_{\mu-\tau}\,. \tag{7.47}$$

Note that this symmetry breaking pattern requires the perturbations in the charged-lepton Yukawa to be flavor diagonal, as shown in Eq. (7.46), therefore predicting no charged lepton flavor violation.

Step III: Finally, the $\mathrm{U}(1)_{\mu-\tau}$ symmetry given by

$$\mathrm{U}(1)_{\mu-\tau}:\ \exp(i\alpha\lambda_3'^{\ell}) \times \exp(i\alpha\lambda_3'^{E}) \times \exp(i\alpha\lambda_7^{\nu_R})\,, \tag{7.48}$$

gets broken around the TeV scale by perturbations of the neutrino Yukawa. As shown in Ref. [107], these small perturbations allow to fully accommodate for the PMNS matrix.

Couplings of the lightest Z' bosons

The breaking pattern illustrated above leads to two massive neutral gauge boson with masses around the TeV scale associated to the $\mathrm{U}(1)_q \times \mathrm{U}(1)_{\mu-\tau}$ flavor symmetry while the other flavor gauge bosons are much heavier.

Quarkphilic $\hat{Z}_q$: The fermion current associated to the $\hat{Z}_q$ field in the gauge basis ($\mathcal{L} \supset g_q \hat{Z}_{q\,\mu} \hat{J}^\mu_{Z_q}$) is

$$\begin{aligned}\hat{J}^\mu_{Z_q} = &-\frac{1}{2}\,\overline{q^0_{kL}}\gamma_\mu q^0_{kL} - \frac{1}{2}\,\overline{u^0_{kR}}\gamma_\mu u^0_{kR} - \frac{1}{2}\,\overline{d^0_{kR}}\gamma_\mu d^0_{kR} \\ &+ \overline{q^0_{3L}}\gamma_\mu q^0_{3L} + \overline{t^0_R}\gamma_\mu t^0_R + \overline{b^0_R}\gamma_\mu b^0_R\,,\end{aligned} \tag{7.49}$$

where $k = 1, 2$. In order to diagonalize $Y_{u(d)}$ after the perturbation in Eq. (7.41), we introduce the unitary matrices $U^{L,R}_{u(d)}$, such that $M_{u(d)} \propto U^{L\dagger}_{u(d)} Y_{u(d)} U^R_{u(d)}$. To the leading order in $\delta^i_{u(d)}$ expansion we find

$$U^L_{u(d)} \simeq \begin{pmatrix} 1 & 0 & \frac{\delta^1_{u(d)}}{y_{t(b)}} \\ 0 & 1 & \frac{\delta^2_{u(d)}}{y_{t(b)}} \\ -\frac{\delta^1_{u(d)}}{y_{t(b)}} & -\frac{\delta^2_{u(d)}}{y_{t(b)}} & 1 \end{pmatrix} \mathcal{R}(\theta^{u(d)}_{12}), \quad U^R_{u(d)} \simeq \mathbb{1}\,, \tag{7.50}$$

where $\theta^{u(d)}_{12}$ is an arbitrary $1-2$ rotation angle, determined beyond the leading order. Note that the CKM mixing matrix, $V_{\mathrm{CKM}} = U^{L\dagger}_u U^L_d$, can already be adjusted at this order with the appropriate choice of parameters. Finally, in the mass basis we get

$$\begin{aligned}\hat{J}^\mu_{Z_q} = &-\frac{1}{2}\,\overline{u_k}\gamma_\mu u_k - \frac{1}{2}\,\overline{d_k}\gamma_\mu d_k + \bar{t}\gamma_\mu t + \bar{b}\gamma_\mu b \\ &+ \left(\Gamma^{u_L}_{ij}\,\overline{u_{iL}}\gamma_\mu u_{jL} + \Gamma^{d_L}_{ij}\,\overline{d_{iL}}\gamma_\mu d_{jL} + \mathrm{h.c.}\right)\,,\end{aligned} \tag{7.51}$$

with $i, j = 1, 2, 3$ and the coupling matrices defined as

$$\Gamma^{u_L(d_L)}_{ij} = \frac{3}{2}\left[\left(U^L_{u(d)}\right)^*_{3i}\left(U^L_{u(d)}\right)_{3j} - \delta_{3i}\delta_{3j}\right]\,. \tag{7.52}$$

Note that the flavor universality of the gauge interactions with respect to the first two generations guarantees a suppression of the FCNCs among them, which are generated only at $\mathcal{O}(\delta^2)$. An interesting scenario is given by the limit $U_u^L \to \mathbb{1}$, where the coupling matrices read

$$\Gamma^{u_L} = 0\,, \quad \Gamma^{d_L} = \frac{3}{2}\begin{pmatrix} |V_{td}|^2 & V_{ts}V_{td}^* & V_{tb}V_{td}^* \\ V_{ts}^*V_{td} & |V_{ts}|^2 & V_{tb}V_{ts}^* \\ V_{tb}^*V_{td} & V_{tb}^*V_{ts} & |V_{tb}|^2 - 1 \end{pmatrix}. \tag{7.53}$$

This limit, characterized by having no FCNCs in the up-quark sector, is realized in the explicit model in Section 7.2.2. In what follows, we will not consider the scenarios with FCNCs in the up-quark sector, given their strong model dependency.

Leptophilic $\hat{Z}_\ell$: Since we assume that the charged lepton Yukawa matrix is generated at a high scale where $\mathrm{U}(1)_{\mu-\tau}$ is unbroken, the $\hat{Z}_\ell$ charged lepton current in the mass basis is given by ($\mathcal{L} \supset g_\ell \hat{Z}_{\ell\,\mu} \hat{J}^\mu_{Z_\ell}$),

$$\hat{J}^\mu_{Z_\ell} = -\overline{\tau}\gamma_\mu\tau + \overline{\mu}\gamma_\mu\mu\,. \tag{7.54}$$

Gauge-boson mixing: At the scale where the two U(1)'s are broken, the most general quadratic Lagrangian in the unitary gauge reads [13]

$$\begin{aligned}\mathcal{L} \subset & -\frac{1}{4}\hat{Z}_{q\,\mu\nu}\hat{Z}_q^{\mu\nu} - \frac{1}{4}\hat{Z}_{\ell\,\mu\nu}\hat{Z}_\ell^{\mu\nu} - \frac{\sin\chi}{2}\hat{Z}_{q\,\mu\nu}\hat{Z}_\ell^{\mu\nu} \\ & + \frac{1}{2}\hat{M}^2_{Z_q}\hat{Z}_{q\,\mu}\hat{Z}_q^\mu + \frac{1}{2}\hat{M}^2_{Z_\ell}\hat{Z}_{\ell\,\mu}\hat{Z}_\ell^\mu + \delta\hat{M}^2\hat{Z}_{q\,\mu}\hat{Z}_\ell^\mu\,,\end{aligned} \tag{7.55}$$

where χ and $\delta\hat{M}$ parametrize the kinetic and mass gauge mixing, respectively. The kinetic and mass mixing terms can be removed by means of a non-unitary and an orthogonal rotation, respectively (see Refs. [21,22] for more details). These are given by

$$\begin{pmatrix}\hat{Z}_\ell \\ \hat{Z}_q\end{pmatrix} = \begin{pmatrix}1 & -t_\chi \\ 0 & 1/c_\chi\end{pmatrix}\begin{pmatrix}c_\xi & -s_\xi \\ s_\xi & c_\xi\end{pmatrix}\begin{pmatrix}Z_1 \\ Z_2\end{pmatrix}, \tag{7.56}$$

where we used the following abbreviations: $c_\xi \equiv \cos\xi$, $s_\xi \equiv \sin\xi$, and $t_\xi \equiv \tan\xi$, and similarly for χ. The induced mass-mixing angle is defined as

$$t_{2\xi} = \frac{-2c_\chi\left(\delta\hat{M}^2 - s_\chi\hat{M}^2_{Z_\ell}\right)}{\hat{M}^2_{Z_q} - c_{2\chi}\hat{M}^2_{Z_\ell} - 2\,s_\chi\delta\hat{M}^2}\,. \tag{7.57}$$

The gauge boson eigenstate masses are

$$M^2_{Z_{1,2}} = \frac{\hat{M}^2_{Z_\ell} + \hat{M}^2_{Z_q} - 2\delta\hat{M}^2 s_\chi \pm \sqrt{\left(\hat{M}^2_{Z_\ell} - \hat{M}^2_{Z_q}\right)^2 + 4\Delta}}{2c_\chi^2}\,, \tag{7.58}$$

[13] For simplicity, and without loss of generality, we assume that the new gauge bosons decouple from the SM gauge sector and there is no relevant kinetic or mass mixing with the SM gauge fields. For the mass mixing, this is expected if the Higgs is not charged under the flavor group and the scalar flavons are SM singlets. The kinectic mixing is also expected to be small given that the flavored U(1) symmetries result from the breaking of a non-abelian group.

	$\mathrm{SU}(2)_Q$	$\mathrm{SU}(2)_U$	$\mathrm{SU}(2)_D$	$\mathrm{U}(1)_q$	$\mathrm{SU}(3)_c$	$\mathrm{SU}(2)_\mathrm{L}$	$\mathrm{U}(1)_\mathrm{Y}$
q_{jL}	**2**	**1**	**1**	$-1/2$	**3**	**2**	$1/6$
u_{jR}	**1**	**2**	**1**	$-1/2$	**3**	**1**	$2/3$
d_{jR}	**1**	**1**	**2**	$-1/2$	**3**	**1**	$-1/3$
q_{3L}	**1**	**1**	**1**	1	**3**	**2**	$1/6$
t_R	**1**	**1**	**1**	1	**3**	**1**	$2/3$
b_R	**1**	**1**	**1**	1	**3**	**1**	$-1/3$
$\mathcal{U}_{jL}$	**1**	**2**	**1**	$-1/2$	**3**	**1**	$2/3$
$\mathcal{D}_{jL}$	**1**	**1**	**2**	$-1/2$	**3**	**1**	$-1/3$
$\mathcal{U}_{jR}$	**2**	**1**	**1**	$-1/2$	**3**	**1**	$2/3$
$\mathcal{D}_{jR}$	**2**	**1**	**1**	$-1/2$	**3**	**1**	$-1/3$
H	**1**	**1**	**1**	0	**1**	**2**	$1/2$
ϕ_u	$\bar{\mathbf{2}}$	**2**	**1**	0	**1**	**1**	0
ϕ_d	$\bar{\mathbf{2}}$	**1**	**2**	0	**1**	**1**	0
ϕ_mix	**1**	**1**	**2**	$-3/2$	**1**	**1**	0

Table 7.4: *Particle content of the quark sector. Particles added to the SM are shown in a gray background.*

where

$$\Delta = \hat{M}^2_{Z_\ell}\hat{M}^2_{Z_q}s^2_\chi + \delta\hat{M}^4 - \left(\hat{M}^2_{Z_\ell} + \hat{M}^2_{Z_q}\right)\delta\hat{M}^2 s_\chi\,. \tag{7.59}$$

Finally, the interactions of the gauge bosons with fermions in the mass eigenstate basis are given by

$$\mathcal{L} \supset \left[(c_\xi - t_\chi s_\xi)\, g_\ell \hat{J}^\mu_{Z_\ell} + \frac{s_\xi}{c_\chi}\, g_q \hat{J}^\mu_{Z_q}\right] Z_{1\,\mu} + \left[\frac{c_\xi}{c_\chi}\, g_q \hat{J}^\mu_{Z_q} - (s_\xi + t_\chi c_\xi)\, g_\ell \hat{J}^\mu_{Z_\ell}\right] Z_{2\,\mu}\,. \tag{7.60}$$

7.2.2 Explicit model example

In this section we present an explicit realization of the framework presented in the previous section. We assume that the maximal flavor group in the absence of Yukawas, $\mathcal{G}$, is a local symmetry of nature that gets broken by the natural minima in Eqs. (7.36) and (7.43) at a very high scale leading to an unbroken $\mathrm{SU}(2)_Q \times \mathrm{SU}(2)_U \times \mathrm{SU}(2)_D \times \mathrm{SU}(2)_E \times \mathrm{U}(1)_q \times \mathrm{U}(1)_l$. For simplicity, we will ignore in this section the generation of neutrino masses, that is not directly relevant to our phenomenological analysis.

Following a similar approach to that in Refs. [108, 110], we introduce a minimal set of fermions to cancel the gauge anomalies, i.e. those of the flavor and SM groups and mixed anomalies among them, see Tables 7.4 and 7.5. The most general renormalizable Lagrangian compatible with the symmetries and particle content of the model reads

$$\begin{aligned}\mathcal{L} = \mathcal{L}_\mathrm{kin} - V(\phi_u, \phi_d, \phi_\mathrm{mix}, \phi_e, \phi_\nu, H) + (&y_t\, \overline{q_{3L}}\widetilde{H} t_R + y_b\, \overline{q_{3L}} H b_R + y_\tau\, \overline{\ell_{3L}} H \tau_R \\ &+ \lambda_u\, \overline{q_{iL}}\widetilde{H}\mathcal{U}_{iR} + \lambda'_u\, \overline{\mathcal{U}_{iL}}(\phi_u)_{ij}\mathcal{U}_{jR} + M_u\, \overline{\mathcal{U}_{iL}} u_{iR} + \lambda_d\, \overline{q_{iL}} H \mathcal{D}_{iR}\end{aligned}$$

$$+ \lambda'_d\, \overline{\mathcal{D}_{iL}}(\phi_d)_{ij}\, \mathcal{D}_{jR} + M_d\, \overline{\mathcal{D}_{iL}} d_{iR} + \lambda_{\rm mix}\, \overline{\mathcal{D}_{iL}}(\phi_{\rm mix})_i\, b_R + \lambda_{e1}\, \overline{\ell_{1L}} H \mathcal{E}_{1R}$$
$$+ \lambda_{e2}\, \overline{\ell_{2L}} H \mathcal{E}_{2R} + \lambda'_{e1}\, \overline{\mathcal{E}_{iL}}(\phi_e)_i\, \mathcal{E}_{1R} + \lambda'_{e2}\, \overline{\mathcal{E}_{iL}}(\widetilde{\phi}_e)_i\, \mathcal{E}_{2R} + M_e\, \overline{\mathcal{E}_{iL}} e_{iR} + h.c.)\,, \quad (7.61)$$

with $i, j = 1, 2$ and where $M_{u,d,e}$ and $\lambda^{(\prime)}_{u,d}$ are universal parameters for the first two generations, and $\widetilde{\phi}_e = i\sigma_2 \phi_e^*$ with σ_2 the Pauli matrix. We assume that the scalar flavons $\phi_{u,d,e}$ take a vev at a high scale with $\langle \phi_f \rangle \gg M_f$ $(f = u, d, e)$. This gives rise to the Yukawa couplings of the first and second generation SM fermions. Through a flavor transformation, we can make $\langle \phi_u \rangle$ diagonal and $\langle \phi_d \rangle \to \langle \phi_d \rangle\, V$, with V a 2×2 unitary matrix that, at leading order, corresponds to the Cabbibo matrix. After step II symmetry breaking, the Yukawa couplings are given by

$$Y_{u(d)} = \begin{pmatrix} y^{(2)}_{u(d)} & 0 \\ 0 & y_{t(b)} \end{pmatrix}\,, \quad Y_e = \begin{pmatrix} y^{(2)}_e & 0 \\ 0 & y_\tau \end{pmatrix}\,. \quad (7.62)$$

At leading order in the $M_f \langle \phi_f \rangle^{-1}$ expansion, the (light generation) Yukawa matrix elements read

$$y^{(2)}_u = \frac{\lambda_u M_u}{\lambda'_u} \langle \phi_u \rangle^{-1}\,, \quad y^{(2)}_d = \frac{\lambda_d M_d}{\lambda'_d} V^\dagger \langle \phi_d \rangle^{-1}\,, \quad (y^{(2)}_e)_{ii} = \frac{\lambda_{ei} M_e}{\lambda'_{ei} v_e}\,, \quad (7.63)$$

with $\langle \phi_e \rangle = (v_e\ 0)^\intercal$. On the other hand, the extra fermions acquire a mass proportional to the vevs of the flavon fields, which are assumed to be large, and they decouple at low energies. The vevs of the flavon fields break the flavor group down to $\mathrm{U}(1)_q \times \mathrm{U}(1)_{\mu-\tau}$. The unbroken $\mathrm{U}(1)_{\mu-\tau}$ symmetry ensures that the charged lepton Yukawa couplings are diagonal, and therefore there are no flavor violating couplings in the charged lepton sector.

Finally in the step III, the scalar flavons $\phi_{\rm mix}$ and ϕ_ν develop a vev around the TeV scale giving a heavy mass to the neutral gauge bosons associated to the U(1)'s ($\hat{M}_{Z_{q(\ell)}} \sim g_{q(\ell)} \langle \phi_{\rm mix(\nu)} \rangle$). Mixing among the third and the first two generations of quarks in the down-quark sector is generated,

$$Y_d \xrightarrow{\langle \phi_{\rm mix} \rangle} Y_d = \begin{pmatrix} y^{(2)}_d & y^{\rm mix}_d \\ 0 & y_b \end{pmatrix}\,, \quad (7.64)$$

where, at leading order in $\langle \phi_d \rangle^{-1} \langle \phi_{\rm mix} \rangle$,

$$y^{\rm mix}_d = y^{(2)}_d\, \frac{\lambda_{\rm mix} \langle \phi_{\rm mix} \rangle}{M_d}\,. \quad (7.65)$$

Note that in this model $V_{ub} \simeq (y^{\rm mix}_d)_1 / y_b$ and $V_{cb} \simeq (y^{\rm mix}_d)_2 / y_b$, and therefore in order to accommodate the measured values of the CKM matrix elements the hierarchy $\lambda_{\rm mix} \langle \phi_{\rm mix} \rangle \gtrsim M_d$ has to be enforced.

Finally, as we will discuss in Section 7.2.3 (see Eq. (7.76)), a relatively large amount of mass mixing between the gauge bosons associated to the flavored U(1)'s is needed in order to accommodate the $b \to s\ell^+\ell^-$ anomalies. In the minimal framework presented in this section, the only connection between the two sectors is given by the portal interaction $(\phi^\dagger_{\rm mix} \phi_{\rm mix})(\phi^\dagger_\nu \phi_\nu)$. This interaction is however unable to induce the required mixing at sufficient level, which in the minimal model is

	$\mathrm{SU}(2)_E$	$\mathrm{U}(1)_l$	$\mathrm{SU}(3)_c$	$\mathrm{SU}(2)_\mathrm{L}$	$\mathrm{U}(1)_\mathrm{Y}$
ℓ_{jL}	**1**	δ_{j2}	**1**	**2**	$-1/2$
e_{jR}	**2**	$1/2$	**1**	**1**	-1
ℓ_{3L}	**1**	-1	**1**	**2**	$-1/2$
τ_R	**1**	-1	**1**	**1**	-1
$\mathcal{E}_{jL}$	**2**	$1/2$	**1**	**1**	-1
$\mathcal{E}_{jR}$	**1**	δ_{j2}	**1**	**1**	-1
H	**1**	0	**1**	**2**	$1/2$
ϕ_e	**2**	$1/2$	**1**	**1**	0
ϕ_ν	**1**	-1	**1**	**1**	0

Table 7.5: *Particle content of the lepton sector. Particles added to the SM are shown in a gray background.*

absent even at the one-loop order. Therefore, the minimal model presented here has to be extended. The necessary amount of mixing can be easily accounted for by the inclusion of additional particles, either fermions or scalars, charged under both $\mathrm{U}(1)_q$ and $\mathrm{U}(1)_{\mu-\tau}$, and with a mass around the TeV scale. For the purpose of this study it is not necessary to provide a precise realization of such extensions but we rather consider the gauge boson mixing as a free parameter.

7.2.3 Phenomenological implications

Rare transitions: $b \to s\mu^+\mu^-$

We start with the effective Hamiltonian for $b \to s\mu^+\mu^-$ transitions introduced in Section 4.2.2. In our model only a contribution to the operator O_9^μ is generated. For our numerical analysis we rely on the results of the fit for the Wilson coefficients reported in Ref. [119] (see also Ref. [99]), where the best fit is $C_9^{\mathrm{NP}\mu} = -1.09 \pm 0.22$ at the 1σ level. In our case, we have

$$C_9^{\mathrm{NP}\mu} = \frac{g_q g_\ell \Gamma^*_{bs}}{V_{tb}V^*_{ts}} \frac{c_\xi s_\xi}{c_\chi} \left[\frac{1 - t_\xi t_\chi}{M^2_{Z_1}} - \frac{1 + t_\chi/t_\xi}{M^2_{Z_2}} \right] \Lambda_\nu^2 \,, \tag{7.66}$$

where $\Lambda_v = \sqrt{\sqrt{2}\pi/(G_F \alpha_{em})} = 7$ TeV.

Naive effective field theory power counting suggests that the contribution due to pure kinetic mixing is expected to be additionally suppressed by a factor $\sim m_b^2/M^2_{Z_{1,2}}$. This is due to the presence of derivatives from the field-strength tensors. Indeed, we explicitly checked that $C_9^{\mathrm{NP}\mu}$ in Eq. (7.66) vanishes in the limit $\delta\hat{M}^2, m_b \to 0$. Therefore, from now on, we set χ to zero and allow for non-zero mass mixing $\delta\hat{M}^2 = \hat{M}_{Z_q}\hat{M}_{Z_\ell}\epsilon$, where the parameter ϵ is expected to be small. Expanding in ϵ, we find

$$C_9^{\mathrm{NP}\mu} = -\frac{\Gamma^*_{bs}}{V_{tb}V^*_{ts}} \left(\frac{g_q \Lambda_v}{M_{Z_2}} \right) \left(\frac{g_\ell \Lambda_v}{M_{Z_1}} \right) \epsilon + \mathcal{O}(\epsilon^2) \,. \tag{7.67}$$

$\Delta F = 2$ processes

Flavor violating Z' couplings to b and s unavoidably induce tree level contribution to $B_s - \bar{B}_s$ mixing. In our model

$$\Delta R_{B_s} = |g_q \Gamma_{bs}|^2 \left(\frac{s_\xi^2}{M_{Z_1}^2} + \frac{c_\xi^2}{M_{Z_2}^2} \right) \left(\frac{g^2 (V_{tb} V_{ts}^*)^2}{16\pi^2 v^2} S_0 \right)^{-1} , \tag{7.68}$$

where the SM loop factor is given by $S_0 = 2.322 \pm 0.018$ [120]. Expanding in ϵ, we find

$$\Delta R_{B_s} = \left| \frac{\Gamma_{bs}}{V_{tb} V_{ts}^*} \right|^2 \left(\frac{g_q \Lambda_v}{M_{Z_2}} \right)^2 \left(\frac{2 s_W^2}{S_0} \right) + \mathcal{O}(\epsilon^2) , \tag{7.69}$$

where s_W is the sine of Weinberg angle. Requiring NP contributions to the mixing amplitude to be at most $\mathcal{O}(10\%)$, we find the following condition

$$\left| \frac{\Gamma_{bs}}{V_{tb} V_{ts}^*} \frac{g_q \Lambda_v}{M_{Z_2}} \right| \lesssim 0.7 . \tag{7.70}$$

In the numerical fit we take NP contributions to the mixing amplitude to be $\Delta R_{B_s} = -0.10 \pm 0.07$ (see discussion in Ref. [121]).

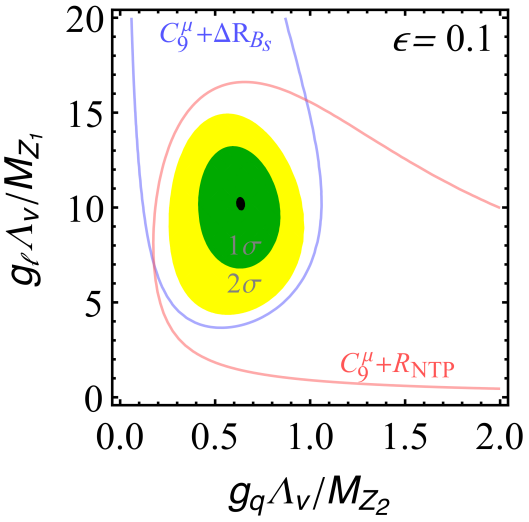

Figure 7.4: *Combined fit to B_s mixing, neutrino trident production and $b \to s\mu^+\mu^-$ observables assuming $\epsilon = 0.1$ (green - 1σ, yellow - 2σ). Relaxing the first (second) constraint is illustrated with red (blue).*

It is worth noting that the contribution to $\Delta F = 2$ processes have necessarily constructive interference and are MFV-like (i.e. a similar relative correction compared to the SM is also expected in $B_d - \overline{B}_d$ and kaon mixing). This conclusion would not hold if the σ_d^i terms in Eq. (7.41) were not negligible. Tuning the σ_d^i one can generate arbitrary contributions to $\Delta F = 2$ amplitudes and relax the bound in Eq. (7.70). However, since this tuning does not find a natural explanation within our framework, we will not consider this possibility any further. Flavon fields also give tree-level MFV-like contributions to $\Delta F = 2$ transitions. However, since they are SM singlets, their contributions to these processes receive an extra suppression of $\mathcal{O}\left(m_b^2/\langle\phi_{\rm mix}\rangle^2\right)$, and can be neglected. We checked this explicitly in the model example and also verified that flavon-Higgs box contributions can be neglected since they are not parametrically enhanced by large masses compared to the Z' contribution.

Neutrino Trident Production

Bounds on flavor-diagonal Z' couplings to muons can also arise from NTP, where a muon pair is created by scattering a muon-neutrino with a nucleon: $\nu_\mu N \to \nu N \mu^+ \mu^-$ [39]. Note that as the flavor of the neutrino in the final state is not detected, one must sum over all three generations in the case of flavor-violating interactions. We obtain for the cross section of NTP

$$\frac{\sigma_{\rm NP}}{\sigma_{\rm SM}} = \frac{1 + \left(1 + 4s_W^2 + 2v^2 V^{\rm NP}\right)^2}{1 + \left(1 + 4s_W^2\right)^2}\,, \tag{7.71}$$

with

$$V^{\rm NP} = g_\ell^2 \left[\left(\frac{c_\xi}{M_{Z_1}} \right)^2 + \left(\frac{s_\xi}{M_{Z_2}} \right)^2 \right] , \tag{7.72}$$

while expanding in ϵ

$$V^{\rm NP} = \frac{g_\ell^2}{M_{Z_1}^2} + \mathcal{O}(\epsilon^2) \,. \tag{7.73}$$

The bound from the CCFR collaboration [42] is given by

$$R_{\rm NTP} \equiv \sigma_{\rm exp}/\sigma_{\rm SM} = 0.82 \pm 0.28\,. \tag{7.74}$$

Requiring this constraint to be satisfied at the 2σ level implies

$$\left| \frac{g_\ell \Lambda_v}{M_{Z_1}} \right| \lesssim 12 \,. \tag{7.75}$$

Combined fit to low-energy data

Using the limits in Eq. (7.70) and Eq. (7.75), and plugging in Eq. (7.67), we find that the NP contribution to C_9^μ can be

$$C_9^{{\rm NP}\mu} \simeq -\,8 \times \epsilon \,. \tag{7.76}$$

We then conclude that $\epsilon \sim \mathcal{O}(0.1)$ is required to reconcile low-energy constraints with the correct size of C_9^μ. To make this point more precise, we perform a combined fit to the set of measurements discussed above. The total likelihood as a function of three parameters: $g_q \Lambda_v / M_{Z_2}$, $g_\ell \Lambda_v / M_{Z_1}$ and ϵ, is constructed by adding the corresponding χ^2 terms from the three measurements: $C_9^{{\rm NP}\mu}$, ΔR_{B_s} and $R_{\rm NTP}$. The preferred region for $g_q \Lambda_v / M_{Z_2}$ and $g_\ell \Lambda_v / M_{Z_1}$ at 1σ (green) and 2σ (yellow), setting $\epsilon = 0.1$, is shown in Figure 7.4. In the numerical analysis, we set $\Gamma_{bs} = V_{tb} V_{ts}^*$ as suggested by Eq. (7.52). Possible $\mathcal{O}(1)$ modifications of this parameter shift accordingly the preferred value of $g_q \Lambda_v / M_{Z_2}$.

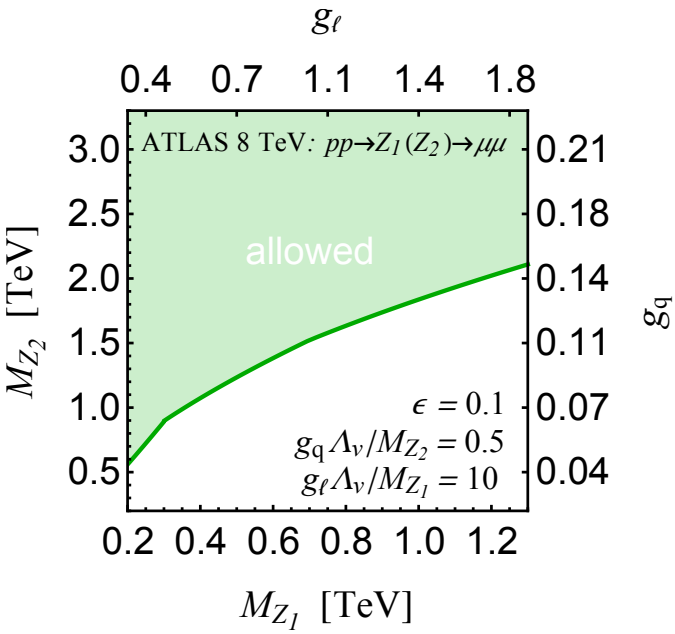

Figure 7.5: *Allowed region in the (M_{Z_1}, M_{Z_2}) plane from direct searches for dimuon resonances in $pp \to Z_1(Z_2) \to \mu^+\mu^-$ at LHC [58]. Here we fix $\epsilon = 0.1$, $g_q\Lambda_v/M_{Z_2} = 0.5$, and $g_\ell\Lambda_v/M_{Z_1} = 10$ in agreement with the preferred region from the low-energy fit. The mixing angle ξ is small for these points, at most ~ 0.1.*

Direct searches at LHC

In this section, we discuss the LHC phenomenology of the two Z' bosons. In the limit of zero mass and kinetic mixing and assuming that right-handed neutrinos are heavy, $Z_1 \simeq \hat{Z}_\ell$ (see Eq. (7.56)) decays predominantly to $\tau^+\tau^-$, $\mu^+\mu^-$ and $\bar{\nu}\nu$ with the partial decay widths

$$\Gamma(\hat{Z}_\ell \to \mu\mu) = \Gamma(\hat{Z}_\ell \to \tau\tau) = \Gamma(\hat{Z}_\ell \to \bar{\nu}\nu) = \frac{g_\ell^2}{12\pi} M_{\hat{Z}_\ell} \,, \tag{7.77}$$

while $Z_2 \simeq \hat{Z}_q$ decays to $\bar{t}t$, $\bar{b}b$ and light jets with the partial widths

$$\Gamma(\hat{Z}_q \to b\bar{b}) = \Gamma(\hat{Z}_\ell \to jj) = \frac{g_q^2}{4\pi} M_{\hat{Z}_q} \,, \tag{7.78}$$

where $jj = u\bar{u} + d\bar{d} + s\bar{s} + c\bar{c}$ and

$$\Gamma(\hat{Z}_q \to t\bar{t}) = \Gamma(\hat{Z}_q \to b\bar{b}) \left(1 + \frac{2m_t^2}{M_{\hat{Z}_q}^2}\right) \sqrt{1 - \frac{4m_t^2}{M_{\hat{Z}_q}^2}} \,, \tag{7.79}$$

in agreement with the general decay formula in Eq. (B9) of Ref. [122]. In the zero mixing limit, only $\hat{Z}_q$ is produced at the LHC. The total hadronic cross section in the narrow width approximation is given by

$$\sigma(q\bar{q} \to \hat{Z}_q) = \frac{8\pi^2}{3 M_{\hat{Z}_q} s_0} \, \Gamma(\hat{Z}_q \to q\bar{q}) \, \mathcal{L}_{q\bar{q}} \,, \tag{7.80}$$

where $\mathcal{L}_{q\bar{q}}$ is the corresponding parton luminosity function. The dominant contribution is for $q = u, d$. We use NNLO MMHT2014 PDF [123] set for numerical studies. Furthermore, we cross-checked the results using MadGraph [124].

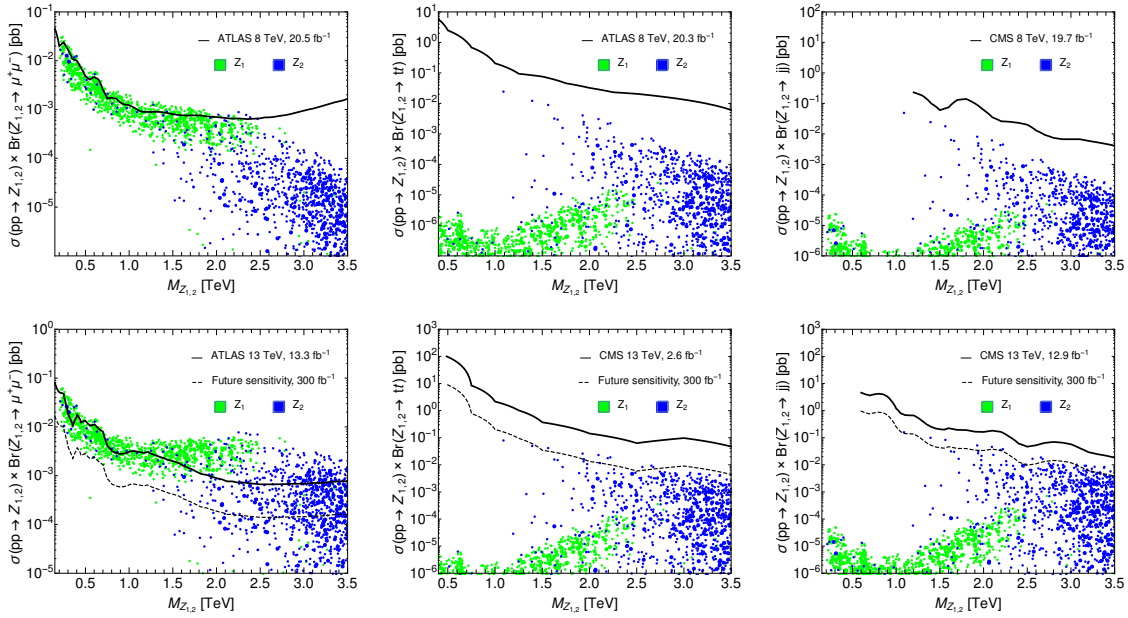

Figure 7.6: *Predictions for the LHC signals ($\sigma \times \mathcal{B}$) at 8 TeV (first row) and 13 TeV (second row) for $\mu^+\mu^-$, $t\bar{t}$ and jj resonance searches for Z_1 (green) and Z_2 (blue). Present limits are shown with black line, and future-projected with dashed line.*

ATLAS searched for a narrow Z' resonance in pp collisions at 8 TeV decaying to $\mu^+\mu^-$ [58]. The reported limits on $\sigma \times \mathcal{B}$ in the mass range $[150 - 3500]$ GeV can be used to set constraints on the parameter space of our model. Production and decay formulas are easily generalized in the case of arbitrary mass mixing ξ. We compute the signal strength for both Z' and confront with these limits.

Interestingly, we find that it is possible to have relatively light vectors ($\lesssim$ TeV) with $\mathcal{O}(1)$ couplings. In particular, fixing $\epsilon = 0.1$, $g_q \Lambda_v / M_{Z_2} = 0.5$, and $g_\ell \Lambda_v / M_{Z_1} = 10$, in agreement with the preferred region from the low-energy fit, we have performed a scan in the (M_{Z_1}, M_{Z_2}) plane. In Figure 7.5 we show in green the region allowed by present dimuon searches from Ref. [58]. The most plausible scenario is the one with a mass hierarchy between the vectors, $M_{Z_1} < M_{Z_2}$, and with small mass mixing. That is, the lighter vector Z_1 is predominantly $\hat{Z}_\ell$, while the heavier Z_2 is predominantly $\hat{Z}_q$. In conclusion, requiring small (perturbative) couplings ($g_\ell \sim 2$ implies $\Gamma_{Z_1}/M_{Z_1} \sim 0.3$), low-energy flavor data together with dimuon resonance searches require a relatively light leptophilic Z', that might be probed in the near future.

In order to check the robustness of the above statement, we have performed an exhaustive parameter scan of the model randomly varying five input parameters with flat priors: $\hat{M}_{Z_q}$ and $\hat{M}_{Z_\ell}$ in the range [150, 4000] GeV, ϵ and g_q in the range [0,1], and g_ℓ in the range [0,2]. We have constructed the combined likelihood function for the low-energy data, together with the dimuon search [58] for both Z's, in terms of the model parameters using the complete formulas (not expanded in small mixing). The best fit point gives $\chi^2_{\rm min} \approx 7$, while the SM point has $\chi^2_{\rm SM} \approx 27$. We have kept the points that provide a good fit to all data, namely $\Delta\chi^2 \equiv \chi^2 - \chi^2_{\rm min} \lesssim 6$.

Shown in Figure 7.6 are the corresponding predictions for $\sigma \times \mathcal{B}$ for $\mu^+\mu^-$, $t\bar{t}$ and jj resonance searches at LHC. In addition, we show the present limits from Refs. [61, 125–128], and estimate the future sensitivity with 300 fb^{-1}. Interestingly enough, the unpublished 13 TeV dimuon resonance search [61] is already probing the relevant region, with conclusive answers expected in the near-future data. On the other hand, we find the impact of the present (and future) $\bar{t}t$ and jj searches to be less relevant. We restricted our scan to the mass range of dimuon resonance searches reported by ATLAS and CMS (namely $M_{\mu\mu} \geq 150$ GeV) but it is interesting to note that a very light (almost leptophilic) Z_1 could evade the experimental bounds provided its gauge coupling is sufficiently small. In this case, $Z \to 4\mu$ provides a bound of $M_{Z_1} \gtrsim 30$ GeV [38, 39, 129], when the three-body decay $Z \to \mu^+\mu^- Z'(\to \mu^+\mu^-)$ is kinematically open. Finally, one can establish a rough estimate on the future mass reach at LHC using the ColliderReach tool for extrapolations [130]. We find that by Run 3, with 300 fb^{-1}, this value should rise to about 5 TeV.

7.2.4 Summary and conclusions

The assumption of dynamically generated Yukawa couplings provides a natural explanation to the observed pattern of fermion masses and mixing angles, both in the quark and lepton sectors [107]. In this framework the maximal $[\mathrm{SU}(3)]^5 \times \mathrm{O}(3)$ flavor group is assumed to be a local symmetry of nature, broken spontaneously (and in several steps) by flavon fields. In this section we have shown that in this context, under reasonable assumptions about the flavor symmetry breaking pattern, it is possible to obtain an explanation of the anomalies observed in $b \to s\mu^+\mu^-$ transitions. The main features of the proposed model can be summarized as follows.

- Two Z' bosons arise as the lowest-lying resonances resulting from the gauging of the flavor group, one corresponding to a gauged $\mathrm{U}(1)_q$ and the other one to a gauged $\mu - \tau$ flavor symmetry. A small but non-vanishing mass-mixing among the Z' bosons is required in order to accommodate the flavor anomalies.

- The flavor symmetry acting on the light quark families ensures a partial protection for quark FCNCs, which turn out to be sufficiently small to avoid the tight existing constraints while allowing for sizable effects in $b \to s\mu^+\mu^-$. The model predicts no FCNCs in the charged lepton sector.

- Concerning $b \to s\mu^+\mu^-$ transitions, our model predicts $C_9^\mu|_{\mathrm{NP}}$ only, and maximal $\mu - e$ universality violation. Therefore, no deviations from the SM predictions in $B_s \to \mu^+\mu^-$ are expected but sizable effects in angular observables measuring lepton flavor universality violation [131–133] should occur.

Present data already provides important restrictions on the parameter space of the model: for small gauge mixing, the bound from B_s mixing implies $g_q/M_{Z_2} \lesssim 0.1$ TeV^{-1} while the constraint from NTP gives the bound $g_\ell/M_{Z_1} \lesssim 1.7$ TeV^{-1}. Direct searches at LHC allow for a very light (almost leptophilic) Z' together with a heavier one (mostly quarkphilic) in the TeV domain. This full region of the parameter space will be explored in the near future by dimuon searches.

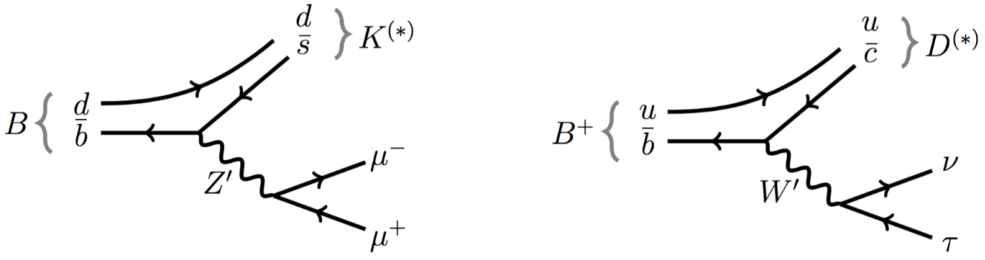

Figure 7.7: *New physics contributions to $B \to K^{(*)}\mu^+\mu^-$ and $B \to D^{(*)}\tau\nu$ from the tree-level exchange of massive vector bosons.*

7.3 Non-universal SU(2) × SU(2) × U(1) models

In this section, based on the publications in Refs. [134, 135], we explore the possibility of having an unified explanation of the $b \to c\ell\nu$ and $b \to s\ell^+\ell^-$ anomalies from the breaking of an SU(2) extended gauge group. In this framework, the new massive gauge vector bosons that arise from the breaking of this group mediate flavor transitions at tree-level as shown in Figure 7.7, providing a possible explanation to the deviations from the SM observed in B-meson decays.

The plan of this section is as follows: In Section 7.3.1 we discuss possible realizations of the SU(2) extended framework, and show that the conditions imposed by the anomalies restrict this extension to a particular model, that we present in more detail in Section 7.3.2. We derive the gauge boson and fermion masses and mixings, as well as the required textures in Section 7.3.3. A detailed description of the flavor and electroweak observables included in the global fit is given in Section 7.3.4. Our global fit main results and predictions are presented in Section 7.3.5 and Section 7.3.6, respectively. Finally, in Section 7.3.7 we provide our conclusions. Details of the model are provided in the Appendices 7.C and 7.D.

7.3.1 Gauge Extensions with Lepton Non-Universality

A common explanation of universality-violating hints in the decays $b \to c\tau\nu$ and $b \to s\ell^+\ell^-$ poses serious challenges for model building. This is mostly because the NP mediators responsible for such processes would have to act at tree level. Indeed, the semileptonic decays $B \to D^{(*)}\tau\nu$ are charged current processes which arise at tree level in the SM. Since the observed deviation from the SM prediction is quite sizable, $\mathcal{O}(25\%)$, this strongly suggests the presence of tree-level charged mediators. The same applies to the decays $B \to K^{(*)}\ell^+\ell^-$ even though they are due, in the SM, to neutral current processes arising at one-loop level. The large deviation from the SM, again $\mathcal{O}(25\%)$, would imply a very light mediator if the new interactions followed the SM pattern. Such a light mediator, $\mathcal{O}(M_Z)$, would be hard to hide from other flavor observables which are in perfect agreement with the SM as well as from direct searches for new states at high energy colliders such as the LHC.

We assume from now on that the anomalies R_K and $R(D^{(*)})$ are genuine and due to new gauge bosons entering at tree level. We are therefore looking for a

non-universal gauge extension of the SM which could explain both anomalies at the same time. We will be interested in scenarios where new physics effects in the lepton sector affect mainly the muon and tau leptons.

There are essentially two strategies to follow in constructing non-universal gauge extensions of the SM:

- **Non-Universality from gauge couplings (g-NU)**: via a non-universal embedding of SM fermions into a larger gauge group, or
- **Non-Universality from Yukawas (y-NU)**: through non-universal interactions between SM fermions and extra particles which are universally coupled to new vector bosons.

This means that, in general, non-universality is either controlled by Yukawa couplings or by gauge couplings. Of course, one can always mix these two approaches, however we keep them separated for the sake of clarity and to gain insights based on generic considerations.

For simplicity and definiteness, we will focus on implementations where the gauge extensions consist of SU(2) and U(1) factors only. The minimal possibilities are denoted generically as $G(221)$ models. In addition to the source of non-universality, $G(221)$ models can be classified according to the gauge symmetry-breaking pattern. We distinguish two broad categories:

- **L-Breaking Pattern (L-BP)**: For this breaking pattern the $\mathrm{U}(1)_\mathrm{Y}$ group appears from a non-trivial breaking of the extended group:

$$\mathrm{SU}(2)_\mathrm{L} \times \mathrm{SU}(2)_\mathrm{H} \times \mathrm{U}(1)_\mathrm{H} \to \mathrm{SU}(2)_\mathrm{L} \times \mathrm{U}(1)_\mathrm{Y} \,. \tag{7.81}$$

- **Y-Breaking Pattern (Y-BP)**:
  The $\mathrm{SU}(2)_\mathrm{L}$ factor is non-trivially embedded in the extended gauge group and arises from the breaking pattern:

$$\mathrm{SU}(2)_1 \times \mathrm{SU}(2)_2 \times \mathrm{U}(1)_\mathrm{Y} \to \mathrm{SU}(2)_\mathrm{L} \times \mathrm{U}(1)_\mathrm{Y} \,. \tag{7.82}$$

We now proceed to review the viability of the different possibilities that are available in our classification.

Non-Universality from gauge couplings

In this scenario, the extended gauge group should distinguish among the different SM fermion flavors. As aforementioned, in this case we have two possibilities:

- **Breaking chain L-BP**: A model within this scenario was already presented in Ref. [136] to explain the $R(D^{(*)})$ anomalies. However, just with the SM particle content one can only couple right-handed fermions to the extra gauge group, making it unable to accommodate R_K.

- **Breaking chain Y-BP**: This model has been studied in Refs. [137–139]. In this scenario it is only possible to reproduce the desired non-universal Z' and W' couplings to leptons if the gauge coupling hierarchy $g_2 \gg g_1 \sim g$ is enforced, with a single SM family coupling to $\mathrm{SU}(2)_2$. However the large g_2 limit has to face constraints from rapid proton decay and perturbativity. Instanton mediated processes will, in general, induce proton decay when a single SM family is coupled to a non-Abelian gauge group, setting a bound on the gauge coupling: $g_2\,(M^2_{Z'}) \lesssim 1.3 - 1.6$, depending on the parameters of the model [140, 141]. This bound can be circumvented by introducing extra fermions that couple to this gauge group, such as VL fermions. However, even in this case, perturbativity sets an upper bound on the gauge coupling of $g_2\,(M^2_{Z'}) < \sqrt{4\pi} \simeq 3.5$. Given these limits, it is not possible to reproduce the requested hierarchy on the lepton couplings, making this framework disfavored for the simultaneous explanation of R_K and $R(D^{(*)})$.

Non-Universality from Yukawa couplings

Here new VL fermions, charged universally under a new force to which the SM fermions are neutral, are Yukawa-coupled to the SM quarks and leptons. The effective coupling of the SM with the new bosons is achieved via mixings with the VL fermions and is hence controlled by the Yukawas, which can be in principle adjusted to get the desired flavor textures. In general these mixings will also modify the SM gauge and Higgs couplings. However one can charge the VL fermions under the gauge group in such a way that GIM protection is enforced at the scale of the first symmetry breaking, making these deviations sufficiently small to avoid experimental constraints. This translates in the two breaking patterns we are considering as follows:

- **Breaking chain L-BP**: In order to obtain an effective coupling $W'^{\pm}$ to left-handed quarks, it is necessary to add VL quarks which mix with the SM weak quark doublet. The electric charge formula of this breaking chain is:

$$Q = T_{3_L} + (T_{3_H} + H)\,, \tag{7.83}$$

  where T_{3_L} (T_{3_H}) and H are respectively the isospin under $\mathrm{SU}(2)_\mathrm{L}$ ($\mathrm{SU}(2)_\mathrm{H}$) and the $\mathrm{U}(1)_\mathrm{H}$ charge. Since the SM fields are neutral under the new $\mathrm{SU}(2)_\mathrm{H}$ interactions, $\mathrm{U}(1)_\mathrm{H}$ charges coincide with the standard hypercharges. In order for two new quarks, Q_b and Q_c, to couple to $W'^{\pm}$ they must belong to the same $\mathrm{SU}(2)_\mathrm{H}$ multiplet and their isospin must satisfy $|T_{3_H}(Q_b) - T_{3_H}(Q_c)| = 1$. On the other hand, to preserve the GIM mechanism in the presence of the new mixings the new quarks must have the same SM quantum numbers (T_{3_L} and $Y \equiv T_{3_H} + H$) as the SM quarks with which they mix [142]. These two requirements are in conflict with each other and so we conclude that models of type L-BP cannot account for a unified description of R_K and $R(D^{(*)})$.

- **Breaking chain Y-BP**: The product $\mathrm{SU}(2)_1 \times \mathrm{SU}(2)_2$ can be broken to the diagonal $\mathrm{SU}(2)_\mathrm{L}$ by a Higgs bidoublet. This specific type of breaking allows for both couplings to W' and GIM suppression. It is enough to charge

	L-BP	Y-BP
g-NU	✗ No left-handed currents	✗ perturbativity
y-NU	✗ No GIM	✓

Table 7.6: *Summary of model building possibilities for $G(221)$ models: source of flavor non-universality versus symmetry-breaking patterns. Blocks denote scenarios which are disfavored as an explanation of the B-decay anomalies while a star denotes a viable framework.*

SM fermions under one of the two SU(2) groups, say $\mathrm{SU}(2)_2$, and copy the exact same assignments for the VL fermions. This is the scenario we deem more promising for the simultaneous explanation of $b \to s\ell^+\ell^-$ and $b \to c\tau\nu$ anomalies.

Summary

In summary, restricted to minimal gauge extensions we have found four broad classes of models that lead to flavor non-universality and can potentially address the flavor anomalies. These classes depend on the breaking pattern (L-BP or Y-BP) and the source of flavor non-universality (g-NU or y-NU). Table 7.6 summarizes our main conclusion: the most promising candidates are gauge extensions where gauge couplings are universal and non-universality arises from Yukawa couplings of the SM fermions with a set of new VL fermions.

7.3.2 Description of the model

In this section we construct in full detail a minimal realization of the type y-NU/Y-BP models discussed in the previous section. We consider a theory with the electroweak gauge group promoted to $\mathrm{SU}(2)_1 \times \mathrm{SU}(2)_2 \times \mathrm{U}(1)_\mathrm{Y}$. The factor $\mathrm{U}(1)_\mathrm{Y}$ corresponds to the usual hypercharge while the SM $\mathrm{SU}(2)_\mathrm{L}$ is contained in the SU(2) product. The gauge bosons and gauge couplings of the extended electroweak group will be denoted as:

$$\begin{aligned} \mathrm{SU}(2)_1 : &\quad g_1, \quad W_i^1 , \\ \mathrm{SU}(2)_2 : &\quad g_2, \quad W_i^2 , \\ \mathrm{U}(1)_\mathrm{Y} : &\quad g', \quad B , \end{aligned} \tag{7.84}$$

where $i = 1, 2, 3$ is the SU(2) index. All of the SM left-handed fermions transform exclusively under the second SU(2) factor, i.e.

$$\begin{aligned} q_L &= (\mathbf{3}, \mathbf{1}, \mathbf{2})_{\frac{1}{6}} , \quad & \ell_L &= (\mathbf{1}, \mathbf{1}, \mathbf{2})_{-\frac{1}{2}} , \\ u_R &= (\mathbf{3}, \mathbf{1}, \mathbf{1})_{\frac{2}{3}} , \quad & e_R &= (\mathbf{1}, \mathbf{1}, \mathbf{1})_{-1} , \\ d_R &= (\mathbf{3}, \mathbf{1}, \mathbf{1})_{-\frac{1}{3}} , \end{aligned} \tag{7.85}$$

	generations	$\mathrm{SU}(3)_\mathrm{c}$	$\mathrm{SU}(2)_1$	$\mathrm{SU}(2)_2$	$\mathrm{U}(1)_\mathrm{Y}$
ϕ	1	**1**	**1**	**2**	1/2
Φ	1	**1**	**2**	$\bar{\mathbf{2}}$	0
ϕ'	1	**1**	**2**	**1**	1/2
q_L	3	**3**	**1**	**2**	1/6
u_R	3	**3**	**1**	**1**	2/3
d_R	3	**3**	**1**	**1**	−1/3
ℓ_L	3	**1**	**1**	**2**	−1/2
e_R	3	**1**	**1**	**1**	−1
$Q_{L,R}$	n_VL	**3**	**2**	**1**	1/6
$L_{L,R}$	n_VL	**1**	**2**	**1**	−1/2

Table 7.7: *Particle content of the model.*

where the representations refer to $\mathrm{SU}(3)_\mathrm{c}$, $\mathrm{SU}(2)_1$ and $\mathrm{SU}(2)_2$, respectively, while the subscript denotes the hypercharge. The SM doublets q_L and ℓ_L can be decomposed in $\mathrm{SU}(2)_2$ components in the usual way,

$$q_L = \begin{pmatrix} u \\ d \end{pmatrix}_L , \qquad \ell_L = \begin{pmatrix} \nu \\ e \end{pmatrix}_L . \tag{7.86}$$

In addition, we introduce n_VL generations of VL fermions transforming as

$$Q_{L,R} \equiv \begin{pmatrix} U \\ D \end{pmatrix}_{L,R} = (\mathbf{3},\mathbf{2},\mathbf{1})_{\frac{1}{6}} , \quad L_{L,R} \equiv \begin{pmatrix} N \\ E \end{pmatrix}_{L,R} = (\mathbf{1},\mathbf{2},\mathbf{1})_{-\frac{1}{2}} . \tag{7.87}$$

For the moment we take the number of generations n_VL as a free parameter to be constrained by phenomenological requirements. Symmetry breaking is achieved via the following set of scalars: a self-dual bidoublet Φ (i.e., $\Phi = \sigma^2 \Phi^* \sigma^2$, with σ^2 the usual Pauli matrix) and two doublets ϕ and ϕ',

$$\phi = (\mathbf{1},\mathbf{1},\mathbf{2})_{\frac{1}{2}} , \qquad \Phi = (\mathbf{1},\mathbf{2},\bar{\mathbf{2}})_0 , \qquad \phi' = (\mathbf{1},\mathbf{2},\mathbf{1})_{\frac{1}{2}} , \tag{7.88}$$

which we decompose as:

$$\phi = \begin{pmatrix} \varphi^+ \\ \varphi^0 \end{pmatrix} , \qquad \Phi = \frac{1}{\sqrt{2}} \begin{pmatrix} \Phi^0 & \Phi^+ \\ -\Phi^- & \bar{\Phi}^0 \end{pmatrix} , \qquad \phi' = \begin{pmatrix} \varphi'^+ \\ \varphi'^0 \end{pmatrix} , \tag{7.89}$$

with $\bar{\Phi}^0 = (\Phi^0)^*$ and $\Phi^- = (\Phi^+)^*$. We summarize the particle content of the model in Table 7.7.

Yukawa interactions

The SM fermions couple to the SM Higgs-like ϕ doublet via the usual Yukawa terms,

$$-\mathcal{L}_\phi = \overline{q_L}\, y^d\, \phi\, d_R + \overline{q_L}\, y^u\, \tilde{\phi}\, u_R + \overline{\ell_L}\, y^e\, \phi\, e_R + h.c. , \tag{7.90}$$

with $\tilde{\phi} \equiv i\sigma^2 \phi^*$. The $y^{u,d,e}$ Yukawa couplings represent 3×3 matrices in family space. The VL fermions, on the other hand, have gauge-invariant Dirac mass terms,

$$-\mathcal{L}_M = \overline{Q_L}\, M_Q\, Q_R + \overline{L_L}\, M_L\, L_R + h.c. , \tag{7.91}$$

and our choice of representations allows us to Yukawa-couple them to the SM fermions via

$$-\mathcal{L}_\Phi = \overline{Q_R}\,\lambda_q^\dagger\,\Phi\,q_L + \overline{L_R}\,\lambda_\ell^\dagger\,\Phi\,\ell_L + h.c.\,, \tag{7.92}$$

and

$$-\mathcal{L}_{\phi'} = \overline{Q_L}\,\widetilde{y}^d\,\phi'\,d_R + \overline{Q_L}\,\widetilde{y}^u\,\tilde{\phi}'\,u_R + \overline{L_L}\,\widetilde{y}^e\,\phi'\,e_R + h.c.\,, \tag{7.93}$$

where $\lambda_{q,\ell}$ and $\widetilde{y}^{u,d,e}$ are $3 \times n_{\rm VL}$ and $n_{\rm VL} \times 3$ Yukawa matrices, respectively. After spontaneous symmetry breaking, these couplings will induce mixings between the VL and SM chiral fermions. This is crucial for the phenomenology of the model, in particular for its flavor sector, as will be clear in the next sections.

Scalar potential and symmetry breaking

The scalar potential can be cast as follows:

$$\begin{aligned}\mathcal{V} = {} & m_\phi^2|\phi|^2 + \frac{\lambda_1}{2}|\phi|^4 + m_{\phi'}^2|\phi'|^2 + \frac{\lambda_2}{2}|\phi'|^4 + m_\Phi^2\,\mathrm{Tr}(\Phi^\dagger\Phi) + \frac{\lambda_3}{2}\left[\mathrm{Tr}(\Phi^\dagger\Phi)\right]^2 \\ & + \lambda_4(\phi^\dagger\phi)(\phi'^\dagger\phi') + \lambda_5(\phi^\dagger\phi)\mathrm{Tr}(\Phi^\dagger\Phi) + \lambda_6(\phi'^\dagger\phi')\mathrm{Tr}(\Phi^\dagger\Phi) + \left(\mu\,\phi'^\dagger\,\Phi\,\phi + h.c.\right)\,.\end{aligned} \tag{7.94}$$

We will assume that the parameters in the scalar potential are such that the scalar fields develop vevs in the following directions:

$$\langle\phi\rangle = \frac{1}{\sqrt{2}}\begin{pmatrix}0\\ v_\phi\end{pmatrix}, \qquad \langle\phi'\rangle = \frac{1}{\sqrt{2}}\begin{pmatrix}0\\ v_{\phi'}\end{pmatrix}, \qquad \langle\Phi\rangle = \frac{1}{2}\begin{pmatrix}u & 0\\ 0 & u\end{pmatrix}\,. \tag{7.95}$$

Assuming $u \gg v_\phi, v_{\phi'}$, the symmetry breaking proceeds via the following pattern:

$$\mathrm{SU(2)}_1 \times \mathrm{SU(2)}_2 \times \mathrm{U(1)_Y} \xrightarrow{u} \mathrm{SU(2)_L} \times \mathrm{U(1)_Y} \xrightarrow{v} \mathrm{U(1)_{em}}\,, \tag{7.96}$$

with the assumed vev hierarchy $u \sim \mathrm{TeV} \gg v \simeq 246$ GeV. With this breaking chain, the charge of the unbroken $\mathrm{U(1)_{em}}$ group is defined as

$$Q = \left(T_3^1 + T_3^2\right) + Y = T_3^L + Y\,, \tag{7.97}$$

with T_3^a the diagonal generator of $\mathrm{SU(2)}_a$. In the first step, the original $\mathrm{SU(2)}_1 \times \mathrm{SU(2)}_2$ group gets broken down to the diagonal $\mathrm{SU(2)_L}$. Under the diagonal subgroup, ϕ and ϕ' transform as doublets and, as usual with 2HDM, we parametrize their vevs as

$$\begin{aligned} v_\phi &= v\,\sin\beta\,,\\ v_{\phi'} &= v\,\cos\beta\,,\end{aligned} \tag{7.98}$$

where $v^2 = v_\phi^2 + v_{\phi'}^2$. Since the two doublets transformed originally in a 'mirror' way under the two original SU(2) factors, it is clear that the ratio between their vevs, $\tan\beta = v_\phi/v_{\phi'}$, controls the size of the gauge mixing effects. In particular, the limit

$\tan\beta = g_1/g_2$ corresponds to the purely diagonal limit with no gauge mixing, see Section 7.3.3 for more details.

The scalar fields $\{\phi, \Phi, \phi'\}$ contain 12 real degrees of freedom, six of these become the longitudinal polarization components of the $W^{(\prime)\pm}$ and $Z^{(\prime)}$ bosons. In the CP-conserving limit the scalar spectrum is composed of three CP-even Higgs bosons, one CP-odd Higgs and one charged scalar, forming an effective (constrained) 2HDM plus CP-even singlet system. The scalar sector will present a decoupling behavior, with a SM-like Higgs boson at the weak scale (to be associated with the 125 GeV boson) and the rest of the scalars at the scale $u \sim$ TeV.[14] Further details of the scalar sector are given in Appendix 7.C.

7.3.3 Gauge boson and fermion masses and interactions

We now proceed to the analysis of the model presented in the previous section. Here we will derive the masses and mixing of the gauge bosons and fermions of the model, as well as the neutral and charged vectorial currents.

Fermion masses

We can combine the SM and the VL fermions as

$$\begin{aligned} \mathcal{U}^I_{L,R} &\equiv \left(u^i_{L,R}, U^k_{L,R}\right) , \qquad \mathcal{D}^I_{L,R} \equiv \left(d^i_{L,R}, D^k_{L,R}\right) , \\ \mathcal{N}^I_{L} &\equiv \left(\nu^i_{L}, N^k_{L}\right) , \qquad\quad \mathcal{N}^I_{R} \equiv \left(0, N^k_{R}\right) , \\ \mathcal{E}^I_{L,R} &\equiv \left(e^i_{L,R}, E^k_{L,R}\right) , \end{aligned} \tag{7.99}$$

where $i = 1, 2, 3$, $k = 1, \ldots, n_{\text{VL}}$ and $I = 1, \ldots, 3 + n_{\text{VL}}$. With this notation the fermion mass Lagrangian after symmetry breaking is given by

$$-\mathcal{L}^f_m = \overline{\mathcal{U}_L}\mathcal{M}_{\mathcal{U}}\mathcal{U}_R + \overline{\mathcal{D}_L}\mathcal{M}_{\mathcal{D}}\mathcal{D}_R + \overline{\mathcal{E}_L}\mathcal{M}_{\mathcal{E}}\mathcal{E}_R + \overline{\mathcal{N}_L}\mathcal{M}_{\mathcal{N}}\mathcal{N}_R + h.c. \tag{7.100}$$

The mass matrices are given in terms of the Yukawa couplings, VL Dirac masses and vevs as

$$\begin{aligned} \mathcal{M}_{\mathcal{U}} &= \begin{pmatrix} \frac{1}{\sqrt{2}} y_u v_\phi & \frac{1}{2}\lambda_q u \\ \frac{1}{\sqrt{2}} \widetilde{y}_u v_{\phi'} & M_Q \end{pmatrix} , \quad \mathcal{M}_{\mathcal{D}} = \begin{pmatrix} \frac{1}{\sqrt{2}} y_d v_\phi & \frac{1}{2}\lambda_q u \\ \frac{1}{\sqrt{2}} \widetilde{y}_d v_{\phi'} & M_Q \end{pmatrix} , \\ \mathcal{M}_{\mathcal{E}} &= \begin{pmatrix} \frac{1}{\sqrt{2}} y_e v_\phi & \frac{1}{2}\lambda_\ell u \\ \frac{1}{\sqrt{2}} \widetilde{y}_e v_{\phi'} & M_L \end{pmatrix} , \quad \mathcal{M}_{\mathcal{N}} = \begin{pmatrix} 0 & \frac{1}{2}\lambda_\ell u \\ 0 & M_L \end{pmatrix} . \end{aligned} \tag{7.101}$$

Note that we did not include any mechanism to generate neutrino masses, and consequently $\mathcal{M}_{\mathcal{N}}$ leads to three massless neutrinos and n_{VL} heavy neutral Dirac fermions. It is nevertheless straightforward to account for neutrino masses without impacting our analysis and conclusions by including one of the usual mechanisms, such as the standard seesaw.

[14] We will assume that μ is of the same order of the largest scale in the scalar potential, i.e. $\mu \sim u$.

In order to have a manageable parameter space and simplify the analysis we will assume that the Yukawa couplings of ϕ' can be neglected, $\widetilde{y}_{u,d,e} \simeq 0$. This can be justified by introducing a softly-broken discrete $\mathcal{Z}_2$ symmetry under which ϕ' is odd and all the other fields are even. We take the Dirac masses of the VL fermions to be generically around the symmetry breaking scale $u \sim$ TeV.

The fermion mass matrices can be block-diagonalized perturbatively in the small ratio $\epsilon = v/u \ll 1$ by means of the following field transformations

$$\begin{aligned} \mathcal{U}_L &\to V_Q^\dagger V_u^\dagger \mathcal{U}_L\,, & \mathcal{U}_R &\to W_u^\dagger \mathcal{U}_R\,, \\ \mathcal{D}_L &\to V_Q^\dagger V_d^\dagger \mathcal{D}_L\,, & \mathcal{D}_R &\to W_d^\dagger \mathcal{D}_R\,, \\ \mathcal{E}_L &\to V_L^\dagger V_e^\dagger \mathcal{E}_L\,, & \mathcal{E}_R &\to W_e^\dagger \mathcal{E}_R\,, \\ \mathcal{N}_L &\to V_L^\dagger \mathcal{N}_L\,, \end{aligned} \tag{7.102}$$

defined in terms of the unitary matrices

$$V_{Q,L} = \left(\begin{array}{c|c} V_{Q,L}^{11} = \sqrt{\mathbb{1} - \frac{1}{4}\lambda_{q,\ell}\widetilde{M}_{Q,L}^{-2}\lambda_{q,\ell}^\dagger} & V_{Q,L}^{12} = -\frac{u}{2} V_{Q,L}^{11} \lambda_{q,\ell} M_{Q,L}^{-1} \\ \hline V_{Q,L}^{21} = \frac{1}{2}\widetilde{M}_{Q,L}^{-1}\lambda_{q,\ell}^\dagger & V_{Q,L}^{22} = \frac{1}{u}\widetilde{M}_{Q,L}^{-1} M_{Q,L}^\dagger \end{array} \right)\,, \tag{7.103}$$

$$V_f = \mathbb{1} + i\epsilon^2 H_V^f + \ldots \quad ; \qquad W_f \;=\; \mathbb{1} + i\epsilon H_W^f + \frac{(i\epsilon)^2}{2} {H_W^f}^2 + \ldots \tag{7.104}$$

Here the freedom in the definition of $V_{Q,L}^{11}$ is removed by choosing it to be hermitian. Furthermore, $u \times \widetilde{M}_{Q,L}$ are the physical VL masses at leading order in ϵ,

$$\widetilde{M}_{Q,L} = \sqrt{\frac{M_{Q,L}^\dagger M_{Q,L}}{u^2} + \frac{\lambda_{q,\ell}^\dagger \lambda_{q,\ell}}{4}} \simeq \mathrm{diag}\left(\widetilde{M}_{Q_1,L_1}, \ldots, \widetilde{M}_{Q_{n_{\rm VL}},L_{n_{\rm VL}}}\right)\,, \tag{7.105}$$

and the matrices H_V^f and H_W^f are given by

$$H_V^f = \frac{i}{2}\left(\begin{array}{c|c} 0 & V_F^{11} y_f y_f^\dagger V_F^{21\dagger} \widetilde{M}_F^{-2} \\ \hline -\widetilde{M}_F^{-2} V_F^{21} y_f y_f^\dagger V_F^{11} & 0 \end{array} \right)\,, \tag{7.106}$$

$$H_W^f = \frac{i}{\sqrt{2}}\left(\begin{array}{c|c} 0 & y_f^\dagger V_F^{21\dagger} \widetilde{M}_F^{-1} \\ \hline -\widetilde{M}_F^{-1} V_F^{21} y_f & 0 \end{array} \right)\,, \tag{7.107}$$

with $F = Q, L$ and $f = u, d, e$. After the block-diagonalization, a further diagonalization of the SM fermion block can be done by means of the 3×3 unitary transformations

$$\begin{aligned} u_L &\to S_u^\dagger u_L\,, & u_R &\to U_u^\dagger u_R\,, \\ d_L &\to S_d^\dagger d_L\,, & d_R &\to U_d^\dagger d_R\,, \\ e_L &\to S_e^\dagger e_L\,, & e_R &\to U_e^\dagger e_R\,. \end{aligned} \tag{7.108}$$

As in the SM, only one combination of these transformations appears in the gauge couplings: the CKM matrix, $V_{\rm CKM} = S_u S_d^\dagger$.

Vector boson masses and gauge mixing

Neutral gauge bosons

The neutral gauge bosons mass matrix in the basis $\mathcal{V}^0 = (W_3^1, W_3^2, B)$ is given by:

$$\mathcal{M}^2_{\mathcal{V}^0} = \frac{1}{4}\begin{pmatrix} g_1^2\left(v_{\phi'}^2+u^2\right) & -g_1 g_2 u^2 & -g_1 g' v_{\phi'}^2 \\ -g_1 g_2 u^2 & g_2^2\left(v_\phi^2+u^2\right) & -g_2 g' v_\phi^2 \\ -g_1 g' v_{\phi'}^2 & -g_2 g' v_\phi^2 & g'^2\left(v_\phi^2+v_{\phi'}^2\right) \end{pmatrix} . \tag{7.109}$$

This matrix has one vanishing eigenvalue, corresponding to the photon and two massive eigenstates which are identified with the Z and Z' bosons. Before fully diagonalizing this mass matrix we consider first the rotation from $(W_3^1,\, W_3^2)$ to $(Z_h,\, W_3)$, with W_3 the electrically neutral $\mathrm{SU(2)_L}$ gauge boson. In order to do this we have to study the first symmetry breaking step, i.e. $u \neq 0$ and $v = 0$, diagonalize the top-left 2×2 block and identify the massless state with W_3 (the $\mathrm{SU(2)_L}$ group remains unbroken in the first step). As a result we get:

$$Z_h = \frac{1}{n_1}\left(g_1\, W_3^1 - g_2\, W_3^2\right) , \qquad W_3 = \frac{1}{n_1}\left(g_2\, W_3^1 + g_1\, W_3^2\right) , \tag{7.110}$$

with $n_1 = \sqrt{g_1^2+g_2^2}$ and the gauge coupling of $\mathrm{SU(2)_L}$ taking the value $g = g_1 g_2/n_1$. In the $(Z_h,\, W_3,\, B)$ basis, the rotation from $(W_3,\, B)$ to $(Z_l,\, A)$ is just like in the SM and we obtain:

$$Z_l = \frac{1}{n_2}\left(g\, W_3 - g'\, B\right) , \qquad A = \frac{1}{n_2}\left(g'\, W_3 + g\, B\right) , \tag{7.111}$$

where $n_2 = \sqrt{g^2+g'^2}$ and the weak angle is defined as usual: $\hat{s}_W = g'/n_2$ and $\hat{c}_W = g/n_2$. We are now in condition to write the neutral gauge boson mass matrix in the $(Z_h,\, Z_l,\, A)$ basis where it takes the form:

$$\mathcal{M}^2_{\mathcal{V}^0} = \frac{1}{4}\begin{pmatrix} \left(g_1^2+g_2^2\right)u^2 + \frac{g^2 g_2^2}{g_1^2} v^2\left(s_\beta^2 + \frac{g_1^4}{g_2^4}c_\beta^2\right) & -g\, n_2 \frac{g_2}{g_1}\, v^2\left(s_\beta^2 - \frac{g_1^2}{g_2^2}c_\beta^2\right) & 0 \\ -g\, n_2 \frac{g_2}{g_1}\, v^2\left(s_\beta^2 - \frac{g_1^2}{g_2^2}c_\beta^2\right) & \left(g^2+g'^2\right)v^2 & 0 \\ 0 & 0 & 0 \end{pmatrix} . \tag{7.112}$$

We see from this mass matrix that in the particular limit $v = 0$, only Z_h gets a mass $M_{Z'} = \frac{1}{4}\left(g_1^2+g_2^2\right)u^2$, which is expected since $\mathrm{SU(2)_L}\times\mathrm{U(1)_Y}$ remains unbroken in that case. Moreover, we can extract the $Z_l - Z_h$ mixing. The mass eigenvectors $(Z',\, Z)$ are given, in terms of $(Z_h,\, Z_l)$, by:

$$Z' = \cos\xi_Z\, Z_h - \sin\xi_Z\, Z_l , \qquad Z = \sin\xi_Z\, Z_h + \cos\xi_Z\, Z_l , \tag{7.113}$$

with the mixing suppressed by the ratio $\epsilon \equiv v/u$,

$$\xi_Z \simeq \frac{g\, n_2}{n_1^2}\frac{g_2}{g_1}\,\epsilon^2\left(s_\beta^2 - \frac{g_1^2}{g_2^2}c_\beta^2\right) = \frac{g}{n_2}\frac{g_2}{g_1}\frac{M_Z^2}{M_{Z'}^2}\left(s_\beta^2 - \frac{g_1^2}{g_2^2}c_\beta^2\right) . \tag{7.114}$$

We define the parameter controlling the mixing as

$$\zeta = s_\beta^2 - \frac{g_1^2}{g_2^2} c_\beta^2 \,. \tag{7.115}$$

In the limit $\zeta \to 0$, the $\mathrm{SU(2)_L}$ sub-group corresponds to the diagonal subgroup of the original SU(2) product and gauge mixing vanishes. As already anticipated, $\zeta \to 0$ corresponds to the limit $\tan\beta \to g_1/g_2$.

Finally, the masses of the neutral massive vector bosons are given by

$$M_{Z'}^2 \simeq \frac{1}{4}\left(g_1^2 + g_2^2\right) u^2 \,, \qquad M_Z^2 \simeq \frac{1}{4}\left(g^2 + g'^2\right) v^2 \,. \tag{7.116}$$

Charged gauge bosons

In the basis $\mathcal{V}^+ = (W_{12}^1, W_{12}^2)$, with $W_{12}^r = \frac{1}{\sqrt{2}}\left(W_1^r - i W_2^r\right)$, the charged gauge boson mass matrix is given by

$$\mathcal{M}_{\mathcal{V}^+}^2 = \frac{1}{4}\begin{pmatrix} g_1^2\left(v_{\phi'}^2 + u^2\right) & -g_1 g_2 u^2 \\ -g_1 g_2 u^2 & g_2^2\left(v_\phi^2 + u^2\right) \end{pmatrix} . \tag{7.117}$$

As before, it is convenient to work in the basis $(W_h,\, W_l)$ where the $\mathrm{SU(2)_L}$ gauge boson appears explicitly. To obtain this basis in terms of the original one, we set $v = 0$, diagonalize the mass matrix and associate the null eigenvalue to W_l ($\mathrm{SU(2)_L}$ remains unbroken in the first stage of symmetry breaking). We get:

$$W_h = \frac{1}{n_1}\left(g_1\, W^1 - g_2\, W^2\right) \,, \qquad W_l = \frac{1}{n_1}\left(g_2\, W^1 + g_1\, W^2\right) \,. \tag{7.118}$$

In the basis $(W_h,\, W_l)$ the mass matrix reads:

$$\mathcal{M}_{\mathcal{V}^+}^2 = \frac{1}{4}\begin{pmatrix} \left(g_1^2 + g_2^2\right) u^2 + \frac{g^2 g_2^2}{g_1^2} v^2 \left(s_\beta^2 + \frac{g_1^4}{g_2^4} c_\beta^2\right) & -g^2 \frac{g_2}{g_1} v^2 \left(s_\beta^2 - \frac{g_1^2}{g_2^2} c_\beta^2\right) \\ -g^2 \frac{g_2}{g_1} v^2 \left(s_\beta^2 - \frac{g_1^2}{g_2^2} c_\beta^2\right) & g^2 v^2 \end{pmatrix} . \tag{7.119}$$

The $W_l - W_h$ mixing presents the same structure as in the neutral gauge boson sector and reads:

$$\xi_W \simeq \zeta \frac{g^2}{n_1^2}\frac{g_2}{g_1}\epsilon^2 = \zeta \frac{g_2}{g_1}\frac{M_W^2}{M_{W'}^2} \,, \tag{7.120}$$

such that the physical eigenstates are given by:

$$W' = \cos\xi_W\, W_h - \sin\xi_W\, W_l \,, \qquad W = \sin\xi_W\, W_h + \cos\xi_W\, W_l \,, \tag{7.121}$$

with masses

$$M_{W'}^2 \simeq M_{Z'}^2 \simeq \frac{1}{4}\left(g_1^2 + g_2^2\right) u^2 \,, \qquad M_W^2 \simeq \frac{1}{4} g^2 v^2 \,. \tag{7.122}$$

Gauge boson couplings to fermions

Neutral currents

The neutral currents of the fermions are given by

$$\begin{aligned}\mathcal{L}_{\rm NC} &= \overline{\psi}\gamma_\mu \left(g' B^\mu Y + g_1 W_3^{1\mu} T_3^1 + g_2 W_3^{2\mu} T_3^2\right)\psi \\ &= \overline{\psi}\gamma_\mu \left\{ e\, Q_\psi\, A^\mu + \frac{g}{c_W} Z_l^\mu [(T_3^1 + T_3^2) - s_W^2\, Q_\psi] + g Z_h^\mu \left[\frac{g_1}{g_2} T_3^1 - \frac{g_2}{g_1} T_3^2\right]\right\}\psi,\end{aligned} \tag{7.123}$$

with $\psi = \mathcal{U}, \mathcal{D}, \mathcal{E}, \mathcal{N}$, and $e = gg'/n_2$ and Q_ψ denoting the electric coupling and the electric charge of the fermions, respectively. Applying the transformations in Eqs. (7.102) and (7.108) we can easily translate the above interactions to the fermion mass eigenbasis

$$\begin{aligned}\mathcal{L}_{\rm NC} \to \mathcal{L}_{\rm NC} = {} & A^\mu\, \overline{\psi}\gamma_\mu\, e Q_\psi \psi + \frac{g}{c_W} Z_l^\mu \Big\{ \overline{\psi}\gamma_\mu \left[(T_3^1 + T_3^2) P_L - s_W^2 Q\right]\psi \\ & - \frac{1}{2}\left(\overline{\mathcal{D}_R}\,\gamma_\mu\, O_R^{dd}\, \mathcal{D}_R - \overline{\mathcal{U}_R}\,\gamma_\mu\, O_R^{uu}\, \mathcal{U}_R + \overline{\mathcal{E}_R}\,\gamma_\mu\, O_R^{ee}\, \mathcal{E}_R - \overline{N_R}\,\gamma_\mu N_R\right)\Big\} \\ & + \frac{\hat{g}}{2} Z_h^\mu \Big[\overline{\mathcal{D}_L}\,\gamma_\mu\, O_L^Q\, \mathcal{D}_L - \overline{\mathcal{U}_L}\,\gamma_\mu\, V O_L^Q V^\dagger\, \mathcal{U}_L + \overline{\mathcal{E}_L}\,\gamma_\mu\, O_L^L\, \mathcal{E}_L - \overline{\mathcal{N}_L}\,\gamma_\mu\, O_L^L\, \mathcal{N}_L \\ & - \frac{g_1^2}{g_2^2}\left(\overline{\mathcal{D}_R}\,\gamma_\mu\, O_R^{dd}\, \mathcal{D}_R - \overline{\mathcal{U}_R}\,\gamma_\mu\, O_R^{uu}\, \mathcal{U}_R + \overline{\mathcal{E}_R}\,\gamma_\mu\, O_R^{ee}\, \mathcal{E}_R - \overline{N_R}\,\gamma_\mu N_R\right)\Big] \\ & + \mathcal{O}\left(\frac{m_f^2}{u^2}\right).\end{aligned} \tag{7.124}$$

Here m_f denotes the mass of a SM fermion with $f = u, d, e$, and we introduced the following definitions:

$$O_L^{Q,L} \equiv \begin{pmatrix} \Delta^{q,\ell} & \Sigma \\ \Sigma^\dagger & \Omega^{Q,L}\end{pmatrix} = \mathbb{1} - \frac{g_1^2 + g_2^2}{g_2^2} \begin{pmatrix} V_{Q,L}^{12}(V_{Q,L}^{12})^\dagger & V_{Q,L}^{12}(V_{Q,L}^{22})^\dagger \\ V_{Q,L}^{22}(V_{Q,L}^{12})^\dagger & V_{Q,L}^{22}(V_{Q,L}^{22})^\dagger\end{pmatrix}, \tag{7.125}$$

$$O_R^{ff'} \equiv \begin{pmatrix} 0 & \hat{\Sigma}^f \\ (\hat{\Sigma}^{f'})^\dagger & 1\end{pmatrix} = \begin{pmatrix} 0 & -\frac{m_f}{u}\left(V_F^{11}\right)^{-1}\left(V_F^{21}\right)^\dagger \widetilde{M}_F^{-1} \\ -\widetilde{M}_F^{-1} V_F^{21}\left(V_F^{11}\right)^{-1}\frac{m_{f'}}{u} & 1\end{pmatrix}, \tag{7.126}$$

$$V = \begin{pmatrix} V_{\rm CKM} & 0 \\ 0 & 1\end{pmatrix}, \tag{7.127}$$

with $F = Q, L$, and finally $\hat{g} \equiv g g_2/g_1$.

Charged currents

Similarly, the charged currents take the following form

$$\begin{aligned}\mathcal{L}_{\rm CC} &= \frac{g_1}{\sqrt{2}} W_\mu^1 \left[\overline{U}\gamma^\mu D + \overline{N}\gamma^\mu E\right] + \frac{g_2}{\sqrt{2}} W_\mu^2 \left[\overline{u}\gamma^\mu P_L\, d + \overline{\nu}\gamma^\mu P_L\, e\right] + h.c. \\ &= \frac{g}{\sqrt{2}} W_l^\mu \left[\overline{\mathcal{U}}\gamma_\mu P_L \mathcal{D} + \overline{\mathcal{N}}\gamma_\mu P_L \mathcal{E} + \overline{U}\gamma_\mu P_R\, D + \overline{N}\gamma_\mu P_R\, E\right] \\ &\quad - \frac{g}{\sqrt{2}} W_h^\mu \left[\frac{g_2}{g_1}\left(\overline{u}\gamma_\mu P_L d + \overline{\nu}\gamma_\mu P_L e\right) - \frac{g_1}{g_2}\left(\overline{U}\gamma_\mu D + \overline{N}\gamma_\mu\, E\right)\right] + h.c.\,,\end{aligned} \tag{7.128}$$

and, in the fermion mass eigenbasis (see Eqs. (7.102) and (7.108)), we have

$$\begin{aligned}\mathcal{L}_{\rm CC} \to \mathcal{L}_{\rm CC} = &\frac{g}{\sqrt{2}} W_l^\mu \left[\overline{\mathcal{U}_L}\,\gamma_\mu\, V \mathcal{D}_L + \overline{\mathcal{N}_L}\,\gamma_\mu\, \mathcal{E}_L + \overline{\mathcal{U}_R}\,\gamma_\mu\, O_R^{ud}\, \mathcal{D}_R + \overline{\mathcal{N}_R}\,\gamma_\mu\, O_R^{\nu e}\, \mathcal{E}_R\right] \\ &- \frac{\hat{g}}{\sqrt{2}} W_h^\mu \left[\overline{\mathcal{U}_L}\,\gamma_\mu\, V O_L^Q\, \mathcal{D}_L + \overline{\mathcal{N}_L}\,\gamma_\mu\, O_L^L\, \mathcal{E}_L - \frac{g_1^2}{g_2^2}\left(\overline{\mathcal{U}_R}\,\gamma_\mu\, O_R^{ud}\, \mathcal{D}_R\right.\right. \\ &\left.\left. + \overline{\mathcal{N}_R}\,\gamma_\mu\, O_R^{\nu e}\, \mathcal{E}_R\right)\right] + h.c. + \mathcal{O}\left(\frac{m_f^2}{u^2}\right)\,.\end{aligned} \tag{7.129}$$

Flavor textures for the gauge interactions

In order to accommodate the hints of lepton universality violation from the recent anomalies in B decays without being in tension with other bounds, we require negligible couplings of the new gauge bosons to the first family of SM-like leptons and a large universality violation among the other two.[15] We now derive the conditions on the number of generations of the exotic fermions to accommodate such constraints.

Using Eqs. (7.125) and (7.103), the matrix $\Delta^{q,\ell}$, that parametrize NP contributions to the left-handed gauge interactions with SM fermions, can be readily written in the following form

$$\Delta^{q,\ell} = \mathbb{1} - \frac{g_1^2 + g_2^2}{4 g_2^2} \lambda_{q,\ell} \widetilde{M}^{-2} \lambda_{q,\ell}^\dagger\,, \tag{7.130}$$

where the second term is the source of lepton non-universality induced by the mixings between the SM and VL fermions generated by the $\lambda_{q,\ell}$ Yukawa couplings. On the other hand, right-handed couplings involving SM fermions, controlled by $O_R^{ff'}$, are mass suppressed and they can be neglected for the interactions we are considering.

If we consider the minimal scenario with $n_{\rm VL} = 1$, the Yukawa couplings $\lambda_{q,\ell}$ can be written generically as

$$\lambda_{q,\ell} = \frac{2 g_2}{n_1} \widetilde{M}_{Q,L} \begin{pmatrix} \Delta_{d,e} \\ \Delta_{s,\mu} \\ \Delta_{b,\tau} \end{pmatrix}\,. \tag{7.131}$$

[15] Note that in this case, and in contrast to the model in presented in Section 7.1, large couplings to the first generation are more dangerous since the NP effects necessary to explain the anomalies in $R(D^{(*)})$ are much larger.

Here $\Delta_{d,e}$, $\Delta_{s,b}$ and $\Delta_{\mu,\tau}$ are free real parameters, and without loss of generality we have chosen an appropriate normalization factor to simplify the expression of $\Delta^{q,\ell}$. We have also ignored possible complex phases in the couplings since we are not interested in CP violating observables. From Eq. (7.130) it is then clear that, for $n_{\rm VL} = 1$, NP contributions to the left-handed gauge couplings to SM fermions are given by

$$\Delta^{q,\ell}_{n_{\rm VL}=1} = \begin{pmatrix} 1-(\Delta_{d,e})^2 & \Delta_{d,e}\Delta_{s,\mu} & \Delta_{d,e}\Delta_{b,\tau} \\ \Delta_{d,e}\Delta_{s,\mu} & 1-(\Delta_{s,\mu})^2 & \Delta_{s,\mu}\Delta_{b,\tau} \\ \Delta_{d,e}\Delta_{b,\tau} & \Delta_{s,\mu}\Delta_{b,\tau} & 1-(\Delta_{b,\tau})^2 \end{pmatrix} . \tag{7.132}$$

As we can see, in the limit of no gauge boson mixing, NP contributions to the first family of SM fermions can only be suppressed if we fix $\Delta_{d,e} \simeq 1$ and $\Delta_{s,\mu}$, $\Delta_{b,\tau} \ll 1$ which then implies approximate universal couplings for the second and the third families. Hence, we need at least two generations of VL fermions in order to have enough freedom to accommodate the observed hints of lepton universality violation.

In the rest of this article we will take the minimal setup consisting of $n_{\rm VL} = 2$ since there is no compelling reason to assume additional VL generations. Moreover, in order to reduce the number of free parameters in the analysis we choose the following texture for the Yukawa matrices $\lambda_{q,\ell}$:

$$\lambda_{q,\ell} = \frac{2g_2}{n_1} \begin{pmatrix} \widetilde{M}_{Q_1,L_1} & 0 \\ 0 & \widetilde{M}_{Q_2,L_2}\,\Delta_{s,\mu} \\ 0 & \widetilde{M}_{Q_2,L_2}\,\Delta_{b,\tau} \end{pmatrix} , \tag{7.133}$$

where, again, $\Delta_{s,b}$ and $\Delta_{\mu,\tau}$ are free real parameters and the normalization factor is chosen for convenience.[16] The left-handed currents, parametrized in terms of $O^{Q,L}_L$ (see Eq. (7.125)) now read

$$\Delta^{q,\ell} = \begin{pmatrix} 0 & 0 & 0 \\ 0 & 1-(\Delta_{s,\mu})^2 & \Delta_{s,\mu}\Delta_{b,\tau} \\ 0 & \Delta_{s,\mu}\Delta_{b,\tau} & 1-(\Delta_{b,\tau})^2 \end{pmatrix} , \tag{7.134}$$

$$\Sigma = \begin{pmatrix} \frac{g_1}{g_2} & 0 \\ 0 & \Delta_{s,\mu}\sqrt{\frac{n_1^2}{g_2^2} - \Delta^2_{s,\mu} - \Delta^2_{b,\tau}} \\ 0 & \Delta_{b,\tau}\sqrt{\frac{n_1^2}{g_2^2} - \Delta^2_{s,\mu} - \Delta^2_{b,\tau}} \end{pmatrix} , \tag{7.135}$$

$$\Omega^{Q,L} = \begin{pmatrix} 1-\frac{g_1^2}{g_2^2} & 0 \\ 0 & \Delta^2_{s,\mu} + \Delta^2_{b,\tau} - \frac{g_1^2}{g_2^2} \end{pmatrix} , \tag{7.136}$$

which, by construction, provide the desired patterns for the NP contributions to accommodate the data.

[16] Note however that the free parameters have to satisfy the condition $(1-g^2/g_2^2)(\Delta^2_{s,\mu}+\Delta^2_{b,\tau}) \leq 1$ for consistency with Eq. (7.105).

7.3.4 Flavor constraints

We consider in our analysis flavor observables receiving new physics contributions at tree-level from the exchange of the massive vector bosons. Additionally, we consider bounds from electroweak precision measurements at the Z and W pole which are affected in our model due to gauge mixing effects.

Regarding electroweak precision observables at the Z and W pole, we use the fit to Z- and W-pole observables performed in Ref. [143]. The fit includes the observables listed in Tables 1 and 2 of [143], and provides mean values, standard deviations and the correlation matrix for the following parameters: the correction to the W mass (δm), anomalous W and Z couplings to leptons ($\delta g_L^{W\ell_i}$, $\delta g_{L,R}^{Z\ell_i}$) and anomalous Z couplings to quarks ($\delta g_{L,R}^{Zu_i}$, $\delta g_{L,R}^{Zd_i}$). The results for these "pseudo-observables" can be found in Eqs. (4.5-4.8) and Appendix B of Ref. [143]. The relevant expressions for these pseudo-observables within our model are given in Appendix 7.D.

We collect the list of flavor observables included in our analysis in Table 7.8 and describe them in more detail in the following sections.

Leptonic Tau decays

Leptonic tau decays pose very stringent constraints on lepton flavor universality [144]. We consider the two decay rates $\Gamma(\tau \to \{e,\mu\}\nu\bar{\nu})$, normalized to the muon decay rate to cancel the dependence on G_F. We take the individual experimental branching ratios and lifetimes from the PDG [23]. For the branching ratios we take the result of the constrained fit, which gives a correlation of 14% between both measurements. Once normalized to the τ lifetime, the decay rates have a correlation of 45%, while the normalization to the muon decay rate has a minor impact on the correlation of the ratios because its uncertainty is negligible. The experimental results are summarized in Table 7.8.

In our model, we have:

$$\frac{\Gamma(\tau \to e\nu\bar{\nu})}{\Gamma(\mu \to e\nu\bar{\nu})} = \frac{\sum_{i,j} |C_{ij}^{e\tau}|^2}{\sum_{i,j} |C_{ij}^{e\mu}|^2} \times \frac{m_\tau^5 \, f(x_{e\tau})}{m_\mu^5 \, f(x_{e\mu})} \,, \tag{7.137}$$

$$\frac{\Gamma(\tau \to \mu\nu\bar{\nu})}{\Gamma(\mu \to e\nu\bar{\nu})} = \frac{\sum_{i,j} |C_{ij}^{\mu\tau}|^2}{\sum_{i,j} |C_{ij}^{e\mu}|^2} \times \frac{m_\tau^5 \, f(x_{\mu\tau})}{m_\mu^5 \, f(x_{e\mu})} \,, \tag{7.138}$$

where $x_{\ell\ell'} = m_\ell^2/m_{\ell'}^2$ and $f(x) = 1 - 8x + 8x^3 - x^4 - 12x^2 \ln x$. The Wilson coefficients $C_{ij}^{\ell_a \ell_b}$ are given by

$$C_{ij}^{\ell_a \ell_b} = \frac{4G_F}{\sqrt{2}} \delta_{aj}\delta_{ib} + \frac{\hat{g}^2}{4M_{W'}^2} \left[2\Delta_{aj}^{\ell}\Delta_{ib}^{\ell} - \Delta_{ab}^{\ell}\Delta_{ij}^{\ell} + \zeta(\Delta_{ab}^{\ell}\delta_{ij} + 2\Delta_{aj}^{\ell}\delta_{ib} + 2\delta_{aj}\Delta_{ib}^{\ell}) \right] . \tag{7.139}$$

The resulting predictions in the SM can be found in Table 7.8. Leading radiative corrections and W-boson propagator effects are included in the SM predictions [145–148].

Leptonic τ decays

Observable	Experiment	Correlation	SM	Theory
$\Gamma_{\tau\to e\nu\bar{\nu}}/\Gamma_{\mu\to e\nu\bar{\nu}}$	$1.350(4)\cdot 10^6$	0.45	$1.3456(5)\cdot 10^6$	Eq. (7.137)
$\Gamma_{\tau\to \mu\nu\bar{\nu}}/\Gamma_{\mu\to e\nu\bar{\nu}}$	$1.320(4)\cdot 10^6$		$1.3087(5)\cdot 10^6$	Eq. (7.138)

$d\to u$ transitions

Observable	Experiment	Correlation	SM	Theory
$\Gamma_{\pi\to\mu\nu}/\Gamma_{\pi\to e\nu}$	$8.13(3)\cdot 10^3$	0.49	$8.096(1)\cdot 10^3$	Eq. (7.140)
$\Gamma_{\tau\to\pi\nu}/\Gamma_{\pi\to e\nu}$	$7.90(5)\cdot 10^7$		$7.91(1)\cdot 10^7$	Eq. (7.141)

$s\to u$ transitions

Observable	Experiment	Correlation	SM	Theory
$\Gamma_{K\to\mu\nu}/\Gamma_{K\to e\nu}$	$4.02(2)\cdot 10^4$	$\begin{bmatrix} \cdot & \cdot & \cdot \\ 0.27 & \cdot & \cdot \\ 0.01 & 0.00 & \cdot \end{bmatrix}$	$4.037(2)\cdot 10^4$	Eq. (7.145)
$\Gamma_{\tau\to K\nu}/\Gamma_{K\to e\nu}$	$1.89(3)\cdot 10^7$		$1.939(4)\cdot 10^7$	Eq. (7.146)
$\Gamma_{K^+\to\pi\mu\nu}/\Gamma_{K^+\to\pi e\nu}$	0.660(3)		0.663(2)	Eq. (7.147)

$c\to s$ transitions

Observable	Experiment		SM	Theory
$\Gamma_{D\to K\mu\nu}/\Gamma_{D\to Ke\nu}$	0.95(5)	$(S=1.3)$	0.921(1)	Eq. (7.149)
$\Gamma_{D_s\to\tau\nu}/\Gamma_{D_s\to\mu\nu}$	10.0(6)		9.6(1)	Eq. (7.150)

$b\to s$ transitions

Observable	Experiment		SM	Theory
$\Delta M_s/\Delta M_d$	35.13(15)		31.2(1.8)	Eq. (7.151)

Coefficient	Fit [119]	Correlation	SM	Theory
$C_9^{\mathrm{NP}\mu}$	$-1.1(0.2)$	$\begin{bmatrix} \cdot & \cdot & \cdot & \cdot \\ -0.08 & \cdot & \cdot & \cdot \\ 0.10 & -0.10 & \cdot & \cdot \\ 0.02 & 0.02 & 0.87 & \cdot \end{bmatrix}$	0.	Eq. (7.153)
$C_{10}^{\mathrm{NP}\mu}$	$+0.3(0.2)$		0.	Eq. (7.153)
$C_9^{\mathrm{NP}e}$	$-0.3(1.7)$		0.	Eq. (7.153)
$C_{10}^{\mathrm{NP}e}$	$+0.6(1.6)$		0.	Eq. (7.153)

$b\to c$ transitions

Observable	Experiment	Correlation	SM	Theory
$\Gamma_{B\to D\mu\bar{\nu}}/\Gamma_{B\to De\bar{\nu}}$	0.95(09)	$+0.51$	0.995(1)	Eq. (7.154)
$\Gamma_{B\to D^*\mu\bar{\nu}}/\Gamma_{B\to D^*e\bar{\nu}}$	0.97(08)		0.996(1)	Eq. (7.154)
$R(D)$	0.397(49)	-0.21	0.297(17)	Eq. (7.155)
$R(D^*)$	0.316(19)		0.252(3)	Eq. (7.155)
$\Gamma_{B\to X_c\tau\nu}/\Gamma_{B\to X_ce\nu}$	0.222(22)		0.223(5)	Eq. (7.156)

Table 7.8: *List of flavor observables used in the fit.*

$d \to u$ transitions

We consider the decay rates $\Gamma(\pi \to \mu\nu)$ and $\Gamma(\tau \to \pi\nu)$, normalized to $\Gamma(\pi \to e\nu)$ in order to cancel the dependence on the combination $G_F|V_{ud}|f_\pi$. These ratios constitute important constraints on flavor non-universality in $d \to u\ell\nu$ transitions.

We calculate the experimental values for these ratios taking the averages for branching fractions and lifetimes from the PDG [23], and imposing the constraint $\mathcal{B}(\pi \to e\nu) + \mathcal{B}(\pi \to \mu\nu) = 1$. We find a correlation of 49% between both ratios. The corresponding results are summarized in Table 7.8.

The model predictions for these ratios are:

$$\frac{\Gamma(\pi \to \mu\bar{\nu})}{\Gamma(\pi \to e\bar{\nu})} = \frac{\sum_j |C_{2j}^{ud}|^2}{\sum_j |C_{1j}^{ud}|^2} \times \left[\frac{\Gamma(\pi \to \mu\bar{\nu})}{\Gamma(\pi \to e\bar{\nu})}\right]_{\rm SM} , \tag{7.140}$$

$$\frac{\Gamma(\tau \to \pi\nu)}{\Gamma(\pi \to e\bar{\nu})} = \frac{\sum_j |C_{3j}^{ud}|^2}{\sum_j |C_{1j}^{ud}|^2} \times \left[\frac{\Gamma(\tau \to \pi\nu)}{\Gamma(\pi \to e\bar{\nu})}\right]_{\rm SM} , \tag{7.141}$$

where the Wilson coefficients $C_{ab}^{u_i d_j}$ are given by

$$C_{ab}^{u_i d_j} = \frac{4G_F}{\sqrt{2}} V_{ij}\delta_{ab} + \frac{\hat{g}^2}{2M_{W'}^2}\left[(V\Delta^q)_{ij}\Delta_{ab}^\ell - \zeta\left(V_{ij}\Delta_{ab}^\ell + (V\Delta^q)_{ij}\delta_{ab}\right)\right] . \tag{7.142}$$

For the SM contributions we follow Ref. [144]. We have:

$$\left[\frac{\Gamma(\pi \to e\bar{\nu})}{\Gamma(\pi \to \mu\bar{\nu})}\right]_{\rm SM} = \frac{m_e^2}{m_\mu^2}\left[\frac{1 - m_e^2/m_\pi^2}{1 - m_\mu^2/m_\pi^2}\right]^2 (1 + \delta R_{\pi \to e/\mu}) , \tag{7.143}$$

$$\left[\frac{\Gamma(\tau \to \pi\nu)}{\Gamma(\pi \to \mu\nu)}\right]_{\rm SM} = \frac{m_\tau^3}{2m_\pi m_\mu^2}\left[\frac{1 - m_\pi^2/m_\tau^2}{1 - m_\mu^2/m_P^2}\right]^2 (1 + \delta R_{\tau/\pi}) . \tag{7.144}$$

The calculation of $\delta R_{\pi \to e/\mu}$ relies on Chiral Perturbation Theory to order $\mathcal{O}(e^2p^2)$ [149]. The radiative correction factor $\delta R_{\tau/\pi}$ can be found in Ref. [150]. The SM predictions for both ratios are collected in Table 7.8.

$s \to u$ transitions

We consider the decay rates $\Gamma(K \to \mu\nu)$ and $\Gamma(\tau \to K\nu)$, normalized to $\Gamma(K \to e\nu)$ in order to cancel the dependence on the combination $G_F|V_{us}|f_K$, as well as the semileptonic ($K_{\ell 3}$) ratio $\Gamma(K^+ \to \pi^0\mu^+\nu)/\Gamma(K^+ \to \pi^0 e^+\nu)$. These ratios pose also important constraints on flavor non-universality.

We take the experimental values for the decay rates $\Gamma(K^+ \to \mu^+\nu)$, $\Gamma(K^+ \to \pi^0 e^+\nu)$ and $\Gamma(K^+ \to \pi^0\mu^+\nu)$ from the constrained fit to K^+ decay data done by the PDG [23], including the correlation matrix. The correlation between $\Gamma(K^+ \to \mu^+\nu)$ and $\Gamma(K^+ \to e^+\nu)$ is calculated comparing the averages for the individual rates with the ratio given by the PDG, resulting in a correlation of 60%. Assuming no correlation between $\Gamma(K^+ \to e^+\nu)$ and the semileptonic modes, and assuming that the τ mode is uncorrelated to the K modes, we construct a 5×5 correlation matrix and calculate the three ratios of interest, including their 3×3 correlation matrix. These results are collected in Table 7.8.

The model predictions for these ratios are:

$$\frac{\Gamma(K \to \mu\bar{\nu})}{\Gamma(K \to e\bar{\nu})} = \frac{\sum_j |C_{2j}^{us}|^2}{\sum_j |C_{1j}^{us}|^2} \times \left[\frac{\Gamma(K \to \mu\bar{\nu})}{\Gamma(K \to e\bar{\nu})}\right]_{\rm SM} , \tag{7.145}$$

$$\frac{\Gamma(\tau \to K\nu)}{\Gamma(K \to e\bar{\nu})} = \frac{\sum_j |C_{3j}^{us}|^2}{\sum_j |C_{1j}^{us}|^2} \times \left[\frac{\Gamma(\tau \to K\nu)}{\Gamma(K \to e\bar{\nu})}\right]_{\rm SM} , \tag{7.146}$$

$$\frac{\Gamma(K^+ \to \pi\mu\bar{\nu})}{\Gamma(K^+ \to \pi e\bar{\nu})} = \frac{\sum_j |C_{2j}^{us}|^2}{\sum_j |C_{1j}^{us}|^2} \times \left[\frac{\Gamma(K^+ \to \pi\mu\bar{\nu})}{\Gamma(K^+ \to \pi e\bar{\nu})}\right]_{\rm SM} , \tag{7.147}$$

with the Wilson coefficients C_{ij}^{us} given in Eq. (7.142). The SM contributions for the first two ratios are given by the analogous expressions to Eqs. (7.143,7.144) [149,150]. The SM contributions to $K_{\ell 3}$ are given by [151, 152]

$$\frac{\Gamma(K^+ \to \pi\mu\bar{\nu})}{\Gamma(K^+ \to \pi e\bar{\nu})} = \frac{I_{K\mu}^{(0)}(\lambda_i)\left(1 + \delta_{\rm EM}^{K\mu} + \delta_{\rm SU(2)}^{K\pi}\right)}{I_{Ke}^{(0)}(\lambda_i)\left(1 + \delta_{\rm EM}^{Ke} + \delta_{\rm SU(2)}^{K\pi}\right)} , \tag{7.148}$$

where quantities $I_{K\ell}^{(0)}(\lambda_i)$, $\delta_{\rm EM}^{K\ell}$, $\delta_{\rm SU(2)}^{K\pi}$ encoding phase-space factors, electromagnetic and isospin corrections can be found in Refs. [151–153]. The numerical results for the SM contributions are collected in Table 7.8.

$c \to s$ transitions

We consider the ratios $\Gamma(D \to K\mu\nu)/\Gamma(D \to Ke\nu)$ and $\Gamma(D_s \to \tau\nu)/\Gamma(D_s \to \mu\nu)$, constraining respectively $\mu - e$ and $\tau - \mu$ non-universality.

For $D \to K\ell\nu$, we consider charged and neutral modes separately. For $D^+ \to \bar{K}^0\ell^+\nu$ we take the separate branching ratios from the PDG assuming no correlation. For $D^0 \to K^-\ell^+\nu$ we take the results from the PDG constrained fit, including the 5% correlation. We construct the D^+ and D^0 ratios separately, obtaining $\Gamma(D^+ \to \bar{K}^0\mu^+\nu)/\Gamma(D^+ \to \bar{K}^0e^+\nu) = 1.05(9)$ and $\Gamma(D^0 \to K^-\mu^+\nu)/\Gamma(D^0 \to K^-e^+\nu) = 0.93(4)$. These two ratios, corresponding to the same theoretical quantity (isospin-breaking effects are neglected here), are combined according to the PDG averaging prescription. Since there is a $\sim 1\,\sigma$ tension between both results, we rescale the error by the factor $S = 1.3$.

For $D_s \to \ell\nu$ we take the individual branching fractions from the PDG, assuming no correlation. The resulting experimental numbers for both ratios are collected in Table 7.8.

The model predictions for these ratios are:

$$\frac{\Gamma(D \to K\mu\bar{\nu})}{\Gamma(D \to Ke\bar{\nu})} = \frac{\sum_j |C_{2j}^{cs}|^2}{\sum_j |C_{1j}^{cs}|^2} \times \left[\frac{\Gamma(D \to K\mu\bar{\nu})}{\Gamma(D \to Ke\bar{\nu})}\right]_{\rm SM} , \tag{7.149}$$

$$\frac{\Gamma(D_s \to \tau\bar{\nu})}{\Gamma(D_s \to \mu\bar{\nu})} = \frac{\sum_j |C_{3j}^{cs}|^2}{\sum_j |C_{2j}^{cs}|^2} \times \left[\frac{\Gamma(D_s \to \tau\bar{\nu})}{\Gamma(D_s \to \mu\bar{\nu})}\right]_{\rm SM} , \tag{7.150}$$

with the Wilson coefficients C_{ij}^{cs} given in Eq. (7.142).

Our SM prediction for the leptonic decay modes includes electromagnetic corrections following [154]. For the SM prediction of the semileptonic modes we use the BESIII determination of the form factor parameters in the simple pole scheme as quoted in HFAG [28]. The resulting SM predictions are given in Table 7.8.

$b \to s$ transitions

We consider here $b \to s$ transitions that are loop-mediated in the SM but receive NP contributions at tree-level in our model (via Z' and Z with anomalous couplings). To the level of precision we are working, the normalization factors in the SM amplitude (G_F and CKM elements) can be taken from tree-level determinations within the SM, and it is not necessary in this case to consider only ratios where these cancel out.

Mass difference in the B_s system

The observable ΔM_s constitutes a strong constraint on the $Z'sb$ coupling, independent of the coupling to leptons. In order to minimize the uncertainty from hadronic matrix elements, we consider the ratio $\Delta M_s/\Delta M_d$. We note that within our model set-up, ΔM_d does not receive NP contributions at tree-level.

The experimental value for the ratio is obtained from the individual measurements for $\Delta M_{d,s}$, which are known to subpercent precision [28]. The result is given in Table 7.8.

The theory prediction is given by:

$$\frac{\Delta M_s}{\Delta M_d} = \frac{M_{B_s}}{M_{B_d}}\,\xi^2\,\left|\frac{C_{sb}}{C_{db}}\right| = \frac{M_{B_s}}{M_{B_d}}\,\xi^2\,\left|\frac{V_{ts}^2}{V_{td}^2} + \frac{C_{sb}^{\rm NP}}{C_{db}^{\rm SM}}\right| \,, \tag{7.151}$$

where the Wilson coefficients $C_{d_ib} = C_{d_ib}^{\rm SM} + C_{d_ib}^{\rm NP}$ are given by

$$C_{d_ib}^{\rm SM} = \frac{G_F^2 M_W^2}{4\pi^2}(V_{ti}V_{tb}^\star)^2 S_0\,, \qquad C_{d_ib}^{\rm NP} = \frac{\hat{g}^2}{8M_{W'}^2}(\Delta_{i3}^q)^2\,. \tag{7.152}$$

Here $S_0 = 2.322 \pm 0.018$ is the loop function in the SM [120]. The parameter $\xi^2 = f_{B_s}^2 B_{B_s}^{(1)}/f_{B_d}^2 B_{B_d}^{(1)}$ is a ratio of decay constants and matrix elements determined from lattice QCD. We consider the latest determination of the parameter ξ from the FNAL/MILC collaborations [155]: $\xi = 1.206(18)(6)$. The SM prediction is given by the first term in Eq. (7.151) and results in $(\Delta M_s/\Delta M_d)_{\rm SM} = 31.2(1.8)$.

$b \to s\ell^+\ell^-$ observables

We consider all $b \to s\ell\ell$ observables used in the fit of Ref. [119]:

- Branching ratios for $B \to X_s\mu^+\mu^-$ and $B_s \to \mu^+\mu^-$ [101, 103, 156–158].
- Branching ratios for $B \to Ke^+e^-$ (in the bin $[1, 6]$ GeV^2) and $B \to K\mu^+\mu^-$ (both at low and high q^2) [84, 159].

- Branching ratios, longitudinal polarization fractions and optimized angular observables [89,160,161] for $B \to K^* e^+ e^-$ (at very low q^2) and $B \to K^* \mu^+ \mu^-$, $B_s \to \phi \mu^+ \mu^-$ (both at low and high q^2) [162–168].

Definitions, theoretical expressions and discussions on theoretical uncertainties can be found in Refs. [89, 119]. We follow the approach of Ref. [169] for $B \to V$ form factors, and take into account the lifetime effect for B_s measurements at hadronic machines [170] for $B_s \to \mu\mu$ [171] and $B_s \to \phi\mu\mu$ [172] decays.

We implement the fit in two different ways. First, we construct the full χ^2 as a function of the model parameters, including all theoretical and experimental correlations, exactly as in Ref. [119].[17] Second, in order to provide simplified expressions to allow the reader to repeat the fit without too much work, we perform a global fit to the relevant coefficients of the effective weak Hamiltonian introduced in Section 4.2.2. We consider the coefficients receiving non-negligible NP contributions within our model, i.e. $(C_9^\mu, C_{10}^\mu, C_9^e, C_{10}^e)$, and provide the best fit points, standard deviations and correlation matrix.[18] These are collected in Table 7.8. The NP contributions to the Wilson coefficients ($C_i^\ell = C_i^{\mathrm{NP}\ell} + C_i^{\mathrm{NP}\ell}$) are

$$\begin{aligned} C_9^{\mathrm{NP}a} &= -\frac{\sqrt{2}}{G_F}\frac{\pi}{\alpha}\frac{1}{V_{tb}V_{ts}^*}\frac{\hat{g}^2}{8M_{W'}^2}(\Delta^q)_{bs}\left[(\Delta^\ell)_{aa} + \zeta\left(4s_W^2 - 1\right)\right] , \\ C_{10}^{\mathrm{NP}a} &= \frac{\sqrt{2}}{G_F}\frac{\pi}{\alpha}\frac{1}{V_{tb}V_{ts}^*}\frac{\hat{g}^2}{8M_{W'}^2}(\Delta^q)_{bs}\left[(\Delta^\ell)_{aa} - \zeta\right] . \end{aligned} \tag{7.153}$$

Using these four coefficients as "pseudo observables" and constructing the χ^2 function leads to a linearized approximation to the fit. We have checked that the result of such a fit is in reasonable agreement with the full fit.

$b \to c$ transitions

We consider the exclusive ratios $R(D^{(*)}) \equiv \Gamma(B \to D^{(*)}\tau\bar{\nu})/\Gamma(B \to D^{(*)}\ell\bar{\nu})$, and the inclusive ratio $R(X_c) \equiv \Gamma(B \to X_c\tau\bar{\nu})/\Gamma(B \to X_c\ell\bar{\nu})$ as measures of flavor non-universality between the τ and the light leptons, as well as the ratios $\Gamma(B \to D^{(*)}\mu\bar{\nu})/\Gamma(B \to D^{(*)}e\bar{\nu})$ constraining $e - \mu$ non-universality.

The experimental value for the inclusive ratio $R(X_c)$ is obtained from the PDG averages for $\mathrm{Br}(\bar{b} \to X\tau^+\nu)$ and $\mathrm{Br}(\bar{b} \to Xe^+\nu)$. The allowed size of lepton flavor universality violating effects in $b \to c\ell\nu$ ($\ell = e, \mu$) transitions is not trivial to account for given that experimental analyses tend to present combined results for the electron and muon data samples. This aspect was also stressed in Ref. [173]. Experimental results are however reported separately for the e and μ samples in an analysis performed by the BaBar collaboration [174]. We use the values of $\mathrm{Br}(B \to D^{(*)}\ell\bar{\nu})$ reported in Table IV of Ref. [174] to extract the ratios $\Gamma(B \to D^{(*)}\mu\bar{\nu})/\Gamma(B \to D^{(*)}e\bar{\nu})$. The correlation between the two ratios is

[17] The fit in Ref. [119] includes $b \to s\gamma$ observables. These observables are not included in our fit.

[18] Contributions to the primed operators $Q_{9',10'}$ are found to be negligible since the right-handed flavor changing $Z^{(\prime)}$ couplings to down-type quarks are suppressed by m_f^2/u^2, see Section 7.3.3.

estimated from the information provided in [174], adding the covariance for the systematic and statistical errors. For the experimental values of $R(D)$ and $R(D^*)$ we consider the latest HFAG average [28]. The latter includes $R(D)$ and $R(D^*)$ measurements performed by BaBar and Belle [175, 176], the LHCb measurement of $R(D^*)$ [177], and the independent Belle measurement of $R(D^*)$ using a semileptonic tagging method [178].[19] The results are summarized in Table 7.8.

The model expressions for these ratios are:

$$\frac{\Gamma(B^- \to D^{(*)}\mu\bar{\nu})}{\Gamma(B^- \to D^{(*)}e\bar{\nu})} = \frac{\sum_j |C_{2j}^{cb}|^2}{\sum_j |C_{1j}^{cb}|^2} \times \left[\frac{\Gamma(B^- \to D^{(*)}\mu\bar{\nu})}{\Gamma(B^- \to D^{(*)}e\bar{\nu})}\right]_{\rm SM} , \tag{7.154}$$

$$R(D^{(*)}) = \frac{2\left(\sum_j |C_{3j}^{cb}|^2\right)}{\sum_j (|C_{1j}^{cb}|^2 + |C_{2j}^{cb}|^2)} \times R(D^{(*)})^{\rm SM} , \tag{7.155}$$

$$R(X_c) = \frac{\sum_j |C_{3j}^{cb}|^2}{\sum_j |C_{1j}^{cb}|^2} \times R(X_c)^{\rm SM} , \tag{7.156}$$

where the Wilson coefficients C_{ij}^{cb} are given in Eq. (7.142). We use the SM predictions of $R(D)$ and $R(D^*)$ obtained in Refs. [181, 182]. Note that recent determinations of $R(D)$ in lattice QCD are compatible with the one used here [183, 184]. For $R(X_c)$ we use the SM prediction reported in Ref. [185]. For the ratios $\Gamma(B^- \to D^{(*)}\mu\bar{\nu})/\Gamma(B^- \to D^{(*)}e\bar{\nu})$ we derive the SM predictions using the Caprini-Lellouch-Neubert parametrization of the form factors [186], with the relevant parameters taken from HFAG [28]. The resulting SM predictions are given in Table 7.8.

Lepton Flavor Violation

We consider current limits on the lepton flavor violating decays $\tau \to 3\mu$ and $Z \to \tau\mu$. The decay $Z \to \tau\mu$ occurs due to gauge mixing effects. The decay rate for $Z \to \tau\mu \equiv (\tau^+\mu^- + \tau^-\mu^+)$ is

$$\Gamma(Z \to \tau\mu) = \frac{M_Z}{48\pi}\left(\zeta\, n_2\, \frac{g_2^4}{n_1^4}\Delta_\mu\Delta_\tau\,\epsilon^2\right)^2 . \tag{7.157}$$

We use the limit $\mathrm{Br}(Z \to \tau\mu) < 1.2 \times 10^{-5}$ [23].

The decay $\tau \to 3\mu$ receives tree-level contributions from $Z^{(\prime)}$ exchange, the decay rate is given by

$$\Gamma(\tau \to 3\mu) = \frac{[2\,(C_{LL}^{\tau\mu})^2 + (C_{LR}^{\tau\mu})^2]\, m_\tau^5}{1536\pi^3} , \tag{7.158}$$

[19] New results for $R(D^*)$ and the tau polarization asymmetry in $B \to D^*\tau\nu$ decays (P_τ) using a hadronic tag have been presented by the Belle collaboration in Ref. [179]. The reported measurements are $R(D^*) = 0.276 \pm 0.034^{+0.029}_{-0.026}$ and $P_\tau = -0.44 \pm 0.47^{+0.20}_{-0.17}$ [179]. These measurements are not included in our analysis but would have a negligible impact if added given that the weighted average for $R(D^*)$ remains basically the same and the experimental uncertainty in P_τ is still very large. Note that the measured tau polarization asymmetry is well compatible with the SM prediction $P_\tau = -0.502^{+0.006}_{-0.005} \pm 0.017$ [180].

$\lambda = 0.22541(^{+30}_{-21})$	[187]	$A = 0.8212(^{+66}_{-338})$	[187]
$\bar{\rho} = 0.132(^{+21}_{-21})$	[187]	$\bar{\eta} = 0.383(^{+22}_{-22})$	[187]
$G_F = 1.16638(1) \times 10^{-5}$ GeV^{-2}	[23]	$M_Z = 91.1876(21)$ GeV	[23]
$\alpha = 1/137.036$	[23]		

Table 7.9: *Electroweak and CKM inputs.*

where the Wilson coefficients $C_{LL}^{\tau\mu}$ and $C_{LR}^{\tau\mu}$ are given by

$$\begin{aligned} C_{LL}^{\ell_a\ell_b} &= \frac{\hat{g}^2}{4M_{W'}^2}\Delta_{ab}^{\ell}\left[\Delta_{bb}^{\ell} + \zeta\left(2s_W^2 - 1\right)\right] , \\ C_{LR}^{\ell_a\ell_b} &= \frac{\hat{g}^2}{2M_{W'}^2}\,\zeta\,\Delta_{ab}^{\ell}\,s_W^2 . \end{aligned} \tag{7.159}$$

We use the HFAG limit $\mathrm{Br}(\tau \to 3\mu) < 1.2 \times 10^{-8}$ [28].

7.3.5 Global fit

Fitting procedure

We first fix the values of g, g' and the electroweak vev v with the values of $\{G_F, \alpha, M_Z\}$ reported in Table 7.9. The $\mathrm{SU}(2)_1$ gauge coupling g_1 is then determined as a function of g_2. The observables considered will depend on seven model parameters:

$$\begin{aligned} M_{Z'} &: \text{The } Z' \text{ mass, note that } M_{W'} \simeq M_{Z'} , \\ g_2 &: \text{The } \mathrm{SU}(2)_2 \text{ gauge coupling} , \\ \zeta &: \text{Controls the size of gauge mixing effects, see Eq. (7.115)} , \\ \Delta_s, \Delta_b, \Delta_\mu, \Delta_\tau &: \text{Determine the gauge couplings to fermions, see Eq. (7.134)} . \end{aligned}$$

The observables will also depend on the CKM inputs $\{\lambda, A, \bar{\rho}, \bar{\eta}\}$. We construct a global χ^2 function that includes information from electroweak precision data at the Z and W poles together with flavor data. It reads

$$\chi^2 \equiv (O - O_{\rm exp})^T \overline{\Sigma}^{-1} (O - O_{\rm exp}) + \sum_{x=\lambda,A,\bar{\rho},\bar{\eta}} \frac{(x - \hat{x})^2}{\sigma_\pm^2} , \tag{7.160}$$

with $\overline{\Sigma}$ being the covariance matrix, O denoting the observables included in the analysis and $O_{\rm exp}$ the corresponding experimental mean values. These are described in Section 7.3.4. The CKM inputs $\{\lambda, A, \bar{\rho}, \bar{\eta}\}$ are included as pseudo-observables in the fit taking into account the values in Table 7.9.[20] The latter are reported in the form $\hat{x}^{+\sigma_+}_{-\sigma_-}$. In the χ^2 we introduce the asymmetric error: $\sigma_\pm = \sigma_+$ (for $x > \hat{x}$) and $\sigma_\pm = \sigma_-$ (for $x < \hat{x}$).

The global fit includes then seven model parameters $\{M_{Z'}, g_2, \Delta_s, \Delta_b, \Delta_\mu, \Delta_\tau, \zeta\}$ and four CKM quantities $\{\lambda, A, \bar{\rho}, \bar{\eta}\}$. To sample the 11-dimensional parameter space we use the affine invariant Markov chain Monte Carlo ensemble sampler `emcee` [188].

[20] These CKM inputs are obtained from a fit by the CKMFITTER group with only tree-level processes [187], as used in Ref. [155].

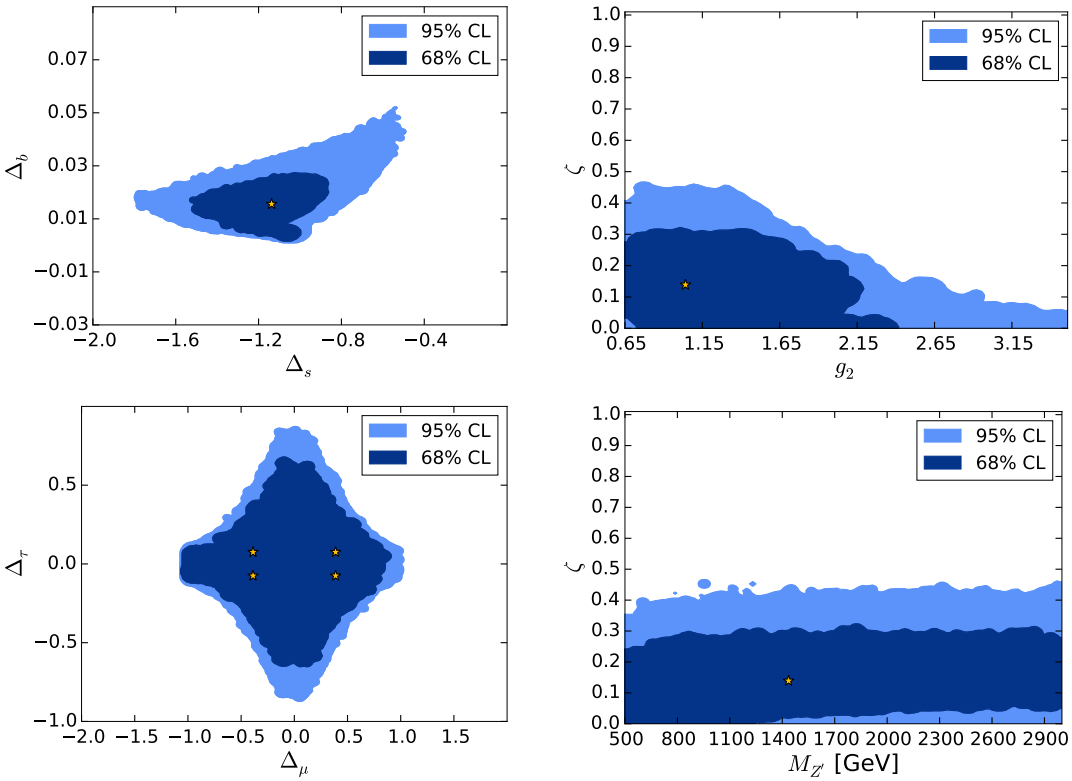

Figure 7.8: *Allowed regions for the model parameters at* 68% *and* 95% *CL from the global fit. The best fit point is illustrated with a star.*

Results of the fit

We restrict the parameter space to 500 GeV $\leq M_{Z'} \leq$ 3000 GeV, $g < g_2 < \sqrt{4\pi}$, $|\Delta_a| \leq 3$ and $0 \leq \zeta \leq 1$. The global minimum of the χ^2 is found to be at

$$\{M_{Z'}\ [\text{GeV}], g_2, \Delta_s, \Delta_b, |\Delta_\mu|, |\Delta_\tau|, \zeta\} = \{1436, 1.04, -1.14, 0.016, 0.39, 0.075, 0.14\}\,, \tag{7.161}$$

with the CKM values $\{\lambda, A, \bar{\rho}, \bar{\eta}\}$ within the 1σ range in Table 7.9. It is enlightening to characterize the best-fit point in terms of the couplings appearing in the Lagrangian. We find that the corresponding Yukawas are, up to a global sign,

$$\lambda_\ell \simeq \begin{pmatrix} -1.2 & 0 \\ 0 & -0.3 \\ 0 & -0.06 \end{pmatrix} \times \frac{M_L}{\text{TeV}}\,, \qquad \lambda_q \simeq \begin{pmatrix} -1.2 & 0 \\ 0 & 1.8 \\ 0 & -0.03 \end{pmatrix} \times \frac{M_Q}{\text{TeV}}\,. \tag{7.162}$$

At the best-fit point we obtain $\chi^2_{\text{min}} = 54.8$, to be compared with the corresponding value in the SM-limit $\chi^2_{\text{SM}} = 93.7$. We derive contours of $\Delta\chi^2 \equiv \chi^2 - \chi^2_{\text{min}}$ in two-dimensional planes after profiling over all the other parameters, taking $\Delta\chi^2 = 2.3$ for 68% CL and $\Delta\chi^2 = 6.18$ for 95% CL. Allowed regions for the model parameters obtained in this way are shown in Figure 7.8.

There is a four-fold degeneracy of the χ^2 minimum with the sign of $\Delta_{\mu,\tau}$ as no observable in the fit is sensitive to the relative sign between Δ_μ and Δ_τ. The

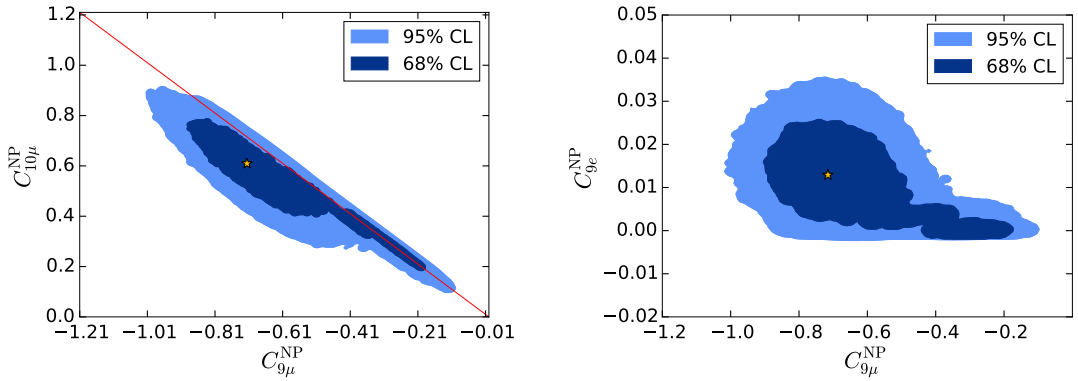

Figure 7.9: *Allowed regions at* 68% *and* 95% *CL from the global fit for the Wilson coefficients of* $b \to s\ell^+\ell^-$ *transitions. The best fit point is illustrated with a star. The red line on the left plot illustrates the correlation* $C_9^{\rm NP\mu} = -C_{10}^{\rm NP\mu}$.

allowed values of $\Delta_{\mu,\tau}$ lie in the region $|\Delta_{\mu,\tau}| \lesssim 1$. While Δ_b is bounded to be very small $\sim 10^{-2}$, the allowed values for Δ_s are around -1. The negative sign obtained for the combination $\Delta_s\Delta_b$ is related to the preference for negative values of $C_9^{\rm NP\mu}$ by $b \to s\ell^+\ell^-$ data. The allowed regions for the Wilson coefficients of $b \to s\ell^+\ell^-$ transitions from the global fit are shown in Figure 7.9. Note that with the assumed flavor structure we have the correlation $C_{10}^{\rm NPe} = (4s_W^2 - 1)C_9^{\rm NPe}$. The relation $C_9^{\rm NP\mu} = -C_{10}^{\rm NP\mu}$ on the other hand holds in our model only in the absence of gauge mixing effects. Departures from this correlation are possible as gauge mixing effects can be sizable, see Figure 7.9 (left).

Allowed values at 68% and 95% CL for R_K and $R(D^*)$ are shown in Figure 7.10. The best fit point presents a sizable deviation from the SM in R_K in the direction of the LHCb measurement while the ratios $R(D^*)$ are SM-like. Note that the NP scaling of $R(D)$ is the same as for $R(D^*)$ because the W' couplings are mostly left-handed, with the right-handed couplings suppressed by m_f^2/u^2. A significant enhancement of $R(D^{(*)})$ is possible within the allowed parameter region. The model presents a positive correlation between R_K and $R(D^{(*)})$ so that R_K is above its best-fit value whenever $R(D^{(*)})$ gets enhanced. The ratios $\Gamma(B \to D^{(*)}\mu\nu)/\Gamma(B \to D^{(*)}e\nu)$ are found to be SM-like with possible deviations only at the $\sim 1\%$ level. As expected, $R(X_c)$ and $R(D^{(*)})$ show a strong correlation, in the region of the parameter space where $R(D^{(*)})$ accommodates the current experimental values one obtains a slight tension in $R(X_c)$ with experiment. The flavor observables with light-mesons and leptonic τ-decays are found to be in good agreement with the SM and experiment, we show the resulting allowed values for $K \to \mu\nu/K \to e\nu$ and $\tau \to \mu\nu\bar{\nu}/\mu \to e\nu\bar{\nu}$ as an example in Figure 7.10.

As noted in Ref. [134], gauge mixing effects play a crucial role in the possible enhancement of $R(D^{(*)})$ in this model. In Figure 7.10 we also show the results of the global fit for $R(D^*)$ as a function of the parameter controlling the size of gauge mixing effects ζ. Having an enhancement of $R(D^*)$ of order $\sim 20\%$ as suggested by the experimental measurements is only possible for $\zeta \ll 1$. The situation is very different for R_K, with the parameter ζ playing no major role in this case as shown in Figure 7.10. We find that the allowed points from the global fit accommodating

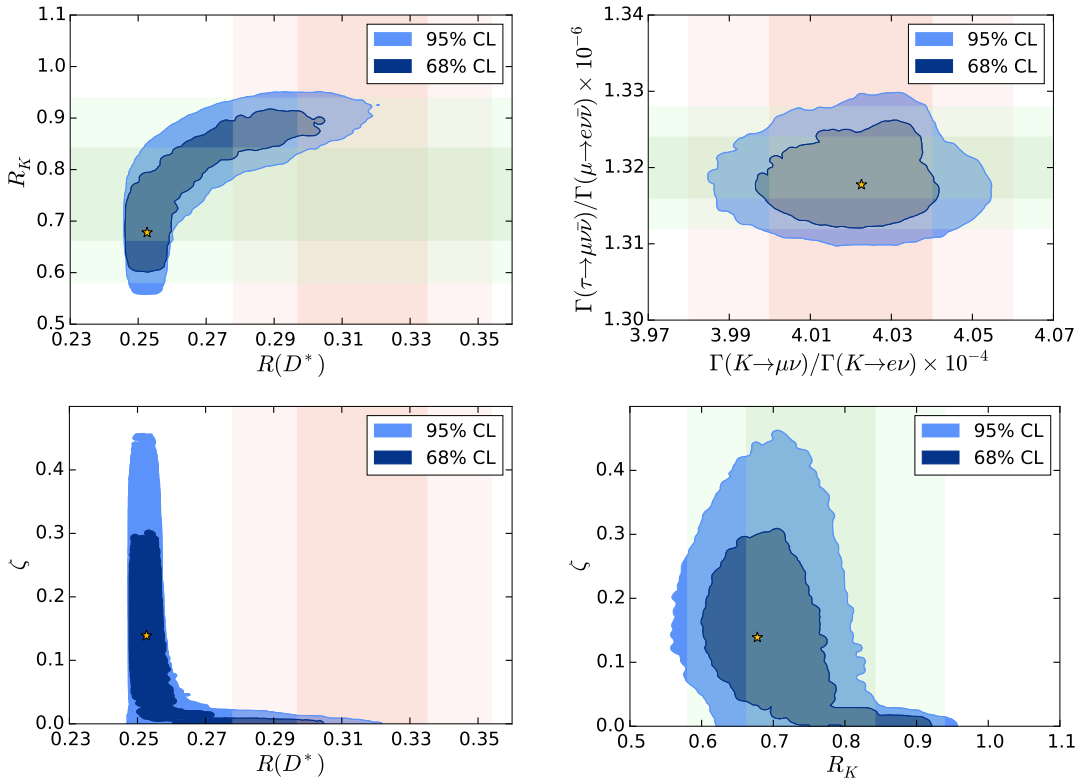

Figure 7.10: *Allowed regions at* 68% *and* 95% *CL from the global fit. Experimental values for these observables are also shown at* 1σ *(dark-band) and* 2σ *(light-band). The best fit point is illustrated with a star.*

both R_K and $R(D^{(*)})$ within 2σ lie within a very restricted region:

$$M_{Z'} \in [500, 1710]\ \text{GeV}\,, \quad g_2 \in [1.2, 3.5]\,, \quad \zeta \in [0, 0.02]\,, \quad \Delta_s \in [-1.16, -0.97]\,,$$
$$\Delta_b \in [0.003, 0.007]\,, \quad |\Delta_\mu| \in [0.94, 0.99]\,, \quad |\Delta_\tau| \in [0, 0.11]\,. \tag{7.163}$$

The Z' mass and the $\mathrm{SU}(2)_2$ gauge coupling g_2 are positively correlated, going from $g_2 \sim 1$ for $M_{Z'} \sim 500$ GeV up to the perturbativity limit $g_2 \leq \sqrt{4\pi}$ for $M_{Z'} \sim 1700$ GeV. A limit on $\tan\beta$ can be derived in this region using Eq. (7.115), we get $\tan\beta \in [0.2, 0.65]$. Similarly, in this region the $\mathrm{SU}(2)_1$ gauge coupling satisfies $0.66 \leq g_1 \leq 0.78$ and the combination $\hat{g} = g g_2/g_1$ is found to be within $1 \leq \hat{g} \leq 3.4$. Note that the Z' and W' interactions with the SM fermions are proportional to $1 - \Delta_a^2$, see Eq. (7.134). In the parameter space region where both R_K and $R(D^{(*)})$ are accommodated within 2σ, the massive gauge bosons, Z' and W', couple predominantly to the third fermion generation.

7.3.6 Predictions

In the following we take the current measured values of R_K and $R(D^{(*)})$ at face value, focusing on the parameter space region described in Eq. (7.163). We are interested in possible signatures that can be used to test or falsify this scenario with upcoming measurements at the LHC and flavor factories.

Differential distributions in $B \to D^{(*)}\tau\nu$ decays

Due to the gauge structure of the model, new physics contributions to the $B \to D^{(*)}\ell\nu$ decay amplitudes have the same Dirac structure as the SM contribution to a good approximation. This gives rise to a clean prediction

$$\frac{R(D)}{R(D^*)} = \left[\frac{R(D)}{R(D^*)}\right]_{\rm SM} , \tag{7.164}$$

which is compatible with current data [28]. The inclusive ratio $R(X_c)$ can provide an additional handle to test the proposed scenario. The model gives rise to an enhancement in $R(X_c)$ within the parameter space region considered, we obtain $0.24 \leq R(X_c) \leq 0.29$. The Dirac structure of the new physics contributions can also be tested by using information from the $q^2 \equiv (p_B - p_{D^{(*)}})^2$ spectra and by measuring additional observables that exploit the rich kinematics and spin of the final state particles. The differential decay rate for $B \to D^{(*)}\tau\nu$ is affected in the model with a global rescaling factor, implying that forward-backward asymmetries as well as the τ and D^* polarization fractions are expected to be as in the SM. For recent studies of differential distributions in $b \to c\tau\nu$ decays see Refs. [180, 182, 189–200]. Future measurements of $b \to c\tau\nu$ transitions at the Belle-II experiment will be crucial to disentangle possible new physics contributions in these decays [201].

Lepton universality tests in R_M

Confirming the violation of lepton flavor universality in other $b \to s$ observables would be definite evidence in favor of new physics at work. Examples of such additional observables are R_M, with $M = K^*, \phi$ [73, 202], defined analogously to R_K,

$$R_M^{[q_1^2, q_2^2]} = \frac{\int_{q_1^2}^{q_2^2} d\Gamma(B_q \to M\mu^+\mu^-)}{\int_{q_1^2}^{q_2^2} d\Gamma(B_q \to M e^+ e^-)} , \tag{7.165}$$

with $q = d, s$ for $M = K^*, \phi$.[21]

The expected values for R_K, R_{K^*} and R_ϕ within each bin are strongly correlated, except for the fact that hadronic uncertainties are mostly independent (but small). From the results of the fit, we find the following expected ranges for the different ratios (q^2 in GeV^2):

$$\begin{aligned}
R_K^{[1,6]} &\in [0.62, 0.91] \text{ at } 68\% \text{ CL} , & R_K^{[1,6]} &\in [0.57, 0.95] \text{ at } 95\% \text{ CL} , \\
R_{K^*}^{[1.1,6]} &\in [0.66, 0.91] \text{ at } 68\% \text{ CL} , & R_{K^*}^{[1.1,6]} &\in [0.62, 0.95] \text{ at } 95\% \text{ CL} , \\
R_{K^*}^{[15,19]} &\in [0.61, 0.90] \text{ at } 68\% \text{ CL} , & R_{K^*}^{[15,19]} &\in [0.56, 0.94] \text{ at } 95\% \text{ CL} , \\
R_\phi^{[1.1,6]} &\in [0.64, 0.91] \text{ at } 68\% \text{ CL} , & R_\phi^{[1.1,6]} &\in [0.60, 0.94] \text{ at } 95\% \text{ CL} , \\
R_\phi^{[15,19]} &\in [0.61, 0.90] \text{ at } 68\% \text{ CL} , & R_\phi^{[15,19]} &\in [0.56, 0.94] \text{ at } 95\% \text{ CL} ,
\end{aligned} \tag{7.166}$$

[21] See Ref. [132] for other observables in $B \to K^*\ell\ell$ testing lepton-flavor non-universality.

where it is understood that a strong (positive) correlation exists among all the predictions, lower values of one observable corresponding to lower values of another and viceversa.[22]

Lepton flavor violation

One of the first *generic* consequences of the violation of lepton flavor universality is lepton flavor violation [12], as explored in connection to the B-meson anomalies in Refs. [14, 40, 197, 203–210]. In our model, the branching fraction for $\tau \to 3\mu$ is proportional to Δ_τ^2 and is therefore suppressed for $|\Delta_\tau| \simeq 0$. When $|\Delta_\tau|$ is near its upper bound, $|\Delta_\tau| \simeq 0.1$, we obtain values for $\mathrm{Br}(\tau \to 3\mu)$ that saturate the current experimental limit 1.2×10^{-8}. Semileptonic decays of the tau lepton into a muon and a pseudo-scalar meson also receive tree-level contributions from $Z^{(\prime)}$ exchange, these will also be proportional to Δ_τ^2 so that the largest rates possible will be obtained for $|\Delta_\tau| \simeq 0.1$. In our model the decays $\tau \to \mu\eta^{(\prime)}$ receive important new physics contributions through the axial-vector strange-quark current. Following [211] we obtain $\mathrm{Br}(\tau \to \mu\eta') \leq 3.9 \times 10^{-8}$ and $\mathrm{Br}(\tau \to \mu\eta) \leq 4.2 \times 10^{-8}$, very close to the current experimental limits $\mathrm{Br}(\tau \to \mu\eta')_{\mathrm{exp}} \leq 1.3 \times 10^{-7}$ and $\mathrm{Br}(\tau \to \mu\eta)_{\mathrm{exp}} \leq 6.5 \times 10^{-8}$ [212]. The observation of lepton flavor violating tau decays decays might therefore lie within the reach of future machines such as Belle-II, where an improvement of the current experimental bounds by an order of magnitude can be expected [201]. On the other hand, due to the suppression of gauge mixing effects ($\zeta \ll 1$) the decay $Z \to \tau\mu$ lies well-below the current experimental limit, for which we obtain $\mathrm{Br}(Z \to \mu\tau) \leq 1.2 \times 10^{-9}$.

Direct searches for new states at the LHC

In this model we expect a plethora of new states lying at the TeV scale: scalar bosons (in the CP-conserving limit we would have two CP-even Higgs bosons, one CP-odd Higgs and one charged scalar, cf. Section 7.3.2), heavy fermions and the massive vector bosons W', Z'.

The heavy VL leptons will be pair-produced at the LHC via Drell-Yan processes due to their coupling to the massive electroweak gauge bosons. These will decay into gauge bosons and charged leptons or neutrinos. Though no dedicated searches for VL leptons have been performed at the LHC, one can obtain limits on their mass and production cross-section by recasting existing multilepton searches [213]. It was found that current limits for a heavy lepton doublet decaying to $\ell = e, \mu$ flavors are around 450 GeV while for decays into τ-leptons the limits are around 270 GeV [213]. Searches for pair production of heavy VL quarks at the LHC focus primarily into final states with a third generation fermion and bosonic states, setting upper limits on the VL quark masses ranging from ~ 700 GeV up to ~ 1 TeV [214–219].

The massive vector bosons W', Z' couple predominantly to the third fermion generation. The LHC phenomenology of this type of states has been discussed in Ref. [173]. The Z' coupling to muons is found to be at most $\sim 12\%$ of its coupling

[22] As it happened for the other models presented in this chapter, the prediction of the model for R_{K^*} in the $q^2 \in [1.1, 6]$ GeV^2 bin is in good agreement with the measured value reported by the LHCb Collaboration [1]. See note added at the beginning of the chapter.

to τ-leptons. In the quark sector, the Z' coupling to the second quark generation is found to be at most $\sim 36\%$ of the coupling to third generation quarks. The Z' boson would be produced at the LHC via Drell-Yan processes due to its coupling to b-quarks and s/c-quarks.

The total Z' width normalized by the Z' mass ($\Gamma_{Z'}/M_{Z'}$) is found to grow with $M_{Z'}$, since $\hat{g}$ and $M_{Z'}$ are positively correlated. Assuming that the Z' can only decay into the SM fermions we have

$$\frac{\Gamma_{Z'}}{M_{Z'}} \simeq \frac{\hat{g}^2}{48\pi}\left[3\sum_{q=s,b}(1-\Delta_q^2)^2+\sum_{\ell=\mu,\tau}(1-\Delta_\ell^2)^2\right], \tag{7.167}$$

where we have neglected fermion mass effects. We obtain that $\Gamma_{Z'}/M_{Z'}$ is between 2% and 31%, with $\Gamma_{Z'}/M_{Z'} \gtrsim 10\%$ for $M_{Z'} \gtrsim 1$ TeV.

If kinematically open, additional decay channels of the Z' boson would reduce the branching fractions to SM particles by enhancing the total Z' width, making the Z' resonance broader. The latter scenario will generically be the case provided the VL fermions are light enough, opening decay channels of the Z' boson into a heavy VL fermion and a SM-like fermion or into a VL fermion pair. The decay rate for these processes is given by:

$$\begin{aligned}
\Gamma(Z'\to F_i\bar{f}_j) &\simeq \frac{\lambda^{1/2}(1,x_i,x_j)\,\hat{g}^2 N_C M_{Z'}}{192\pi}\left[2-x_i-x_j-(x_i-x_j)^2\right](\Sigma_{ij})^2\,,\\
\Gamma(Z'\to F_i\bar{F}_i) &\simeq \frac{\lambda^{1/2}(1,x_i,x_i)\,\hat{g}^2 N_C M_{Z'}}{96\pi}\left\{(1-x_i)\left((\Omega^{Q,L}_{ii})^2+\frac{g_1^4}{g_2^4}\right)-6\,\frac{g_1^2}{g_2^2}\,x_i\,\Omega^{Q,L}_{ii}\right\}.
\end{aligned} \tag{7.168}$$

Here $\lambda(x,y,z) = x^2+y^2+z^2-2(xy+yz+xz)$, $N_C = 3(1)$ for (un)colored fermions and $x_i = m_i^2/M_{Z'}^2$. We have denoted by F_i a generic heavy fermion and by f_j one of the SM-like fermions. The matrices Σ and $\Omega^{Q,L}$ have been defined in Eqs. (7.135) and (7.136). The Z' decays into a heavy fermion and a SM-like fermion are accidentally suppressed due to the small entries of the Σ matrix within the parameter region of interest. These decays therefore give small contributions to the total width in general. The decays into a pair of heavy fermions, on the other hand, can give a significant contribution to the total Z' width when kinematically allowed. For instance, if the masses of the heavy leptons lie around 450 GeV we obtain a contribution to $\Gamma_{Z'}/M_{Z'}$ from the decays $Z' \to E_i\bar{E}_i, N_i\bar{N}_i$ ($i = 1,2$) of about 20% for $M_{Z'} \sim 1.2$ TeV, making the Z' boson a very wide resonance in this case: $\Gamma_{Z'}/M_{Z'} \sim 30\% - 50\%$.

The ATLAS and CMS collaborations have searched for a resonance in the $\tau^+\tau^-$ channel at $\sqrt{s} = 8$ TeV [58, 60, 220, 221]. Among these, the strongest limits are those coming from ATLAS and they place important bounds on the model. We have evaluated the Z' production cross-section at the LHC using the computer tool `MadGraph (MG5_aMC_2.4.2)` [124]. We find that it is possible to exclude the low-mass region where the Z' resonance remains reasonably narrow and there is not much room for additional decay channels giving large contributions to the total width. The latter would require having very light exotic fermions, entering in conflict with direct searches for these states at colliders. In the heavy Z' mass region ($\gtrsim 1$ TeV) the

Z' resonance becomes wide ($\Gamma_{Z'}/M_{Z'} \gtrsim 10\%$) and the interpretation of the current experimental results based on the search of a relatively narrow resonance is not valid anymore. Dedicated searches at the LHC for a broad resonance in the $\tau^+\tau^-$ channel within the mass range $\sim 1 - 1.7$ TeV would then be needed in order to test this scenario.[23] In this regard, a recast of the existing 8 TeV and 13 TeV LHC analyses in $\tau^+\tau^-$ resonance searches allowing for a large resonance width was done in Ref. [222]. This recast of the LHC bounds severely constraints the parameter space of the model; however a dedicated analysis including these constraints lies the scope of this thesis.

The proposed scenario also gives some predictions in the scalar sector relevant for collider searches. Neglecting mixing between the scalar bidoublet Φ and the Higgs doublets $\phi^{(\prime)}$, the scalar spectrum will contain a heavy CP-even neutral scalar transforming as an $\mathrm{SU(2)_L}$ singlet originating from Φ. We will denote this state by h_2. The mass of this scalar is expected to be around the symmetry breaking scale $u \sim$ TeV. The dominant interactions of h_2 are with the heavy fermions and the heavy gauge vector bosons, these are described by

$$\mathcal{L} \supset 2(M_{W'}^2 W_\mu'^+ W'^{-\mu} + \frac{1}{2} M_{Z'}^2 Z'_\mu Z'^\mu)\frac{h_2}{u} - (y_Q)_{ii}\,\bar{Q}_i Q_i\,h_2 - (y_L)_{ii}\,\bar{L}_i L_i\,h_2\,, \quad (7.169)$$

with $Q_i^T = (U_i, D_i)$, $L_i^T = (N_i, E_i)$ $(i = 1, 2)$ and

$$y_Q = \frac{g_2^2}{n_1^2}\begin{pmatrix} \widetilde{M}_{Q_1} & 0 \\ 0 & \widetilde{M}_{Q_2}(\Delta_s^2 + \Delta_b^2) \end{pmatrix}, \qquad y_L = \frac{g_2^2}{n_1^2}\begin{pmatrix} \widetilde{M}_{L_1} & 0 \\ 0 & \widetilde{M}_{L_2}(\Delta_\mu^2 + \Delta_\tau^2) \end{pmatrix}. \quad (7.170)$$

The production of h_2 at the LHC is dominated by gluon fusion mediated by the heavy quarks and is determined by the same parameters entering in the low-energy global fit. At the center-of mass energy $\sqrt{s}$ the production cross-section reads

$$\sigma(pp \to h_2) \simeq \frac{c_{gg}\Gamma(h_2 \to gg)}{M_{h_2} s}\,, \qquad \Gamma(h_2 \to gg) \simeq \frac{\alpha_s^2 M_{h_2}^3}{18\pi^3}\left|\sum_{i=1}^{2}\frac{(y_Q)_{ii}}{u\widetilde{M}_{Q_i}}\right|^2. \quad (7.171)$$

Here c_{gg} represents a dimensionless partonic integral which we estimate using the set of parton distribution functions MSTW2008NLO [223] evaluated at the scale $\mu = M_{h_2}$. In writing the decay rate for $h_2 \to gg$ we have taken the local approximation for the fermionic loops. For $M_{h_2} \sim 1$ TeV, and restricting the rest of the parameters to the region described in Eq. (7.163), we obtain $\sigma(pp \to h_2) \simeq 110 - 290$ fb at $\sqrt{s} = 13$ TeV center-of-mass energy. For $M_{Z'} \sim 1.7$ TeV (and $M_{h_2} \sim 1$ TeV) the production cross-section converges towards ~ 110 fb. The interactions of h_2 in Eq. (7.169) will induce loop-mediated decays into gluons (which will hadronize into jets) and electroweak gauge bosons W^+W^-, ZZ, $\gamma\gamma$, $Z\gamma$. Assuming negligible tree-level decays, the h_2 boson will manifest in this case as a very narrow resonance decaying mainly into a pair of jets. The current experimental sensitivity for dijet-resonances at the LHC around this mass range ($M_{h_2} \sim 1$ TeV) is at

[23] We find our main conclusions in this regard to agree with those posed previously by the authors of Ref. [173] while analyzing a similar new physics case.

the level of 10^3 fb [224, 225]. The decays into electroweak gauge bosons are found to be subdominant and for $M_{Z'} \in [1, 1.7]$ TeV we have: $\text{Br}(h_2 \to WW) \sim 10^{-2}$, $\text{Br}(h_2 \to ZZ, Z\gamma)/\text{Br}(h_2 \to WW) \sim 25\%$, $\text{Br}(h_2 \to \gamma\gamma)/\text{Br}(h_2 \to WW) \sim 1\%$. Note however that in the case where some of the heavy fermions are below the threshold $M_{h_2}/2$, tree-level decay of h_2 into these fermions becomes kinematically open and will generically dominate over the loop-induced decays commented above.

7.3.7 Conclusions

We have performed a phenomenological analysis of a renormalizable and perturbative gauge extension of the SM. We took into account flavor observables sensitive to tree-level new physics contributions as well as bounds from electroweak precision measurements at the Z and W pole. More specifically, we have analyzed the model in light of the current hints of new physics in $b \to c\ell\nu$ and $b \to s\ell^+\ell^-$ semileptonic decays, finding that the flavor anomalies can be accommodated within the allowed regions of the parameter space.

As derived from the phenomenological analysis, strong hierarchies in the flavor structure of the Yukawa couplings are required in order to accommodate both $b \to s\ell^+\ell^-$ and $b \to c\ell\nu$ anomalies. We have taken a phenomenologically oriented approach in this section, not invoking any flavor symmetry behind such structure. One interesting question would be the exploration of possible flavor symmetries accommodating the observed flavor structure. We confirm the conclusions of Ref. [134] regarding the importance of suppressing gauge bosons mixing. This translates in a tuning of $\tan\beta$. Such accidental tuning would be more satisfactory if there was a dynamical or symmetry-based explanation behind. These last points also bring us to the question of the validity of our analysis, based on tree-level new physics effects, once quantum corrections are considered. These corrections might alter the flavor structure of the theory, remove accidental tunings which hold at the classical level as well as introduce new constraints from loop-induced processes such as $b \to s\gamma$. Though such analysis lies beyond the scope of this thesis, it would be relevant in order to establish the viability of the proposed framework if the present deviations in $b \to s\ell^+\ell^-$ and $b \to c\ell\nu$ are confirmed in the future.

From the model building point of view, there are many open questions which we have not addressed in this thesis and would deserve further investigation, one of them being the implementation of a mechanism for the generation of the observed neutrino masses and lepton mixing angles. Our model also lacks a dark matter candidate, motivating the extension of our framework. It would be interesting to pursue the investigation of possible embeddings of the model within a larger gauge group, where the mass of the heavy fermions arise from spontaneous symmetry breaking.

Appendices

7.A Anomaly cancellation conditions in the $\mathrm{U(1)_{BGL}}$ model

In this appendix we present the restrictions on the charges derived from the requisite gauge anomaly cancellation for quarks transforming according to Eq. (2.38) and allowing the leptons to transform in the most general way:

$$\begin{aligned} \mathcal{X}_L^\ell &= \mathrm{diag}\,(X_{eL}, X_{\mu L}, X_{\tau L})\ , \\ \mathcal{X}_R^e &= \mathrm{diag}\,(X_{eR}, X_{\mu R}, X_{\tau R})\ . \end{aligned} \tag{7.A.1}$$

As mentioned in Section 7.1.1, the QCD anomaly condition is automatically satisfied within BGL models. On the other hand, the anomaly conditions involving a single $\mathrm{U(1)'}$ gauge boson together with $\mathrm{SU(2)_L}$ or $\mathrm{U(1)_Y}$ ones, and the mixed gravitational-$\mathrm{U(1)'}$ anomaly are non-trivial and read

$$\begin{aligned} \mathcal{A}_{221'} &= 3X_{uR} + \frac{3}{2}X_{tR} + \frac{9}{2}X_{dR} + \sum_{\alpha=e,\mu,\tau} X_{\alpha L}\,, \\ \mathcal{A}_{111'} &= -\frac{5}{2}X_{uR} - \frac{5}{4}X_{tR} - \frac{3}{4}X_{dR} + \sum_{\alpha=e,\mu,\tau}\left(\frac{1}{2}X_{\alpha L} - X_{\alpha R}\right)\,, \\ \mathcal{A}_{GG1'} &= \sum_{\alpha=e,\mu,\tau}\left(2X_{\alpha L} - X_{\alpha R}\right)\ . \end{aligned} \tag{7.A.2}$$

The triangle diagrams involving two or three $\mathrm{U(1)'}$ gauge bosons result in more complicated conditions for the BGL charges, which include a quadratic and a cubic equation:

$$\begin{aligned} \mathcal{A}_{11'1'} &= -\frac{7}{2}X_{uR}^2 - \frac{7}{4}X_{tR}^2 + \frac{15}{4}X_{dR}^2 + X_{uR}X_{dR} + \frac{1}{2}X_{tR}X_{dR} \\ &\quad - \sum_{\alpha=e,\mu,\tau}\left(X_{\alpha L}^2 - X_{\alpha R}^2\right)\,, \\ \mathcal{A}_{1'1'1'} &= -\frac{9}{4}\left[2X_{uR}^3 + X_{tR}^3 + 3X_{dR}^3 - X_{dR}\left(2X_{uR}^2 + X_{tR}^2\right)\right. \\ &\quad \left. -X_{dR}^2\left(2X_{uR} + X_{tR}\right)\right] + \sum_{\alpha=e,\mu,\tau}\left(2X_{\alpha L}^3 - X_{\alpha R}^3\right)\ . \end{aligned} \tag{7.A.3}$$

Satisfying these conditions with rational charges is non-trivial and there is only one class of solutions giving an anomaly-free model, up to lepton flavor permutations:

$$\begin{aligned} X_{uR} &= -X_{dR} - \frac{1}{3}X_{\mu R}\,, \quad X_{tR} = -4X_{dR} + \frac{2}{3}X_{\mu R}\,, \\ X_{eL} &= X_{dR} + \frac{1}{6}X_{\mu R}\,, \quad X_{\mu L} = -X_{dR} + \frac{5}{6}X_{\mu R}\,, \\ X_{\tau L} &= \frac{9}{2}X_{dR} - X_{\mu R}\,, \\ X_{eR} &= 2X_{dR} + \frac{1}{3}X_{\mu R}\,, \quad X_{\tau R} = 7X_{dR} - \frac{4}{3}X_{\mu R}\,. \end{aligned} \tag{7.A.4}$$

At this point we have two free charges in the above relations, i.e. X_{dR} and $X_{\mu R}$. Using $X_{\Phi_2} = 0$, as discussed in Section 7.1.1, yields one relation between the two charges. The remaining free charge, e.g. X_{dR}, is fixed by some normalization convention.

7.B Scalar potential of the $\mathrm{U(1)_{BGL}}$ model

The Higgs doublets are parametrized as

$$\Phi_i = \begin{pmatrix} \Phi_i^+ \\ \Phi_i^0 \end{pmatrix} = e^{i\theta_i} \begin{pmatrix} \varphi_i^+ \\ \frac{1}{\sqrt{2}}\left(v_i + \rho_i + i\eta_i\right) \end{pmatrix} \quad (i = 1, 2)\,. \tag{7.B.1}$$

Their neutral components acquire vevs given by $\langle \Phi_j^0 \rangle = e^{i\theta_j} v_j/\sqrt{2}$ with $v_i > 0$ and $(v_1^2 + v_2^2)^{1/2} \equiv v$. In full generality we can rotate away the phase of Φ_1, leaving the second doublet with the phase $\theta = \theta_2 - \theta_1$. We parametrize the complex scalar singlet as

$$S = e^{-i\alpha_S/2} \frac{(v_S + R_0 + iI_0)}{\sqrt{2}}\,, \tag{7.B.2}$$

with $v_S > 0$.

Since we have in our model three scalar fields, $\{\Phi_1, \Phi_2, S\}$, the phase-blind part of the scalar potential has a $\mathrm{U}(1)^3$ global invariance. In order to avoid massless Goldstone bosons, we need to charge the S field in such a way that the phase-sensitive part breaks this symmetry down to $\mathrm{U}(1)^2 = \mathrm{U}(1)_\mathrm{Y} \times \mathrm{U}(1)'$. Gauge-invariant combinations can be built only from $\Phi_1^\dagger \Phi_2$ and S, leaving us with the possibilities $\Phi_1^\dagger \Phi_2 S$, $\Phi_1^\dagger \Phi_2 S^2$ and combinations involving complex conjugates. For concreteness we choose $\Phi_1^\dagger \Phi_2 S^2$ to be invariant, which imposes $X_S = -9/8$. The scalar potential then reads

$$\begin{aligned} V =& m_i^2 |\Phi_i|^2 + \frac{\lambda_i}{2}|\Phi_i|^4 + \lambda_3 |\Phi_1|^2 |\Phi_2|^+ \lambda_4 |\Phi_1^\dagger \Phi_2|^2 + \frac{b_2}{2}|S|^2 2 + \frac{d_2}{4}|S|^4 \\ &+ \frac{\delta_i}{2}|\Phi_i|^2 |S|^2 - \frac{\delta_3}{4}\left(\Phi_1^\dagger \Phi_2 S^2 + \Phi_2^\dagger \Phi_1 (S^*)^2\right)\,. \end{aligned} \tag{7.B.3}$$

All the parameters of the scalar potential but δ_3 are real due to hermiticity. The parameter δ_3 has been chosen to be real and positive by rephasing the scalar field S appropriately.

The vacuum expectation value of the potential is given by

$$\begin{aligned} V_0 =& \frac{v^4}{16}\Big[8\frac{m_1^2}{v^2}c_\beta^2 + 2\lambda_1 c_\beta^4 + 4 s_\beta^2 \left(2\frac{m_2^2}{v^2} + (\lambda_3 + \lambda_4) c_\beta^2\right) + 2\lambda_2 s_\beta^4 \\ &+ 2\hat{v}^2 \left(2\frac{b_2}{v^2} + \delta_1 c_\beta^2 + \delta_2 s_\beta^2\right) + d_2 \hat{v}^4 - 2\,\delta_3\, c_\beta s_\beta \hat{v}^2 \cos(\alpha_S - \theta)\Big]\,. \end{aligned} \tag{7.B.4}$$

Here we have defined the ratio $\hat{v} = v_S/v$. The stability of the vacuum requires that

$$0 = \frac{\partial V_0}{\partial \theta} = -\frac{\delta_3 v^2 v_S^2}{16} s_{2\beta} \sin(\alpha_S - \theta)\,. \tag{7.B.5}$$

By convention we choose $\alpha_S = \theta$, the other possibilities in $\alpha_S = \theta \mod 2\pi$ simply amount to an unphysical rephasing of the scalar field S. Stability also requires $\partial V_0/\partial v_i = 0$, to which the only non-trivial solution reads

$$\begin{aligned} b_2 &= \frac{v^2}{2}\left[-\delta_1 c_\beta^2 + \delta_3 c_\beta s_\beta - \delta_2 s_\beta^2 - d_2 \hat{v}^2\right], \\ m_1^2 &= \frac{v^2}{8}\left[-4\left(\lambda_3+\lambda_4\right) s_\beta^2 - 4\lambda_1 c_\beta^2 + \delta_3 t_\beta \hat{v}^2 - 2\delta_1 \hat{v}^2\right], \\ m_2^2 &= \frac{v^2}{8}\left[-4\left(\lambda_3+\lambda_4\right) c_\beta^2 - 4\lambda_2 s_\beta^2 + \delta_3 t_\beta^{-1} \hat{v}^2 - 2\delta_2 \hat{v}^2\right]. \end{aligned} \tag{7.B.6}$$

Since $\theta = \alpha_S$ does not appear explicitly, the scalar potential is then determined in terms of 10 unknown parameters $\{v_S, \beta, \lambda_{1-4}, d_2, \delta_{1-3}\}$.

The masses of the physical CP-odd boson A and the charged scalar are quasidegenerate and are given by

$$\begin{aligned} M_A^2 &= \frac{\delta_3\, v_S^2}{4 s_{2\beta}}\left(1 + \frac{s_{2\beta}^2}{\hat{v}^2}\right) \simeq \frac{\delta_3\, v_S^2}{4 s_{2\beta}}, \\ M_{H^\pm}^2 &= \frac{\delta_3\, v_S^2}{4 s_{2\beta}}\left(1 - \frac{2 s_{2\beta}\lambda_4}{\hat{v}^2 \delta_3}\right) \simeq \frac{\delta_3 v_S^2}{4 s_{2\beta}}, \end{aligned} \tag{7.B.7}$$

respectively. The physical states $H_{1,2,3}$ are expressed in terms of $\{\rho_1, \rho_2, R_0\}$ via an orthogonal transformation,

$$\begin{pmatrix} H_1 \\ H_2 \\ H_3 \end{pmatrix} = \mathcal{R}_S \begin{pmatrix} \rho_1 \\ \rho_2 \\ R_0 \end{pmatrix}. \tag{7.B.8}$$

The mass matrix for the CP-even bosons can be diagonalized analytically in a perturbative expansion around $1/\hat{v} \ll 1$. Including the leading corrections in $1/\hat{v}$ one obtains

$$\mathcal{R}_S \simeq \begin{pmatrix} c_\beta & s_\beta & \omega_{13} \\ -s_\beta & c_\beta & \omega_{23} \\ \omega_{23} s_\beta - \omega_{13} c_\beta & -(\omega_{23} c_\beta + \omega_{13} s_\beta) & 1 \end{pmatrix}, \tag{7.B.9}$$

with

$$\begin{aligned} \omega_{13} &= -\frac{2\delta_1 c_\beta^2 - \delta_3 s_{2\beta} + 2\delta_2 s_\beta^2}{2\hat{v} d_2}, \\ \omega_{23} &= \frac{\delta_3 s_{4\beta} + 2(\delta_1 - \delta_2) s_{2\beta}^2}{2\hat{v}(2 d_2 s_{2\beta} - \delta_3)}. \end{aligned} \tag{7.B.10}$$

The resulting masses for the CP-even scalars are given by

$$M_{H_1}^2 \simeq \frac{\tilde{\lambda} v^2}{2 d_2}, \quad M_{H_2}^2 \simeq \frac{\delta_3 v_S^2}{4 s_{2\beta}}, \quad M_{H_3}^2 \simeq \frac{d_2 v_S^2}{2}, \tag{7.B.11}$$

with

$$\begin{aligned} \tilde{\lambda} = {} & (2 d_2 \lambda_1 - \delta_1^2) c_\beta^4 + (\delta_1 c_\beta^2 + \delta_2 s_\beta^2)\delta_3 s_{2\beta} - \frac{2\delta_1\delta_2 + \delta_3^2}{4} s_{2\beta}^2 \\ & - (\delta_2^2 - 2 d_2 \lambda_2) s_\beta^4 + d_2(\lambda_3 + \lambda_4) s_{2\beta}^2. \end{aligned} \tag{7.B.12}$$

The exact expression for their Yukawa couplings in Eq. (7.19) is

$$v\, Y_f^{H_k} = [c_\beta(\mathcal{R}_S)_{k1} + s_\beta(\mathcal{R}_S)_{k2}]\, D_f + [s_\beta(\mathcal{R}_S)_{k1} - c_\beta(\mathcal{R}_S)_{k2}]\, N_f\,. \tag{7.B.13}$$

Finally, the vacuum solution in our models allows for complex vevs but that is not sufficient to have spontaneous CP violation. In the weak gauge sector CP violation is manifest through the invariant $\mathrm{Tr}\,[H_d, H_u]^3$ [226]. In the CP-invariant scenario, i.e. with real Yukawa matrices, the Hermitian combinations $H_{u,d}$ are given by

$$\begin{aligned} 2H_u &= v_1^2\Delta_1\Delta_1^T + v_2^2\Delta_2\Delta_2^T + v_1v_2(\Delta_1\Delta_2^T + \Delta_2\Delta_1^T)c_\theta + iv_1v_2(\Delta_1\Delta_2^T - \Delta_2\Delta_1^T)s_\theta\,, \\ 2H_d &= v_1^2\Gamma_1\Gamma_1^T + v_2^2\Gamma_2\Gamma_2^T + v_1v_2(\Gamma_2\Gamma_1^T + \Gamma_1\Gamma_2^T)c_\theta + iv_1v_2(\Gamma_2\Gamma_1^T - \Gamma_1\Gamma_2^T)s_\theta\,. \end{aligned} \tag{7.B.14}$$

In our model we get $\mathrm{Tr}\,[H_d, H_u]^3 = 0$, implying the absence of CP violation in the gauge interactions when the only phase is carried by the scalar vev. As a consequence, the source of CP violation for the weak currents in our model is present in the Yukawa couplings and will appear in the observables through the CKM mechanism.

7.C Details of the SU(2) × SU(2) × U(1) model

7.C.1 Tadpole equations

The vev configuration introduced in Section 7.3.2 leads to three minimization conditions or tadpole equations. In the following we will consider all the parameters in the scalar potential to be real. Defining

$$t_i = \frac{\partial \mathcal{V}}{\partial v_i} = 0\,, \tag{7.C.1}$$

these are

$$\begin{aligned} t_\phi &= m_\phi^2 v_\phi + \frac{1}{2}v_\phi\left(\lambda_4 v_{\phi'}^2 + \lambda_5 u^2\right) + \frac{1}{2}v_{\phi'}u\,\mu + \frac{1}{2}\lambda_1 v_\phi^3\,, \\ t_{\phi'} &= m_{\phi'}^2 v_{\phi'} + \frac{1}{2}v_{\phi'}\left(\lambda_4 v_\phi^2 + \lambda_6 u^2\right) + \frac{1}{2}v_\phi u\,\mu + \frac{1}{2}\lambda_2 v_{\phi'}^3\,, \\ t_u &= m_\Phi^2 u + \frac{1}{2}u\left(\lambda_5 v_\phi^2 + \lambda_6 v_{\phi'}^2\right) + \frac{1}{2}v_\phi v_{\phi'}\mu + \frac{1}{2}\lambda_3 u^3\,. \end{aligned} \tag{7.C.2}$$

These three conditions can be solved for the mass squared parameters m_ϕ^2, $m_{\phi'}^2$ and m_Φ^2.

7.C.2 Scalar mass matrices

The neutral scalar fields can be decomposed as

$$\begin{aligned}
\varphi^0 &= \frac{1}{\sqrt{2}}\left(v_\phi + S_\phi + i\,A_\phi\right) , \\
\varphi'^0 &= \frac{1}{\sqrt{2}}\left(v_{\phi'} + S_{\phi'} + i\,A_{\phi'}\right) , \\
\Phi^0 &= \frac{1}{\sqrt{2}}\left(u + S_\Phi + i\,A_\Phi\right) .
\end{aligned} \tag{7.C.3}$$

Since we assume that CP is conserved in the scalar sector, the CP-even and CP-odd states do not mix. In this case, one can define the bases

$$\begin{aligned}
\mathcal{S}^T &\equiv (S_\phi, S_{\phi'}, S_\Phi) \quad , & \mathcal{P}^T &\equiv (A_\phi, A_{\phi'}, A_\Phi) , \\
(\mathcal{H}^-)^T &\equiv \left(\left(\varphi^+\right)^*, \left(\varphi'^+\right)^*, \left(\Phi^+\right)^*\right) \quad , & (\mathcal{H}^+)^T &\equiv \left(\varphi^+, \varphi'^+, \Phi^+\right) ,
\end{aligned} \tag{7.C.4}$$

which allow us to obtain the scalar mass Lagrangian

$$-\mathcal{L}_m^s = \frac{1}{2}\mathcal{S}^T\mathcal{M}_\mathcal{S}^2\mathcal{S} + \frac{1}{2}\mathcal{P}^T\mathcal{M}_\mathcal{P}^2\mathcal{P} + \left(\mathcal{H}^-\right)^T\mathcal{M}_{\mathcal{H}^\pm}^2\mathcal{H}^+ . \tag{7.C.5}$$

The mass matrix for the CP-even scalars is given by

$$\mathcal{M}_\mathcal{S}^2 = \begin{pmatrix} \mathcal{M}^2_{S_\phi S_\phi} & \mathcal{M}^2_{S_\phi S_{\phi'}} & \mathcal{M}^2_{S_\phi S_\Phi} \\ \mathcal{M}^2_{S_\phi S_{\phi'}} & \mathcal{M}^2_{S_{\phi'} S_{\phi'}} & \mathcal{M}^2_{S_{\phi'} S_\Phi} \\ \mathcal{M}^2_{S_\phi S_\Phi} & \mathcal{M}^2_{S_{\phi'} S_\Phi} & \mathcal{M}^2_{S_\Phi S_\Phi} \end{pmatrix} , \tag{7.C.6}$$

with

$$\begin{aligned}
\mathcal{M}^2_{S_\phi S_\phi} &= m_\phi^2 + \frac{1}{2}\Big(3v_\phi^2\lambda_1 + v_{\phi'}^2\lambda_4 + u^2\lambda_5\Big) , \\
\mathcal{M}^2_{S_\phi S_{\phi'}} &= v_\phi v_{\phi'}\lambda_4 + \frac{1}{2}u\mu , \\
\mathcal{M}^2_{S_\phi S_\Phi} &= v_\phi u\lambda_5 + \frac{1}{2}v_{\phi'}\mu , \\
\mathcal{M}^2_{S_{\phi'} S_{\phi'}} &= m_{\phi'}^2 + \frac{1}{2}\Big(3v_{\phi'}^2\lambda_2 + v_\phi^2\lambda_4 + u^2\lambda_6\Big) , \\
\mathcal{M}^2_{S_{\phi'} S_\Phi} &= v_{\phi'} u\lambda_6 + \frac{1}{2}v_\phi\mu , \\
\mathcal{M}^2_{S_\Phi S_\Phi} &= m_\Phi^2 + \frac{1}{2}\Big(v_\phi^2\lambda_5 + v_{\phi'}^2\lambda_6 + 3u^2\lambda_3\Big) .
\end{aligned} \tag{7.C.7}$$

The lightest CP-even state, $\mathcal{S}_1 \equiv h$, is identified with the recently discovered SM-like Higgs boson with a mass ~ 125 GeV. Similarly, in the Landau gauge ($\xi = 0$), the mass matrix for the CP-odd scalars is given by

$$\mathcal{M}_\mathcal{P}^2 = \begin{pmatrix} \mathcal{M}^2_{A_\phi A_\phi} & \mathcal{M}^2_{A_\phi A_{\phi'}} & \mathcal{M}^2_{A_\phi A_\Phi} \\ \mathcal{M}^2_{A_\phi A_{\phi'}} & \mathcal{M}^2_{A_{\phi'} A_{\phi'}} & \mathcal{M}^2_{A_{\phi'} A_\Phi} \\ \mathcal{M}^2_{A_\phi A_\Phi} & \mathcal{M}^2_{A_{\phi'} A_\Phi} & \mathcal{M}^2_{A_\Phi A_\Phi} \end{pmatrix} , \tag{7.C.8}$$

with

$$\begin{aligned}
\mathcal{M}^2_{A_\phi A_\phi} &= m^2_\phi + \frac{1}{2}\Big(v^2_\phi\lambda_1 + v^2_{\phi'}\lambda_4 + u^2\lambda_5\Big)\,,\\
\mathcal{M}^2_{A_\phi A_{\phi'}} &= \frac{1}{2}u\mu\,,\\
\mathcal{M}^2_{A_\phi A_\Phi} &= \frac{1}{2}v_{\phi'}\mu\,,\\
\mathcal{M}^2_{A_{\phi'} A_{\phi'}} &= m^2_{\phi'} + \frac{1}{2}\Big(v^2_{\phi'}\lambda_2 + v^2_\phi\lambda_4 + u^2\lambda_6\Big)\,,\\
\mathcal{M}^2_{A_{\phi'} A_\Phi} &= -\frac{1}{2}v_\phi\mu\,,\\
\mathcal{M}^2_{A_\Phi A_\Phi} &= m^2_\Phi + \frac{1}{2}\Big(v^2_\phi\lambda_5 + v^2_{\phi'}\lambda_6 + u^2\lambda_3\Big)\,.
\end{aligned} \tag{7.C.9}$$

After application of the tadpole equations in Eq. (7.C.2), it is straightforward to show that the matrix $\mathcal{M}^2_{\mathcal{P}}$ has two vanishing eigenvalues. These correspond to the Goldstone bosons that constitute the longitudinal modes for the massive Z and Z' bosons. Finally, the mass matrix for the charged scalars in the Landau gauge ($\xi = 0$) is given by

$$\mathcal{M}^2_{\mathcal{H}^\pm} = \begin{pmatrix} \mathcal{M}^2_{\varphi^+\varphi^+} & \mathcal{M}^2_{\varphi^+\varphi'^+} & \mathcal{M}^2_{\varphi^+\Phi^+} \\ \mathcal{M}^2_{\varphi^+\varphi'^+} & \mathcal{M}^2_{\varphi'^+\varphi'^+} & \mathcal{M}^2_{\varphi'^+\Phi^+} \\ \mathcal{M}^2_{\varphi^+\Phi^+} & \mathcal{M}^2_{\varphi'^+\Phi^+} & \mathcal{M}^2_{\Phi^+\Phi^+} \end{pmatrix}\,, \tag{7.C.10}$$

with

$$\begin{aligned}
\mathcal{M}^2_{\varphi^+\varphi^+} &= m^2_\phi + \frac{1}{2}\Big(v^2_\phi\lambda_1 + v^2_{\phi'}\lambda_4 + u^2\lambda_5\Big)\,,\\
\mathcal{M}^2_{\varphi^+\varphi'^+} &= \frac{1}{2}u\mu\,,\\
\mathcal{M}^2_{\varphi^+\Phi^+} &= -\frac{1}{2}v_{\phi'}\mu\,,\\
\mathcal{M}^2_{\varphi'^+\varphi'^+} &= m^2_{\phi'} + \frac{1}{2}\Big(v^2_{\phi'}\lambda_2 + v^2_\phi\lambda_4 + u^2\lambda_6\Big)\,,\\
\mathcal{M}^2_{\varphi'^+\Phi^+} &= \frac{1}{2}v_\phi\mu\,,\\
\mathcal{M}^2_{\Phi^+\Phi^+} &= m^2_\Phi + \frac{1}{2}\Big(v^2_\phi\lambda_5 + v^2_{\phi'}\lambda_6 + u^2\lambda_3\Big)\,.
\end{aligned} \tag{7.C.11}$$

Again, one can find two vanishing eigenvalues in $\mathcal{M}^2_{\mathcal{H}^\pm}$ after applying the tadpole equations in Eqs. (7.C.2). These correspond to the Goldstone bosons *eaten-up* by the W and W' gauge bosons.

7.D Pseudo-observables for Z- and W-pole observables

In our model, the pseudo-observables considered in Ref. [143] are given by:

$$\begin{aligned}
\delta m &= -\delta v \, \frac{g'^2}{g^2 - g'^2} \ , \\
\delta g_L^{W\ell_i} &= -\zeta \, \epsilon^2 \, \frac{g_2^4}{n_1^4} \Delta_{ii}^{\ell} + f(1/2, 0) - f(-1/2, -1) \, , \\
\delta g_L^{Z\ell_i} &= \zeta \, \epsilon^2 \, \frac{g_2^4}{2n_1^4} \Delta_{ii}^{\ell} + f(-1/2, -1) \, , \\
\delta g_R^{Z\ell_i} &= f(0, -1) \, , \\
\delta g_L^{Zu_i} &= -\zeta \, \epsilon^2 \frac{g_2^4}{2n_1^4} (V_{\rm CKM} \Delta^q V_{\rm CKM}^\dagger)_{ii} + f(1/2, 2/3) \, , \\
\delta g_R^{Zu_i} &= f(0, 2/3) \, , \\
\delta g_L^{Zd_i} &= \zeta \, \epsilon^2 \frac{g_2^4}{2n_1^4} \Delta_{ii}^{q} + f(-1/2, -1/3) \, , \\
\delta g_R^{Zd_i} &= f(0, -1/3) \, ,
\end{aligned} \tag{7.D.1}$$

where

$$\delta v = -\zeta \epsilon^2 \frac{1}{2} \frac{g_2^4}{n_1^4} \Delta_{22}^{\ell} \quad \text{and} \quad f(T^3, Q) = -\delta v \left(T^3 + Q \frac{g'^2}{g^2 - g'^2} \right) . \tag{7.D.2}$$

The family index i for these shifts covers the three fermion generations except for $\delta g_R^{Zu_i}$, for which $i = 1, 2$. We neglect corrections to the right-handed Z and W couplings that are suppressed by the fermion masses, see Section 7.3.3. We also neglect loop contributions, which we estimate to be comparable to the tree-level contributions for $\zeta \lesssim 0.02$. However, the resulting δg's in that case would be below the limits quoted in [143].

Bibliography

[1] Simone Bifani on behalf of the LHCb Collaboration, LHCb seminar at CERN, 18 April 2017.

[2] The ATLAS collaboration [ATLAS Collaboration], ATLAS-CONF-2017-027.

[3] A. Celis, J. Fuentes-Martin, M. Jung and H. Serodio, Phys. Rev. D **92** (2015) no.1, 015007 [arXiv:1505.03079 [hep-ph]].

[4] G. C. Branco, W. Grimus and L. Lavoura, Phys. Lett. B **380** (1996) 119 [hep-ph/9601383].

[5] A. Celis, J. Fuentes-Martin and H. Serodio, Phys. Lett. B **741** (2015) 117 [arXiv:1410.6217 [hep-ph]].

[6] A. Celis, J. Fuentes-Martín and H. Serôdio, JHEP **1412** (2014) 167 [arXiv:1410.6218 [hep-ph]].

[7] A. J. Buras, F. De Fazio and J. Girrbach, JHEP **1402** (2014) 112 [arXiv:1311.6729 [hep-ph]].

[8] R. Gauld, F. Goertz and U. Haisch, JHEP **1401** (2014) 069 [arXiv:1310.1082 [hep-ph]].

[9] M. B. Green and J. H. Schwarz, Phys. Lett. **149B** (1984) 117.

[10] M. B. Green and J. H. Schwarz, Nucl. Phys. B **255** (1985) 93.

[11] M. B. Green, J. H. Schwarz and P. C. West, Nucl. Phys. B **254** (1985) 327.

[12] S. L. Glashow, D. Guadagnoli and K. Lane, Phys. Rev. Lett. **114** (2015) 091801 [arXiv:1411.0565 [hep-ph]].

[13] B. Bhattacharya, A. Datta, D. London and S. Shivashankara, Phys. Lett. B **742** (2015) 370 [arXiv:1412.7164 [hep-ph]].

[14] S. M. Boucenna, J. W. F. Valle and A. Vicente, Phys. Lett. B **750** (2015) 367 [arXiv:1503.07099 [hep-ph]].

[15] P. Binetruy, S. Lavignac, S. T. Petcov and P. Ramond, Nucl. Phys. B **496** (1997) 3 [hep-ph/9610481].

[16] N. F. Bell and R. R. Volkas, Phys. Rev. D **63** (2001) 013006 [hep-ph/0008177].

[17] S. Choubey and W. Rodejohann, Eur. Phys. J. C **40** (2005) 259 [hep-ph/0411190].

[18] J. Heeck and W. Rodejohann, Phys. Rev. D **84** (2011) 075007 [arXiv:1107.5238 [hep-ph]].

[19] L. M. Cebola, D. Emmanuel-Costa and R. González Felipe, Phys. Rev. D **88** (2013) no.11, 116008 [arXiv:1309.1709 [hep-ph]].

[20] A. Crivellin, G. D'Ambrosio and J. Heeck, Phys. Rev. D **91** (2015) no.7, 075006 [arXiv:1503.03477 [hep-ph]].

[21] P. Langacker, Rev. Mod. Phys. **81** (2009) 1199 [arXiv:0801.1345 [hep-ph]].

[22] K. S. Babu, C. F. Kolda and J. March-Russell, Phys. Rev. D **57** (1998) 6788 [hep-ph/9710441].

[23] K. A. Olive *et al.* [Particle Data Group], Chin. Phys. C **38** (2014) 090001.

[24] J. Erler and P. Langacker, Phys. Lett. B **456** (1999) 68 [hep-ph/9903476].

[25] R. Foot, A. Kobakhidze, K. L. McDonald and R. R. Volkas, Phys. Rev. D **89** (2014) no.11, 115018 [arXiv:1310.0223 [hep-ph]].

[26] F. J. Botella, G. C. Branco, A. Carmona, M. Nebot, L. Pedro and M. N. Rebelo, JHEP **1407** (2014) 078 [arXiv:1401.6147 [hep-ph]].

[27] G. Bhattacharyya, D. Das and A. Kundu, Phys. Rev. D **89** (2014) 095029 [arXiv:1402.0364 [hep-ph]].

[28] Y. Amhis *et al.* [Heavy Flavor Averaging Group (HFAG)], arXiv:1412.7515 [hep-ex].

[29] C. M. Bouchard *et al.* [Fermilab Lattice and MILC Collaborations], PoS LATTICE **2014** (2014) 378 [arXiv:1412.5097 [hep-lat]].

[30] R. J. Dowdall, C. T. H. Davies, R. R. Horgan, G. P. Lepage, C. J. Monahan and J. Shigemitsu, arXiv:1411.6989 [hep-lat].

[31] Y. Aoki, T. Ishikawa, T. Izubuchi, C. Lehner and A. Soni, Phys. Rev. D **91** (2015) no.11, 114505 [arXiv:1406.6192 [hep-lat]].

[32] M. Blanke and A. J. Buras, Eur. Phys. J. C **76** (2016) no.4, 197 [arXiv:1602.04020 [hep-ph]].

[33] S. Aoki *et al.*, Eur. Phys. J. C **74** (2014) 2890 [arXiv:1310.8555 [hep-lat]].

[34] J. Charles *et al.* [CKMfitter Group], Eur. Phys. J. C **41** (2005) no.1, 1 [hep-ph/0406184].

[35] A. J. Buras, R. Fleischer, J. Girrbach and R. Knegjens, JHEP **1307** (2013) 77 [arXiv:1303.3820 [hep-ph]].

[36] A. J. Buras, F. De Fazio, J. Girrbach, R. Knegjens and M. Nagai, JHEP **1306** (2013) 111 [arXiv:1303.3723 [hep-ph]].

[37] M. Ciuchini, G. D'Agostini, E. Franco, V. Lubicz, G. Martinelli, F. Parodi, P. Roudeau and A. Stocchi, JHEP **0107** (2001) 013 [hep-ph/0012308].

[38] W. Altmannshofer, S. Gori, M. Pospelov and I. Yavin, Phys. Rev. D **89** (2014) 095033 [arXiv:1403.1269 [hep-ph]].

[39] W. Altmannshofer, S. Gori, M. Pospelov and I. Yavin, Phys. Rev. Lett. **113** (2014) 091801 [arXiv:1406.2332 [hep-ph]].

[40] A. Crivellin, L. Hofer, J. Matias, U. Nierste, S. Pokorski and J. Rosiek, Phys. Rev. D **92** (2015) no.5, 054013 [arXiv:1504.07928 [hep-ph]].

[41] D. Geiregat *et al.* [CHARM-II Collaboration], Phys. Lett. B **245** (1990) 271.

[42] S. R. Mishra *et al.* [CCFR Collaboration], Phys. Rev. Lett. **66** (1991) 3117.

[43] T. Adams *et al.* [NuTeV Collaboration], Phys. Rev. D **61** (2000) 092001 [hep-ex/9909041].

[44] C. S. Wood, S. C. Bennett, D. Cho, B. P. Masterson, J. L. Roberts, C. E. Tanner and C. E. Wieman, Science **275** (1997) 1759.

[45] S. C. Bennett and C. E. Wieman, Phys. Rev. Lett. **82** (1999) 2484 Erratum: [Phys. Rev. Lett. **83** (1999) 889] [hep-ex/9903022].

[46] A. Derevianko, Phys. Rev. Lett. **85** (2000) 1618 [hep-ph/0005274].

[47] M. Carpentier and S. Davidson, Eur. Phys. J. C **70** (2010) 1071 [arXiv:1008.0280 [hep-ph]].

[48] R. Diener, S. Godfrey and I. Turan, Phys. Rev. D **86** (2012) 115017 [arXiv:1111.4566 [hep-ph]].

[49] V. A. Dzuba, J. C. Berengut, V. V. Flambaum and B. Roberts, Phys. Rev. Lett. **109** (2012) 203003 [arXiv:1207.5864 [hep-ph]].

[50] B. M. Roberts, V. A. Dzuba and V. V. Flambaum, Ann. Rev. Nucl. Part. Sci. **65** (2015) 63 [arXiv:1412.6644 [physics.atom-ph]].

[51] F. J. Botella, G. C. Branco and M. N. Rebelo, Phys. Lett. B **722** (2013) 76 [arXiv:1210.8163 [hep-ph]].

[52] M. Jung and A. Pich, JHEP **1404** (2014) 076 [arXiv:1308.6283 [hep-ph]].

[53] A. Crivellin, A. Kokulu and C. Greub, Phys. Rev. D **87** (2013) no.9, 094031 [arXiv:1303.5877 [hep-ph]].

[54] C. W. Chiang, N. G. Deshpande and J. Jiang, JHEP **0608** (2006) 075 [hep-ph/0606122].

[55] F. Jegerlehner and A. Nyffeler, Phys. Rept. **477** (2009) 1 [arXiv:0902.3360 [hep-ph]].

[56] F. S. Queiroz and W. Shepherd, Phys. Rev. D **89** (2014) no.9, 095024 [arXiv:1403.2309 [hep-ph]].

[57] G. Aad *et al.* [ATLAS Collaboration], JHEP **1211** (2012) 138 [arXiv:1209.2535 [hep-ex]].

[58] G. Aad *et al.* [ATLAS Collaboration], Phys. Rev. D **90** (2014) no.5, 052005 [arXiv:1405.4123 [hep-ex]].

[59] S. Chatrchyan *et al.* [CMS Collaboration], Phys. Lett. B **714** (2012) 158 [arXiv:1206.1849 [hep-ex]].

[60] V. Khachatryan *et al.* [CMS Collaboration], JHEP **1504** (2015) 025 [arXiv:1412.6302 [hep-ex]].

[61] The ATLAS collaboration [ATLAS Collaboration], ATLAS-CONF-2016-045.

[62] CMS Collaboration [CMS Collaboration], CMS-PAS-EXO-16-031.

[63] V. Khachatryan *et al.* [CMS Collaboration], Phys. Lett. B **768** (2017) 57 [arXiv:1609.05391 [hep-ex]].

[64] A. Greljo and D. Marzocca, arXiv:1704.09015 [hep-ph].

[65] E. Accomando, D. Becciolini, A. Belyaev, S. Moretti and C. Shepherd-Themistocleous, JHEP **1310** (2013) 153 [arXiv:1304.6700 [hep-ph]].

[66] M. Carena, A. Daleo, B. A. Dobrescu and T. M. P. Tait, Phys. Rev. D **70** (2004) 093009 [hep-ph/0408098].

[67] E. Accomando, A. Belyaev, L. Fedeli, S. F. King and C. Shepherd-Themistocleous, Phys. Rev. D **83** (2011) 075012 [arXiv:1010.6058 [hep-ph]].

[68] G. Aad *et al.* [ATLAS Collaboration], Eur. Phys. J. C **74** (2014) no.12, 3134 [arXiv:1407.2410 [hep-ex]].

[69] S. Schael *et al.* [ALEPH and DELPHI and L3 and OPAL and LEP Electroweak Collaborations], Phys. Rept. **532** (2013) 119 [arXiv:1302.3415 [hep-ex]].

[70] A. J. Buras, F. De Fazio and J. Girrbach, JHEP **1302** (2013) 116 [arXiv:1211.1896 [hep-ph]].

[71] R. Alonso, B. Grinstein and J. Martin Camalich, Phys. Rev. Lett. **113** (2014) 241802 [arXiv:1407.7044 [hep-ph]].

[72] G. Hiller and F. Kruger, Phys. Rev. D **69** (2004) 074020 [hep-ph/0310219].

[73] G. Hiller and M. Schmaltz, JHEP **1502** (2015) 055 [arXiv:1411.4773 [hep-ph]].

[74] I. de Medeiros Varzielas and G. Hiller, JHEP **1506** (2015) 072 [arXiv:1503.01084 [hep-ph]].

[75] G. Hiller and M. Schmaltz, Phys. Rev. D **90** (2014) 054014 [arXiv:1408.1627 [hep-ph]].

[76] T. Blake, T. Gershon and G. Hiller, Ann. Rev. Nucl. Part. Sci. **65** (2015) 113 [arXiv:1501.03309 [hep-ex]].

[77] S. Godfrey and T. Martin, arXiv:1309.1688 [hep-ph].

[78] D. A. Demir, G. L. Kane and T. T. Wang, Phys. Rev. D **72** (2005) 015012 [hep-ph/0503290].

[79] A. Hayreter, Phys. Lett. B **649** (2007) 191 [hep-ph/0703269].

[80] S. Godfrey and T. A. W. Martin, Phys. Rev. Lett. **101** (2008) 151803 [arXiv:0807.1080 [hep-ph]].

[81] M. C. Chen and J. Huang, Phys. Rev. D **81** (2010) 055007 [arXiv:0910.5029 [hep-ph]].

[82] E. Salvioni, A. Strumia, G. Villadoro and F. Zwirner, JHEP **1003** (2010) 010 [arXiv:0911.1450 [hep-ph]].

[83] R. Diener, S. Godfrey and T. A. W. Martin, Phys. Rev. D **83** (2011) 115008 [arXiv:1006.2845 [hep-ph]].

[84] R. Aaij *et al.* [LHCb Collaboration], Phys. Rev. Lett. **113** (2014) 151601 [arXiv:1406.6482 [hep-ex]].

[85] C. Bobeth, G. Hiller and G. Piranishvili, JHEP **0712** (2007) 040 [arXiv:0709.4174 [hep-ph]].

[86] C. Bobeth, G. Hiller, D. van Dyk and C. Wacker, JHEP **1201** (2012) 107 [arXiv:1111.2558 [hep-ph]].

[87] C. Bouchard *et al.* [HPQCD Collaboration], Phys. Rev. Lett. **111** (2013) no.16, 162002 Erratum: [Phys. Rev. Lett. **112** (2014) no.14, 149902] [arXiv:1306.0434 [hep-ph]].

[88] R. Aaij *et al.* [LHCb Collaboration], Phys. Rev. Lett. **111** (2013) 191801 [arXiv:1308.1707 [hep-ex]].

[89] S. Descotes-Genon, T. Hurth, J. Matias and J. Virto, JHEP **1305** (2013) 137 [arXiv:1303.5794 [hep-ph]].

[90] R. R. Horgan, Z. Liu, S. Meinel and M. Wingate, Phys. Rev. Lett. **112** (2014) 212003 [arXiv:1310.3887 [hep-ph]].

[91] R. R. Horgan, Z. Liu, S. Meinel and M. Wingate, PoS LATTICE **2014** (2015) 372 [arXiv:1501.00367 [hep-lat]].

[92] W. Altmannshofer and D. M. Straub, Eur. Phys. J. C **75** (2015) no.8, 382 [arXiv:1411.3161 [hep-ph]].

[93] S. Descotes-Genon, J. Matias and J. Virto, Phys. Rev. D **88** (2013) 074002 [arXiv:1307.5683 [hep-ph]].

[94] W. Altmannshofer and D. M. Straub, Eur. Phys. J. C **73** (2013) 2646 [arXiv:1308.1501 [hep-ph]].

[95] F. Beaujean, C. Bobeth and D. van Dyk, Eur. Phys. J. C **74** (2014) 2897 Erratum: [Eur. Phys. J. C **74** (2014) 3179] [arXiv:1310.2478 [hep-ph]].

[96] T. Hurth and F. Mahmoudi, JHEP **1404** (2014) 097 [arXiv:1312.5267 [hep-ph]].

[97] D. Ghosh, M. Nardecchia and S. A. Renner, JHEP **1412** (2014) 131 [arXiv:1408.4097 [hep-ph]].

[98] T. Hurth, F. Mahmoudi and S. Neshatpour, JHEP **1412** (2014) 053 [arXiv:1410.4545 [hep-ph]].

[99] W. Altmannshofer and D. M. Straub, arXiv:1503.06199 [hep-ph].

[100] S. Jäger and J. Martin Camalich, Phys. Rev. D **93** (2016) no.1, 014028 [arXiv:1412.3183 [hep-ph]].

[101] V. Khachatryan *et al.* [CMS and LHCb Collaborations], Nature **522** (2015) 68 [arXiv:1411.4413 [hep-ex]].

[102] R. Aaij *et al.* [LHCb Collaboration], arXiv:1703.05747 [hep-ex].

[103] C. Bobeth, M. Gorbahn, T. Hermann, M. Misiak, E. Stamou and M. Steinhauser, Phys. Rev. Lett. **112** (2014) 101801 [arXiv:1311.0903 [hep-ph]].

[104] A. Crivellin, J. Fuentes-Martin, A. Greljo and G. Isidori, Phys. Lett. B **766** (2017) 77 [arXiv:1611.02703 [hep-ph]].

[105] G. D'Ambrosio, G. F. Giudice, G. Isidori and A. Strumia, Nucl. Phys. B **645** (2002) 155 [hep-ph/0207036].

[106] V. Cirigliano, B. Grinstein, G. Isidori and M. B. Wise, Nucl. Phys. B **728** (2005) 121 [hep-ph/0507001].

[107] R. Alonso, M. B. Gavela, G. Isidori and L. Maiani, JHEP **1311** (2013) 187 [arXiv:1306.5927 [hep-ph]].

[108] B. Grinstein, M. Redi and G. Villadoro, JHEP **1011** (2010) 067 [arXiv:1009.2049 [hep-ph]].

[109] M. E. Albrecht, T. Feldmann and T. Mannel, JHEP **1010** (2010) 089 [arXiv:1002.4798 [hep-ph]].

[110] R. Alonso, E. Fernandez Martinez, M. B. Gavela, B. Grinstein, L. Merlo and P. Quilez, JHEP **1612** (2016) 119 [arXiv:1609.05902 [hep-ph]].

[111] X. G. He, G. C. Joshi, H. Lew and R. R. Volkas, Phys. Rev. D **43** (1991) 22.

[112] R. Foot, Mod. Phys. Lett. A **6** (1991) 527.

[113] X. G. He, G. C. Joshi, H. Lew and R. R. Volkas, Phys. Rev. D **44** (1991) 2118.

[114] G. Dutta, A. S. Joshipura and K. B. Vijaykumar, Phys. Rev. D **50** (1994) 2109 [hep-ph/9405292].

[115] J. Heeck, M. Holthausen, W. Rodejohann and Y. Shimizu, Nucl. Phys. B **896** (2015) 281 [arXiv:1412.3671 [hep-ph]].

[116] R. Alonso, M. B. Gavela, L. Merlo and S. Rigolin, JHEP **1107** (2011) 012 [arXiv:1103.2915 [hep-ph]].

[117] C. S. Fong and E. Nardi, Phys. Rev. D **89** (2014) no.3, 036008 [arXiv:1307.4412 [hep-ph]].

[118] J. R. Espinosa, C. S. Fong and E. Nardi, JHEP **1302** (2013) 137 [arXiv:1211.6428 [hep-ph]].

[119] S. Descotes-Genon, L. Hofer, J. Matias and J. Virto, JHEP **1606** (2016) 092 [arXiv:1510.04239 [hep-ph]].

[120] A. Lenz *et al.*, Phys. Rev. D **83** (2011) 036004 [arXiv:1008.1593 [hep-ph]].

[121] D. Buttazzo, A. Greljo, G. Isidori and D. Marzocca, JHEP **1608** (2016) 035 [arXiv:1604.03940 [hep-ph]].

[122] F. Bishara, A. Greljo, J. F. Kamenik, E. Stamou and J. Zupan, JHEP **1512** (2015) 130 [arXiv:1505.03862 [hep-ph]].

[123] L. A. Harland-Lang, A. D. Martin, P. Motylinski and R. S. Thorne, Eur. Phys. J. C **75** (2015) no.5, 204 [arXiv:1412.3989 [hep-ph]].

[124] J. Alwall *et al.*, JHEP **1407** (2014) 079 [arXiv:1405.0301 [hep-ph]].

[125] G. Aad *et al.* [ATLAS Collaboration], JHEP **1508** (2015) 148 [arXiv:1505.07018 [hep-ex]].

[126] V. Khachatryan *et al.* [CMS Collaboration], Phys. Rev. D **91** (2015) no.5, 052009 [arXiv:1501.04198 [hep-ex]].

[127] CMS Collaboration [CMS Collaboration], CMS-PAS-EXO-16-032.

[128] CMS Collaboration [CMS Collaboration], CMS-PAS-B2G-15-002.

[129] F. del Aguila, M. Chala, J. Santiago and Y. Yamamoto, JHEP **1503** (2015) 059 [arXiv:1411.7394 [hep-ph]].

[130] Gavin Salam and Andreas Weiler, *Collider Reach*, [`http://collider-reach.web.cern.ch/`].

[131] S. Descotes-Genon, L. Hofer, J. Matias and J. Virto, arXiv:1605.06059 [hep-ph].

[132] B. Capdevila, S. Descotes-Genon, J. Matias and J. Virto, JHEP **1610** (2016) 075 [arXiv:1605.03156 [hep-ph]].

[133] N. Serra, R. Silva Coutinho and D. van Dyk, Phys. Rev. D **95** (2017) no.3, 035029 [arXiv:1610.08761 [hep-ph]].

[134] S. M. Boucenna, A. Celis, J. Fuentes-Martin, A. Vicente and J. Virto, Phys. Lett. B **760** (2016) 214 [arXiv:1604.03088 [hep-ph]].

[135] S. M. Boucenna, A. Celis, J. Fuentes-Martin, A. Vicente and J. Virto, JHEP **1612** (2016) 059 [arXiv:1608.01349 [hep-ph]].

[136] X. G. He and G. Valencia, Phys. Rev. D **87** (2013) no.1, 014014 [arXiv:1211.0348 [hep-ph]].

[137] X. Li and E. Ma, Phys. Rev. Lett. **47** (1981) 1788.

[138] D. J. Muller and S. Nandi, Phys. Lett. B **383** (1996) 345 [hep-ph/9602390].

[139] C. W. Chiang, N. G. Deshpande, X. G. He and J. Jiang, Phys. Rev. D **81** (2010) 015006 [arXiv:0911.1480 [hep-ph]].

[140] D. E. Morrissey, T. M. P. Tait and C. E. M. Wagner, Phys. Rev. D **72** (2005) 095003 [hep-ph/0508123].

[141] J. Fuentes-Martin, J. Portoles and P. Ruiz-Femenia, JHEP **1501** (2015) 134 [arXiv:1411.2471 [hep-ph]].

[142] P. Langacker and D. London, Phys. Rev. D **38** (1988) 886.

[143] A. Efrati, A. Falkowski and Y. Soreq, JHEP **1507** (2015) 018 [arXiv:1503.07872 [hep-ph]].

[144] A. Pich, Prog. Part. Nucl. Phys. **75** (2014) 41 [arXiv:1310.7922 [hep-ph]].

[145] T. Kinoshita and A. Sirlin, Phys. Rev. **113** (1959) 1652.

[146] S. M. Berman, Phys. Rev. **112** (1958) 267.

[147] W. J. Marciano and A. Sirlin, Phys. Rev. Lett. **61** (1988) 1815.

[148] W. J. Marciano, Phys. Rev. D **60** (1999) 093006 [hep-ph/9903451].

[149] V. Cirigliano and I. Rosell, JHEP **0710** (2007) 005 [arXiv:0707.4464 [hep-ph]].

[150] R. Decker and M. Finkemeier, Nucl. Phys. B **438** (1995) 17 [hep-ph/9403385].

[151] V. Cirigliano, M. Giannotti and H. Neufeld, JHEP **0811** (2008) 006 [arXiv:0807.4507 [hep-ph]].

[152] V. Cirigliano, G. Ecker, H. Neufeld, A. Pich and J. Portoles, Rev. Mod. Phys. **84** (2012) 399 [arXiv:1107.6001 [hep-ph]].

[153] A. Kastner and H. Neufeld, Eur. Phys. J. C **57** (2008) 541 [arXiv:0805.2222 [hep-ph]].

[154] S. Fajfer, I. Nisandzic and U. Rojec, Phys. Rev. D **91** (2015) no.9, 094009 [arXiv:1502.07488 [hep-ph]].

[155] A. Bazavov *et al.* [Fermilab Lattice and MILC Collaborations], Phys. Rev. D **93** (2016) no.11, 113016 [arXiv:1602.03560 [hep-lat]].

[156] B. Aubert *et al.* [BaBar Collaboration], Phys. Rev. Lett. **93** (2004) 081802 [hep-ex/0404006].

[157] M. Iwasaki *et al.* [Belle Collaboration], Phys. Rev. D **72** (2005) 092005 [hep-ex/0503044].

[158] T. Huber, T. Hurth and E. Lunghi, JHEP **1506** (2015) 176 [arXiv:1503.04849 [hep-ph]].

[159] R. Aaij *et al.* [LHCb Collaboration], JHEP **1405** (2014) 082 [arXiv:1403.8045 [hep-ex]].

[160] J. Matias, F. Mescia, M. Ramon and J. Virto, JHEP **1204** (2012) 104 [arXiv:1202.4266 [hep-ph]].

[161] S. Descotes-Genon, J. Matias, M. Ramon and J. Virto, JHEP **1301** (2013) 048 [arXiv:1207.2753 [hep-ph]].

[162] R. Aaij *et al.* [LHCb Collaboration], JHEP **1308** (2013) 131 [arXiv:1304.6325 [hep-ex]].

[163] R. Aaij *et al.* [LHCb Collaboration], JHEP **1305** (2013) 159 [arXiv:1304.3035 [hep-ex]].

[164] R. Aaij *et al.* [LHCb Collaboration], JHEP **1406** (2014) 133 [arXiv:1403.8044 [hep-ex]].

[165] R. Aaij *et al.* [LHCb Collaboration], JHEP **1602** (2016) 104 [arXiv:1512.04442 [hep-ex]].

[166] R. Aaij *et al.* [LHCb Collaboration], JHEP **1307** (2013) 084 [arXiv:1305.2168 [hep-ex]].

[167] R. Aaij *et al.* [LHCb Collaboration], JHEP **1509** (2015) 179 [arXiv:1506.08777 [hep-ex]].

[168] R. Aaij *et al.* [LHCb Collaboration], JHEP **1504** (2015) 064 [arXiv:1501.03038 [hep-ex]].

[169] S. Descotes-Genon, L. Hofer, J. Matias and J. Virto, JHEP **1412** (2014) 125 [arXiv:1407.8526 [hep-ph]].

[170] S. Descotes-Genon, J. Matias and J. Virto, Phys. Rev. D **85** (2012) 034010 [arXiv:1111.4882 [hep-ph]].

[171] K. De Bruyn, R. Fleischer, R. Knegjens, P. Koppenburg, M. Merk, A. Pellegrino and N. Tuning, Phys. Rev. Lett. **109** (2012) 041801 [arXiv:1204.1737 [hep-ph]].

[172] S. Descotes-Genon and J. Virto, JHEP **1504** (2015) 045 Erratum: [JHEP **1507** (2015) 049] [arXiv:1502.05509 [hep-ph]].

[173] A. Greljo, G. Isidori and D. Marzocca, JHEP **1507** (2015) 142 [arXiv:1506.01705 [hep-ph]].

[174] B. Aubert *et al.* [BaBar Collaboration], Phys. Rev. D **79** (2009) 012002 [arXiv:0809.0828 [hep-ex]].

[175] J. P. Lees *et al.* [BaBar Collaboration], Phys. Rev. Lett. **109** (2012) 101802 [arXiv:1205.5442 [hep-ex]].

[176] M. Huschle *et al.* [Belle Collaboration], Phys. Rev. D **92** (2015) no.7, 072014 [arXiv:1507.03233 [hep-ex]].

[177] R. Aaij *et al.* [LHCb Collaboration], Phys. Rev. Lett. **115** (2015) no.11, 111803 Erratum: [Phys. Rev. Lett. **115** (2015) no.15, 159901] [arXiv:1506.08614 [hep-ex]].

[178] A. Abdesselam *et al.* [Belle Collaboration], arXiv:1603.06711 [hep-ex].

[179] A. Abdesselam *et al.*, arXiv:1608.06391 [hep-ex].

[180] A. Celis, M. Jung, X. Q. Li and A. Pich, JHEP **1301** (2013) 054 [arXiv:1210.8443 [hep-ph]].

[181] J. F. Kamenik and F. Mescia, Phys. Rev. D **78** (2008) 014003 [arXiv:0802.3790 [hep-ph]].

[182] S. Fajfer, J. F. Kamenik and I. Nisandzic, Phys. Rev. D **85** (2012) 094025 [arXiv:1203.2654 [hep-ph]].

[183] J. A. Bailey *et al.* [MILC Collaboration], Phys. Rev. D **92** (2015) no.3, 034506 [arXiv:1503.07237 [hep-lat]].

[184] H. Na *et al.* [HPQCD Collaboration], Phys. Rev. D **92** (2015) no.5, 054510 Erratum: [Phys. Rev. D **93** (2016) no.11, 119906] [arXiv:1505.03925 [hep-lat]].

[185] Z. Ligeti and F. J. Tackmann, Phys. Rev. D **90** (2014) no.3, 034021 [arXiv:1406.7013 [hep-ph]].

[186] I. Caprini, L. Lellouch and M. Neubert, Nucl. Phys. B **530** (1998) 153 [hep-ph/9712417].

[187] CKMfitter Group collaboration, J. Charles, A. Hocker, H. Lacker, S. Laplace, F. R. Le Diberder, J. Malcles et al., *CP violation and the CKM matrix: Assessing the impact of the asymmetric B factories*, *Eur. Phys. J.* **C41** (2005) 1–131, [hep-ph/0406184].

[188] D. Foreman-Mackey, D. W. Hogg, D. Lang and J. Goodman, Publ. Astron. Soc. Pac. **125** (2013) 306 [arXiv:1202.3665 [astro-ph.IM]].

[189] A. Datta, M. Duraisamy and D. Ghosh, Phys. Rev. D **86** (2012) 034027 [arXiv:1206.3760 [hep-ph]].

[190] Y. Sakaki and H. Tanaka, Phys. Rev. D **87** (2013) no.5, 054002 [arXiv:1205.4908 [hep-ph]].

[191] P. Biancofiore, P. Colangelo and F. De Fazio, Phys. Rev. D **87** (2013) no.7, 074010 [arXiv:1302.1042 [hep-ph]].

[192] Y. Sakaki, M. Tanaka, A. Tayduganov and R. Watanabe, Phys. Rev. D **91** (2015) no.11, 114028 [arXiv:1412.3761 [hep-ph]].

[193] M. Duraisamy, P. Sharma and A. Datta, Phys. Rev. D **90** (2014) no.7, 074013 [arXiv:1405.3719 [hep-ph]].

[194] S. Shivashankara, W. Wu and A. Datta, Phys. Rev. D **91** (2015) no.11, 115003 [arXiv:1502.07230 [hep-ph]].

[195] S. Bhattacharya, S. Nandi and S. K. Patra, Phys. Rev. D **93** (2016) no.3, 034011 [arXiv:1509.07259 [hep-ph]].

[196] D. Becirevic, S. Fajfer, I. Nisandzic and A. Tayduganov, arXiv:1602.03030 [hep-ph].

[197] S. Sahoo and R. Mohanta, New J. Phys. **18** (2016) no.9, 093051 [arXiv:1607.04449 [hep-ph]].

[198] R. Alonso, A. Kobach and J. Martin Camalich, Phys. Rev. D **94** (2016) no.9, 094021 [arXiv:1602.07671 [hep-ph]].

[199] A. K. Alok, D. Kumar, S. Kumbhakar and S. U. Sankar, arXiv:1606.03164 [hep-ph].

[200] F. U. Bernlochner and Z. Ligeti, Phys. Rev. D **95** (2017) no.1, 014022 [arXiv:1606.09300 [hep-ph]].

[201] T. Abe *et al.* [Belle-II Collaboration], arXiv:1011.0352 [physics.ins-det].

[202] W. Altmannshofer and I. Yavin, Phys. Rev. D **92** (2015) no.7, 075022 [arXiv:1508.07009 [hep-ph]].

[203] L. Calibbi, A. Crivellin and T. Ota, Phys. Rev. Lett. **115** (2015) 181801 [arXiv:1506.02661 [hep-ph]].

[204] D. Guadagnoli and K. Lane, Phys. Lett. B **751** (2015) 54 [arXiv:1507.01412 [hep-ph]].

[205] S. Sahoo and R. Mohanta, Phys. Rev. D **93** (2016) no.11, 114001 [arXiv:1512.04657 [hep-ph]].

[206] A. Crivellin, G. D'Ambrosio, M. Hoferichter and L. C. Tunstall, Phys. Rev. D **93** (2016) no.7, 074038 [arXiv:1601.00970 [hep-ph]].

[207] D. Bečirević, O. Sumensari and R. Zukanovich Funchal, Eur. Phys. J. C **76** (2016) no.3, 134 [arXiv:1602.00881 [hep-ph]].

[208] G. Kumar, Phys. Rev. D **94** (2016) no.1, 014022 [arXiv:1603.00346 [hep-ph]].

[209] D. Guadagnoli, D. Melikhov and M. Reboud, Phys. Lett. B **760** (2016) 442 [arXiv:1605.05718 [hep-ph]].

[210] C. S. Kim, X. B. Yuan and Y. J. Zheng, Phys. Rev. D **93** (2016) no.9, 095009 [arXiv:1602.08107 [hep-ph]].

[211] A. Celis, V. Cirigliano and E. Passemar, Phys. Rev. D **89** (2014) no.9, 095014 [arXiv:1403.5781 [hep-ph]].

[212] Y. Miyazaki *et al.* [Belle Collaboration], Phys. Lett. B **648** (2007) 341 [hep-ex/0703009 [HEP-EX]].

[213] A. Falkowski, D. M. Straub and A. Vicente, JHEP **1405** (2014) 092 [arXiv:1312.5329 [hep-ph]].

[214] G. Aad *et al.* [ATLAS Collaboration], JHEP **1411** (2014) 104 [arXiv:1409.5500 [hep-ex]].

[215] G. Aad *et al.* [ATLAS Collaboration], JHEP **1508** (2015) 105 [arXiv:1505.04306 [hep-ex]].

[216] G. Aad *et al.* [ATLAS Collaboration], JHEP **1510** (2015) 150 [arXiv:1504.04605 [hep-ex]].

[217] G. Aad *et al.* [ATLAS Collaboration], Eur. Phys. J. C **76** (2016) no.8, 442 [arXiv:1602.05606 [hep-ex]].

[218] V. Khachatryan *et al.* [CMS Collaboration], JHEP **1506** (2015) 080 [arXiv:1503.01952 [hep-ex]].

[219] V. Khachatryan *et al.* [CMS Collaboration], Phys. Rev. D **93** (2016) no.1, 012003 [arXiv:1509.04177 [hep-ex]].

[220] G. Aad *et al.* [ATLAS Collaboration], JHEP **1507** (2015) 157 [arXiv:1502.07177 [hep-ex]].

[221] CMS Collaboration [CMS Collaboration], CMS-PAS-EXO-12-046.

[222] D. A. Faroughy, A. Greljo and J. F. Kamenik, Phys. Lett. B **764** (2017) 126 [arXiv:1609.07138 [hep-ph]].

[223] A. D. Martin, W. J. Stirling, R. S. Thorne and G. Watt, Eur. Phys. J. C **63** (2009) 189 [arXiv:0901.0002 [hep-ph]].

[224] G. Aad *et al.* [ATLAS Collaboration], Phys. Lett. B **754** (2016) 302 [arXiv:1512.01530 [hep-ex]].

[225] V. Khachatryan *et al.* [CMS Collaboration], Phys. Rev. Lett. **116** (2016) no.7, 071801 [arXiv:1512.01224 [hep-ex]].

[226] J. Bernabeu, G. C. Branco and M. Gronau, Phys. Lett. **169B** (1986) 243.

CHAPTER

8 Invisible axion models with non-trivial flavor structure

> There is a theory which states that if ever anyone discovers exactly what the Universe is for and why it is here, it will instantly disappear and be replaced by something even more bizarre and inexplicable. There is another theory which states that this has already happened.
>
> — *Douglas Adams*, The Hitchhiker's Guide to the Galaxy

The benchmark invisible axion models introduced in Chapter 3 are characterized by presenting a minimal scalar sector and no FCNCs. In this chapter we consider the possibility of extending the DFSZ framework presented in Section 3.3.1 to account for a more general class of models, with richer Yukawa and scalar structures. More concretely, in Section 8.1 we will introduce a model able to accommodate Yukawa alignment[1] within an effective DFSZ-like framework. This way we provide for an ultraviolet completion of the A2HDM that, at the same time, solves the Strong CP problem. In Section 8.2 we present a class of invisible axion models based on the BGL model [1] introduced in Section 2.2.2. Contrary to the previously presented models, this implementation is characterized by having flavor changing axion interactions at tree-level, which are controlled by the fermion mixing matrices. We will see that these models introduce new features, both in the axion and in the Higgs sectors, that are absent in the benchmark invisible axion models and that give rise to a new interesting phenomenology.

8.1 Effective A2HDM with a DFSZ-like invisible axion

This section is based in the publication in Ref. [2] where we discuss the possibility of having invisible axion models with a non-minimal scalar sector at the EW scale. In particular, we consider in Section 8.1.1 a simple extension of the DFSZ model with two additional Higgs doublets that are blind to the PQ symmetry, and show that, due to mixing effects among the scalar fields, the decoupling structure of the theory becomes richer than in the DFSZ model. We also show that in certain cases it is

[1] See Section 2.2.1 for a discussion on the hypothesis of Yukawa alignment and its implications.

even possible to obtain an effective 2HDM with a Yukawa aligned structure. While the number of fields that are blind to the PQ symmetry could be reduced to just one for many of the issues discussed, by having two of these fields we guarantee that the scalar potential of the effective theory at the weak scale will be the most general one. The properties of the axion from this model are discussed in Section 8.1.2. A study of the possible decoupling limits of the model is given in Section 8.1.3. In Section 8.1.4 we present two ways of implementing small neutrino masses. We conclude in Section 8.1.5.

8.1.1 Framework

We consider the DFSZ invisible axion model with two additional complex Higgs doublets that are not charged under the PQ symmetry. The scalar sector of the model contains then four complex $\mathrm{SU}(2)_\mathrm{L}$ doublets with hypercharge $Y = 1/2$ and a complex scalar gauge singlet S. We denote by $\Phi_{1,2}$ the Higgs doublets that carry a PQ charge, while the doublets that are blind to the PQ symmetry are denoted by $\phi_{1,2}$. All the Higgs doublets take part in the spontaneous breaking of the EW gauge symmetry by acquiring vevs $\langle \Phi_j^0 \rangle = u_j/\sqrt{2}$ and $\langle \phi_j^0 \rangle = v_j/\sqrt{2}$ $(j = 1, 2)$, with $(u_1^2 + \cdots + v_2^2)^{1/2} \equiv v = (\sqrt{2} G_F)^{-1/2}$ being fixed by the massive gauge boson masses. As in the DFSZ model we assume that the global $\mathrm{U}(1)_\mathrm{PQ}$ symmetry is spontaneously broken by a very large vev of the scalar field $\langle S \rangle = v_\mathrm{PQ}/\sqrt{2}$ $(v_\mathrm{PQ} \gg v)$.

Our scalar content will transform under the PQ symmetry as

$$S \to e^{i X_S \theta} S \,, \quad \Phi_j \to e^{i X_j \theta} \Phi_j \,, \quad \phi_j \to \phi_j \,. \tag{8.1}$$

The most relevant terms in the scalar potential, as will be explained in Section 8.1.3, are the trilinear interactions

$$\mu_{1,j} \Phi_1^\dagger \phi_j S \quad \text{and} \quad \mu_{2,j} \Phi_2^\dagger \phi_j S^* \,, \tag{8.2}$$

where the implicit sum on $j = 1, 2$ is assumed. The parameters $\mu_{1(2),j}$ have mass dimension and determine the size of the mixing between both types of doublets. The above interactions lead to the following charge constraints

$$X_1 = -X_2 = X_S \,. \tag{8.3}$$

The PQ charge normalization is unphysical and therefore we shall set $X_S = 1$, as it is usually done. The full scalar potential, built with the above constraints, can be written as $V = V_S + V_\Phi + V_\phi$, with

$$\begin{aligned}
V_S =& \mu_S^2 |S|^2 + \lambda_S |S|^4 + \lambda_i^{\Phi S} (\Phi_i^\dagger \Phi_i) |S|^2 \\
&+ \left[\lambda_{12}^{\Phi S} (\Phi_1^\dagger \Phi_2) S^2 + \text{h.c.} \right] \\
&+ \lambda_i^{\phi S} (\phi_i^\dagger \phi_i) |S|^2 + \left[\lambda_{12}^{\phi S} (\phi_1^\dagger \phi_2) |S|^2 + \text{h.c.} \right] \\
&+ \left[\mu_{1,i} \Phi_1^\dagger \phi_i S + \mu_{2,i} \Phi_2^\dagger \phi_i S^* + \text{h.c.} \right] \,, \\
V_\Phi =& M_i^2 \Phi_i^\dagger \Phi_i + \lambda_{ii,jj}^{\Phi} (\Phi_i^\dagger \Phi_i)(\Phi_j^\dagger \Phi_j)
\end{aligned}$$

$$
\begin{aligned}
&+ \lambda^{\Phi\phi}_{ii,jj}(\Phi_i^\dagger\Phi_i)(\phi_j^\dagger\phi_j) + \lambda'^{\Phi\phi}_{ii,jj}(\Phi_i^\dagger\phi_j)(\phi_j^\dagger\Phi_i) \\
&+ \lambda^{\Phi}_{12,21}(\Phi_1^\dagger\Phi_2)(\Phi_2^\dagger\Phi_1) + \Big[\lambda^{\Phi\phi}_{ii,12}(\Phi_i^\dagger\Phi_i)(\phi_1^\dagger\phi_2) \\
&+\lambda'^{\Phi\phi}_{ii,12}(\Phi_i^\dagger\phi_2)(\phi_1^\dagger\Phi_i) + \text{h.c.}\Big] \,, \\
V_\phi =& m^2_{ij}\phi_i^\dagger\phi_j + \frac{1}{2}\lambda_{ij,kl}(\phi_i^\dagger\phi_j)(\phi_k^\dagger\phi_l) \,,
\end{aligned}
\tag{8.4}
$$

with $\lambda_{ij,kl} = \lambda_{kl,ij}$, $m^2_{ij} = (m^2_{ji})^*$ and $\lambda_{ij,kl} = \lambda^*_{ji,lk}$. For the Yukawa interactions we shall only couple the doublets Φ_j, we call them active fields. Given our choice of PQ charges, the doublets ϕ_j do not couple to fermions and thus we call them passive fields. For simplicity, we choose the left-handed doublets to be blind under the chiral $\mathrm{U}(1)_{\mathrm{PQ}}$. The charge assignments for the fermions are the same as in the original axion and the DFSZ models (see Eq. (3.34))

$$
\begin{aligned}
&Q_{Lp} \to Q_{Lp}, && \ell_{Lp} \to \ell_{Lp}, \\
&u_{Rp} \to e^{iX_u\theta}u_{Rp}, && e_{Rp} \to e^{iX_e\theta}e_{Rp} \,, \\
&d_{Rp} \to e^{iX_d\theta}d_{Rp} \,.
\end{aligned}
\tag{8.5}
$$

Here $p = 1, 2, 3$ is a family index. The Yukawa Lagrangian reads

$$
-\mathcal{L}_Y = \overline{Q_L}\,\Gamma\,\Phi_1 d_R + \overline{Q_L}\,\Delta\,\tilde{\Phi}_2 u_R + \overline{\ell_L}\,\Pi\,\Phi_k e_R + \text{h.c.} \,,
\tag{8.6}
$$

where $\tilde{\Phi}_2 \equiv i\sigma_2\Phi_2^*$ with σ_2 the Pauli matrix. The mass matrices for the fermions in the flavor basis are given by

$$
M_d = \frac{\Gamma\, u_1}{\sqrt{2}} \,, \qquad M_u = \frac{\Delta\, u_2}{\sqrt{2}} \,, \qquad M_e = \frac{\Pi\, u_k}{\sqrt{2}} \,.
\tag{8.7}
$$

The Yukawa interactions in Eq. (8.6) impose the charge constraints

$$
X_d = -X_1 \,, \quad X_u = X_2 \,, \quad X_e = -X_k \,.
\tag{8.8}
$$

Depending on the values of k, we will have different implementations of the NFC condition [3, 4]: $k = 1$ (type-II); and $k = 2$ (flipped). These are just the usual implementations of NFC in the DFSZ model. Other implementations of the NFC condition, i.e. type-I and lepton-specific [4], where both up and down sectors couple to the same scalar doublet, would not solve the strong CP problem and are not considered.

8.1.2 Axion properties

Given its similarities with the DFSZ model, the invisible axion model from this implementation share many properties with the DFSZ axion presented in Section 3.3.1. In particular, its mass and coupling to photons, determined by the color and electromagnetic anomalies, are the same as in the DFSZ model. However, there is an important difference in what concerns its couplings to matter. As we saw in Chapter 8, in order to determine the axion-matter couplings it is convenient to define the

axion so that it does not mix with the longitudinal component of the Z. Since the information on the passive fields enter through the neutral Goldstone boson, our model will differ from the DFSZ on the axion couplings to matter. As a result, the PQ charges are modified in the following way [5] (see Eqs. (3.54) and (3.55) for the DFSZ analogue)

$$X'_k = X_k - \frac{1}{v^2}\sum_{m=1}^{2} u_m^2 X_m \,, \tag{8.9}$$

with $k = 1, 2$. As a result, the axion coupling to electrons (see Eq. (3.25)) is given by

$$g_e = X'_k = \begin{cases} 2\dfrac{u_2^2}{v^2} + \dfrac{v_1^2+v_2^2}{v^2} & \text{for } k=1 \\ -2\dfrac{u_1^2}{v^2} - \dfrac{v_1^2+v_2^2}{v^2} & \text{for } k=2 \end{cases} , \tag{8.10}$$

where Eq. (8.3) has been used. As expected, we recover the DFSZ result for the axion properties in the limit $v_{1,2} = 0$, when the passive fields do not take part in the breaking of the EW symmetry. However, we can have significant deviations when this is not the case. In Figure 8.1 we plot the absolute value of the axion-electron coupling, $|g_e|$, in terms of the ratios u_k/v. The black solid line corresponds to the DFSZ scenario, while the dashed red and dotted blue lines to our cases $k = 1$ and $k = 2$, respectively. Let us take the $k = 1$ implementation as an example; the dashed red lines are contours and their intersection with the solid black line give the same value of $|g_e|$ as in the DFSZ model. Fixing, for example, the top Yukawa to $y_{top} = 1.5$ (horizontal dashed line) the DFSZ scenario gives $|g_e| = 0.9$. However, this horizontal line crosses not only one dashed red contour but many. In particular, for this specific y_{top} we have $|g_e| \in [0.9\,,\, 1.44]$. This allow us to increase the axion-electron coupling up to 60%. For the scenario $k = 2$ the opposite happens, i.e. we can decrease the axion-electron coupling. The adimensional axion-electron coupling constant defined as

$$|h_{aee}| = \frac{m_e|g_e|}{v_{\rm PQ}} \simeq 1.4\times 10^{-14} \times \left(\frac{m_a}{\rm meV}\right) \times |g_e| \,, \tag{8.11}$$

is constrained from white dwarfs and stellar evolution considerations, see Section 3.3.4, requiring $|h_{aee}| \lesssim 1.3\times 10^{-13}$ [6, 7]. This leads to the mass bound

$$m_a|g_e| \lesssim 10\,{\rm meV}\,. \tag{8.12}$$

Taking the scenario $k = 1$ and fixing the value of the top Yukawa, we see that the axion mass is more constrained as we depart from the DFSZ limit. For the scenario $k = 2$ the inverse happens, as we depart from the DFSZ limit we soften the bound on the axion mass (for a fixed value of the top Yukawa). Therefore, the presence of the passive fields can have important implications for the energy-loss in stars by modifying the axion coupling to electrons.

Taking into account perturbativity of the top Yukawa, the allowed range for $|g_e|$ is roughly $[0.2, 2]$ and $[0, 1.8]$ for $k = 1$ and $k = 2$, respectively. This implies the

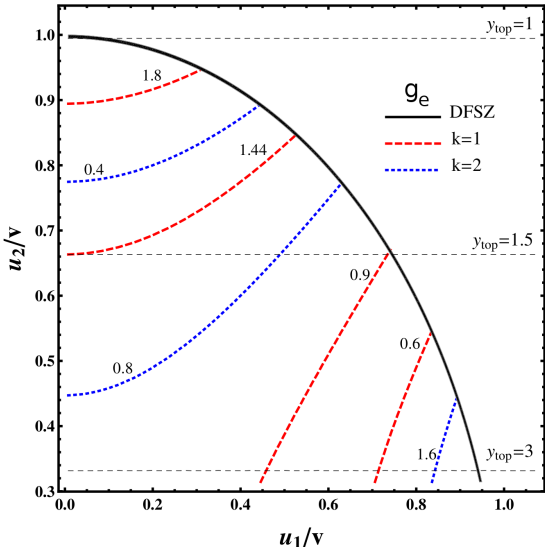

Figure 8.1: *Axion coupling to electrons, $|g_e|$, in the u_2/v vs. u_1/v plane. The DFSZ model is represented by the solid black line, our framework with red dashed line for $k = 1$ and blue dotted one for $k = 2$. Very small values of u_2/v would lead to a non-perturbative top Yukawa and are not shown.*

following bound on the axion mass $m_a \lesssim 5\,\text{meV}$. Such bound is well compatible with the region where the invisible axion could constitute all of the dark matter in the Universe, see Ref. [8] and references therein.

The presence of the passive fields would also give rise to similar modifications of the axion coupling to hadrons [5], relevant for interpreting the supernova SN 1987A limits [6]. The passive fields, on the other hand, do not change the axion coupling to photons since they are blind to the PQ symmetry. In our scenario this implies that bounds relying on the axion coupling to photons that we discussed in Section 3.3.4 would be the same as in the DFSZ model. In particular, constraints from the Solar age, helioseismology, the Solar neutrino flux as well as direct axion searches via axion-photon conversion are not sensitive to the passive fields [6].

8.1.3 Mixing active and passive doublets and the decoupling limit

A distinctive feature of invisible axion models is that the large PQ symmetry breaking scale usually brings the scalar sector to a decoupling scenario. A SM-like Higgs remains at the weak scale while the other scalar fields (with the exception of the axion) get masses around v_{PQ}. In the DFSZ model for example, decoupling arises due to terms in the scalar potential mixing the Higgs doublets with the scalar singlet; these terms are crucial so that the axion actually becomes invisible. Under specific circumstances one can avoid decoupling in the DFSZ model and have the two Higgs doublets at the weak scale, protection against dangerous flavor changing scalar couplings is guaranteed by the NFC condition. In order to illustrate the decoupling limit, let us consider the DFSZ scalar potential which is a particular case of our more general scalar sector, where the passive fields are absent, i.e. $V_{\text{DFSZ}} = V|_{\phi_j=0}$. Due to the large hierarchy on the vevs, i.e. $v_{\text{PQ}} \gg v$, we can extract

$$v_{\text{PQ}}^2 = -2\mu_S^2/\lambda_S + \mathcal{O}(v^2)\,. \tag{8.13}$$

Up to $\mathcal{O}(v^2)$, we can deal with this mixing as being $\mathrm{SU}(2)_\mathrm{L}$ preserving. The mass matrix for the doublets reads

$$V_{\mathrm{DFSZ}}^{\mathrm{mass}} \;=\; \Phi_i^\dagger\;(\mathcal{M}_A)_{ij}\;\Phi_j + \mathcal{O}(v^2)\,, \tag{8.14}$$

with $\mathcal{M}_A$ given in Eq. (8.17a). The decoupling condition can be readily obtained by going to the Higgs basis in which only one Higgs doublet takes a vev, the Higgs doublet that does not acquire a vev will decouple if

$$\frac{|\lambda_{12}^{\Phi S}|\,v_{\mathrm{PQ}}^2}{2\cos\beta\sin\beta} \gg v^2\,. \tag{8.15}$$

Here $\tan\beta \equiv \langle\Phi_2^0\rangle/\langle\Phi_1^0\rangle$ and $\lambda_{12}^{\Phi S}$ is defined in Eq. (8.4). In the decoupling limit the Higgs doublet that gets a vev remains at the EW scale: three degrees of freedom of this doublet correspond to the Goldstone bosons that give mass to the massive gauge vector bosons while the remaining degree of freedom is a SM-like Higgs boson. If $|\lambda_{12}^{\Phi S}|$ happens to be small enough, both doublets remain at the weak scale and a plethora of new physics phenomena associated with the Higgs sector becomes accessible to experiments.

In the framework presented in Section 8.1.1, the breaking of $\mathrm{U}(1)_{\mathrm{PQ}}$ by the large vev v_{PQ} induces a non-negligible mixing between the active and passive scalar doublets. The decoupling structure of this framework will then be richer than in the DFSZ model. Defining the scalar field $\varphi = (\Phi_1,\,\Phi_2,\,\phi_1,\,\phi_2)^T$, we want to diagonalize the mass terms for the doublets $\varphi_i^\dagger \mathcal{M}_{ij}\,\varphi_j$, where

$$\mathcal{M} \;=\; \begin{pmatrix} \mathcal{M}_A & \mathcal{M}_B \\ \mathcal{M}_B^\dagger & \mathcal{M}_C \end{pmatrix}. \tag{8.16}$$

Here $\mathcal{M}$ is a 4×4 hermitian matrix and the specific form of the 2×2 blocks is given by

$$\mathcal{M}_A = \begin{pmatrix} M_1^2 + \frac{\lambda_1^{\Phi S}}{2} v_{\mathrm{PQ}}^2 & \frac{\lambda_{12}^{\Phi S}}{2} v_{\mathrm{PQ}}^2 \\ \frac{(\lambda_{12}^{\Phi S})^*}{2} v_{\mathrm{PQ}}^2 & M_2^2 + \frac{\lambda_2^{\Phi S}}{2} v_{\mathrm{PQ}}^2 \end{pmatrix}, \tag{8.17a}$$

$$\mathcal{M}_B = \frac{1}{\sqrt{2}} v_{\mathrm{PQ}}^2 \begin{pmatrix} \mu_{1,1} & \mu_{1,2} \\ \mu_{2,1} & \mu_{2,2} \end{pmatrix}, \tag{8.17b}$$

$$\mathcal{M}_C = \begin{pmatrix} m_{11}^2 + \frac{\lambda_1^{\phi S}}{2} v_{\mathrm{PQ}}^2 & m_{12}^2 + \frac{\lambda_{12}^{\phi S}}{2} v_{\mathrm{PQ}}^2 \\ (m_{12}^2)^* + \frac{(\lambda_{12}^{\phi S})^*}{2} v_{\mathrm{PQ}}^2 & m_{22}^2 + \frac{\lambda_2^{\phi S}}{2} v_{\mathrm{PQ}}^2 \end{pmatrix}. \tag{8.17c}$$

The block $\mathcal{M}_B$ is responsible for the mixing of active and passive fields, it comes solely from the interaction in Eq. (8.2). Let us denote by H_j ($j = 1,\ldots,4$) the mass eigenstates, ordered from the heaviest to the lightest one ($|M_{H_m}| \geq |M_{H_n}|$ for $m < n$). We must find the unitary transformation $\mathcal{R}$, i.e. $\varphi_i = \mathcal{R}_{ij}\,H_j$, that makes $\mathcal{M}$ diagonal. The Yukawa interactions will contain, in general, the four mass eigenstates H_j coupling to the fermions.

We are interested in the two following decoupling limits: (1) $H_{3,4}$ at the weak scale; (2) H_4 at the weak scale. In case (2) we will get a SM-like Higgs sector at

the weak scale. Therefore, we shall focus on case (1) (case (2) can be seen as a limiting case of (1) where H_3 decouples). Working in the decoupling limit (1), we do not need the full information on the entries of $\mathcal{R}$ in order to check the low energy Yukawa interactions. The relevant entries are the block that mixes the active fields with the lightest mass eigenstates, that is

$$\begin{pmatrix}\Phi_1\\ \Phi_2\end{pmatrix} = \widehat{\mathcal{R}}\begin{pmatrix}H_3\\ H_4\end{pmatrix}, \quad \text{with} \quad \widehat{\mathcal{R}} = \begin{pmatrix}\mathcal{R}_{13} & \mathcal{R}_{14}\\ \mathcal{R}_{23} & \mathcal{R}_{24}\end{pmatrix}. \tag{8.18}$$

The matrix $\widehat{\mathcal{R}}$ is in general not unitary. The effective Yukawa interactions will be given by

$$\begin{aligned}-\mathcal{L}_Y^{\text{eff}} &= \overline{Q_L}\,\Gamma\,(\mathcal{R}_{13}H_3 + \mathcal{R}_{14}H_4)d_R + \overline{Q_L}\,\Delta\,(\mathcal{R}_{23}^*\tilde{H}_3 + \mathcal{R}_{24}^*\tilde{H}_4)u_R\\ &\quad + \overline{\ell_L}\,\Pi\,(\mathcal{R}_{k3}H_3 + \mathcal{R}_{k4}H_4)e_R + \text{h.c.}\end{aligned} \tag{8.19}$$

In the decoupling limit, the EW vev should reside completely in the light doublets $\langle H_{3,4}^0\rangle = w_{3,4}/\sqrt{2}$, with $(w_3^2 + w_4^2)^{1/2} = v$. We describe below the Yukawa structures that can arise at the weak scale for different forms of the matrix $\widehat{\mathcal{R}}$. The entries denoted by $\times$ shall represent not only nonzero entries, but also of $\mathcal{O}(1)$. The last requirement guarantees perturbative Yukawa couplings. We then have the following cases:

- $\widehat{\mathcal{R}} = \begin{pmatrix}\times & 0\\ \times & \times\end{pmatrix}$

  A mixing matrix $\widehat{\mathcal{R}}$ with this structure will give rise to Yukawa alignment [9] in the effective theory. A possible texture for the mass matrix is

  $$\frac{\mathcal{M}_A}{2b} \sim \begin{pmatrix}1+\dfrac{\epsilon}{2b} & 1\\ 1 & 1\end{pmatrix}, \quad \frac{\mathcal{M}_B}{b} \sim \begin{pmatrix}1 & 1\\ 1 & 1\end{pmatrix}, \quad \frac{\mathcal{M}_C}{b} \sim \begin{pmatrix}2 & -1\\ -1 & 2\end{pmatrix}, \tag{8.20}$$

  with b and ϵ being parameters of $\mathcal{O}(b) \sim \mathcal{O}(v_{\text{PQ}}^2) \gg \mathcal{O}(\epsilon)$. The mass spectrum is of the form, up to $\mathcal{O}(v^2)$,

  $$M_{H_1}^2 \sim 5b\,, \quad M_{H_2}^2 \sim 3b\,, \quad M_{H_3}^2 \sim \epsilon\,, \quad M_{H_4}^2 \sim 0\,. \tag{8.21}$$

  Since one is free to perform a basis transformation among the light Higgs doublets, other forms of the mixing matrix $\widehat{\mathcal{R}}$ leading to Yukawa alignment at the weak scale are equivalent to the one presented previously. In this framework one can only obtain two independent alignment parameters, contrary to the most general hypothesis of Yukawa alignment formulated in Ref. [9] with three independent alignment parameters.

- $\widehat{\mathcal{R}} = \begin{pmatrix}\times & 0\\ \times & 0\end{pmatrix}$

  Any UV implementation will always lead in this case to an effective type-I scenario, where all the fermions couple to the same doublet at the weak scale. A possible texture for the mass matrix is

  $$\frac{\mathcal{M}_A}{b} \sim \begin{pmatrix}1+\dfrac{\epsilon}{b} & 1\\ 1 & 1+\dfrac{\epsilon}{b}\end{pmatrix}, \qquad \frac{\mathcal{M}_B}{c} \sim \frac{\mathcal{M}_C}{b} \sim \begin{pmatrix}1 & 1\\ 1 & 1\end{pmatrix}. \tag{8.22}$$

Here c is a parameter of $\mathcal{O}(c) \sim \mathcal{O}(b) \sim \mathcal{O}(v_{\rm PQ}^2) \gg \mathcal{O}(\epsilon)$. This leads to a spectrum of the form

$$M_{H_{1,2}}^2 \simeq 2(b \pm c)\,, \quad M_3^2 \simeq \epsilon\,, \quad M_4^2 \simeq 0\,, \tag{8.23}$$

with the same hierarchy as before.

In the previous cases, the original Yukawa structure of the active fields is not manifest at the weak scale. A large mixing $\mu_{1(2),j} \sim v_{\rm PQ}$ between the active and passive fields generates a decoupling scenario where the light scalar states contain a significant admixture of both types of fields. However, a large mixing between active and passive fields does not guarantee that the Yukawa structure will be different in the effective theory.

- $\widehat{\mathcal{R}} = \begin{pmatrix} \times & 0 \\ 0 & \times \end{pmatrix}$

  The original UV implementation will remain at the effective level. A possible texture for the mass matrix is

  $$\frac{\mathcal{M}_A}{b} \sim \begin{pmatrix} 1+\dfrac{\epsilon}{b} & 0 \\ 0 & 1 \end{pmatrix}\,, \quad \frac{\mathcal{M}_B}{b} \sim \begin{pmatrix} 0 & 1 \\ 1 & 0 \end{pmatrix}\,, \quad \frac{\mathcal{M}_C}{b} \sim \begin{pmatrix} 1 & 0 \\ 0 & 1 \end{pmatrix}\,. \tag{8.24}$$

  We get the mass spectrum

  $$M_{H_{1,2}}^2 \sim 2b\,, \quad M_{H_3}^2 \sim \epsilon\,, \quad M_{H_4}^2 \sim 0\,. \tag{8.25}$$

  In general, the original Yukawa structure in Eq. (8.6) will remain in the effective theory if the mixing matrix $\widehat{\mathcal{R}}$ can be brought into diagonal form by a basis transformation of the light doublets. Finally, if the mixing between the active and passive doublets is negligible $\mu_{1(2),j} \ll v_{\rm PQ}$, the only way to get the desired decoupling is that the light fields $H_{3,4}$ are simply two independent combinations of the active doublets. In this case the Yukawa structure is not altered.

As noted in Section 8.1.1, only the type-II or flipped implementations can solve the strong CP problem. However, in our scenario we are able to mimic the DFSZ axion and still allow (at the effective level) for a type-I, type-II, flipped or even aligned Yukawa structure. Also, recall that in contrast with the usual two-Higgs-doublet models with NFC, our effective scalar potential has the most general form. Finally, we are not able to reproduce (at the effective level) the lepton-specific scenario since the active field coupling to the charged leptons at the UV level is always one of the active fields coupling to the up or down quarks.

8.1.4 Adding right-handed neutrinos

We shall work in the canonical extension with three right-handed neutrinos N_{Rp} ($p = 1, 2, 3$). Since the Dirac or Majorana nature of the light neutrinos is still unknown we shall present an implementation for both scenarios.

The Majorana neutrinos can be implemented in the well known Type-I seesaw mechanism [10]. In this framework the fermionic interaction Lagrangian gets extended by

$$-\mathcal{L}_\nu = \overline{\ell_L} Y \tilde{\Phi}_j N_R + \overline{N_R^c}\, A\, N_R\, S + \text{h.c.} \tag{8.26}$$

Here $j = 1, 2$ depending on the implementation of the NFC condition and A is a dimensionless 3×3 symmetric complex matrix. We need to impose a non-trivial transformation of N_R under the $\mathrm{U}(1)_{\mathrm{PQ}}$ symmetry. With the field transformation

$$N_{Rp} \to e^{iX_N\theta} N_{Rp}\,, \tag{8.27}$$

the above Lagrangian implies the charge constraints[2]

$$X_N = -\frac{1}{2}\,, \quad X_\ell = X_N - X_j\,. \tag{8.28}$$

After the breaking of the PQ-symmetry, a mass term for the right-handed fields is generated and the resulting low-energy neutrino mass matrix will then be given by

$$m_\nu \simeq -\frac{u_j^{*2}}{2\sqrt{2} v_{\mathrm{PQ}}}\, Y\, A^{-1}\, Y^T\,. \tag{8.29}$$

If in Eq. (8.26) instead of Φ_j we had the passive doublets coupling to neutrinos, X_ℓ becomes $-1/2$ and in Eq. (8.29) we must do the replacement $u_j^* Y \to \sum_k v_k^* Y_k$.

In general, the introduction of a Majorana mass term for the right-handed neutrinos breaks lepton number. The presence of a complex scalar singlet allows the definition of a conserved lepton number $\mathrm{U}(1)_L$ in Eq. (8.26), where all leptons have associated a $+1$ charge (-1 for anti-leptons) and the complex scalar S a -2 charge [11]. However, the presence in the scalar potential of the interaction terms in Eq. (8.2) explicitly violates lepton number. One could see these type of interactions as a soft breaking, allowing lepton number conservation in a natural limit. As explained in Ref. [11], in that symmetric limit we get a majoron (the Goldstone of the $\mathrm{U}(1)_L$). In these models the majoron can transmute into the invisible axion as the soft symmetry breaking term is turned on. Our scenario is a bit different, since we cannot define a lepton number up to a soft breaking. The trilinear terms in Eq. (8.2) must be close to the PQ scale in order to obtain a Yukawa aligned structure at the weak scale while avoiding non-perturbative Yukawa couplings at the same time. Besides, the interaction terms in Eq. (8.26), we also have the dimension four lepton number violating term $\Phi_1^\dagger \Phi_2 S^2$.[3] In this way, lepton number is not at all softly broken.

Summing up, in our scenario lepton number is explicitly (and not softly) broken and the invisible axion will have no remnant of a majoron. Therefore, the seesaw scale can be related with the PQ scale, but the dynamical origin of lepton number violation is not approached in this model.

Choosing the charge assignment $X_\ell = X_N \neq 0, \pm 1/2$, we can avoid the Majorana mass term for the right-handed neutrinos as well as their Yukawa coupling with the

[2] Allowing instead for the term $\overline{N_R^c}\, A\, N_R\, S^*$ in Eq. (8.26) would imply $X_N = \frac{1}{2}$.

[3] This term can be eliminated choosing a different PQ charge assignment, in that case the trilinear couplings are promoted to a dimension four term.

active doublets. In this case the neutrinos obtain Dirac masses from their Yukawa interaction with the passive fields,

$$-\mathcal{L}_\nu = \overline{\ell_L} Y_j \, \tilde{\phi}_j N_R + \text{h.c.} \tag{8.30}$$

The neutrino mass matrix will be given by

$$m_\nu = \frac{v_j^*}{\sqrt{2}} Y_j \, . \tag{8.31}$$

This scenario is not as popular as the seesaw mechanism for two main reasons: the requirement of very small Yukawa couplings, without any dynamical origin; and the need for a new imposed symmetry, a global $B - L$, that forbids the Majorana term.

In our framework the very small Yukawa couplings can be avoided if we are working near the DFSZ limit. In this limiting case we have the strong hierarchy $\mathcal{O}(u_j) \gg \mathcal{O}(v_j)$, allowing the neutrino Yukawas to be as tuned as the charged lepton ones. Concerning the global $B - L$ symmetry; due to the particular charge assignments under $\mathrm{U}(1)_{\mathrm{PQ}}$, the theory posses an accidental $B - L$ global symmetry which remains unbroken. Note that, while the previous seesaw scenario can be implemented in the usual DFSZ model, the Dirac case is only possible (without resorting to very small Yukawa couplings) if the scalar fields coupling to neutrinos do not couple to other type of matter, i.e. are passive fields.

8.1.5 Conclusions

In this section we have considered the DFSZ invisible axion model with an additional pair of Higgs doublets that are blind to the PQ symmetry. Due to mixing effects among the scalar fields it is possible to obtain a rich scalar sector at the weak scale with an underlying natural flavor conservation condition which guarantees the absence of dangerous flavor changing scalar couplings. We have shown that in a particular decoupling limit, two Higgs doublets remain at the weak scale with a Yukawa aligned structure [9], while all the other scalars (with the exemption of the axion) have masses close to the PQ symmetry breaking scale. In this limit, the model can then be regarded as an UV completion of the A2HDM. Compared with the original formulation of the A2HDM, our framework posses some important differences. In our scenario a chiral global $\mathrm{U}(1)_{\mathrm{PQ}}$ symmetry provides a dynamical solution to the strong CP problem via the PQ mechanism, with a DFSZ-like axion. On the other hand, our model contains at most two independent complex alignment parameters while the general A2HDM contains three (with the same fermionic content than the SM). We can also extend it to accommodate small active neutrino masses with either Dirac or Majorana neutrinos.

Other models that can give rise to Yukawa alignment at the weak scale have been formulated [12], none of these however solve the strong CP problem. Having an UV completion of the A2HDM that solves the strong CP problem is crucial for example when interpreting the stringent limits from hadronic electric dipole moments [13].

Finally, it is worth stressing that invisible axion models as the one proposed in this section have some drawbacks; besides the fact that the PQ symmetry and the particle content might seem ad hoc. Being $\mathrm{U}(1)_{\mathrm{PQ}}$ a continuous symmetry,

gravitational effects can introduce large contributions to the axion mass and spoil the solution to the strong CP problem, see Section 3.3.3 for a discussion. While this is out of the scope of the work presented in this thesis, we call the attention that in order to make this model more natural a mechanism to avoid these effects, such as the one discussed in Section 3.3.3, should be implemented.

8.2 Invisible axion models with controlled FCNCs at tree-level

Up to now, the invisible axion models presented in this thesis are characterized by having no flavor changing interactions. In this section we will exploit the $\mathrm{U}(1)_{\mathrm{BGL}}$ introduced in Section 2.2.1 to build a class of invisible axion models where the PQ symmetry is not family universal but rather a horizontal symmetry.[4] As we saw in Section 2.2.1, the minimal version of the BGL model leads to the presence of a dangerous Goldstone boson that calls for the extension of such framework. By promoting the BGL symmetry to a PQ symmetry, we get rid of this dangerous Goldstone boson, which now becomes an axion or familon, while at the same time, we provide a solution to the Strong CP problem within this framework.

The model considered in this section is characterized by several interesting features. Among these, we stress the possibility of avoiding the domain wall problem [16–18]. Moreover, the presence of flavor changing axion interactions can introduce experimental constraints stronger than the astrophysical ones in some cases [19]. Invisible axion models with a horizontal PQ symmetry have been built previously in Refs. [20–24] and in the context of horizontal gauge symmetries in Ref. [25].

The structure of this section is as follows: in Section 8.2.1 we show that it is not possible to implement axion models within the 2HDM BGL model presented in Section 2.2.2 and that an extension of the scalar sector is needed to promote this symmetry to a PQ symmetry. In Section 8.2.2, we provide a simple extension of the BGL model for which the proposed mechanism is possible. This model can be minimally extended to account for neutrino masses, we explore this possibility within a concrete implementation in Section 8.2.3. A full study of the axion properties of the model, including the domain wall problem and the protection from gravitational effects, is done in Section 8.2.4. All the results shown in the previous sections will be obtained in the top-BGL implementation where the top quark is singled out and the FCNCs appear in the down-quark sector; Section 8.2.5 is intended to the study of all the possible models variations. In Section 8.2.6 we perform a phenomenological analysis of the axion in these models taking into account flavor experiments, astrophysical considerations and axion searches via axion-photon conversion. Some details concerning Higgs decoupling scenarios and possible new physics signatures related to the Higgs sector can also be found in Section 8.2.7. We summarize our results and conclude in Section 8.2.8.

[4] Such models were introduced in Refs. [14, 15] in which the following section is based.

8.2.1 The anomalous condition for a BGL-like model

The aim of this section is to consider whether the $\mathrm{U}(1)_{\mathrm{BGL}}$ symmetry introduced in Section 2.2.2 can be promoted to a PQ symmetry. As we saw in Section 3.2, for a global U(1) to act as a $\mathrm{U}(1)_{\mathrm{PQ}}$ and solve the Strong CP problem, this symmetry has to be chiral and $\mathrm{SU}(3)_c$ anomalous. The BGL symmetry introduced in Eq. (2.38) is a chiral symmetry, however the color anomaly cancellation condition

$$[\mathrm{SU}(3)_c]^2 \times \mathrm{U}(1)_{\mathrm{PQ}} : \quad 2X_{tL} - X_{tR} + X_{uR} = 0\,. \tag{8.32}$$

is automatically satisfied for this charge implementation. This result, that also applies to the other 2HDM BGL model variations, is the consequence of having to match the $\mathcal{S}_\Phi^{\mathrm{up}}$ and $\mathcal{S}_\Phi^{\mathrm{down}}$ generators (see Eqs. (2.33) and (2.36)) to make the two Higgs BGL implementation consistent. A simple solution to bypass this matching condition is to extend the model beyond two Higgs, making the three-Higgs doublet model the minimal extension. In the three Higgs implementation we can just join the scalar generators $\mathcal{S}_\Phi^{\mathrm{up}}$ and $\mathcal{S}_\Phi^{\mathrm{down}}$ into a single one

$$\mathcal{S}_\Phi = \mathrm{diag}\left(e^{iX_{uR}\,\theta}, e^{i(X_{tR}-X_{tL})\,\theta}, e^{i(X_{tL}-X_{dR})\,\theta}\right)\,. \tag{8.33}$$

In this three-Higgs doublet model implementation we get the following Yukawa textures

$$\begin{gathered}
\Gamma_1 = \begin{pmatrix} \times & \times & \times \\ \times & \times & \times \\ 0 & 0 & 0 \end{pmatrix}\,, \qquad \Gamma_2 = 0\,, \qquad \Gamma_3 = \begin{pmatrix} 0 & 0 & 0 \\ 0 & 0 & 0 \\ \times & \times & \times \end{pmatrix}\,, \\
\Delta_1 = \begin{pmatrix} \times & \times & 0 \\ \times & \times & 0 \\ 0 & 0 & 0 \end{pmatrix}\,, \qquad \Delta_2 = \begin{pmatrix} 0 & 0 & 0 \\ 0 & 0 & 0 \\ 0 & 0 & \times \end{pmatrix}\,, \qquad \Delta_3 = 0\,,
\end{gathered} \tag{8.34}$$

with the charge constraints

$$\begin{gathered}
\text{Texture Matching Conditions:} \begin{cases} X_{uR} = -X_{dR}, \\ X_{uR} \neq X_{tR}, \\ X_{tL} \neq X_{tR} - X_{uR}, \end{cases} \\
\text{Anomaly condition: } X_{tL} \neq -\frac{1}{2}\left(X_{uR} - X_{tR}\right).
\end{gathered} \tag{8.35}$$

Since we extended the Higgs sector, in principle it is no longer necessary to have Γ_1^{BGL} and Δ_1^{BGL} (see Eq. (2.21) for their definition) coupling to the same Higgs doublet. We can have another three different implementations:

- Γ_1^{BGL} with Δ_2^{BGL}. This implies $-X_{dR} = X_{tR} - X_{tL}$;
- Γ_2^{BGL} with Δ_1^{BGL}. This implies $X_{uR} = X_{tL} - X_{dR}$;
- Γ_2^{BGL} with Δ_2^{BGL}. This implies $X_{tR} - X_{tL} = X_{tL} - X_{dR}$.

However, the first two implementations violate the charge restrictions in Eq. (2.37) whereas the third one is a safe implementation and gives

$$\mathcal{S}_\Phi = \text{diag}\left(e^{iX_{uR}\,\theta}, e^{-iX_{dR}\,\theta}, e^{i(X_{tL}-X_{dR})\,\theta}\right)\,, \tag{8.36}$$

so we get the following Yukawa textures implementation

$$\begin{gathered}\Gamma_1 = 0\,, \qquad \Gamma_2 = \begin{pmatrix}\times & \times & \times\\ \times & \times & \times\\ 0 & 0 & 0\end{pmatrix}\,, \quad \Gamma_3 = \begin{pmatrix}0 & 0 & 0\\ 0 & 0 & 0\\ \times & \times & \times\end{pmatrix}\,,\\ \Delta_1 = \begin{pmatrix}\times & \times & 0\\ \times & \times & 0\\ 0 & 0 & 0\end{pmatrix}\,, \qquad \Delta_2 = 0\,, \qquad \Delta_3 = \begin{pmatrix}0 & 0 & 0\\ 0 & 0 & 0\\ 0 & 0 & \times\end{pmatrix}\,.\end{gathered} \tag{8.37}$$

For this symmetry to be anomalous and in order not to introduce additional textures that spoil the desired behavior of the model we need to guarantee, in analogy to the previous case, the following charge restrictions

$$\begin{gathered}\text{Texture Matching Conditions: } \begin{cases} X_{tR} = 2X_{tL} - X_{dR},\\ X_{tL} \neq X_{uR} + X_{dR},\\ X_{tL} \neq \frac{1}{2}\left(X_{uR} + X_{dR}\right), \end{cases}\\ \text{Anomaly Condition: } X_{uR} \neq -X_{dR}.\end{gathered} \tag{8.38}$$

The BGL 2HDM needs to satisfy the condition B in Eq. (2.32). However, when extending it to a three Higgs scenario, with the possibility of null couplings, this condition no longer needs to be satisfied. Relaxing this condition by setting $X_{tR} = X_{uR} + X_{tL}$, we get a new type of texture in the up sector (the combination of Δ_1^{BGL} and Δ_2^{BGL}). Three new possible implementations become available:

- New texture coupling to Γ_1^{BGL}. This implies $X_{dR} = -X_{uR}$;
- New texture coupling to Γ_2^{BGL}. This implies $X_{dR} - X_{tL} = -X_{uR}$;
- New texture coupling to a null texture.

The first two cases violate the charge conditions in Eq. (2.37), this is the reason why there is no BGL 2HDM with this texture. However, the third possibility gives a safe implementation in a three Higgs scenario with the same scalar charge assignments as in the previous case, i.e. Eq. (8.36). The Yukawa textures implementation is then given by

$$\begin{gathered}\Gamma_1 = 0\,, \qquad \Gamma_2 = \begin{pmatrix}\times & \times & \times\\ \times & \times & \times\\ 0 & 0 & 0\end{pmatrix}\,, \quad \Gamma_3 = \begin{pmatrix}0 & 0 & 0\\ 0 & 0 & 0\\ \times & \times & \times\end{pmatrix}\,,\\ \Delta_1 = \begin{pmatrix}\times & \times & 0\\ \times & \times & 0\\ 0 & 0 & \times\end{pmatrix}\,, \qquad \Delta_2 = 0\,, \qquad \Delta_3 = 0\,.\end{gathered} \tag{8.39}$$

For the symmetry to be anomalous and to guarantee that we introduce no additional Yukawa textures, the following charge conditions apply

$$\begin{aligned} &\text{Texture Matching Conditions: } \begin{cases} X_{uR} \neq -X_{dR}, \\ X_{tL} \neq X_{uR} + X_{dR}, \\ X_{tL} \neq -\left(X_{uR} + X_{dR}\right), \\ X_{tL} \neq \frac{1}{2}\left(X_{uR} + X_{dR}\right), \end{cases} \\ &\text{Anomaly Condition: } X_{tL} \neq 3\left(X_{uR} + X_{dR}\right). \end{aligned} \tag{8.40}$$

In conclusion, in this section we have shown that it is not possible to build an anomalous two-Higgs-doublet model à la BGL and we have found three different implementations of the PQ symmetry for the three-Higgs-doublet model, up to permutations in the family or in the up-down sectors. These three cases are built from the generators in Eqs. (2.29) and (2.34). They read as follows:

- **Case I:** where the Yukawa textures are given by Eq. (8.34), satisfies conditions A and B in Eqs. (2.30) and (2.32), and the texture matching and anomaly conditions in Eq. (8.35).

  The charges associated with the Higgs fields are

  $$X_{\Phi 1} = X_{uR}\,, \quad X_{\Phi 2} = X_{tR} - X_{tL}\,, \quad X_{\Phi 3} = X_{tL} + X_{uR}\,. \tag{8.41}$$

- **Case II:** with the Yukawa textures shown in Eq. (8.37), satisfies conditions A and B, and the texture matching and anomaly conditions in Eq. (8.38).

  The charges associated with the Higgs fields are

  $$X_{\Phi 1} = X_{uR}\,, \quad X_{\Phi 2} = -X_{dR}\,, \quad X_{\Phi 3} = X_{tL} - X_{dR}\,. \tag{8.42}$$

- **Case III:** with the Yukawa textures shown in Eq. (8.39), satisfies the constraint $X_{tR} = X_{uR} + X_{tL}$, condition A, and the texture matching and anomaly conditions in Eq. (8.40).

  The charges associated with the Higgs fields are the same as in case II.

8.2.2 The three-Higgs-doublet class of anomalous models

In the previous section we have shown that the Yukawa textures in the BGL 2HDM cannot be imposed by a chiral PQ symmetry. We also derived the necessary conditions to build three-Higgs doublet models with FCNC at tree-level completely determined by the fermion mixing matrices. In the latter scenario, we obtained all the possible Yukawa texture implementations imposed by a PQ symmetry and determined the restrictions to the PQ charges in each case. In what follows we provide details about the quark Yukawa sector, the scalar sector, and the extension to the leptonic sector in these type of models.

The Yukawa quark sector

In similar a fashion to what was done in Section 2.1, we shall build the relevant flavor matrix combinations that mediate the FCNCs. The Yukawa Lagrangian in the three Higgs scenario is now written as

$$-\mathcal{L}_{\rm Y} = \overline{Q_L^0}\,\left[\Gamma_1\,\Phi_1 + \Gamma_2\,\Phi_2 + \Gamma_3\,\Phi_3\right] d_R^0 + \overline{Q_L^0}\,\left[\Delta_1\,\widetilde{\Phi}_1 + \Delta_2\,\widetilde{\Phi}_2 + \Delta_3\,\widetilde{\Phi}_3\right] u_R^0 + \text{h.c.}\,, \tag{8.43}$$

where we just keep the same notation as in Eq. (2.1), but for $j = 1, 2, 3$ in this case. We go once more to the Higgs basis, by performing the following transformations

$$\begin{pmatrix} G^+ \\ H^+ \\ H'^+ \end{pmatrix} = O_3 \begin{pmatrix} \varphi_1^+ \\ \varphi_2^+ \\ \varphi_3^+ \end{pmatrix}\,, \quad \begin{pmatrix} G^0 \\ I \\ I' \end{pmatrix} = O_3 \begin{pmatrix} \eta_1 \\ \eta_2 \\ \eta_3 \end{pmatrix}\,, \quad \begin{pmatrix} H^0 \\ R \\ R' \end{pmatrix} = O_3 \begin{pmatrix} \rho_1 \\ \rho_2 \\ \rho_3 \end{pmatrix}\,, \tag{8.44}$$

with

$$O_3 = \begin{pmatrix} \frac{v_1}{v} & \frac{v_2}{v} & \frac{v_3}{v} \\ \frac{v_2}{v'} & -\frac{v_1}{v'} & 0 \\ \frac{v_1}{v''} & \frac{v_2}{v''} & -\frac{v'^2}{v'' v_3} \end{pmatrix}\,, \quad v = \sqrt{v_1^2 + v_2^2 + v_3^2}\,, \quad v' = \sqrt{v_1^2 + v_2^2}\,, \quad v'' = \frac{v' v}{v_3}\,. \tag{8.45}$$

In the Higgs basis the mass and Yukawa interactions are given by

$$\begin{aligned} -\mathcal{L}_{\rm Y} =& \overline{d_L^0}\left[M_d + \frac{1}{v} M_d H^0 + \frac{1}{v'} N_d^0 R + \frac{1}{v''} N_d'^0 R' + i\frac{1}{v'} N_d^0 I + i\frac{1}{v''} N_d'^0 I'\right] d_R^0 \\ &+ \overline{u_L^0}\left[M_u + \frac{1}{v} M_u H^0 + \frac{1}{v'} N_u^0 R + \frac{1}{v''} N_u'^0 R' - i\frac{1}{v'} N_u^0 I - i\frac{1}{v''} N_u'^0 I'\right] u_R^0 \\ &+ \frac{\sqrt{2}}{v'} H^+ \left(\overline{u_L^0} N_d^0 d_R^0 - \overline{u_R^0} N_u^{0\dagger} d_L^0\right) + \frac{\sqrt{2}}{v''} H'^+ \left(\overline{u_L^0} N_d'^0 d_R^0 - \overline{u_R^0} N_u'^{0\dagger} d_L^0\right) + \text{h.c.}\,, \end{aligned} \tag{8.46}$$

with the flavor matrices given by

$$\begin{aligned} M_d &= \frac{1}{\sqrt{2}}(v_1 e^{i\alpha_1}\Gamma_1 + v_2 e^{i\alpha_2}\Gamma_2 + v_3 e^{i\alpha_3}\Gamma_3)\,, \\ M_u &= \frac{1}{\sqrt{2}}(v_1 e^{-i\alpha_1}\Delta_1 + v_2 e^{-i\alpha_2}\Delta_2 + v_3 e^{-i\alpha_3}\Delta_3)\,, \end{aligned} \tag{8.47}$$

and

$$\begin{aligned} N_d^0 =& \frac{1}{\sqrt{2}}\left(v_2 e^{i\alpha_1}\Gamma_1 - v_1 e^{i\alpha_2}\Gamma_2\right)\,, \\ N_u^0 =& \frac{1}{\sqrt{2}}\left(v_2 e^{-i\alpha_1}\Delta_1 - v_1 e^{-i\alpha_2}\Delta_2\right)\,, \\ N_d'^0 =& \frac{1}{\sqrt{2}}\left(v_1 e^{i\alpha_1}\Gamma_1 + v_2 e^{i\alpha_2}\Gamma_2 - \frac{v'^2}{v_3} e^{i\alpha_3}\Gamma_3\right)\,, \\ N_u'^0 =& \frac{1}{\sqrt{2}}\left(v_1 e^{-i\alpha_1}\Delta_1 + v_2 e^{-i\alpha_2}\Delta_2 - \frac{v'^2}{v_3} e^{-i\alpha_3}\Delta_3\right)\,. \end{aligned} \tag{8.48}$$

These last flavor matrix combinations are the ones mediating the FCNCs in our framework. We can now evaluate them for each of the three cases. In the basis where the quarks are mass eigenstates we get:

- **Case I:**

$$\begin{aligned}
(N_d)_{ij} &= \frac{v_2}{v_1}\,(D_d)_{ij} - \frac{v_2}{v_1}(V^\dagger)_{i3}(V)_{3j}(D_d)_{jj}\,,\\
(N'_d)_{ij} &= (D_d)_{ij} - \frac{v^2}{v_3^2}(V^\dagger)_{i3}(V)_{3j}(D_d)_{jj}\,,\\
N_u &= -\frac{v_1}{v_2}\mathrm{diag}(0,0,m_t) + \frac{v_2}{v_1}\mathrm{diag}(m_u,m_c,0)\,,\\
N'_u &= D_u\,.
\end{aligned} \tag{8.49}$$

- **Case II:**

$$\begin{aligned}
(N_d)_{ij} &= -\frac{v_1}{v_2}\,(D_d)_{ij} + \frac{v_1}{v_2}(V^\dagger)_{i3}(V)_{3j}(D_d)_{jj}\,,\\
(N'_d)_{ij} &= (D_d)_{ij} - \frac{v^2}{v_3^2}(V^\dagger)_{i3}(V)_{3j}(D_d)_{jj}\,,\\
N_u &= \frac{v_2}{v_1}\mathrm{diag}(m_u,m_c,0)\,,\\
N'_u &= \mathrm{diag}(m_u,m_c,0) - \frac{v'^2}{v_3^2}\mathrm{diag}(0,0,m_t)\,.
\end{aligned} \tag{8.50}$$

- **Case III:**

$$\begin{aligned}
(N_d)_{ij} &= -\frac{v_1}{v_2}\,(D_d)_{ij} + \frac{v_1}{v_2}(V^\dagger)_{i3}(V)_{3j}(D_d)_{jj}\,,\\
(N'_d)_{ij} &= (D_d)_{ij} - \frac{v^2}{v_3^2}(V^\dagger)_{i3}(V)_{3j}(D_d)_{jj}\,,\\
N_u &= \frac{v_2}{v_1}D_u\,,\\
N'_u &= D_u\,.
\end{aligned} \tag{8.51}$$

As expected, in all cases the FCNCs will be mediated by quark masses and off-diagonal elements of the CKM quark mixing matrix. This is virtually the same type of suppression as the one obtained in the BGL 2HDM implementation. The difference lies in the vevs ratios that we get in front of each term. This actually contrasts with the anomaly-free three Higgs BGL implementation [26]. In that scenario the Yukawa textures, which differ from the 2HDM implementation, cannot give such a strong suppression to $|\Delta S| = 2$ processes as compared to the original BGL implementation. One generally gets suppressions of the order of $(V_{cd}^* V_{cs})^2 \sim \lambda^2$ ($\lambda \simeq 0.225$), requiring heavy neutral scalar fields. However, the fact that we kept the same Yukawa textures in passing from the two to the three Higgs implementation allows us to have suppressions of the type $(V_{td}^* V_{ts})^2 \sim \lambda^{10}$ for $|\Delta S| = 2$ processes, just like the original BGL scenario.

The scalar potential

As we saw in Section 3.2.1, current experimental limits exclude axions coming from a PQ symmetry broken at the EW scale [23, 27–29]. To obtain a viable axion model the PQ symmetry must be broken at a scale much higher than the EW scale. The axion is then called invisible since its mass and couplings are suppressed by the large PQ symmetry breaking scale. We can achieve this in a similar way as in the DFSZ and KSVZ invisible axion models, that is, by introducing a complex scalar singlet which acquires a very large vev $\langle 0|S|0\rangle = e^{i\alpha_{\rm PQ}} v_{\rm PQ}/\sqrt{2}$, with $v_{\rm PQ} \gg v$. The new complex field S will have the following symmetry transformation

$$S \to e^{iX_S\,\theta} S\,. \tag{8.52}$$

The introduction of the complex scalar singlet increases the number of independent charges in one unity. From the Yukawa sector alone, with fermion charges chosen in order for the symmetry to be anomalous, we are able to reduce the number of independent PQ charges to just three. In this way the number of independent charges increases to four.

The scalar doublets transform as in Eq. (2.25) with the charges $X_{\Phi i}$ expressed in terms of the three quark charges, their explicit form will depend on whether we are working in case I or II/III (as detailed in the previous section). We shall split the potential in two parts: the phase blind part $[V(\Phi,S)]_{\rm blind}$, and the phase sensitive part $[V(\Phi,S)]_{\rm sen}$, i.e.

$$V(\Phi,S) \;=\; [V(\Phi,S)]_{\rm blind} + [V(\Phi,S)]_{\rm sen}\;. \tag{8.53}$$

The phase blind terms do not constrain the charge assignments, they are given by

$$\begin{aligned}[V(\Phi,S)]_{\rm blind} =& m_i^2 \Phi_i^\dagger \Phi_i + \lambda_{ii,jj}\left(\Phi_i^\dagger\Phi_i\right)\left(\Phi_j^\dagger\Phi_j\right) + \lambda'_{ij,ji}\left(\Phi_i^\dagger\Phi_j\right)\left(\Phi_j^\dagger\Phi_i\right) \\ &+ m_S^2|S|^2 + \lambda_S|S|^4 + \lambda_i^{\Phi S}(\Phi_i^\dagger\Phi_i)|S|^2\,.\end{aligned} \tag{8.54}$$

The parameters $\lambda_i^{\Phi S}$ and $\lambda_{ii,jj}$ run for all $i,j = 1,2,3$, while the parameter $\lambda'_{ij,ji}$ runs for $i \neq j$. This part of the potential possesses a $\mathrm{U}(1)^4$ global symmetry. The role of the phase sensitive part is to introduce terms which break (explicitly) this symmetry down to $\mathrm{U}(1)_{\rm Y} \times \mathrm{U}(1)_{\rm PQ}$. With this symmetry we will have two complex phases to which the scalar potential will not be sensitive, one will be the neutral Goldstone boson and the other the axion. This will introduce two new additional constraints, reducing the number of independent charges down to two.

We shall now present the possible phase sensitive terms that we may built and their constraints in terms of the PQ charges. We note that any term of the form $\Phi_i^\dagger\Phi_j$ (or any combination where this is the only phase sensitive part) implies the charge relation $X_{\Phi i} = X_{\Phi j}$, which is automatically excluded by the charge conditions, see Eqs. (8.41) and (8.42). Also, terms that are only sensitive to phases of one single field such as S^k, $\Phi_i^\dagger\Phi_i S^k$, etc. would imply a discrete phase, which is not allowed in our framework.

In Table 8.1 we present all the possible, renormalizable and gauge invariant, phase sensitive terms (up to hermitic conjugation). We now have to check all the

Case	Phase sensitive	Constraint
(1)	$\left(\Phi_1^\dagger\Phi_2\right)\left(\Phi_1^\dagger\Phi_3\right)$	$X_{\Phi 2}+X_{\Phi 3}-2X_{\Phi 1}=0$
(2)	$\left(\Phi_2^\dagger\Phi_1\right)\left(\Phi_2^\dagger\Phi_3\right)$	$X_{\Phi 3}+X_{\Phi 1}-2X_{\Phi 2}=0$
(3)	$\left(\Phi_3^\dagger\Phi_1\right)\left(\Phi_3^\dagger\Phi_2\right)$	$X_{\Phi 1}+X_{\Phi 2}-2X_{\Phi 3}=0$
(4)	$\left(\Phi_1^\dagger\Phi_2\right)\{S,S^*\}^{k_1}$	$k_1X_S=\mp(X_{\Phi 2}-X_{\Phi 1})$
(5)	$\left(\Phi_1^\dagger\Phi_3\right)\{S,S^*\}^{k_2}$	$k_2X_S=\mp(X_{\Phi 3}-X_{\Phi 1})$
(6)	$\left(\Phi_2^\dagger\Phi_3\right)\{S,S^*\}^{k_3}$	$k_3X_S=\mp(X_{\Phi 3}-X_{\Phi 2})$

Table 8.1: *We consider $k_i=1,2$ due to renormalizability. The minus sign $(-)$ is associated with S and the plus $(+)$ with the conjugated field S^*.*

possible combinations of two terms from (1) to (6). Combining just the first three cases will lead to a constraint of the type $X_{\Phi i}=X_{\Phi j}$, which is excluded. When combining cases (1) to (3) with cases (4) to (6) all of these last three cases will be allowed simultaneously. After finding all the possible combinations and using the information about the explicit forms of $X_{\Phi i}$ in terms of the quark charges we get the following charge constraints:

- **Case I:**

$$X_{tL}=C_I(X_{uR}-X_{tR})\,,\quad X_S=C_S^I X_{tL}\,. \tag{8.55}$$

- **Case II/III:**

$$X_{tL}=C_{II(III)}(X_{uR}+X_{dR})\,,\quad X_S=C_S^{II(III)}X_{tL}\,. \tag{8.56}$$

We must also have $C_I\neq 0,-1,-1/2$, $C_{II}\neq 0,1,1/2$ and $C_{III}\neq -1,0,\frac{1}{2},1,3$ (see Eqs. (8.35), (8.38) and (8.40), respectively) in order to preserve the Yukawa textures and the symmetry to be anomalous. In Table 8.2 we present all possible values for $C_{I,II,III}$ and $C_S^{I,II,III}$ in each possible phase sensitive potential implementation.

At this point we have two free charges which we choose to be X_{uR} and X_S, for all cases. We can normalize all charges to the scalar singlet charge, without loss of generality, just by setting the condition $X_S=1$. This allows the PQ quark charges to be written in terms of the values $C_S^{I,II,III}$, $C_{I,II,III}$ and one free charge, X_{uR}. They will now take the form:

- **Case I:**

$$X_{tL}=\frac{1}{C_S^I}\,,\quad X_{dR}=-X_{uR}\,,\quad X_{tR}=X_{uR}-\frac{1}{C_S^I C_I}\,. \tag{8.57}$$

- **Case II:**

$$X_{tL}=\frac{1}{C_S^{II}}\,,\quad X_{dR}=-X_{uR}+\frac{1}{C_S^{II}C_{II}}\,,\quad X_{tR}=X_{uR}-\frac{1-2C_{II}}{C_S^{II}C_{II}}\,. \tag{8.58}$$

Term	Combination		C_I	C_S^I	$C_{II(III)}$	$C_S^{II(III)}$
T_1	(4)+(5)	$k_1=1,\, k_2=2\,(S,S^*)$	-2	$1/2$	3	$1/3$
T_2	(4)+(5)	$k_1=2,\, k_2=1\,(S,S^*)$	1	1	$3/2$	$1/3$
T_3	(4)+(6)	$k_1=1,\, k_3=2\,(S,S)$	$-3/4$	$-1/3$	-2	$-1/2$
T_4	(4)+(6)	$k_1=2,\, k_3=1\,(S,S)$	$-3/5$	$-1/3$	$-1/2$	-1
T_5	(5)+(6)	$k_2=1,\, k_3=2\,(S,S^*)$	$-1/4$	-1	$2/3$	$1/2$
T_6	(5)+(6)	$k_2=2,\, k_3=1\,(S,S^*)$	$-2/5$	$-1/2$	$1/3$	1
T_7	(1)+(4)+(5)	$k_1=k_2=2\,(S,S^*)$	$-$	$-$	2	$1/4$
T_8	(2)+(4)+(6)	$k_1=k_3=2\,(S,S)$	$-2/3$	$-1/4$	-1	$-1/2$
T_9	(3)+(5)+(6)	$k_2=k_3=2\,(S,S^*)$	$-1/3$	$-1/2$	$-$	$-$
T_{10}	(1)+(4)+(5)+(6)	$k_1=1,\, k_2=1,\, k_3=2\,(S,S^*,S^*)$	$-$	$-$	2	$1/2$
T_{11}	(2)+(4)+(5)+(6)	$k_1=1,\, k_2=2,\, k_3=1\,(S,S,S)$	$-2/3$	$-1/2$	-1	-1
T_{12}	(3)+(4)+(5)+(6)	$k_1=2,\, k_2=1,\, k_3=1\,(S,S,S^*)$	$-1/3$	-1	$-$	$-$

Table 8.2: *Allowed values for the charge combinations $C_{I,II,III}$ and $C_S^{I,II,III}$. Half of the possible values are not shown in the table as they can be trivially obtained by interchanging $S \leftrightarrow S^*$ in the above combinations, which amounts to a replacement $C_S^{I,II,III} \to -C_S^{I,II,III}$. The scenarios T_1, T_8 and T_{11} are not possible in case III.*

- **Case III:**

$$X_{tL} = \frac{1}{C_S^{III}}\,, \quad X_{dR} = -X_{uR} + \frac{1}{C_S^{III} C_{III}}\,, \quad X_{tR} = X_{uR} + \frac{1}{C_S^{III}}\,. \tag{8.59}$$

In this section we have found up to 12 distinct phase sensitive potential implementations, see Table 8.2. For case I, T_7 and T_{10} implementations are not compatible with the flavor PQ symmetry in the fermionic sector. In case II, the incompatible implementations are T_9 and T_{12}. Finally, case III has the same incompatible implementations as case II plus T_1, T_8 and T_{11} implementations. As an illustrative example, let us choose the implementation T_2. The scalar potential would take the form

$$V(\Phi,S) = \left[V(\Phi,S)\right]_{\text{blind}} + \left[\lambda(\Phi_1^\dagger\Phi_2)S^2 + \mu(\Phi_1^\dagger\Phi_3)S^* + \text{h.c.}\right]\,, \tag{8.60}$$

with λ dimensionless and μ with mass dimension. Under this particular potential implementation, and with our normalization, the PQ quark charges read

- **Case I:** $X_{tL} = 1\,, \quad X_{dR} = -X_{uR}\,, \quad X_{tR} = X_{uR} - 1.$
- **Case II:** $X_{tL} = 3\,, \quad X_{dR} = -X_{uR} + 2\,, \quad X_{tR} = X_{uR} + 4.$
- **Case III:** $X_{tL} = 3\,, \quad X_{dR} = -X_{uR} + 2\,, \quad X_{tR} = X_{uR} + 3.$

While the scalar charges are: $X_{\Phi 1} = X_{uR}\,, \quad X_{\Phi 2} = X_{uR} - 2\,, \quad X_{\Phi 3} = X_{uR} + 1$. The fact that the scalar charges are the same for all the three cases should not be surprising. The scalar potential itself knows nothing about the distinct Yukawa implementations, that information enters only when we use the explicit expression of the scalar charges in terms of the quark ones. Therefore, the scalars charges will only depend on the distinct potential implementations.

The Yukawa leptonic sector

In this section we shall only be interested in the Yukawa couplings of the charged leptons and therefore we will say nothing on the Dirac or Majorana nature of the neutrinos. We will assume that the final neutrino mass matrix texture contains enough freedom, such that, in combination with the lepton mass matrix, accommodates the full low-energy neutrino data. However, note that the neutrino Yukawa textures should satisfy some conditions such that the BGL quark and lepton textures are not spoiled through radiative corrections [30]. In the next section we will present a particular model implementation were the neutrino sector is worked out. However, since we are mostly interested in the axion properties of this class of models, we will focus our attention just to the charged lepton implementation for the general case.

The Yukawa leptonic Lagrangian is of the form

$$-\mathcal{L}_{\rm Y}^{\rm lep} = \overline{L_L^0}\,\left[\Pi_1\,\Phi_1 + \Pi_2\,\Phi_2 + \Pi_3\,\Phi_3\right] l_R^0 + \text{h.c.} \tag{8.61}$$

In a similar way as it happens in the quark Yukawa sector, it is convenient to rewrite the Yukawa lepton Lagrangian by rotating the Higgs doublets to the Higgs basis (see Eq. (8.44)) and by diagonalizing the lepton mass matrices through the bi-unitary transformations

$$\nu_L^0 = U_{\nu L}\,\nu_L\,, \quad l_{L,R}^0 = U_{eL,R}\,e_{L,R}\,. \tag{8.62}$$

The Yukawa Lagrangian now reads as

$$\begin{aligned} -\mathcal{L}_{\rm Y}^{\rm lep} =& \overline{e_L}\left[D_e + \frac{1}{v}D_e H^0 + \frac{1}{v'}N_e R + \frac{1}{v''}N_e' R' + i\frac{1}{v'}N_e I + i\frac{1}{v''}N_e' I'\right] e_R \\ &+ \frac{\sqrt{2}}{v'}H^+\overline{\nu_L}N_e e_R + \frac{\sqrt{2}}{v''}H'^+\overline{\nu_L}N_e' e_R + \text{h.c.} \end{aligned} \tag{8.63}$$

where, as it happened with the quarks, N_e and N_e' mediate the FCNCs. These flavor combinations have the same expression, in the flavor basis, as N_d and N_d' present in Eq. (8.48) with the replacement $\Gamma_i \to \Pi_i$.

Regarding the PQ symmetry transformations, the scalar field transformations are given in Eqs. (8.41) and (8.42) for cases I and II/III respectively. We now need to determine the PQ charges of the leptonic fields. In general these transform under the continuous symmetry as

$$L_L^0 \to \mathcal{S}_L^\ell\,L_L^0\,, \quad l_R^0 \to \mathcal{S}_R^\ell l_R^0\,, \tag{8.64}$$

with

$$\mathcal{S}_L^\ell = \text{diag}(e^{iX_{eL}\theta}, e^{iX_{\mu L}\theta}, e^{iX_{\tau L}\theta})\,, \quad \mathcal{S}_R^\ell = \text{diag}(e^{iX_{eR}\theta}, e^{iX_{\mu R}\theta}, e^{iX_{\tau R}\theta})\,. \tag{8.65}$$

A global phase transformation allows us to set $X_{eL} = 0$ without loss of generality, just as we did in the quark sector.

We could proceed with the symmetry implementation just like in the quark sector, however, we can also combine the BGL-like textures in the quark sector with NFC for the charged lepton such that we have several phenomenological models available. We shall then split these implementations into two classes:

(1) With FCNCs in the charged lepton sector.

This is the extension to three Higgs doublets of the symmetry implementation in Ref. [30]. In this case, in order to have the FCNCs under control we choose the implementation *à la* BGL, i.e.

$$\{\Pi_1, \Pi_2, \Pi_3\} \sim \left\{\Gamma_1^{\rm BGL}, \Gamma_2^{\rm BGL}, 0\right\} . \tag{8.66}$$

Just like in the quark sector, we need the other sector mass matrix (i.e. neutrino mass matrix) to be block diagonal, in order to have the PMNS mediating the FCNCs. The way to achieve this will depend on the Dirac or Majorana nature of the neutrinos and is out of the scope of this section (see next section for more details). The symmetry implementation is just like the one in the quark sector, i.e. $X_{eL} = X_{\mu L} \equiv X_{l'L}$ and $X_{eR} = X_{\mu R} = X_{\tau R} \equiv X_{lR}$. The constraints are

$$X_{l'L} - X_{lR} = X_{\Phi i} , \quad X_{\tau L} - X_{lR} = X_{\Phi j} . \tag{8.67}$$

The equivalent to conditions A and B in the quark sector also apply to the lepton charges. Since we have set $X_{eL} = 0$, the charged lepton charges become completely defined by the known scalar charges, i.e.

$$X_{\tau L} = X_{\Phi j} - X_{\Phi i} , \quad X_{lR} = -X_{\Phi i} . \tag{8.68}$$

(2) Without FCNCs in the charged lepton sector.

In this case there are six implementations possible, as it was shown in Ref. [31]. Using the information that all the charges of the scalar fields are different we get

(a)

$$\{\Pi_1, \Pi_2, \Pi_3\} \sim \left\{ \begin{pmatrix} \times & \times & \times \\ \times & \times & \times \\ \times & \times & \times \end{pmatrix} , \quad \begin{pmatrix} & & \\ & & \\ & & \end{pmatrix} , \quad \begin{pmatrix} & & \\ & & \\ & & \end{pmatrix} \right\} . \tag{8.69}$$

In this scenario both left and right generators must be fully degenerate, i.e. $X_{eL} = X_{\mu L} = X_{\tau L} \equiv X_{lL}$ and $X_{eR} = X_{\mu R} = X_{\tau R} \equiv X_{lR}$. This implies the following constraint

$$X_{lL} - X_{lR} = X_{\Phi i} \quad (\text{or} \quad X_{lR} = -X_{\Phi i}) . \tag{8.70}$$

(b)

$$\{\Pi_1, \Pi_2, \Pi_3\} \sim \left\{ \begin{pmatrix} \times & \times & 0 \\ \times & \times & 0 \\ 0 & 0 & \times \end{pmatrix} , \quad \begin{pmatrix} & & \\ & & \\ & & \end{pmatrix} , \quad \begin{pmatrix} & & \\ & & \\ & & \end{pmatrix} \right\} . \tag{8.71}$$

In this scenario both left and right generators must be two-fold degenerate, i.e. $X_{eL} = X_{\mu L} \equiv X_{l'L}$ and $X_{eR} = X_{\mu R} \equiv X_{l'R}$. This implies the following constraints

$$X_{l'L} - X_{l'R} = X_{\Phi i} , \quad X_{\tau L} - X_{\tau R} = X_{\Phi i} . \tag{8.72}$$

(c)

$$\{\Pi_1,\,\Pi_2,\,\Pi_3\} \sim \left\{ \begin{pmatrix} \times & \times & 0 \\ \times & \times & 0 \\ 0 & 0 & 0 \end{pmatrix}, \quad \begin{pmatrix} 0 & 0 & 0 \\ 0 & 0 & 0 \\ 0 & 0 & \times \end{pmatrix}, \quad \begin{pmatrix} & & \\ & & \\ & & \end{pmatrix} \right\}. \tag{8.73}$$

In this scenario the left and right generators have the same form as in the previous one. However, the constraints are

$$X_{l'L} - X_{l'R} = X_{\Phi i}\,, \quad X_{\tau L} - X_{\tau R} = X_{\Phi j}\,. \tag{8.74}$$

(d)

$$\{\Pi_1,\,\Pi_2,\,\Pi_3\} \sim \left\{ \begin{pmatrix} \times & 0 & 0 \\ 0 & \times & 0 \\ 0 & 0 & \times \end{pmatrix}, \quad \begin{pmatrix} & & \\ & & \\ & & \end{pmatrix}, \quad \begin{pmatrix} & & \\ & & \\ & & \end{pmatrix} \right\}. \tag{8.75}$$

In this scenario the left and right generators must have no degeneracy. The constraint is given by

$$X_{\alpha L} - X_{\alpha R} = X_{\Phi i} \quad (\alpha = e,\,\mu,\,\tau)\,. \tag{8.76}$$

(e)

$$\{\Pi_1,\,\Pi_2,\,\Pi_3\} \sim \left\{ \begin{pmatrix} \times & 0 & 0 \\ 0 & \times & 0 \\ 0 & 0 & 0 \end{pmatrix}, \quad \begin{pmatrix} 0 & 0 & 0 \\ 0 & 0 & 0 \\ 0 & 0 & \times \end{pmatrix}, \quad \begin{pmatrix} & & \\ & & \\ & & \end{pmatrix} \right\}. \tag{8.77}$$

In this scenario the left and right generators are the same as before. The constraints are given by

$$X_{\alpha' L} - X_{\alpha' R} = X_{\Phi i}\,, \quad X_{\tau L} - X_{\tau R} = X_{\Phi j} \quad (\alpha' = e,\,\mu)\,. \tag{8.78}$$

(f)

$$\{\Pi_1,\,\Pi_2,\,\Pi_3\} \sim \left\{ \begin{pmatrix} \times & 0 & 0 \\ 0 & 0 & 0 \\ 0 & 0 & 0 \end{pmatrix}, \quad \begin{pmatrix} 0 & 0 & 0 \\ 0 & \times & 0 \\ 0 & 0 & 0 \end{pmatrix}, \quad \begin{pmatrix} 0 & 0 & 0 \\ 0 & 0 & 0 \\ 0 & 0 & \times \end{pmatrix} \right\}. \tag{8.79}$$

In this scenario the left and right generators are the same as before. The constraints are given by

$$X_{eL} - X_{eR} = X_{\Phi i}\,, \quad X_{\mu L} - X_{\mu R} = X_{\Phi j}\,, \quad X_{\tau L} - X_{\tau R} = X_{\Phi k}\,. \tag{8.80}$$

In general, we have only information on the difference between left- and right-handed charged lepton charges. The condition $X_{eL} = 0$ allows us to have the charged lepton charges fully determined by the known scalar charges only in cases (1) and ($2a$). For the other cases we would need to know the neutrino sector implementation. Nevertheless, as we shall see in Section 8.2.4, the knowledge of the difference is enough to get most of the axion properties.

8.2.3 Adding right-handed neutrinos: an explicit implementation

With the purpose of illustration, in this section we will extend one of the implementations discussed in the previous sections to accommodate for neutrino masses and mixing. For simplicity we will focus in the particular flavored PQ charges for the quark fields,

$$X_{tL} = -2\,,\; X_{uR} = \frac{5}{2}\,,\; X_{tR} = -\frac{1}{2}\,,\; X_{dR} = -\frac{5}{2}\,, \tag{8.81}$$

that are compatible with the conditions found in Section 8.2.1. For the leptonic sector many possible implementations of the PQ symmetry are available either with Dirac or Majorana neutrinos. We shall focus on the last scenario, introducing two right-handed neutrino fields, N_{Ri} $(i = 1, 2)$. These two fields transform under the PQ symmetry with the same phase, X_{NR}. The charge transformation for this sector takes the form

$$X_{\tau L} = 1\,, \quad X_{lR} = -1/2\,, \quad X_{NR} = 1/2\,, \tag{8.82}$$

where we have defined $X_{eR} = X_{\mu R} = X_{\tau R} \equiv X_{lR}$ and we have set $X_{eL} = X_{\mu L} = 0$, without loss of generality, just as we did in the quark sector. Finally, the scalar charges are given by

$$X_{\Phi 1} = 5/2\,, \quad X_{\Phi 2} = 3/2\,, \quad X_{\Phi 3} = 1/2\,, \quad X_S = 1\,, \tag{8.83}$$

and the only allowed phase sensitive terms in the scalar potential are

$$(\Phi_1^\dagger \Phi_2) S\,,\; (\Phi_1^\dagger \Phi_3) S^2\,,\; (\Phi_2^\dagger \Phi_3) S\,,\; (\Phi_2^\dagger \Phi_1)(\Phi_2^\dagger \Phi_3)\,, \tag{8.84}$$

which correspond to the implementation T_{11} in Table 8.2.

The Yukawa Lagrangian will then take the form

$$\begin{aligned} -\mathcal{L}_{\rm Y} =& \overline{Q_L^0}\,[\Gamma_1\,\Phi_1 + \Gamma_3\,\Phi_3]\,d_R^0 + \overline{Q_L^0}\,[\Delta_1\,\widetilde{\Phi}_1 + \Delta_2\,\widetilde{\Phi}_2]u_R^0 \\ &+ \overline{L_L^0}\,[\Pi_2\,\Phi_2 + \Pi_3\,\Phi_3]\,l_R^0 + \overline{L_L^0}\,\Sigma_3\,\widetilde{\Phi}_3 N_R^0 \\ &+ \overline{(N_R^0)^c} A N_R^0 S^* + \text{h.c.}\,, \end{aligned} \tag{8.85}$$

where A is a general 2×2 complex symmetric matrix. In this three-Higgs-doublet model implementation we get the following Yukawa textures:

$$\begin{aligned} \text{Down:} \quad & \Gamma_1 = \Gamma_1^{\rm BGL}\,,\; \Gamma_3 = \Gamma_2^{\rm BGL}\,; \\ \text{Up:} \quad & \Delta_1 = \Delta_1^{\rm BGL}\,,\; \Delta_2 = \Delta_2^{\rm BGL}\,; \\ \text{Charged leptons:} \quad & \Pi_2 = \Gamma_2^{\rm BGL}\,,\; \Pi_3 = \Gamma_1^{\rm BGL}\,; \\ \text{Neutrinos:} \quad & \Sigma_3 = \Delta_1^{\rm BGL}\big|_{\not 3}\,. \end{aligned} \tag{8.86}$$

The matrix $\Delta_1^{\rm BGL}\big|_{\not 3}$ corresponds to the original BGL texture but with the third column removed. The Yukawa textures implemented in this framework are stable under renormalization group evolution [30].

As discussed in Section 8.2.2 this implementation possesses FCNCs in the down-quark sector controlled by the matrices in Eq.(8.49). The model also possesses tree-level FCNCs in the charged lepton sector, although not as suppressed as in the quark sector. These will be completely controlled by the PMNS matrix [32]. The flavor matrices encoding the FCNC interactions among charged leptons take the form

$$\begin{aligned}(N'_e)_{ij} &= -\frac{(v_1^2+v_2^2)}{v_3^2}(D_e)_{ij} + \frac{v^2}{v_3^2}(U^\dagger)_{i3}(U)_{3j}(D_e)_{jj}\,,\\ (N_e)_{ij} &= -\frac{v_1}{v_2}(U^\dagger)_{i3}(U)_{3j}(D_e)_{jj}\,,\end{aligned} \tag{8.87}$$

in the fermion mass basis. Here U represents the PMNS mixing matrix and D_e the diagonal charged lepton mass matrix.

The smallness of active neutrino masses is understood in this framework via a type I seesaw mechanism [10] once the scalar singlet, S, gets a vev. This way the PQ symmetry breaking scale provides a dynamical origin for the heavy seesaw scale [11]. The effective neutrino mass matrix is given by

$$m_\nu \simeq -\frac{v_3^2 e^{i\left(\alpha_{\rm PQ}-2\alpha_3\right)}}{2\sqrt{2}v_{\rm PQ}}\Sigma_3 A^{-1}\Sigma_3^T\,. \tag{8.88}$$

One active neutrino remains massless because m_ν is singular, fixing the size of the other two neutrino masses. For a normal hierarchy: $m_2 = \sqrt{\Delta m^2_{21}} \simeq 9$ meV and $m_3 = \sqrt{|\Delta m^2_{31}|} \simeq 50$ meV [33]. An inverted hierarchy on the other hand implies two quasi-degenerate neutrinos: $m_1 \sim m_2 \simeq 50$ meV.

8.2.4 Axion properties

The anomalous $\mathrm{U}(1)_{\rm PQ}$ symmetry of the class of models built in the previous sections is spontaneously broken by the vev of the singlet field S at a very high scale, just like in the standard DFSZ and KSVZ models. Non-perturbative QCD effects induce a potential for the axion field, allowing us to shift away the strong CP phase and giving a small mass to the axion [34]. The axion mass is given by Eq. (3.56), where the color anomaly coefficient is given in this class of models by

$$C_{ag} \equiv \sum_{i=\text{colored}} X_{iR} - X_{iL} = 2X_{uR} + 3X_{dR} + X_{tR} - 2X_{tL}\,. \tag{8.89}$$

This quantity turns out to be independent of the free charges and can be expressed as C_{ag}^M (with $M = I,\, II,\, III$), which takes the form

$$\begin{gathered}\textbf{Case I:}\quad C_{ag}^I = -\frac{1+2C_I}{C_I C_S^I}\,,\quad \textbf{Case II:}\quad C_{ag}^{II} = \frac{2}{C_{II}C_S^{II}}\,,\\ \textbf{Case III:}\quad C_{ag}^{III} = \frac{3-C_{III}}{C_{III}C_S^{III}}\,.\end{gathered} \tag{8.90}$$

Here we have introduced the parameters $C_{I,II,III}$ and $C_S^{I,II,III}$ specified in Table 8.2. The quantity C_{ag}^M is therefore only dependent of the scalar implementation once the

	T_1	T_2	T_3	T_4	T_5	T_6	T_7	T_8	T_9	T_{10}	T_{11}	T_{12}
$N_{\rm DW}^{I}$	3	3	2	1	2	1	–	2	2	–	1	1
$N_{\rm DW}^{II}$	2	4	2	4	6	6	4	4	–	2	2	–
$N_{\rm DW}^{III}$	–	3	5	7	7	8	2	–	–	1	–	–

Table 8.3: *Values for the domain wall number in each of the possible scenarios.*

Yukawa textures are specified. One of the interesting features of having a flavored PQ symmetry is that it is possible to avoid the formation of domain walls during the evolution of the Universe [16,19]. As we saw in Section 3.3.2 the domain wall number is determined by the color anomaly coefficient with $N_{\rm DW} = |C_{ag}^{M}|$. In Table 8.3 we present the values of the domain wall number for the different implementations of the models we are presenting. As we can see, while some of the implementations also suffer from the domain wall problem, others have $N_{\rm DW} = 1$, for which the resulting domain wall structure is harmless [35]. This is the case for instance for the specific implementation that we extended in Section 8.2.3.

The most significant differences of our 3HFPQ framework with the usual benchmarks invisible axion models is the presence of tree-level flavor changing axion couplings as well as large deviations from the axion coupling to photons, that was given in Eq. (3.30). In this class of models the electromagnetic factor $C_{a\gamma}$ is given by

$$\begin{aligned} C_{a\gamma} =& 2 \sum_{i=\text{charged}} (X_{iR} - X_{iL}) Q_i^2 \\ =& 2 \left[\frac{8}{3} X_{uR} + X_{dR} + \frac{4}{3} X_{tR} - \frac{5}{3} X_{tL} + \sum_{\alpha=e,\mu,\tau} (X_{\alpha R} - X_{\alpha L}) \right] . \end{aligned} \tag{8.91}$$

This quantity can be expressed as

$$C_{a\gamma}^{M} = \frac{2}{3} \frac{A_M}{C_M C_S^M} , \tag{8.92}$$

with $M = I,\, II,\, III$ and where the combination of fermionic charges $A_{I,II,II}$ are defined in Table 8.4. The charged lepton combinations are denoted by a vector (i, j, k), which represents the Higgs doublet that is coupled to the left-handed leptons (e, μ, τ). For example, the case $(1, 1, 3)$ tell us that Φ_1 is coupled to e_L and μ_L while Φ_3 couples to τ_L. This can correspond to the charged lepton Yukawa implementations (1), (2c) or (2e). Note also that the case $(3, 3, 1)$ is not a relabeling of the scalar fields since we keep the quark sector unchanged and, therefore, we will get a distinct result. Once the choice on the Yukawa textures is made, the parameter $C_{a\gamma}^{M}$ will depend on the potential implementation and the way the charged leptons transform under the PQ symmetry.

Cases	A_I	A_{II}	A_{III}
$(1,1,1)$	$-4-5C_I$	$-1+3C_{II}$	$3-C_{III}$
$(2,2,2)$	$5+4C_I$	$8+3C_{II}$	$12-C_{III}$
$(3,3,3)$	$-4-14C_I$	$8-6C_{II}$	$12-10C_{III}$
$(1,1,2)$	$-1-2C_I$	$2+3C_{II}$	$6-C_{III}$
$(1,1,3)$	$-4-8C_I$	2	$6-4C_{III}$
$(2,2,1)$	$2+C_I$	$5+3C_{II}$	$9-C_{III}$
$(2,2,3)$	$2-2C_I$	8	$12-4C_{III}$
$(3,3,1)$	$-4-11C_I$	$5-3C_{II}$	$9-7C_{III}$
$(3,3,2)$	$-1-8C_I$	$8-3C_{II}$	$12-7C_{III}$
$(1,2,3)$	$-1-5C_I$	5	$9-4C_{III}$

Table 8.4: *Charge combinations A_I, A_{II} and A_{III} entering in the description of the axion coupling to photons. The numbers in the first column label the Higgs doublet that is coupled to the left-handed charged leptons (e,μ,τ).*

Axion couplings to matter

As already explained in Chapter 3, when calculating the axion couplings to matter one should redefine the axion current in such a way that it does not mix with the neutral Goldstone boson associated with the spontaneous symmetry breaking of the electroweak gauge symmetry. This redefinition results in a shift of the original scalar charges [5],

$$X'_{\Phi i} = X_{\Phi i} - X\,, \tag{8.93}$$

which in terms of the fermion charges reads

$$\begin{aligned} X'_{u,t\,R} = X_{u,t\,R} - X\,, \quad X'_{dR} = X_{dR} + X\,, \quad X'_{tL} = X_{tL}\,, \\ X'_{\ell L} = X_{\ell L}\,, \quad X'_{\ell R} = X_{\ell R} + X\,, \end{aligned} \tag{8.94}$$

with $\ell = \{e,\mu,\tau\}$ and

$$X = \frac{1}{v^2}\sum_i v_i^2 X_{\Phi i}\,. \tag{8.95}$$

The explicit expression for X will take the same form in cases II and III (they share the same Higgs charge assignments) but a different form in case I, i.e.

$$X = \begin{cases} X_{uR} - \dfrac{v_2^2\,(1+C_I) - v_3^2 C_I}{v^2 C_S^I C_I} & \text{for case I,} \\ X_{uR} - \dfrac{v_2^2 + v_3^2\left(1 - C_{II(III)}\right)}{v^2 C_S^{II(III)} C_{II(III)}} & \text{for case II and III}\,. \end{cases} \tag{8.96}$$

We now define the shifted charge matrix as

$$\mathcal{X}_X \equiv \frac{1}{i}\,\frac{d\mathcal{S}'_X}{d\theta}\bigg|_{\theta=0}\,, \tag{8.97}$$

which take the explicit form

$$\begin{aligned}\mathcal{X}_{uL} =&\mathcal{X}_{dL} = \mathrm{diag}(0,\, 0,\, X'_{tL})\,, \quad \mathcal{X}_{eL} = \mathrm{diag}(X'_{eL},\, X'_{\mu L},\, X'_{\tau L})\,,\\ \mathcal{X}_{uR} =&\mathrm{diag}(X'_{uR},\, X'_{uR},\, X'_{tR})\,, \quad \mathcal{X}_{dR} = X'_{dR}\,\mathbb{1}\,, \quad \mathcal{X}_{eR} = \mathrm{diag}(X'_{eR},\, X'_{\mu R},\, X'_{\tau R})\,.\end{aligned} \tag{8.98}$$

These charge matrices determine the couplings of the axion to fermions in the flavor basis. By going to the mass basis the fermion fields are rotated through the unitary transformations in Eq. (1.21). These transformations will change the charge matrix to

$$\widetilde{\mathcal{X}}_X = U_X^\dagger \mathcal{X}_X U_X\,. \tag{8.99}$$

In this new basis the quark charge matrices take the explicit form

$$\widetilde{\mathcal{X}}_{uL} = \mathcal{X}_{uL}\,, \quad \widetilde{\mathcal{X}}_{uR} = \mathcal{X}_{uR}\,, \quad \widetilde{\mathcal{X}}_{dL} = X_{tL} \begin{pmatrix} |V_{td}|^2 & V_{td}^* V_{ts} & V_{td}^* V_{tb} \\ V_{ts}^* V_{td} & |V_{ts}|^2 & V_{ts}^* V_{tb} \\ V_{tb}^* V_{td} & V_{tb}^* V_{ts} & |V_{tb}|^2 \end{pmatrix}\,, \quad \widetilde{\mathcal{X}}_{dR} = \mathcal{X}_{dR}\,, \tag{8.100}$$

where we have used $X'_{tL} = X_{tL}$. For the charged leptons we have in scenario (1)

$$\widetilde{\mathcal{X}}_{eL} = X_{\tau L} \begin{pmatrix} |V_{\tau 1}|^2 & V_{\tau 1}^* V_{\tau 2} & V_{\tau 1}^* V_{\tau 3} \\ V_{\tau 2}^* V_{\tau 1} & |V_{\tau 2}|^2 & V_{\tau 2}^* V_{\tau 3} \\ V_{\tau 3}^* V_{\tau 1} & V_{\tau 3}^* V_{\tau 2} & |V_{\tau 3}|^2 \end{pmatrix}\,, \quad \widetilde{\mathcal{X}}_{eR} = \mathcal{X}_{eR}\,, \tag{8.101}$$

where we have used $X'_{\tau L} = X_{\tau L}$, in scenario (2) we get

$$\widetilde{\mathcal{X}}_{eL} = \mathcal{X}_{eL}\,, \quad \widetilde{\mathcal{X}}_{eR} = \mathcal{X}_{eR}\,. \tag{8.102}$$

The axion vector and axial-vector couplings to matter are then given by

$$C_{au}^{V,A} = \mathcal{X}_{uL} \pm \mathcal{X}_{uR}\,, \quad C_{ad}^{V,A} = \widetilde{\mathcal{X}}_{dL} \pm \mathcal{X}_{dR}\,, \quad C_{ae}^{V,A} = \widetilde{\mathcal{X}}_{eL} \pm \mathcal{X}_{eR}\,. \tag{8.103}$$

From the above equations we can see that the flavor changing axion interactions will be mediated by the off-diagonal elements of $\widetilde{\mathcal{X}}_{dL}$ (and $\widetilde{\mathcal{X}}_{eL}$ in case (1)). This is a common property of Goldstone bosons in flavor models, however it is an additional feature for the axion compared to the standard DFSZ and KSVZ scenarios. Regarding the vector couplings, it is interesting to remark that, while the flavor-diagonal interactions yield a null contribution for on-shell axions, this is not the case for the flavor-violating terms. This reflects the scalar (beside the pseudoscalar) nature of the axion field in models with FCNCs.

The axion axial-vector couplings to light quarks are explicitly given by (see Eq. (3.25))

$$g_u \equiv (C_{au}^A)_{11} = \begin{cases} -\dfrac{v_2^2\,(1+C_I) - v_3^2 C_I}{v^2 C_S^I C_I} & \text{for case I,} \\ -\dfrac{v_2^2 + v_3^2\,\big(1 - C_{II(III)}\big)}{v^2 C_S^{II(III)} C_{II(III)}} & \text{for case II and III}\,, \end{cases}$$

$$g_d \equiv (C^A_{ad})_{11} = -g_u + \begin{cases} \dfrac{|V_{td}|^2}{C^I_S} & \text{for case I}\,, \\ \dfrac{|V_{td}|^2 C_{II(III)} - 1}{C^{II(III)}_S C_{II(III)}} & \text{for case II and III}\,, \end{cases} \tag{8.104}$$

$$g_s \equiv (C^A_{ad})_{22} = g_d \quad (\text{with the replacement } V_{td} \to V_{ts})\,,$$

from which one can obtain the corresponding couplings to protons and neutrons, see Eq. (3.29)

The coupling to electrons in scenario (1) is given by

$$g_e \equiv \left(C^A_{ae}\right)_{11} = X_{\tau L}|U_{\tau 1}|^2 - X_{eR} - X\,. \tag{8.105}$$

For the particular implementation presented in Section 8.2.3 this coupling reads

$$g_e = -2 + |U_{\tau 1}|^2 + \frac{v_2^2 + 2v_3^2}{v^2}\,. \tag{8.106}$$

As we can see, the explicit form of g_e depends on the scalar potential implementation and the vevs of the doublet fields. Finally, in scenario (2) the electron coupling can be obtained from Eq. (8.105) by taking the limit $|U_{\tau 1}|^2 \to 0$.

Protecting the axion against gravity

This section is intended to extend the discussion on the protection of the PQ solution against gravity introduced in Section 3.3.3, and apply it to the class of models presented here. In what follows we will identify the PQ symmetry as an accidental global symmetry at low energies, associated with the spontaneous breaking of a gauge symmetry, $\mathrm{U(1)_A}$, at high energies down to a discrete subgroup. We shall follow Ref. [36], using a discrete gauge symmetry to stabilize the axion without enlarging the low energy particle content. To this end, we shall use the discrete version of the Green-Schwarz anomaly cancellation mechanism [37].

From the effective theory point of view, since we have at low energies the $\mathrm{SU(3)_c} \times \mathrm{SU(2)_L} \times \mathrm{U(1)_Y}$ gauge group, there are several possible anomalies we must consider:

$$\mathcal{A}_1 :\ [\mathrm{U(1)_Y}]^2 \times \mathrm{U(1)_A}\,, \qquad \mathcal{A}_2 :\ [\mathrm{SU(2)_L}]^2 \times \mathrm{U(1)_A}\,, \qquad \mathcal{A}_3 :\ [\mathrm{SU(3)_c}]^2 \times \mathrm{U(1)_A}\,,$$
$$\mathcal{A}_A :\ [\mathrm{U(1)_A}]^3\,, \qquad \mathcal{A}_G :\ [\text{gravity}]^2 \times \mathrm{U(1)_A}\,. \tag{8.107}$$

The Green-Schwarz anomaly cancellation conditions are then given by

$$\frac{\mathcal{A}_1}{k_1} = \frac{\mathcal{A}_2}{k_2} = \frac{\mathcal{A}_3}{k_3} = \frac{\mathcal{A}_A}{k_A} = \frac{\mathcal{A}_G}{12} = \delta_{\mathrm{GS}}\,, \tag{8.108}$$

with δ_{GS} a constant that cannot be specified by the low energy theory and $k_{1,2,3,A}$ the levels of the Kac-Moody algebra [38] which are integers for non-Abelian groups. The equality involving the hypercharge currents, $\mathcal{A}_1$, gives no useful constraints since the associated level k_1 is not an integer in general [39]. Similarly, the anomaly $\mathcal{A}_A$ can be canceled by the Green-Schwarz mechanism but with no useful constraints due to

the arbitrariness in the normalization of $\mathrm{U}(1)_\mathrm{A}$. Finally, the anomaly $\mathcal{A}_G$ gives no useful constraint either.

When the $\mathrm{U}(1)_\mathrm{A}$ is broken down to a $\mathbb{Z}_P$, the effective low energy theory will satisfy the discrete version of the Green-Schwarz cancellation condition [39, 40]

$$\frac{\mathcal{A}_3 + mP/2}{k_3} = \frac{\mathcal{A}_2 + m'P/2}{k_2}\,, \tag{8.109}$$

with m and m' integers. The model under discussion is non-supersymmetric, nevertheless, the Green-Schwarz mechanism should still be available since the breaking of supersymmetry can happen at the scale much higher that the weak scale.

Our goal is to build a $\mathrm{U}(1)_\mathrm{A}$ symmetry that contains a discrete subgroup capable of solving the strong CP problem. The $\mathrm{U}(1)_\mathrm{PQ}$ group is anomalous and, therefore, capable of giving such a solution (as it was seen in the previous sections). However, $\mathrm{U}(1)_\mathrm{PQ}$ cannot be identified with $\mathrm{U}(1)_\mathrm{A}$ as the PQ symmetry alone is, in general, not enough to satisfy the Green-Schwarz anomaly conditions. Fortunately, the model also presents baryon number conservation (+1 charge for quarks, −1 for anti-quarks), which is QCD anomaly free but it is anomalous under $\mathrm{SU}(2)_\mathrm{L}$. We shall then try to see if the combination $\mathrm{U}(1)_\mathrm{PQ} + \gamma\mathrm{U}(1)_B$ is suitable to be our axial symmetry. As the lepton charges depend on the specific representation in the neutrino sector, we will focus on the quark sector. The generalization to the lepton sector will be discussed at the end. From the $\mathrm{U}(1)_\mathrm{PQ}$ charge assignments in Eqs. (8.57), (8.58) and (8.59) we can find the anomaly coefficients

$$\begin{aligned}
\mathcal{A}_2 =& \frac{3}{2}\left(3\gamma + X_{tL}\right) = \frac{3}{2}\left(3\gamma + \frac{1}{C_S^M}\right)\,,\\
\mathcal{A}_3 =& \frac{1}{2}\left(2X_{tL} - 2X_{uR} - X_{tR} - 3X_{dR}\right) = -\frac{C_{ag}^M}{2}\,,
\end{aligned} \tag{8.110}$$

with $M = I,\, II,\, III$. The factor γ is then found to be

$$\gamma = -\frac{1}{9}\left(\frac{k_2}{k_3}C_{ag}^M + \frac{3}{C_S^M}\right)\,. \tag{8.111}$$

Using the simplest realization of the Kac–Moody algebra, i.e. $k_2 = k_3 = 1$, we get for each case

$$\begin{aligned}
&\textbf{Case I:}\quad \gamma = \frac{1 - C_I}{9C_S^I C_I}\,, \quad \textbf{Case II:}\quad \gamma = -\frac{2 + 3C_{II}}{9C_S^{II}C_{II}}\,,\\
&\textbf{Case III:}\quad \gamma = -\frac{3 + 2C_{III}}{9C_S^{III}C_{III}}\,.
\end{aligned} \tag{8.112}$$

Normalizing the combination so that all the charges are integers, we define the axial Abelian symmetry as

$$\mathrm{U}(1)_\mathrm{A} = 9\mathrm{U}(1)_\mathrm{PQ} + 9\gamma\mathrm{U}(1)_B\,. \tag{8.113}$$

The charges under this new symmetry are given in Table 8.5. Finally, note that the inclusion of PQ lepton charges would modify $\mathcal{A}_2$ in the following way

$$\mathcal{A}_2 \to \mathcal{A}_2 + \frac{1}{2}\left(X_{eL} + X_{\mu L} + X_{\tau L}\right)\,, \tag{8.114}$$

$\mathrm{U}(1)_\mathrm{A}$	Case I	Case II	Case III
$Q_{L1,2}$	$\frac{1-C_I}{C_S C_I}$	$-\frac{2+3C_{II}}{C_S^{II} C_{II}}$	$-\frac{3+2C_{III}}{C_S^{III} C_{III}}$
Q_{L3}	$\frac{8C_I+1}{C_S C_I}$	$\frac{6C_{II}-2}{C_S^{II} C_{II}}$	$\frac{7C_{III}-3}{C_S^{III} C_{III}}$
$u_{R1,2}$	$x+\frac{1-C_I}{C_S C_I}$	$x-\frac{2+3C_{II}}{C_S^{II} C_{II}}$	$x-\frac{3+2C_{III}}{C_S^{III} C_{III}}$
u_{R3}	$x-\frac{C_1+8}{C_S C_I}$	$x+\frac{15C_{II}-11}{C_S^{II} C_{II}}$	$x+\frac{7C_{III}-3}{C_S^{III} C_{III}}$
$d_{R1,2,3}$	$-x+\frac{1-C_I}{C_S C_I}$	$-x+\frac{7-3C_{II}}{C_S^{II} C_{II}}$	$-x+\frac{6-2C_{III}}{C_S^{III} C_{III}}$
Φ_1	x	x	x
Φ_2	$x-\frac{9+9C_I}{C_S^I C_I}$	$x-\frac{9}{C_S^{II} C_{II}}$	$x-\frac{9}{C_S^{III} C_{III}}$
Φ_3	$x+\frac{9}{C_S^I}$	$x+\frac{9C_{II}-9}{C_S^{II} C_{II}}$	$x+\frac{9C_{III}-9}{C_S^{III} C_{III}}$
S	9	9	9

Table 8.5: *Charge assignments under* $\mathrm{U}(1)_\mathrm{A}$, $x = 9X_{uR}$.

while $\mathcal{A}_3$ would remain unaltered. This accounts to a correction of γ of the form

$$\gamma \to \gamma - \frac{1}{9}\left(X_{eL} + X_{\mu L} + X_{\tau L}\right) , \tag{8.115}$$

which transforms the quark charges in Table 8.5 to

$$\begin{aligned} Q_{Li} &\to Q_{Li} - \left(X_{eL} + X_{\mu L} + X_{\tau L}\right) , \\ u_{Ri} &\to u_{Ri} - \left(X_{eL} + X_{\mu L} + X_{\tau L}\right) , \\ d_{Ri} &\to d_{Ri} - \left(X_{eL} + X_{\mu L} + X_{\tau L}\right) , \end{aligned} \tag{8.116}$$

and leaves the lepton and scalar charges unchanged.

In Table 8.6 we present the axial symmetry and its discrete $\mathbb{Z}_{13}$ version in the T_6 scenario, for each case I, II and III. The discrete anomaly coefficients are $\mathcal{A}_3 = -2$ and $\mathcal{A}_2 = 24$ for case I, $\mathcal{A}_3 = -15/2$ and $\mathcal{A}_2 = 12$ for case II, and $\mathcal{A}_3 = 3$ and $\mathcal{A}_2 = 45/2$ for case III. In each case, by construction, the anomaly coefficients satisfy the discrete Green-Schwarz cancellation condition in Eq. (8.109).

In this example the phase sensitive terms are explicitly given by

$$T_6 : \quad \Phi_1^\dagger \Phi_3 S^2 , \quad \Phi_2^\dagger \Phi_3 S^* . \tag{8.117}$$

Due to gravity effects we expect the most relevant $\mathrm{U}(1)_{\mathrm{PQ}}$ breaking contributions to be of the type

$$[\mathcal{O}_{4-d}] \times \frac{S^k}{M_{Pl}^{k-d}} : \quad \begin{cases} d=4 & \mathcal{O}_0 \sim \text{const} \\ d=2 & \mathcal{O}_2 \sim |\Phi_i|^2, |S|^2, \cdots \\ d=1 & \mathcal{O}_3 \sim \Phi_2^\dagger \Phi_3 S^* \\ d=0 & \mathcal{O}_4 \sim |\Phi_i|^4, |S|^4, \cdots \end{cases} \tag{8.118}$$

with k integer. The largest contribution will be the one coming from the $\mathcal{O}_0$ operator. Due to the $\mathbb{Z}_{13}$ symmetry this contribution will only take place for $k = 13$, i.e. S^{13}/M_{Pl}^9. This operator will give a contribution to the axion mass squared of the order $v_{\mathrm{PQ}}^{11}/M_{Pl}^9 \sim [10^{-72}, 10^{-39}]$ GeV^2 for PQ scales between 10^9 to 10^{12} GeV. The

T_6	$Q_{L1,2}$	Q_{L3}	$u_{R1,2}$	u_{R3}	$d_{R1,2,3}$	Φ_1	Φ_2	Φ_3	X_S
Case I:									
$\mathrm{U(1)_A}$	7	-11	$x+7$	$x-38$	$-x+7$	x	$x-27$	$x-18$	9
$\mathbb{Z}_{13}$	7	2	$x+7$	$x+1$	$-x+7$	x	$x+12$	$x+8$	9
Case II:									
$\mathrm{U(1)_A}$	-9	0	$x-9$	$x-18$	$-x+18$	x	$x-27$	$x-18$	9
$\mathbb{Z}_{13}$	4	0	$x+4$	$x+8$	$-x+5$	x	$x+12$	$x+8$	9
Case III:									
$\mathrm{U(1)_A}$	-11	-2	$x-11$	$x-2$	$-x+16$	x	$x-27$	$x-18$	9
$\mathbb{Z}_{13}$	2	11	$x+2$	$x+11$	$-x+3$	x	$x+12$	$x+8$	9

Table 8.6: *Particular example with the phase sensitive scalar potential T_6.*

contribution to the $\bar{\theta}$ will be between 10^{-54} to 10^{-15}. These are extremely small contributions, making the model safe against large gravitational corrections.

In this section we have shown how we could avoid large contributions to the axion mass, as well as to the $\bar{\theta}$ parameter, just by invoking a discrete gauge symmetry. However, there are many more effective operators that will be induced by gravity than those presented above. Some of them could give contributions to the original Yukawa textures potentially spoiling the good behavior of the BGL-like textures.

Let us choose case I as a particular scenario. From the $\mathbb{Z}_{13}$ charge assignments we have the Yukawa term $\overline{Q}_{L1}\, u_{R3}\, \tilde{\Phi}_2$ carrying a net charge 8. This term is not allowed at the renormalizable level, but the gravity induced effects can introduce the $\mathbb{Z}_{13}$ invariant term $\overline{Q}_{L1}\, u_{R3}\, \tilde{\Phi}_2\, (S/M_{Pl})^2$. This term will contribute to the Yukawa textures once S spontaneously breaks the PQ symmetry with a correction of the order $y \times v_{\mathrm{PQ}}^2/M_{Pl}^2$, with y the associated Yukawa coupling. For a PQ breaking scale of order $v_{\mathrm{PQ}} \lesssim \mathcal{O}\,(10^{15})$ GeV this operator gives a harmless contribution. However, for higher scales this term could give significant corrections to the BGL-like suppression when $y \sim \mathcal{O}(1)$. Nevertheless, even for a high PQ breaking scale, we could have $\mathcal{O}(y) \ll 1$ suppressing this additional contribution. This is not so strange taking into account that in our framework no information on the Yukawa hierarchy is given. We know that $\mathcal{O}(y_u,\, y_d,\, \cdots) \ll 1$ and in our framework this is imposed by hand. In a more complete model, these hierarchies could be made dynamical and there we should also take attention to these additional gravity induced terms.

8.2.5 Model variations

The class of models presented above had FCNCs in the down-quark sector and the top quark was singled out. However, there are many other possible implementations that will still give the same minimal flavor violating scenario. These model variations can be found by performing any of the two operations:

(i) Symmetric permutations in the flavor space;

(ii) Changing up and down right-handed generators.

We can apply these two operations to the models previously studied in order to get all possible model variants.

Type (*i*) operation

The permutations in flavor space will change the textures in the sector with no FCNCs, i.e the up sector if we apply this operation in the original formulation. The symmetry generators take now the form

$$\mathcal{S}_L \to P^T \mathcal{S}_L P\,, \quad \mathcal{S}_R^{u,d} \to P^T \mathcal{S}_R^{u,d} P\,, \quad \mathcal{S}_L^e \to P'^T \mathcal{S}_L P'\,, \quad \mathcal{S}_R^e \to P'^T \mathcal{S}_R^e P'\,, \tag{8.119}$$

with P and P' 3×3 permutation matrices. The 2 by 2 block in the NFC sector will change structure, we get

$$P, P' = P_{23} \quad \longrightarrow \quad \left\{ \begin{pmatrix} \times & \times \\ \times & \times \end{pmatrix}, \begin{pmatrix} & \\ & \times \end{pmatrix}, \begin{pmatrix} \times & & \times \\ & \times & \\ \times & & \times \end{pmatrix} \right\} : \text{Block } 1-3 \tag{8.120a}$$

$$P, P' = P_{13} \quad \longrightarrow \quad \left\{ \begin{pmatrix} & & \\ & \times & \times \\ & \times & \times \end{pmatrix}, \begin{pmatrix} \times & & \\ & & \\ & & \end{pmatrix}, \begin{pmatrix} \times & & \\ & \times & \times \\ & \times & \times \end{pmatrix} \right\} : \text{Block } 2-3 \tag{8.120b}$$

Where P_{ij} permutes the lines i and j (when applied on the left) and columns i and j (when applied on the right). Besides the textures the only changes due to (i) are in the axion-matter couplings. The permutation matrices single out other flavors. Therefore, the action of the permutation matrices will change the CKM and PMNS elements entering in Eq. (8.100) and Eq. (8.101), respectively. We get the following redefinition

$$\begin{aligned} P, P' = P_{23} \quad &\longrightarrow \quad t \to c, \tau \to \mu \\ P, P' = P_{13} \quad &\longrightarrow \quad t \to u, \tau \to e \end{aligned} \tag{8.121}$$

Consequently, the couplings u, d, s and e are appropriately changed.

Type (*ii*) operation

We change the sector where the FCNCs are present, that can be accounted with the following symmetry generators

$$\mathcal{S}_L = \text{diag}(1, 1, e^{iX_{tL}\theta})\,, \quad \mathcal{S}_R^u = e^{iX_{dR}\theta}\mathbb{1}\,, \quad \mathcal{S}_R^d = \text{diag}(e^{iX_{uR}\theta}, e^{iX_{uR}\theta}, e^{iX_{tR}\theta})\,. \tag{8.122}$$

We have switched the $\mathcal{S}_R^u$ and $\mathcal{S}_R^d$ generators, keeping the same labels for the charges. Thus, in this scenario the $\mathcal{S}_R^u$ is completely degenerate, but instead of labeling the charge X_{uR} we keep it labeled as X_{dR}, just as in the previous case. By keeping the same label we can easily compare this new case with the previous scenario where the FCNCs where in the down sector. The Higgs charges, for the three cases, take the same form as in the original scenario (see Eqs. (8.41) and (8.42)) but with an overall minus sign.

$$\textbf{Case I:} \quad X_{\Phi 1} = -X_{uR}\,, \quad X_{\Phi 2} = -(X_{tR} - X_{tL})\,, \quad X_{\Phi 3} = -(X_{tL} + X_{uR})\,.$$

Cases	A_I	A_{II}	A_{III}
$(1,1,1)$	$-1-5C_I$	$11-3C_{II}$	$12-4C_{III}$
$(2,2,2)$	$-10-14C_I$	$2-3C_{II}$	$3-4C_{III}$
$(3,3,3)$	$-1+4C_I$	$2+6C_{II}$	$3+5C_{III}$
$(1,1,2)$	$-4-8C_I$	$8-3C_{II}$	$9-4C_{III}$
$(1,1,3)$	$-1-2C_I$	8	$9-C_{III}$
$(2,2,1)$	$-7-11C_I$	$5-3C_{II}$	$6-4C_{III}$
$(2,2,3)$	$-7-8C_I$	2	$3-C_{III}$
$(3,3,1)$	$-1+C_I$	$5+3C_{II}$	$6+2C_{III}$
$(3,3,2)$	$-4-2C_I$	$2+3C_{II}$	$3+2C_{III}$
$(1,2,3)$	$-4-5C_I$	5	$6-C_{III}$

Table 8.7: *Charge combinations A_I, A_{II} and A_{III} entering in the description of the axion coupling to photons. The numbers in the first column label the Higgs doublet giving mass to the charged leptons (e,μ,τ); for example $(1,1,2)$ stands for the case where Φ_1 gives mass to e and μ while Φ_2 to τ.*

$$\begin{aligned}
&\textbf{Case II:} \quad X_{\Phi 1} = -X_{uR}\,, \quad X_{\Phi 2} = X_{dR}\,, \quad X_{\Phi 3} = -(X_{tL} - X_{dR})\,. \\
&\textbf{Case III:} \quad X_{\Phi 1} = -X_{uR}\,, \quad X_{\Phi_2} = X_{dR}\,, \quad X_{\Phi_3} = -(X_{tL} - X_{dR})\,.
\end{aligned} \tag{8.123}$$

The quark charges take the same form as in Eq. (8.57), (8.58) and (8.59) as long as in the scalar sector the role of the S field is substituted by the S^*, keeping the $X_S = 1$ normalization. This will account for the overall minus sign coming from the Higgs charges. While the left-handed quark charges have the same expression as in the original scenario, the right-handed ones switched sectors. The coupling to gluons will not change, however the coupling to photons changes since the up and down electric charges are different. It will be given by

$$C_{a\gamma} = 2\left[4X_{dR} + \frac{2}{3}X_{uR} + \frac{1}{3}X_{tR} - \frac{5}{3}X_{tL} + \sum_{\alpha}(X_{\alpha R} - X_{\alpha L})\right]. \tag{8.124}$$

This will have the same form as Eq. (8.92), but now the coefficients take the form given in Table 8.7

The axion coupling to matter will also change, since we have changed the FCNC sector. The shift we need to perform in order to account for the orthogonality between the axion and the Goldstone boson will get an overall minus sign with respect to Eq. (8.96). Because we changed sectors without changing the labels of the charges the quark charges shifts will coincide with the ones in Eq. (8.94). The shift charge matrix takes the form

$$\begin{aligned}
&\mathcal{X}_{uL} = \mathcal{X}_{dL} = \mathrm{diag}(0,\, 0,\, X'_{tL})\,, \quad \mathcal{X}_{eL} = \mathrm{diag}(X'_{eL},\, X'_{\mu L},\, X'_{\tau L})\,, \\
&\mathcal{X}_{uR} = X'_{dR}\mathbb{1}\,, \quad \mathcal{X}_{dR} = \mathrm{diag}(X'_{uR},\, X'_{uR},\, X'_{tR})\,, \quad \mathcal{X}_{eR} = \mathrm{diag}(X'_{eR},\, X'_{\mu R},\, X'_{\tau R})\,.
\end{aligned} \tag{8.125}$$

In the mass basis they take the explicit form

$$\widetilde{\mathcal{X}}_{uL} = X_{tL} \begin{pmatrix} |V_{ub}|^2 & V_{ub}V_{cb}^* & V_{ub}V_{tb}^* \\ V_{cb}V_{ub}^* & |V_{cb}|^2 & V_{ub}V_{tb}^* \\ V_{tb}V_{ub}^* & V_{tb}V_{cb}^* & |V_{tb}|^2 \end{pmatrix}, \quad \widetilde{\mathcal{X}}_{uR} = \mathcal{X}_{uR}\,, \quad \widetilde{\mathcal{X}}_{dL} = \mathcal{X}_{dL}\,, \quad \widetilde{\mathcal{X}}_{dR} = \mathcal{X}_{dR}\,, \tag{8.126}$$

The axial-vector couplings to the light quarks are now given by

$$\begin{aligned} g_d \equiv (C_{ad}^A)_{11} &= \begin{cases} -\dfrac{v_2^2\,(1+C_I) - v_3^2 C_I}{v^2 C_S^I C_I} & \text{for case I,} \\ -\dfrac{v_2^2 + v_3^2\,\big(1 - C_{II(III)}\big)}{v^2 C_S^{II(III)} C_{II(III)}} & \text{for case II and III}\,, \end{cases} \\ g_s \equiv (C_{ad}^A)_{22} &= g_d\,, \\ g_u \equiv (C_{au}^A)_{11} &= -g_d + \begin{cases} \dfrac{|V_{ub}|^2}{C_S^I} & \text{for case I}\,, \\ \dfrac{|V_{ub}|^2 C_{II(III)} - 1}{C_S^{II(III)} C_{II(III)}} & \text{for case II and III}\,. \end{cases} \end{aligned} \tag{8.127}$$

Model variations dictionary

In this section we present a compilation of the most significant changes resulting from applying the operations (i) or (ii) to the original formulation. These can be found in Table 8.8.

8.2.6 Experimental constraints on the invisible axion

The framework presented here has two important differences with respect to the benchmark invisible axion models introduced in Chapter 3 that are of phenomenological interest:

- As we saw in Section 3.3.4, the axion mass and coupling to photons are related by Eq. (3.66), with ξ taking the approximate values 0.5 for the KSVZ model, and 1.4 (0.8) for the DFSZ type II (flipped). However, in this framework we can get, besides the standard values, an additional set of discrete values depending on the model implementation, which allows us to cover a larger range of axion-photon couplings.

- Contrarily to what happens in the DFSZ and KSVZ models, the axion couples differently to different flavors and has flavor changing interactions at tree level. This class of models presents non-diagonal couplings in the up-quark sector or in the down-quark sector depending on the model considered, and has flavor changing axion interactions in the charged lepton sector for some of the leptonic implementations.

Searches constraining invisible axion models based on astrophysical considerations, and on the axion-photon conversion mechanism where already discussed in

	Original	Operation (i)		Operation (ii)
		P_{23}	P_{13}	
Yukawa textures	Eq. (8.34), (8.37), (8.39)	Eq. (8.120a)	Eq. (8.120b)	Original
Symmetry generators	Eqs. (2.29), (2.34)	Eq. (8.119)		Eq. (8.122)
Scalar charges	Eqs. (8.41), (8.42)			Eq. (8.123)
Coupling to photons	Table 8.4			Table 8.7
Orthogonality shift	Eq. (8.96)			Overall minus sign
Mass basis charges	Eqs. (8.98), (8.100)	$t \to c$ $\tau \to \mu$	$t \to u$ $\tau \to e$	Eqs. (8.125), (8.126)
u, d, s couplings	Eqs. (8.104)	$t \to c$	$t \to u$	Eqs. (8.127)
Electron coupling	Eqs. (8.105)	$\tau \to \mu$	$\tau \to e$	Original

Table 8.8: *This table summarizes the changes we need to do in order to get all possible model variations. The firs column, i.e. Original, presents the various relevant equations in the scenario where the down sector has FCNCs and the top is singled out. The second column, i.e. Operation (i), represents models with permutations in the flavor space of each sector. The last column, i.e. Operation (ii), represent models with quark sectors interchanged.*

Section 3.3.4. However, the presence of flavor-violating axion couplings introduce new experimental bounds that were not considered before. The most stringent bounds on flavor-changing axion interactions are extracted from flavor violating decays of kaons or muons into the axion and some other particle(s). Flavor processes in which the axion enters with a double insertion of the axion coupling ($\mu \to e\gamma$, $\mu - e$ conversion in nuclei, $K^0 - \bar{K}^0$ mixing, $B_s \to \mu^+\mu^-$, among others) are very suppressed by an extra $v_{\rm PQ}^{-1}$ factor at the amplitude level and do not put relevant bounds.

The leptonic decay $\mu^+ \to e^+ a$ can in principle be used to constrain charged lepton flavor violating interactions of the axion. In Ref. [41] the authors reported the experimental bound $\text{Br}(\mu^+ \to e^+ a) < 2.6 \times 10^{-6}$ at 90% CL. This result however relies on the assumption that the positron is emitted isotropically to avoid large backgrounds from the ordinary muon decay $\mu^+ \to e^+ \nu_e \bar{\nu}_\mu$. This assumption would be valid if we only had vector couplings but not axial-vector ones. In our scenarios, the lepton flavor violating axial-vector and vector couplings are equal, so the assumptions behind the $\mu^+ \to e^+ a$ bound do not apply. In this case the best process to bound the charged lepton flavor violating axion couplings is the radiative decay $\mu^+ \to e^+ a\,\gamma$. With this process it is possible to extract limits which are independent of the chirality properties of the axion couplings [42]. The most stringent experimental bound at the moment is $\text{Br}(\mu^+ \to e^+ a\,\gamma) < 1.1 \times 10^{-9}$ at 90% CL [43], obtained at LAMPF using the Crystal Box detector. From this process we can extract

$$v_{\rm PQ} > \left[\left|g_{\mu e}^V\right|^2 + \left|g_{\mu e}^A\right|^2\right]^{1/2} \times \left(1.6 \times 10^9\,\text{GeV}\right) = \left|g_{\mu e}^V\right| \times \left(2.3 \times 10^9\,\text{GeV}\right)\,, \quad (8.128)$$

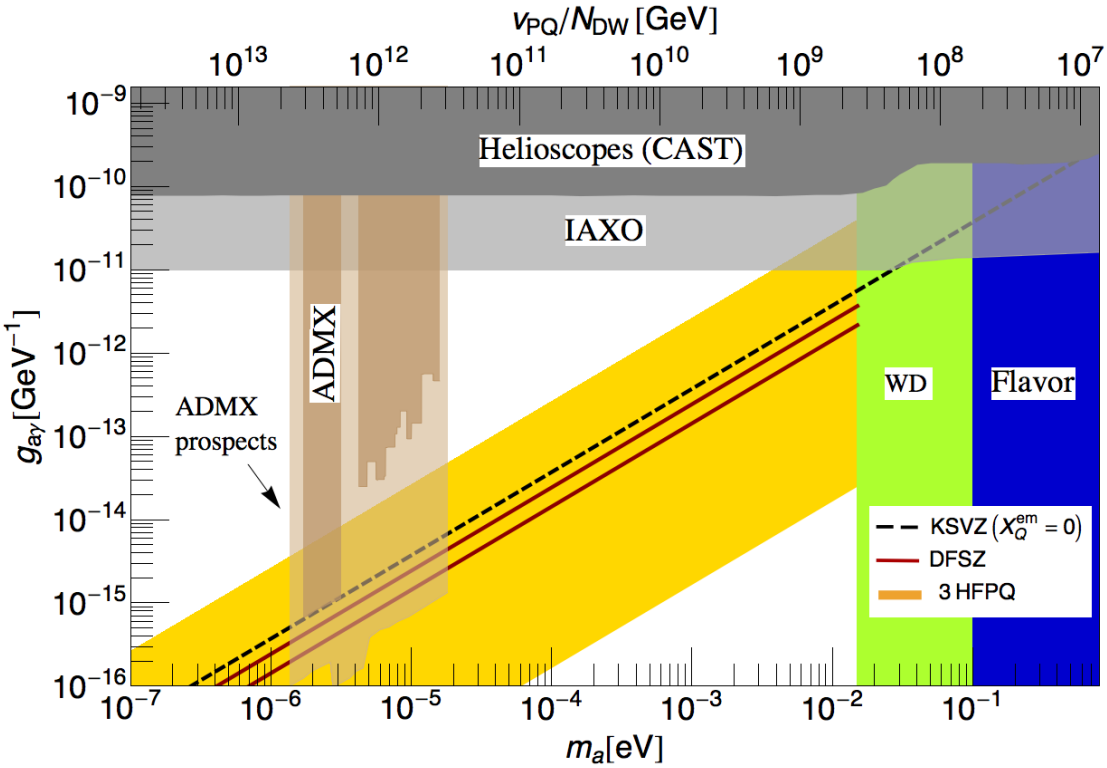

Figure 8.2: *Constraints on the invisible axion of the 3HFPQ models where the top-quark is singled out. Familon searches in flavor experiments, astrophysical considerations and axion-photon conversion experiments are taken into account. The yellow wide band represents a scan over all possible 3HFPQ models considered. Constraints from WD cooling are shown taking the benchmark point $|g_e|/N_{DW} = 10^{-1}$. The dark blue band represents the most conservative upper bound on the axion mass from $\mu^+ \to e^+ a\gamma$. Predictions for the KSVZ and DFSZ models (type II and flipped) are also shown.*

with the axion-lepton couplings $g^V_{\mu e} = g^A_{\mu e} = \left(C^A_{ae}\right)_{21}$ in the scenario with FCNCs in the charged lepton sector. We obtain a robust bound from this process since the flavor changing couplings $g^{V,A}_{\mu e}$ are completely determined by elements of the PMNS lepton mixing matrix due to the underlying PQ symmetry. The bound extracted on the PQ scale, or equivalently the axion mass, from $\mu^+ \to e^+ a\gamma$ does not vary much between all the models with FCNCs in the charged lepton sector. The reason being that the PMNS matrix is very anarchical, that is, $|V^*_{\tau 2} V_{\tau 1}| \sim |V^*_{\mu 2} V_{\mu 1}| \sim |V^*_{e2} V_{e1}|$. Obviously, models without tree-level FCNCs in the charged lepton sector avoid the constraints coming from $\mu^+ \to e^+ a\gamma$.

Models with FCNCs in the up-quark sector do not receive strong constraints from flavor observables, all the relevant observables involve a double insertion of the axion couplings in this case. On the other hand, models with FCNCs in the down-quark sector are strongly constrained by limits on $K^+ \to \pi^+ a$. To the best of our knowledge, the strongest bound on $K^+ \to \pi^+ a$ decays has been set by the E787 Collaboration at Brookhaven National Laboratory, achieving $\mathrm{Br}(K^+ \to \pi^+ a) <$

4.5×10^{-11} at 90% CL [44]. The partial decay width for this process is given by

$$\Gamma(K^+ \to \pi^+ a) = \frac{1}{64\pi} \frac{m_K^3}{v_{\rm PQ}^2} \left|g_{sd}^V\right|^2 \beta^3 \left|F_1(0)\right|^2 , \tag{8.129}$$

with $\beta = 1 - m_\pi^2/m_K^2$ and $g_{sd}^V = \left(C_{ad}^V\right)_{21}$. The relevant hadronic matrix element

$$\left\langle \pi^+(p') \right| \overline{s}\gamma^\mu d \left| K^+(p) \right\rangle = F_1(q^2)(p+p')^\mu , \tag{8.130}$$

can be extracted in the limit of exact SU(3) flavor symmetry. At the zero momentum transfer the form factor has the fixed normalization $F_1(0) = 1$ [45]. We have $\langle \pi^+(p') | \, \overline{s}\gamma^\mu\gamma_5 d \, | K^+(p) \rangle = 0$ because K^+ and π^+ are pseudoscalar mesons. From this result we can extract a lower bound on the PQ scale

$$v_{\rm PQ} > \left|g_{sd}^V\right| \times \left(4.4 \times 10^{11}\,{\rm GeV}\right) . \tag{8.131}$$

Just like in the charged lepton sector, the coupling g_{sd}^V is fixed in terms of elements of the CKM quark mixing matrix due to the underlying PQ symmetry. A robust bound can then be extracted on the axion mass which is independent of the many free parameters of the model.

Future improvements on the $\mu^+ \to e^+ a\gamma$ bounds are difficult to achieve with present facilities, see discussion in Ref. [46]. On the other hand, improvements on the $K^+ \to \pi^+ a$ limits can be expected from the NA62 experiment at CERN [47].

In Figs. 8.2 and 8.3 we summarize all the relevant constraints on the axion properties. In Figure 8.2 we show constraints on models with FCNCs in the charged lepton sector and in the down-quark sector which select the top-quark. The strongest bound from flavor observables arises in this case from $\mu^+ \to e^+ a\gamma$ because of the strong suppression factor $|V_{ts}^* V_{td}|$ entering in $K^+ \to \pi^+ a$ decays. The wide yellow band represents the prediction scanning over all the 3HFPQ models of this type. For this type of models astrophysical bounds from WD cooling put in general a stronger limit on the axion mass than flavor processes, the WD bound however depends strongly on the vevs of the Higgs doublets while the flavor limits do not. This is precisely what occurs for the model analyzed in Ref. [14], which corresponds to a case I model with scalar potential implementation T_{11} and leptonic implementation $(3, 3, 2)$. Predictions for the KSVZ and DFSZ invisible axion models are also shown in Figs. 8.2 and 8.3. For the KSVZ model we assume that the exotic color triplet has no electric charge ($X_Q^{em} = 0$). In both Figures, the upper DFSZ line corresponds to the flipped scenario while the bottom one to the type II case.

In Figure 8.3 we show the constraints on those models with FCNCs in the down-quark sector which select the up or charm quark. The most relevant limit on the axion mass comes now from $K^+ \to \pi^+ a$ due to the value of the product of CKM matrix elements $|V_{ud}^* V_{us}|^2 \sim |V_{cd}^* V_{cs}|^2 \gg |V_{td}^* V_{ts}|^2$ lifting the decay rate. For some models of this type the bound from kaon decays can be as strong as $m_a \lesssim 2 \times 10^{-5}$ eV. This is one of the main results of this chapter. Among all the models with FCNCs in the down-quark sector, those which select the top quark are much less constrained because of the very effective CKM suppression entering in $K^+ \to \pi^+ a$ decays.

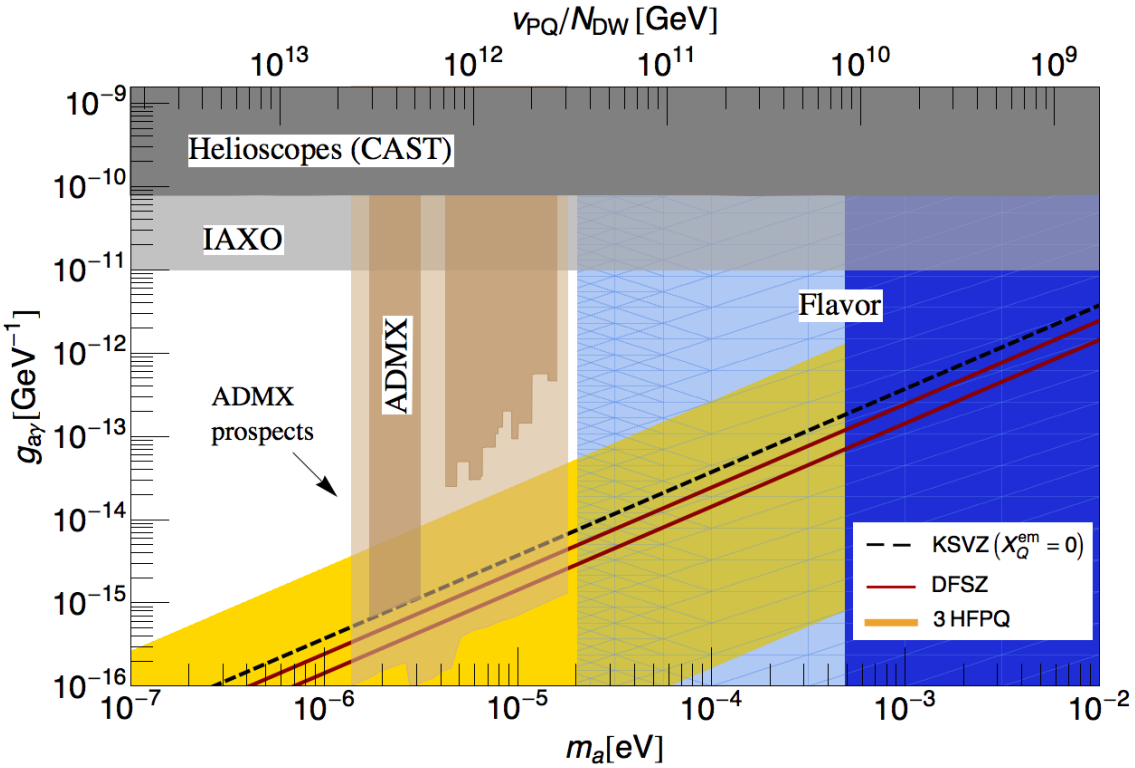

Figure 8.3: *Constraints on the invisible axion of the 3HFPQ models where the up-quark and charm quarks are singled out. Familon searches in flavor experiments, astrophysical considerations and axion-photon conversion experiments are taken into account. The yellow wide band represents a scan over all possible 3HFPQ models considered. The dark blue band corresponds to the most conservative upper bound on the axion mass extracted from $K^+ \to \pi^+ a$, the light blue band corresponds to the strongest upper bound from this process. Predictions for the KSVZ and DFSZ models (type II and flipped) are also shown.*

8.2.7 The scalar sector

The scalar sector of this class of models contains three complex Higgs doublets Φ_j $(j = 1, 2, 3)$ and a complex scalar gauge singlet S. The scalar fields are then parametrized in terms of 14 real degrees of freedom (each doublet carrying 4 and the singlet 2). Three degrees of freedom correspond to the usual Goldstone bosons $G^{\pm,0}$ responsible of giving mass to the massive weak gauge bosons. These have already being isolated by going to the Higgs basis in Eq. (8.44). Another degree of freedom corresponds to the axion which, up to corrections of order $\mathcal{O}(v/v_{\rm PQ})$, is given by the phase of the scalar gauge singlet. The other 10 degrees of freedom become physical scalar fields, leaving 2 electrically charged and 6 neutral physical scalars. It is not our intent to present a detailed analysis of the Higgs phenomenology in this class of models. We will, nevertheless, say a few words on some of these aspects. However, before discussing the Higgs phenomenology it is necessary to have some basic grasp of the decoupling structure of the kind of models considered.

Decoupling in the scalar sector

After the scalar fields acquire a vev, mixing among the scalars with the same charge is induced. Due to the large hierarchy between the vevs, i.e. $v_{\rm PQ} \gg v$, the radial part of the gauge singlet acquires a large mass and we can treat the mixing as $\mathrm{SU(2)_L}$-conserving. The scalar potential of the $\mathrm{SU(2)_L}$ doublets is then given by

$$V(\Phi) = (\Phi_i^\dagger \mathcal{M}_{ij}^2 \Phi_j + \mathcal{O}(v^2) + \text{h.c.}) + \text{quartic terms on } \Phi_i\,, \tag{8.132}$$

with the square mass matrix taking the form

$$\mathcal{M}^2 = v_{\rm PQ}^2 \begin{pmatrix} \frac{m_1^2}{v_{\rm PQ}^2} + \lambda_1^{\Phi S} & \lambda_4 & \lambda_5 \\ \lambda_4^* & \frac{m_2^2}{v_{\rm PQ}^2} + \lambda_2^{\Phi S} & \lambda_6 \\ \lambda_5^* & \lambda_6^* & \frac{m_3^2}{v_{\rm PQ}^2} + \lambda_3^{\Phi S} \end{pmatrix}. \tag{8.133}$$

The couplings λ_i are associated with the phase sensitive terms (i) of Table 8.1. In the case where a phase sensitive term has mass dimension, such as in cases (4), (5) and (6) with $k_i = 1$, we parametrize it as $\mu_i = v_{\rm PQ}\lambda_i$. Additionally, note that for models T_1 to T_9 the PQ symmetry forces one of the couplings to be zero, that is $\lambda_k = 0$ with $k = 4, 5$ or 6, while for models T_{10} to T_{12} all the couplings are expected to be non-zero.

Because of the large value of the PQ symmetry breaking scale, the scalar sector of invisible axion models usually presents a decoupling scenario. This way only the axion and a SM-like Higgs remains at the EW scale while the others acquire a mass of order $v_{\rm PQ}$. However, it is possible to achieve specific values for the parameters in order to avoid the decoupling limit in such a way that two (or three) Higgs doublets get masses around the EW scale.

In what follows, we analyze the different decoupling limits and give a possible texture reproducing each scenario. In the textures we use the parameters $b, c \sim \mathcal{O}(1)$ and $\epsilon \sim \mathcal{O}\left(v^2/v_{\rm PQ}^2\right)$. The last parameter, ϵ, has been introduced in order to show how EW corrections coming from the terms we have neglected in Eq. (8.132) can lift the zero eigenvalues to the EW scale. We also distinguish between the case where one of the λ-couplings is zero as in models T_1 to T_9 and the case where all the couplings are non-zero, corresponding to models T_{10} to T_{12}.

- **One doublet at the electroweak scale.**
  This scenario is characterized by the presence of a SM-like Higgs at the EW scale, with the other two scalar doublets having masses at the PQ symmetry breaking scale. As a result, the infrared theory will correspond to the SM plus the axion (whose properties and couplings were discussed in Section 8.2.4) supplemented by higher dimension operators suppressed by the PQ breaking scale which can be neglected.[5]

[5] Additionally, one should take special care of higher dimension operators coming from gravitational effects as they give non-negligible contributions. For a detailed analysis see Sections 3.3.3 and 8.2.4.

We list two textures generating this scenario

$$\mathcal{M}^2 = v_{\rm PQ}^2 \begin{pmatrix} \sqrt{2}\,b + \epsilon & b & b \\ b & \sqrt{2}\,b & 0 \\ b & 0 & \sqrt{2}\,b \end{pmatrix} . \tag{8.134}$$

This texture can be implemented in models T_1 to T_9, even though the zero has been located in the position of λ_5. The same mass spectrum is generated by permuting the value of the parameters appropriately. On the other hand, for the models T_{10} to T_{12} one possible texture is given by

$$\mathcal{M}^2 = v_{\rm PQ}^2 \begin{pmatrix} b + \epsilon & b & c \\ b & b + \epsilon & c \\ c & c & c \end{pmatrix} , \tag{8.135}$$

where the constraint $b \neq c$ needs to be satisfied to have just one doublet at the EW scale.

- **Two doublets at the electroweak scale.**
  In this decoupling scenario we obtain a 2HDM with tree-level FCNCs controlled by the CKM and PMNS matrices, the quark masses and the ratio of the vevs of the two-Higgs-doublets whose masses are at the EW scale (in a similar fashion as in the BGL 2HDM). However, the values of the flavor changing scalar couplings cannot be determined in general as it will depend on the specific implementation of the scalar parameters in $\mathcal{M}^2$. In any case, as these couplings present the same structure as in the BGL models, similar constraints in the parameter space are expected.

  For models T_1 to T_9 it is not possible to reproduce this scenario unless some of the parameters are ultraweak, i.e. of order $\mathcal{O}\left(v^2/v_{\rm PQ}^2\right)$. In this case one possible texture is given by

$$\mathcal{M}^2 = v_{\rm PQ}^2 \begin{pmatrix} b + \epsilon & b & \epsilon \\ b & b + \epsilon & 0 \\ \epsilon & 0 & \epsilon \end{pmatrix} , \tag{8.136}$$

  which is only valid for models T_1, T_2 and T_7. The equivalent texture for models T_3 to T_6, T_8 and T_9 can be directly obtained from the previous texture by permuting the entries in the matrix. Finally, one texture reproducing this scenario in models T_{10} to T_{12} is

$$\mathcal{M}^2 = v_{\rm PQ}^2 \begin{pmatrix} b + \epsilon & b & b \\ b & b + \epsilon & b \\ b & b & b \end{pmatrix} . \tag{8.137}$$

- **Three doublets at the electroweak scale.**
  Having the three doublets at the EW scale is only possible if we force all the parameters in Eq. (8.133) to be ultraweak, that is if every term in $\mathcal{M}^2$ take values around the EW scale. As we have discussed in Section 8.2.2, this scenario gives rise to FCNCs which are suppressed by the CKM and the PMNS matrices with the explicit scalar flavor violating couplings depending on the model implementation.

This simple analysis of the possible decoupling scenarios is by no means a full and detailed study of the scalar spectrum. The textures above are just illustrative and many other textures with different degrees of tuning might be present for any of the three relevant decoupling scenarios. Finally, it should be noted that the scalar sector in this class of models suffers from a fine tuning problem (commonly known as the hierarchy problem), just like most models where more than one scale is present in the theory. A solution for this problem is out of the scope of the work presented in this thesis. However, it is worth mentioning that some promising directions have been pursued in the literature within the framework of invisible axion models, see e.g. [48, 49].

Higgs phenomenology

If there is a decoupling in the scalar sector where one Higgs doublet remains at the weak scale while the other scalar fields become very heavy, three degrees of freedom of this doublet correspond to the Goldstone bosons giving mass to the massive gauge bosons while the remaining degree of freedom corresponds to a SM-like Higgs boson. The possibility of a richer decoupling structure in the scalar sector, with two or three Higgs doublets at the weak scale would give rise to potentially new physics signatures at flavor factories and collider experiments like the LHC. The latter scenario would imply the existence of additional neutral Higgs boson (besides the 125 GeV SM-like Higgs boson) and charged scalars with masses around the EW scale. Neglecting mixing effects among the scalar fields, the phenomenology of these scalars would be basically the same than in the BGL 2HDMs analyzed in Refs. [50–52]. For example, dangerous $|\Delta S| = 2$ contributions to $K^0 - \bar{K}^0$ mixing due to neutral scalars would be very suppressed in the top BGL models because the flavor changing couplings are proportional to $|V_{ts}^* V_{td}|$, allowing the mass of these scalars to be at the weak scale [50].

A classification of flavor observables which receive important contributions in the BGL 2HDMs and a comprehensive phenomenological analysis of these models was presented in Ref. [50]. Additional neutral scalars with flavor changing couplings will enter at tree level in pseudoscalar meson leptonic decays $M^0 \to \ell^+\ell^-$, neutral meson mixing $M^0 - \bar{M}^0$, as well as in lepton flavor violating transitions of the type: $\ell_1^- \to \ell_2^-\ell_3^+\ell_4^-$, $\tau \to \ell\pi\pi$ and $\mu - e$ conversion in nuclei. The previous processes arise in the SM at the loop level and receive strong suppressions due to the GIM mechanism or the smallness of neutrino masses, this makes these processes very sensitive to small new physics contributions. Charged scalars will also contribute at tree-level to semi-leptonic pseudoscalar meson decays ($M \to \ell\nu$, $B \to D^{(*)}\ell\nu$) and leptonic τ decays ($\tau \to \ell\bar{\nu}_\ell\nu_\tau$), possibly causing observable violations of lepton universality. Neutral and charged scalars will contribute at the loop level in processes like $\bar{B} \to X_s\gamma$ and $\ell_1 \to \ell_2\gamma$ and will in general dominate over the SM contribution which appears at the same level. The discovery of additional scalars at the LHC and characteristic decay signatures of the nonstandard scalars in the BGL 2HDMs have been analyzed in Ref. [51, 52]. The main results of these analyses is that within BGL 2HDMs additional charged and neutral scalars can be as light as 150 GeV while being compatible with present 125 GeV Higgs, flavor, electroweak precision and collider data [50–52].

Models	KSVZ	DFSZ	3HFPQ
BSM fields	Q+S	Φ_2+S	Φ_2+Φ_3+S
PQ fields	Q, S	q, l, $\Phi_{1,2}$, S (flavor blind)	q, l, $\Phi_{1,2,3}$, S (flavor sensitive)
$C_{a\gamma}/C_{ag}$	$6(X_Q^{em})^2$	$2/3, 8/3$	$[-34/3, 44/3]$
Tree-level CtM	No	Yes	Yes
Tree-level FCAI	No	No	Yes
$N_{\rm DW}$	1	$3, 6$	$1, 2, \cdots, 8$

Table 8.9: *Comparison of the class of models constructed here with the usual invisible axion model benchmarks. The different values for $C_{a\gamma}/C_{ag}$ and N_{DW} in the DFSZ and the 3HFPQ models correspond to different implementations of the PQ symmetry. We use the notation: CtM=Coupling to Matter; FCAI=Flavor Changing Axion Interaction.*

8.2.8 Conclusions

In this section we have built a class of invisible axion models with FCNCs at tree level which are controlled by the fermion mixing matrices. The scalar sector contains three-Higgs doublets and a complex scalar gauge singlet field. A flavored Peccei-Quinn symmetry provides a solution to the strong CP problem via the Peccei-Quinn mechanism, giving rise to an invisible axion which could account for the cold dark matter in the Universe. Moreover, it is possible to explain the smallness of active neutrino masses via a type I seesaw mechanism, providing a dynamical origin for the heavy seesaw scale, which is related to the PQ breaking scale in this class of models. The main features of such 3HFPQ class of models are summarized in Table 8.9, making the relevant comparisons with the KSVZ and DFSZ axion models. Experimental limits on the axion have been analyzed taking into account familon searches in rare kaon and muon decays, astrophysical considerations and axion-photon conversion experiments.
The most important findings of our analysis are:

- Models with tree-level FCNCs in the down-quark or charged lepton sectors receive important constraints on the PQ scale from familon searches in kaon and muon decays. These bounds are very robust for the class of models considered here since the flavor changing axion couplings are completely controlled by elements of the fermion mixing matrices due to the underlying PQ symmetry.

- Models with tree-level FCNCs in the down-quark sector for which the top quark is singled out receive the strongest upper bound on the axion mass from white-dwarf cooling arguments in general, though these bounds depend strongly on the vevs of the Higgs doublets. Bounds from $K^+ \to \pi^+ a$ are very weak due to the strong CKM suppression. Figure 8.2 summarizes all the constraints on this scenario.

- Models with tree-level FCNCs in the down-quark sector for which the up (or charm) quark is singled out receive the strongest upper bound on the axion mass from $K^+ \to \pi^+ a$ decays since in this case the flavor changing couplings

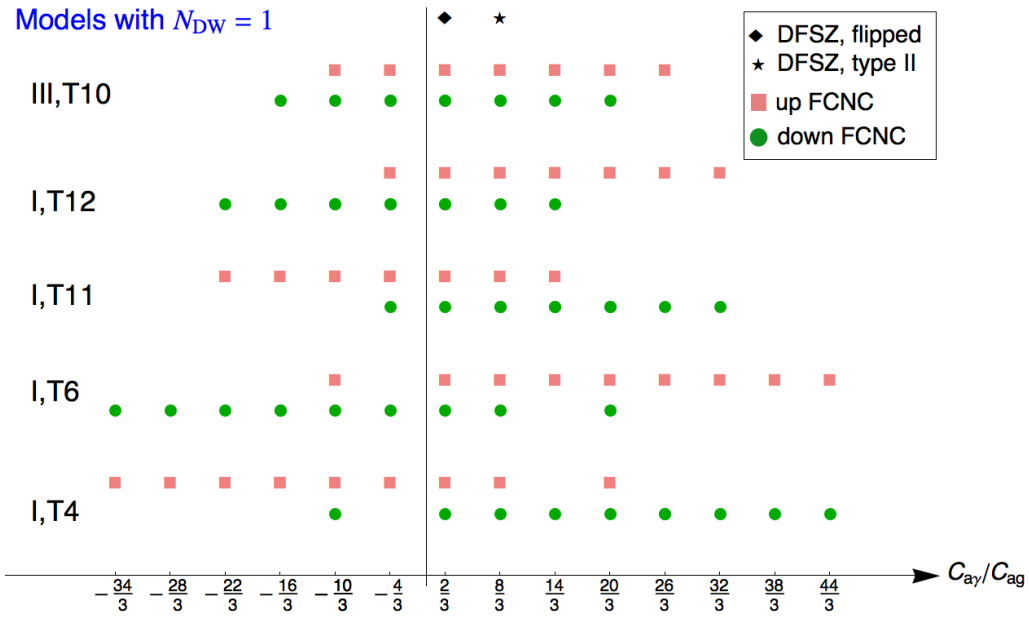

Figure 8.4: *Values of $C_{a\gamma}/C_{ag}$ in 3HFPQ models with $N_{DW} = 1$. Squares stand for models with FCNC in the up-quark sector while those with FCNC in the down-quark sector are denoted with circles. The corresponding values for $C_{a\gamma}/C_{ag}$ in the DFSZ models (type II and flipped) are also shown.*

are not as suppressed $|V_{us}^* V_{ud}| \sim |V_{cs}^* V_{cd}| \gg |V_{ts}^* V_{td}|$. Figure 8.3 summarizes all the constraints on this scenario.

- Constraints from $\mu^+ \to e^+ a\gamma$ are very similar in all models with FCNCs in the charged lepton sector due to the anarchical structure of the PMNS matrix. The bounds derived from $\mu^+ \to e^+ a\gamma$ are stronger than those obtained from $K^+ \to \pi^+ a$ in models with tree-level FCNCs in the down-quark sector for which the top quark is singled out.

- The axion of models without FCNCs in the down-quark and charged lepton sectors does not receive important constraints from flavor observables. In this case the strongest bounds on the axion can be derived from the axion-photon coupling and white-dwarf cooling arguments.

- A large variety of the models considered have $N_{\rm DW} = 1$, avoiding the domain wall problem. Allowed values for the model dependent quantity $C_{a\gamma}/C_{ag}$ (see Eqs. (8.89) and (8.91)) in these models are presented in Figure 8.4. As we can see, large deviations on the axion-photon coupling compared with the DFSZ model are obtained in some cases. One interesting aspect is the fact that we are able to mimic the DFSZ axion coupling to photons and have at the same time $N_{\rm DW} = 1$. A zero $C_{a\gamma}$ can be achieved but only in models with $N_{\rm DW} > 1$.

Bibliography

[1] G. C. Branco, W. Grimus and L. Lavoura, Phys. Lett. B **380** (1996) 119 [hep-ph/9601383].

[2] A. Celis, J. Fuentes-Martín and H. Serôdio, Phys. Lett. B **737** (2014) 185 [arXiv:1407.0971 [hep-ph]].

[3] S. L. Glashow and S. Weinberg, Phys. Rev. D **15** (1977) 1958.

[4] G. C. Branco, P. M. Ferreira, L. Lavoura, M. N. Rebelo, M. Sher and J. P. Silva, Phys. Rept. **516** (2012) 1 [arXiv:1106.0034 [hep-ph]].

[5] M. Srednicki, Nucl. Phys. B **260** (1985) 689.

[6] G. G. Raffelt, Lect. Notes Phys. **741** (2008) 51 [hep-ph/0611350].

[7] M. M. Miller Bertolami, B. E. Melendez, L. G. Althaus and J. Isern, JCAP **1410** (2014) no.10, 069 [arXiv:1406.7712 [hep-ph]].

[8] A. G. Dias, A. C. B. Machado, C. C. Nishi, A. Ringwald and P. Vaudrevange, JHEP **1406** (2014) 037 [arXiv:1403.5760 [hep-ph]].

[9] A. Pich and P. Tuzon, Phys. Rev. D **80** (2009) 091702 [arXiv:0908.1554 [hep-ph]].

[10] P. Minkowski, Phys. Lett. **67B** (1977) 421.

[11] Y. Chikashige, R. N. Mohapatra and R. D. Peccei, Phys. Lett. **98B** (1981) 265.

[12] K. J. Bae, Phys. Rev. D **82** (2010) 055004 [arXiv:1003.5869 [hep-ph]].

[13] M. Jung and A. Pich, JHEP **1404** (2014) 076 [arXiv:1308.6283 [hep-ph]].

[14] A. Celis, J. Fuentes-Martin and H. Serodio, Phys. Lett. B **741** (2015) 117 [arXiv:1410.6217 [hep-ph]].

[15] A. Celis, J. Fuentes-Martín and H. Serôdio, JHEP **1412** (2014) 167 [arXiv:1410.6218 [hep-ph]].

[16] Y. B. Zeldovich, I. Y. Kobzarev and L. B. Okun, Zh. Eksp. Teor. Fiz. **67** (1974) 3 [Sov. Phys. JETP **40** (1974) 1].

[17] P. Sikivie, Phys. Rev. Lett. **48** (1982) 1156.

[18] A. Vilenkin, Phys. Rept. **121** (1985) 263.

[19] F. Wilczek, Phys. Rev. Lett. **49** (1982) 1549.

[20] A. Davidson and M. A. H. Vozmediano, Phys. Lett. **141B** (1984) 177.

[21] A. Davidson and M. A. H. Vozmediano, Nucl. Phys. B **248** (1984) 647.

[22] M. Hindmarsh and P. Moulatsiotis, Phys. Rev. D **56** (1997) 8074 [hep-ph/9708281].

[23] M. Hindmarsh and P. Moulatsiotis, Phys. Rev. D **59** (1999) 055015 [hep-ph/9807363].

[24] Y. H. Ahn, Phys. Rev. D **91** (2015) 056005 [arXiv:1410.1634 [hep-ph]].

[25] Z. G. Berezhiani and M. Y. Khlopov, Sov. J. Nucl. Phys. **51** (1990) 739 [Yad. Fiz. **51** (1990) 1157].

[26] F. J. Botella, G. C. Branco and M. N. Rebelo, Phys. Lett. B **687** (2010) 194 [arXiv:0911.1753 [hep-ph]].

[27] L. M. Krauss and M. B. Wise, Phys. Lett. B **176** (1986) 483.

[28] W. A. Bardeen, R. D. Peccei and T. Yanagida, Nucl. Phys. B **279** (1987) 401.

[29] J. L. Feng, T. Moroi, H. Murayama and E. Schnapka, Phys. Rev. D **57** (1998) 5875 [hep-ph/9709411].

[30] F. J. Botella, G. C. Branco, M. Nebot and M. N. Rebelo, JHEP **1110** (2011) 037 [arXiv:1102.0520 [hep-ph]].

[31] H. Serôdio, Phys. Rev. D **88** (2013) no.5, 056015 [arXiv:1307.4773 [hep-ph]].

[32] B. Pontecorvo, Sov. Phys. JETP **7** (1958) 172 [Zh. Eksp. Teor. Fiz. **34** (1957) 247].

[33] D. V. Forero, M. Tortola and J. W. F. Valle, Phys. Rev. D **90** (2014) no.9, 093006 [arXiv:1405.7540 [hep-ph]].

[34] S. Weinberg, Phys. Rev. Lett. **40** (1978) 223.

[35] S. M. Barr, K. Choi and J. E. Kim, Nucl. Phys. B **283** (1987) 591.

[36] K. S. Babu, I. Gogoladze and K. Wang, Phys. Lett. B **560** (2003) 214 [hep-ph/0212339].

[37] M. B. Green and J. H. Schwarz, Phys. Lett. **149B** (1984) 117.

[38] V. G. Kac, Funct. Anal. Appl. **1** (1967) 328.

[39] T. Banks and M. Dine, Phys. Rev. D **45** (1992) 1424 [hep-th/9109045].

[40] L. E. Ibanez and G. G. Ross, Phys. Lett. B **260** (1991) 291.

[41] A. Jodidio *et al.*, Phys. Rev. D **34** (1986) 1967 Erratum: [Phys. Rev. D **37** (1988) 237].

[42] J. T. Goldman *et al.*, Phys. Rev. D **36** (1987) 1543.

[43] R. D. Bolton *et al.*, Phys. Rev. D **38** (1988) 2077.

[44] S. S. Adler *et al.* [E787 Collaboration], Phys. Lett. B **537** (2002) 211 [hep-ex/0201037].

[45] H. Leutwyler and M. Roos, Z. Phys. C **25** (1984) 91.

[46] M. Hirsch, A. Vicente, J. Meyer and W. Porod, Phys. Rev. D **79** (2009) 055023 Erratum: [Phys. Rev. D **79** (2009) 079901] [arXiv:0902.0525 [hep-ph]].

[47] R. Fantechi [NA62 Collaboration], arXiv:1407.8213 [physics.ins-det].

[48] S. Bertolini and A. Santamaria, Nucl. Phys. B **357** (1991) 222. doi:10.1016/0550-3213(91)90467-C

[49] K. Allison, C. T. Hill and G. G. Ross, Nucl. Phys. B **891** (2015) 613 [arXiv:1409.4029 [hep-ph]].

[50] F. J. Botella, G. C. Branco, A. Carmona, M. Nebot, L. Pedro and M. N. Rebelo, JHEP **1407** (2014) 078 [arXiv:1401.6147 [hep-ph]].

[51] G. Bhattacharyya, D. Das, P. B. Pal and M. N. Rebelo, JHEP **1310** (2013) 081 [arXiv:1308.4297 [hep-ph]].

[52] G. Bhattacharyya, D. Das and A. Kundu, Phys. Rev. D **89** (2014) 095029 [arXiv:1402.0364 [hep-ph]].

CHAPTER

9 Final remarks

> It's good to have an end to journey toward; but it is the journey that matters, in the end.
>
> — *Ursula K. Le Guin*, The Left Hand of Darkness

The SM possesses several "weak points" that seem to suggest that there might be something beyond, possibly even at the reach of LHC and/or future flavor facilities. Motivated by some of these SM weaknesses, this thesis was devoted to the exploration of NP extensions from three different approaches: EFTs and their extension to one-loop order, the study of the flavor anomalies from a gauge extended sector, and invisible axion models and their interplay with the flavor sector.

Given the lack of positive direct searches at LHC, and with the increasing precision reached in many observables, EFTs provide an essential tool in the search for NP, since they allow for a systematic and model-independent analysis of the experimental data. EFTs are extensively used, for example, in flavor physics, where the masses of some of the particles mediating the relevant processes, either from the SM or from NP, are expected to lay well beyond the typical scale of the system. In some EFT analyses, the inclusion of one-loop corrections becomes crucial. This is the case, for instance, when radiative corrections introduce new effects that are not present or appear strongly suppressed at tree-level. In order to connect these EFT analyses with existing models, it is rather useful to have systematic techniques that allow for a simple determination of the EFT of a given (arbitrary) UV model. In this sense, functional integration techniques seem more powerful than the diagrammatic matching procedure when one aims to the determination of the full EFT, since they directly provide the whole set of EFT operators together with their matching conditions. Moreover, universal expansions that are applicable in certain limits have been derived in the literature using these techniques.

Lately, there has been an intense debate on how to determine, from the path integral, the contributions to one-loop WCs involving both heavy and light fields. In Chapter 6, we addressed this issue and developed a simplified framework based on functional techniques for the construction of one-loop EFTs. In this chapter we have shown that the one-loop WCs are completely determined by the hard region (i.e. the region where the loop momenta is of the same order as the high-energy scale) of a functional determinant that contains all one-loop contributions to the Green functions. This method provides a new insight into the matching procedure

and introduces important simplifications with respect to previous approaches in the literature.

Although so far no new particles have been found at the LHC there are some interesting hints of NP in the flavor sector. These consist in a series of deviations in B-meson decays involving $b \to s\mu^+\mu^-$ transitions, and in the theoretically-clean ratios $R_{K^{(*)}}$, pointing to a large LFUV in the $e-\mu$ sector. Global fits to $b \to s\mu^+\mu^-$ data and/or $R_{K^{(*)}}$ show compatible results and provide a very good fit when allowing for rather large non-universal NP effects in $b \to s\ell^+\ell^-$ transitions. This situation is preferred over the SM hypothesis by $4-5\,\sigma$.

While it is still early to know whether these are genuine NP effects, it is interesting to analyze these hints from a model-building approach and try to search for implications in other observables. We followed this approach in Chapter 7. In particular, in Section 7.1 we explored a possible explanation of the anomalies based on a minimal U(1)′ extension of the SM characterized to have *all* their fermion couplings related *exactly* to the CKM matrix elements, avoiding the strong flavor bounds in a natural way while providing a very predictive model. In this framework, gauge anomaly cancellation can be achieved with the SM fermion content alone by fixing the extension of the symmetry to the lepton sector in a very specific way, giving rise to lepton-flavor-conserving family-non-universal Z' couplings. Given the predictability of these models, with most of the couplings completely fixed by the gauge symmetry, they provide a very interesting phenomenology.

A different approach in the explanation of the anomalies consists in searching for possible connections between these anomalies and other problems of the SM. Indeed, the SM flavor puzzle, may be hinting to the same underlying dynamics in the flavor sector as the one needed to explain the anomalies. In Section 7.2 we analyzed this possibility from the hypothesis of dynamical Yukawa couplings, that provides a natural explanation to the general structure of the Yukawa matrices. In this framework, it is assumed that the SM Yukawas appear from the vev of scalar flavon fields that are charged under the non-Abelian flavor symmetry $[\mathrm{SU}(3)]^5\times\mathrm{O}(3)$, which is promoted to a local symmetry. We have shown that the desired pattern of the SM Yukawa couplings can naturally lead to a sequential breaking of the flavor symmetry down to $\mathrm{U}(1)_\mathrm{q}\times\mathrm{U}(1)_{\mu-\tau}$, which finally gets spontaneously broken around the TeV scale. In order to explain the aforementioned experimental hints, the Z' bosons resulting from this last breaking are required to mix, yielding very distinctive collider signatures that will be tested in the near future.

As also discussed in this thesis, other hints of lepton-universality violation have been reported in the $R(D^{(*)})$ ratios, implying a combined deviation from the SM at the 4σ level, and hinting for a large LFUV in the tau sector. In Section 7.3 we explored the possibility of accommodating both sets of anomalies by extending the SM gauge group with an extra SU(2) symmetry and analyzed the phenomenological implications of such extension in detail. In particular, we have shown that the model presented in this thesis can significantly ease the tensions with B-physics data while satisfying the stringent bounds from other flavor observables and electroweak precision data. An important issue for this model is whether it is able to avoid the strong bounds from $\tau^+\tau^-$ resonance searches at LHC. Present experimental bounds

force the Z' of the model to have a large width, which requires an extension of the minimal framework.

Another interesting direction in the search for NP is provided by the Strong CP problem, i.e. the lack of explanation in the SM to why the QCD vacuum angle cancels with the chiral phase of the quark mass matrix to an accuracy of $\mathcal{O}(10^{-11})$. The PQ mechanism provides an elegant solution and predicts the existence of a very light and weakly coupled pseudo-Goldstone boson, the axion, whose phenomenology is particularly interesting. This solution consists on the introduction of a global chiral symmetry with mixed anomalies with QCD, $\mathrm{U}(1)_{\mathrm{PQ}}$, that gets spontaneously broken. In order to avoid experimental constraints, the breaking should take place at very high energies, so that the mass and the couplings of the axion are suppressed by this high scale, giving rise to the so-called invisible axion models.

In Chapter 8 we explored different invisible axion implementations that extend the minimal frameworks. In Section 8.1 we presented an invisible axion model that offers a UV completion to the A2HDM. Additionally, in Section 8.2 we have introduced a class of models where the PQ symmetry is not universal but rather a flavor symmetry. This has several interesting features that are not present in the minimal benchmark models. For instance, these models predict flavor-changing axion transitions that yield interesting signatures in $\mu^+ \to e^+ a\gamma$ and $K^+ \to \pi^+ a$. The presence of flavor violations in the axion and scalar sectors controlled by the CKM matrix, and the possibility to avoid the domain wall problem stand as the main features of the models presented in this section. Moreover, the smallness of active neutrinos masses is naturally accounted for in both frameworks via the type-I see-saw mechanism, providing a common origin for PQ symmetry breaking and the see-saw scales.

Part III

Resumen en español

CAPÍTULO

10 Resumen de la tesis

> ¿Qué duda cabe que el mundo que conocemos es el resultado del reflejo de la parte de cosmos del horizonte sensible en nuestro cerebro? Este reflejo unido, contrastado, con las imágenes reflejadas en los cerebros de los demás hombres que han vivido y que viven, es nuestro conocimiento del mundo, es nuestro mundo. ¿Es así, en realidad, fuera de nosotros? No lo sabemos, no lo podremos saber jamás.
>
> — *Pío Baroja*, El árbol de la ciencia

La física de partículas está viviendo actualmente una era de exploración que comenzó con la observación en el LHC del bosón de Higgs, proporcionando así al Modelo Estándar de la Física de Partículas la elusiva pieza final que lo completa. Si bien esta teoría es extremadamente exitosa, se acepta comúnmente que no es la teoría final ya que no puede responder a todas las preguntas teóricas ni a ciertas observaciones experimentales. Por lo tanto, se espera que Nueva Física que extienda al Modelo Estándar aparezca pronto, aunque esto bien podría ser sólo una esperanza. Esta tesis recoge algunas de las aventuras en la búsqueda de Nueva Física. Se organiza en tres partes: la Parte I introduce, en inglés, los principales temas de la tesis y establece la notación y marcos teóricos que se utilizan más tarde. Esta parte contiene temas que son de conocimiento general en la literatura y pretende ser una introducción amplia. Por el contrario, la Parte II, también en inglés, se dedica específicamente a compilar la investigación científica que se hizo durante el doctorado y, por tanto, es de naturaleza más técnica que la parte anterior.

La Parte I está organizada de la siguiente forma. En el Capítulo 1 introducimos el Modelo Estándar, sus principales características, y varias cuestiones teóricas y experimentales que este marco teórico no puede explicar. El resto de esta parte se dedica al análisis de varias extensiones del Modelo Estándar. En particular, en el Capítulo 2 presentamos el modelo de dos dobletes de Higgs, una extensión mínima del Modelo Estándar donde se añade un doblete de Higgs adicional al sector escalar de la teoría. En este capítulo se hace especial hincapié en el problema del sabor del modelo de dos dobletes de Higgs y se estudian sus soluciones. El Capítulo 3 presenta el problema de violación de CP en el sector fuerte en cierto detalle, junto

con una discusión sobre la solución de Peccei–Quinn y su fenomenología asociada. En el Capítulo 4 introducimos el concepto de Teorías Efectivas y mostramos cómo construirlas a partir de un modelo ultravioleta dado usando técnicas funcionales. También mostramos ejemplos de Teorías Efectivas dentro del marco teórico del Modelo Estándar que introducen un enfoque complementario en la búsqueda de Nueva Física. Finalmente, en el Capítulo 5 presentamos las recientes anomalías experimentales en desintegraciones del mesón B y discutimos sus principales implicaciones.

Mientras que la Parte I sigue una discusión más lineal, con cada capítulo basado en los anteriores, la Parte II está estructurada en tres capítulos esencialmente independientes. El Capítulo 6 extiende los métodos funcionales para la construcción de Teorías Efectivas introducidos en el Capítulo 4. En el Capítulo 7 presentamos tres modelos construidos para proporcionar una explicación a las anomalías en la física del mesón B. Estos se basan en varias extensiones del sector gauge del Modelo Estándar, cada una de las cuales da lugar a predicciones experimentales características diferentes. En el Capítulo 8 se introducen dos modelos de axión invisible que incluyen propiedades adicionales no presentes en las implementaciones originales.

A continuación detallamos los principales objetivos, metodología y conclusiones de la presente tesis.

10.1 Objetivos: Non Terrae Plus Ultra?

El Modelo Estándar es la teoría que recopila todo nuestro conocimiento actual sobre las interacciones fuertes y electrodébiles. En esta teoría el concepto de simetría juega un papel central. Sus grados de libertad fundamentales son campos que corresponden a representaciones de la simetría de Lorentz; y el Lagrangiano que caracteriza las interacciones entre estos campos está basado en la invariancia bajo la simetría local $\mathrm{SU(3)_c \times SU(2)_L \times U(1)_Y}$. El uso de estos principios de simetría proporciona un marco teórico elegante y simple que es capaz de describir con gran precisión la mayoría de los datos experimentales conocidos en física de partículas, haciendo del Modelo Estándar uno de los mayores éxitos de la Física Moderna. Entre las principales características del Modelo Estándar destacan las siguientes:

- El Modelo Estándar es una teoría cuántica de campos basada en los principios de localidad, causalidad y renormalizabilidad, invariante bajo la simetría de Lorentz y la simetría local (también llamada gauge) $\mathcal{G}_{\mathrm{SM}} \equiv \mathrm{SU(3)_c \times SU(2)_L \times U(1)_Y}$.

- En este marco teórico, los bosones, partículas de espín entero entre las que se encuentran el bosón Higgs y los bosones gauge, son los mediadores de las interacciones. Al contrario que el bosón de Higgs, los bosones gauge están completamente definidos en términos de la simetría gauge del Modelo Estándar. Tenemos ocho gluones sin masa para las interacciones fuertes, G^{α}_{μ}, asociados a la simetría local $\mathrm{SU(3)_c}$; mientras que los bosones gauge correspondientes a la simetría $\mathrm{SU(2)_L \times U(1)_Y}$ son el fotón, A_{μ}, que no tiene masa y que media las interacciones electromagnéticas, y tres bosones masivos, el $W^{\pm}_{\mu}$ y el Z_{μ}, mediadores de las interacciones débiles. Puesto que en el Modelo Estándar

Tipo	Partícula	$\mathrm{SU(3)_c}$	$\mathrm{SU(2)_L}$	$\mathrm{U(1)_Y}$
Quarks	q_L	**3**	**2**	$1/6$
	u_R	**3**	**2**	$2/3$
	d_R	**3**	**2**	$-1/3$
Leptones	ℓ_L	**1**	**2**	$-1/2$
	e_R	**1**	**1**	-1

Tabla 10.1: *Contenido de materia del Modelo Estándar y sus números cuánticos respecto a la simetría gauge.*

tanto los mediadores del electromagnetismo como los de la fuerza débil están asociados a la misma simetría, se dice que estas fuerzas están unificadas y a la simetría $\mathrm{SU(2)_L \times U(1)_Y}$ se le conoce como simetría electrodébil.

- La materia observada está constituida por fermiones, que están descritos en términos de partículas de espín un medio de quiralidad bien definida

$$\begin{aligned} q_L &= \begin{pmatrix} u_L \\ d_L \end{pmatrix}, \qquad u_R\,, \qquad d_R\,, \\ \ell_L &= \begin{pmatrix} \nu_L \\ e_L \end{pmatrix}, \qquad e_R\,. \end{aligned} \tag{10.1}$$

  Las interacciones de los fermiones con los bosones gauge viene determinadas por cómo transforman bajo la simetría local del Modelo Estándar. Los fermiones del Modelo Estándar aparecen en cinco representaciones diferentes de la simetría gauge (ver Tabla 10.1). Los fermiones que no transforman bajo la simetría asociada a la interacción fuerte, $\mathrm{SU(3)_c}$, no sienten esta fuerza y reciben el nombre de leptones. En contrapartida, a los fermiones que sí sienten esta interacción se les denomina quarks. Los quarks y los leptones aparecen en tres copias, denominadas comúnmente como familias o sabores:

$$u \equiv \begin{pmatrix} u \\ c \\ t \end{pmatrix}, \qquad d \equiv \begin{pmatrix} d \\ b \\ s \end{pmatrix}, \qquad e \equiv \begin{pmatrix} e \\ \mu \\ \tau \end{pmatrix}, \qquad \nu \equiv \begin{pmatrix} \nu_e \\ \nu_\mu \\ \nu_\tau \end{pmatrix}. \tag{10.2}$$

  Los fermiones de distintos sabor sienten las interacciones gauge forma idéntica, situación que recibe el nombre de *universalidad*, y sólo se distinguen entre sí por sus masas y sus interacciones de Yukawa con el Higgs.

- La simetría gauge impide que los bosones gauge masivos, el W y el Z, y los fermiones adquieran una masa, en contradicción de las observaciones experimentales. En el Modelo Estándar estas partículas adquieren masa por medio del mecanismo de Higgs. Este mecanismo se basa en el hecho de que, mientras que el Lagrangiano es invariante bajo la simetría gauge, el vacío (el estado fundamental) del potencial de Higgs no lo es. De este modo el bosón de Higgs adquiere un valor esperado en el vacío que induce una ruptura espontánea de

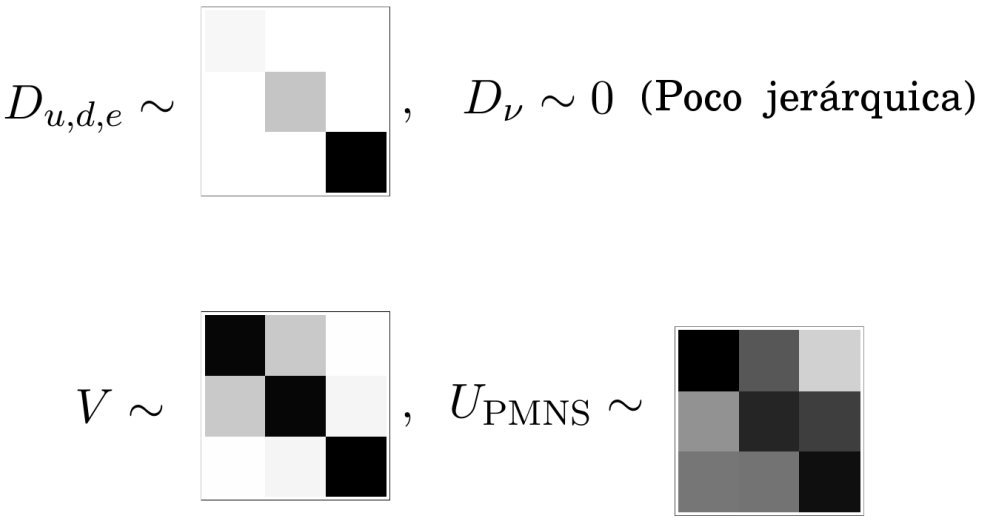

Figura 10.1: *Ilustración de los patrones observados en las masas, denotadas como D_f ($f = u, d, e, \nu$), y las mezclas fermiónicas, con V para la matriz CKM y U_{PMNS} para la matriz PMNS. Los colores más claros en los elementos de matriz indican valores más suprimidos comparados con los colores más oscuros.*

la simetría electrodébil, dando lugar a las masas observadas y, al mismo tiempo, introduciendo mezclas entre las distintas familias en las interacciones con el bosón W. Éstas están parametrizadas en términos de las llamadas matrices CKM y PMNS que describen, respectivamente, las mezclas en el sector de quarks y de leptones.[1]

El Modelo Estándar proporciona un marco teórico sólido y consistente para la descripción de los fenómenos físicos que tienen lugar a altas energías. Además reproduce una inmensa mayoría de los datos experimentales actuales con un acuerdo asombroso. Sin embargo, existen varias indicaciones, tanto teóricas como experimentales, que parecen apuntar a la posible existencia de Física más allá del Modelo Estándar. Desde el punto de vista teórico, el Modelo Estándar presenta varias cuestiones insatisfactorias:

- **El problema de violación de CP en el sector fuerte:** La inclusión de efectos no perturbativos en el sector que describe las interacciones fuertes da lugar a la aparición de un nuevo término en el Lagrangiano. Este nuevo término viola la simetría CP; sin embargo, no hay evidencia experimental para tal fuente de violación de CP. Puesto que el Modelo Estándar carece de un mecanismo para prohibir la presencia de este término, es necesario realizar un ajuste de los parámetros de la teoría, del orden de una parte en diez mil millones, para encontrar buen acuerdo con las observaciones experimentales.

[1] En sentido estricto, en el Modelo Estándar no existe ningún mecanismo para dar masa a los neutrinos y como consecuencia la matriz PMNS es igual a la identidad en este marco teórico, en contradicción con los resultados observados (ver discusión más adelante).

- **El puzzle del sabor:** No hay ninguna explicación en el Modelo Estándar que explique la existencia de tres familias. Por otra parte, como se puede ver en la Figura 10.1, las masas y mezclas de fermiones del Modelo Estándar siguen una estructura bastante peculiar, caracterizada por tener elementos de matriz muy jerárquicos en el sector de quarks y leptones cargados, que contrasta fuertemente con el patrón anárquico observado en el sector de los neutrinos. La falta de una explicación, dentro del Modelo Estándar, para estas características del sector del sabor, constituye el llamado puzzle del sabor del Modelo Estándar.

- **El problema de las jerarquías:** A diferencia de lo que ocurre con los fermiones y los bosones gauge, la masa del bosón de Higgs, que es una partícula escalar, es muy sensible a las posibles extensiones del Modelo Estándar. En presencia de Nueva Física, la masa del bosón de Higgs recibiría correcciones cuánticas proporcionales a la escala de energía de esta Nueva Física. La existencia de estas correcciones cuánticas requerirían, una vez más, la introducción de un ajuste de parámetros para mantener la masa del bosón de Higgs en su valor observado.

- **Gran Unificación:** En teoría de cuántica de campos, los acoplamientos de una teoría dada varían con la energía a la que se miden. Una característica interesante del Modelo Estándar es que, si evolucionamos los acoplamientos gauge de cada uno de sus tres grupos de simetría, se puede ver que se vuelven aproximadamente iguales a una energía muy alta. Esto podría estar indicando que, al igual que sucede con las fuerzas débiles y electromagnéticas, las fuerzas del Modelo Estándar se unifican. Del mismo modo que ocurre con las interacciones electrodébiles, esta posible unificación podría estar insinuando la existencia de una dinámica subyacente alrededor de la escala de unificación. Las teorías más allá del Modelo Estándar basadas en esta idea de unificación de fuerzas reciben el nombre de Teorías de Gran Unificación.

- **Gravedad:** El Modelo Estándar no incluye los efectos de la gravedad. Por lo tanto *debe* ser extendido para proporcionar una descripción de la gravedad cuántica. Estos efectos se pueden agregar al Modelo Estándar usando Teorías Efectivas siempre que uno se restrinja a energías por debajo de la escala de Planck. Sin embargo, más allá de esa escala uno debe confiar en una teoría completa de la gravedad cuántica.

Por otro lado, a pesar del enorme éxito fenomenológico del Modelo Estándar, hay observaciones experimentales que no pueden explicarse en esta teoría, y que sugieren la presencia de física más allá de este marco teórico:

- **Masas y mezclas de neutrinos:** Los neutrinos son partículas sin masa en el Modelo Estándar. Sin embargo, los experimentos de oscilación de neutrinos han demostrado que estos tienen masa. Aunque el Modelo Estándar se puede extender fácilmente para dar cuenta de estas masas, existen diferentes mecanismos. Además, relacionado con esta cuestión, no está claro si los neutrinos

son sus propias antipartículas. Cuál es la extensión del Modelo Estándar escogida por la Naturaleza para explicar las masas de los neutrinos permanece como una de las preguntas abiertas en la Física de Partículas.

- **Las anomalías en física del sabor:** Las colaboraciones experimentales de LHCb, Belle y Babar han reportado un conjunto de interesantes anomalías que involucran varios observables en el desintegración del mesón B, formado por un quark d y un anti-quark b. Aunque estas medidas todavía no son lo suficientemente significativas para anunciar el descubrimiento de Nueva Física, el conjunto de desviaciones observadas parece mostrar un patrón bastante coherente. El valor nominal de estas anomalías experimentales implican una gran violación de la universalidad del sabor de leptónico que no puede explicarse en el Modelo Estándar.

- **Asimetría materia-antimateria:** El Modelo Estándar predice que la materia y la antimateria deben ser creadas en el universo primitivo prácticamente en la misma cantidad. Sin embargo, el universo observado está hecho principalmente de materia. Para explicar esta asimetría el Modelo Estándar necesita ser extendido.

- **Materia oscura y energía oscura:** Según las observaciones cosmológicas, el Modelo Estándar sólo representa el 5 % de la energía en el universo observable. De la energía restante, un 26 % debe corresponder a nueva materia que no interacciona ni fuertemente ni electromagnéticamente, la llamada *materia oscura*. El resto (un 69 %) debe consistir en *energía oscura*, cuya naturaleza aún está en debate.

En esta tesis hemos tratado de abordar algunos de estos problemas. En particular, en el Capítulo 2 se discuten posibles extensiones del sector escalar del Modelo Estándar, lo cuál puede ser de interés para la explicación de la asimetría materia-antimateria o para la materia oscura. El objetivo del Capítulo 3 es introducir el problema de violación de CP en el sector fuerte y presentar un mecanismo capaz de resolverlo; mientras que en el Capítulo 8 hemos presentado modelos explícitos que amplían los mecanismos más minimalistas para incluir características adicionales. A falta de una indicación clara acerca de cuál podría ser la teoría subyacente que extienda al Modelo Estándar, es muy útil hacer uso de descripciones efectivas que parametrizan esta posible nueva dinámica de una manera independiente del modelo. Hemos introducido estas técnicas en el Capítulo 4, mientras que en el Capítulo 6 las hemos extendido al siguiente orden en teoría de perturbaciones, es decir, a un *loop*. Finalmente, en el Capítulo 5 se presentan las anomalías de sabor en detalle, y el Capítulo 7 se dedica al estudio de posibles explicaciones de las anomalías a través un sector de gauge extendido.

10.2 Metodología y conclusiones: La búsqueda de terra incognita

Como hemos comentado en la sección anterior, el Modelo Estándar posee varios "puntos débiles" que parecen sugerir que podría haber algo más allá, posiblemente incluso al alcance del LHC y/o futuras factorías de sabor. Motivados por algunas de estas debilidades del Modelo Estándar, en esta tesis hemos explorado extensiones de este modelo mediante tres enfoques diferentes: Teorías Efectivas y su extensión a un *loop*, el estudio de las anomalías del sabor a través de un sector gauge extendido, y modelos de axiones y su interacción con el sector del sabor.

Dada la ausencia actual de resultados positivos en las búsquedas directas de Nueva Física en el LHC, y con la creciente precisión que se está alcanzando en muchos observables, las Teorías Efectivas proporcionan una herramienta esencial en la búsqueda de Nueva Física, ya que permiten un análisis sistemático e independiente de modelo de los datos experimentales. Las Teorías Efectivas son ampliamente utilizadas, por ejemplo, en la física del sabor, donde se espera que las masas de algunas de las partículas que median los procesos de interés, ya sean del Modelo Estándar o nuevas partículas, estén más allá de la escala típica del sistema. En algunos análisis de Teorías Efectivas, la inclusión de correcciones a un *loop* resulta crucial. Este es el caso, por ejemplo, cuando estas correcciones introducen nuevos efectos que no están presentes o que aparecen fuertemente suprimidos a primer orden en teoría de perturbaciones. Con el fin de conectar estos análisis con los modelos existentes, es bastante útil tener técnicas sistemáticas que permitan una simple determinación de la Teoría Efectiva de un modelo ultravioleta arbitrario. En este sentido, cuando se pretende determinar la totalidad de la Teoría Efectiva las técnicas de integración funcional resulta mucho más eficientes que el el proceso de *matching*, consistente en la comparación directa entre la Teoría Efectiva y la teoría ultravioleta a bajas energías. Esto es porque los métodos funcionales proporcionan directamente todo el conjunto de operadores de la Teoría Efectiva junto con sus condiciones de correspondencia. Además, existen ciertas expresiones universales que son aplicables bajo ciertos límites y que han sido derivadas en la literatura usando estas técnicas.

Últimamente ha habido un intenso debate sobre cómo determinar, a partir de estos métodos funcionales, las contribuciones a los coeficientes de la Teoría Efectiva cuando estos provienen de procesos a un *loop* que involucran tanto partículas pesadas como ligeras. En el Capítulo 6, hemos abordado esta cuestión y hemos desarrollado un marco teórico simplificado, basado en técnicas funcionales, para la construcción de Teorías Efectivas a un *loop*. En este capítulo hemos demostrado que los acoplamientos de la Teoría Efectiva quedan completamente determinados por la región *hard*, donde el momento que involucra las correcciones cuánticas es del mismo orden que la escala de altas energías, de un determinante funcional que contiene toda la información relativa a los efectos a un *loop* que involucran a las partículas pesadas. Este método proporciona una nueva visión al proceso de construcción de Teorías Efectivas e introduce importantes simplificaciones con respecto a enfoques previos presentes en la literatura.

A pesar de que por el momento no se han encontrado nuevas partículas en el LHC, existen interesantes discrepancias experimentales en el sector del sabor que parecen apuntar a efectos de Nueva Física (ver Capítulo 5 para una discusión en inglés). Estas anomalías experimentales consisten en una serie de desviaciones respecto a la predicción teórica del Modelo Estándar en los desintegraciones del mesón B que involucran las transiciones a nivel partónico $b \to s\ell^+\ell^-$ (con $\ell = \mu, e$). Estas desviaciones parecen indicar la existencia de una fuerte violación de universalidad en el sector $e - \mu$. Los ajustes globales de todos los datos experimentales relacionados con estas transiciones dan un ajuste muy bueno cuando se incluyen grandes contribuciones de Nueva Física de carácter no universal en acoplamientos relacionados con transiciones $b \to s\ell^+\ell^-$. Esta situación es preferida a la predicción del Modelo Estándar por $4 - 5\,\sigma$.

Aunque todavía es pronto para saber si estos efectos son realmente Nueva Física, es interesante estudiar estas anomalías desde posibles extensiones del Modelo Estándar e intentar buscar implicaciones en otros observables. Éste es el camino que seguimos en el Capítulo 7. En particular en la Sección 7.1 hemos explorado una posible explicación de las anomalías basada en una extensión $\mathrm{U}(1)'$ del Modelo Estándar que se caracteriza por tener *todos* sus acoplamientos a quarks *exactamente* relacionados con los elementos de su matriz de mezcla. De este modo, estos modelos evitan de forma natural los fuertes límites que reciben los procesos que violan sabor al tiempo que proporcionan un marco teórico muy predictivo. En estos modelos, la cancelación de anomalías gauge se puede lograr únicamente con el contenido fermiónico del Modelo Estándar, fijando la extensión de la simetría al sector leptónico de manera unívoca. Como resultado, estos modelos dan lugar a un Z' con acoplamientos no-universales en el sector leptónico pero que conserva sabor. Dada la predictibilidad de estos modelos, con la mayor parte de sus acoplamientos completamente fijados por la simetría gauge, estos proporcionan una fenomenología muy interesante.

Un enfoque diferente en la explicación de las anomalías consiste en buscar posibles conexiones entre éstas y otros problemas del Modelo Estándar. Por ejemplo, el puzzle del sabor del Modelo Estándar, que introdujimos en la sección anterior, podría estar sugiriendo la existencia de la misma dinámica subyacente en el sector del sabor que la que se necesitaría para explicar las anomalías. En la Sección 7.2 hemos explorado esta idea mediante la hipótesis de los acoplamientos de Yukawa dinámicos, que proporciona una explicación natural a la estructura general de las matrices de masa y de mezcla fermiónicas mostrada en la Figura 10.1. En este marco teórico, se asume que los Yukawas del Modelo Estándar surgen a partir del valor esperado en el vacío de nuevos campos escalares cargados bajo la simetría de sabor $[\mathrm{SU}(3)]^5 \times \mathrm{O}(3)$, que es tomada como a una simetría local de la naturaleza. En esta tesis hemos mostrado que el patrón de Yukawas observado puede conducir naturalmente a una rotura secuencial de la simetría del sabor que preserva a bajas energías la simetría $\mathrm{U}(1)_{\mathrm{q}} \times \mathrm{U}(1)_{\mu-\tau}$, la cual a su vez se rompe espontáneamente alrededor de la escala del TeV. Con el fin de explicar las anomalías experimentales antes mencionadas, los bosones Z' que resultan de esta última ruptura de simetría se deben mezclar, dando lugar a predicciones muy distintivas que serán testadas en el LHC en un futuro próximo.

Junto a las anomalías ya mencionadas, también se han reportado otros indicios de violación de la universalidad leptónica en los ratios $R(D^{(*)})$, dando lugar a una desviación combinada con respecto a la predicción del Modelo Estándar de 4σ, sugiriendo una gran violación de universalidad en la tercera familia de leptones. En la Sección 7.3 hemos exploramos la posibilidad de acomodar ambos conjuntos de anomalías extendiendo el sector gauge del Modelo Estándar mediante la inclusión de una simetría SU(2) adicional, y hemos analizado en detalle las implicaciones fenomenológicas de dicha extensión. En particular, hemos demostrado que el modelo presentado en esta tesis puede aliviar significativamente las tensiones experimentales observadas, al tiempo que puede evadir los fuertes límites experimentales impuestos por otros observables de física del sabor y por medidas de precisión en el sector electrodébil. Una cuestión que este tipo de extensiones debe abordar, es su capacidad para evadir los fuertes límites experimentales procedentes de búsquedas directas de resonancias con estado final $\tau^+\tau^-$, que se están llevando a cabo actualmente en el LHC. Los límites experimentales actuales obligan a el Z' de estos modelos a tener una anchura de desintegración muy grande, lo que requiere una extensión del marco teórico mínimo presentado en esta tesis.

Por otro lado el problema de CP en el sector fuerte, que ya fue comentado en la sección anterior y que ha sido discutido en más detalle en el Capítulo 3, también ofrece una dirección interesante en la búsqueda de Nueva Física. El mecanismo de Peccei–Quinn proporciona una solución elegante y predice la existencia de un bosón escalar muy ligero y débilmente acoplado, el axión, cuya fenomenología es particularmente interesante. Esta solución consiste en la introducción de una simetría quiral global, $\mathrm{U}(1)_{\mathrm{PQ}}$, que presenta anomalías mixtas con la simetría de la interacción fuerte y que debe estar espontáneamente rota a bajas energías. Para evadir los fuertes límites experimentales sobre esta nueva partícula, la ruptura de la simetría debe tener lugar a una escala de energías muy elevadas, haciendo que la masa y los acoplamientos del axión estén fuertemente suprimidos por esta escala. Al axión resultante de estos modelos se le conoce como axión invisible, dados sus acoplamientos extremadamente débiles con el resto de las partículas.

En el Capítulo 8 hemos presentado dos modelos de axiones invisibles que extienden los modelos mínimos para incorporar nuevas propiedades que están ausentes en estos últimos. En particular, en la Sección 8.1 hemos presentado un modelo de axiones invisibles que, al tiempo que resuelve el problema de CP en el sector fuerte, ofrece una compleción ultravioleta para el modelo alineado de dos dobletes de Higgs. También hemos explorado en la Sección 8.2 una clase de modelos donde la simetría de Peccei–Quinn no es universal sino una simetría de sabor. Los modelos de este tipo introducen interesantes características nuevas. Por ejemplo, los axiones de estas teorías poseen acoplamientos que violan sabor, dando lugar a interesantes predicciones en los desintegraciones $\mu^+ \to e^+ a\gamma$ y $K^+ \to \pi^+ a$. Entre las características fundamentales de los modelos de axiones presentados en esta sección, destacan el que las violaciones de sabor mediadas por el axión y el resto de escalares están controladas por la matriz de mezcla fermiónica, así como la posibilidad de evitar el problema de los *domain walls*, uno de los principales obstáculos en la construcción de modelos de axiones en los que la rotura de la simetría de Peccei-Quinn se produce por debajo de la escala de inflación. Por otra parte, el pequeño tamaño de las masas

de los neutrinos activos se puede explicar naturalmente en ambas implementaciones por medio del mecanismo de *see-saw* de tipo I, proporcionando un origen común para la ruptura de la simetría de Peccei–Quinn y la escala de *see-saw*.